REDE NORDESTE DE BIOTECNOLOGIA
UNIVERSIDADE FEDERAL DE SERGIPE

CELIA WAYLAN PEREIRA

ATUAÇÃO DO NÚCLEO INCERTUS NA AQUISIÇÃO E EXTINÇÃO DE MEMÓRIAS DE MEDO CONDICIONADO

São Cristovão - SE
2012

REDE NORDESTE DE BIOTECNOLOGIA
UNIVERSIDADE FEDERAL DE SERGIPE

CELIA WAYLAN PEREIRA

ATUAÇÃO DO NÚCLEO INCERTUS NA AQUISIÇÃO E EXTINÇÃO DE MEMÓRIAS DE MEDO CONDICIONADO

Tese apresentada ao Programa de Pós-Graduação Biotecnologia da Rede Nordeste de Biotecnologia, como requisito parcial à obtenção do título de Doutor em Biotecnologia.

Orientador: Prof. Dr. Murilo Marchioro.
Co-orientador: Prof. Dr. Francisco E. Olucha Bordonau

São Cristovão - SE
2012

FICHA CATALOGRÁFICA ELABORADA PELA BIBLIOTECA CENTRAL
UNIVERSIDADE FEDERAL DE SERGIPE

Pereira, Celia Waylan
P436a Atuação do núcleo incertus na aquisição e extinção de memórias de medo condicionado / Celia Waylan Pereira ; orientador Murilo Marchioro. – São Cristóvão, 2012.
180 f. : il.

Tese (Doutorado em Biotecnologia) – Rede Nordeste de Biotecnologia – RENORBIO, Universidade Federal de Sergipe, 2012.

1. Biotecnologia – Aplicações médicas. 2. Neurologia. 3. Emoções. 4. Medo. 5. Comportamento. I. Marchioro, Murilo, orient. II. Título.

CDU 606:616.8

CELIA WAYLAN PEREIRA

ATUAÇÃO DO NÚCLEO INCERTUS NA AQUISIÇÃO E EXTINÇÃO DE MEMÓRIAS DE MEDO CONDICIONADO

Tese apresentada ao Programa de Pós-Graduação Biotecnologia da Rede Nordeste de Biotecnologia, como requisito parcial à obtenção do título de Doutor em Biotecnologia.

BANCA EXAMINADORA

Prof. Dr.:Murilo Marchioro Instituição:Universidade Federal de Sergipe/Renorbio

Assinatura: _____

Profª. Drª.: Deise Maria Furtado de Mendonça Instituição: Universidade Federal de Sergipe

Assinatura: _____

Prof. Dr.: Edilson Divino de Araújo Instituição:Universidade Federal de Sergipe/Renorbio

Assinatura: _____

Prof. Dr.: Roberto Rodrigues de Souza Instituição:Universidade Federal de Sergipe/Renorbio

Assinatura: _____

Profª. Drª.: Vera Lucia Correa Feitosa Instituição: Universidade Federal de Sergipe

Assinatura: _____

São Cristovão, 27 de agosto de 2012

A Deus por me conceder o privilégio de ser chamada de Sua filha mediante Sua graça e por ter me dado os dons para que eu realizasse esse trabalho.

AGRADECIMENTOS

O caminho do doutorado é cheio de provações, angústias e também alegrias. Para chegar até aqui é necessário equilíbrio emocional, mental e espiritual. Porém, isso não se obtém sozinha e por isso agradeço sinceramente àqueles que me auxiliaram nessa jornada:

Agradeço a Deus por estar ao meu lado em todos esses momentos e por ter iluminado minha mente nos momentos mais difíceis;

Agradeço à minha mãe, Celia Serra, sinônimo de mulher batalhadora, por me apoiar e lembrar-me que era possível realizar os meus sonhos, ensinando-me a trabalhar para atingir meus objetivos;

Agradeço aos meus tios e a minha avó pelo carinho, pelas palavras e pelos doces sorrisos que me deram o ânimo necessário para continuar;

Agradeço ao meu esposo, Fabio, que participou de todo o processo junto comigo, encorajando-me e apoiando-me, principalmente nos momentos em que eu perdia a serenidade;

Agradeço aos meus orientadores, Murilo Marchioro e “Paco” Olucha por mostrarem-me o caminho, dando-me sugestões e aceitando também meus pontos de vista. Agradeço pela oportunidade de trabalhar com vocês que conhecem os princípios da profissão e da pesquisa, sempre preocupados com resultados de qualidade;

Agradeço aos demais membros dessa equipe: Ana Sánchez-Pérez, Marcos Otero-García, Juan e Rocío pelo convívio e colaboração.

A Capes pela bolsa concedida;

Agradeço a todos aqueles, que apesar de não terem sido citados, colaboraram com meu crescimento e com a realização desse trabalho através de manifestações de carinho e amizade.

"Aplica teu coração ao ensino e teu ouvido às palavras que trazem conhecimento (...). Escuta teu pai, que te gerou, e não desprezes tua mãe envelhecida. Adquire a verdade, mas não a vendas; adquire a sabedoria, a instrução e o entendimento."

Pr 23, 12. 22-23

"A ciência humana de maneira nenhuma nega a existência de Deus. Quando considero quantas e quão maravilhosas coisas o homem compreende, pesquisa e consegue realizar, então reconheço claramente que o espírito humano é obra de Deus, e a mais notável."

Galileu Galilei

RESUMO

A pesquisa dos mecanismos neurais relacionados à formação das emoções tem crescido nos últimos anos. O medo é um comportamento originado em resposta aos perigos enfrentados pelos animais, tendo sua origem nas reações defensivas exibidas quando da exposição a estímulos ameaçadores. A memória do medo ajuda os animais e os seres humanos a reconhecem as fontes putativas de perigo e adotar a resposta comportamental apropriada. Os circuitos neurais primárias envolvidos nos mecanismo de aquisição de medo e extinção envolvem conexões entre o córtex pré-frontal, hipocampo ventral e a amígdala, e estas áreas são moduladas por redes do tronco cerebral. O núcleo incertus (NI) no tegmento dorsal pontino fornece uma forte projeção GABAérgica a estes centros prosencéfalicos e é fortemente ativado por estressores neurogênicos. Neste estudo em ratos adultos machos foi injetado o traçador anterógrado miniruby no NI, delineado as suas projeções para a amígdala e examinado o efeito de lesões eletrolíticas no NI sobre diferentes fases do processo de condicionamento do medo-extinção. Fibras derivadas do NI foram observadas na amígdala medial anterior, núcleo endopiriforme, parte intra-amígdala do núcleo do leito da estria terminalis, área de transição amígdala-hipocampal, e o núcleo ventromedial da amígdala lateral, com uma ampla faixa de fibra presentes entre a amígdala basolateral e os núcleos olfativos da amígdala. Em um paradigma de condicionamento contextual de medo convencional, comparou-se o comportamento de congelamento em ratos controle (não operados) (n = 13), com ratos operados sem lesão do NI e ratos com lesão do núcleo incertus (n = 9). Não houve diferenças entre os três grupos nas fases de habituação, aquisição ou condicionamento ao contexto, mas ratos com lesão no NI exibiram uma extinção nitidamente mais lenta (com atraso) de respostas condicionadas de congelamento em comparação com ratos operados sem lesão do NI e controles, sugerindo que circuitos NI relacionados normalmente promovem a extinção através de projeções inibitórias para a amígdala e o córtex pré-frontal. Os resultados encontrados auxiliam na compreensão dos mecanismos neurobiológicos envolvidos e no desenvolvimento futuro de técnicas terapêuticas biotecnológicas visando minimizar os efeitos dos distúrbios associados ao medo em humanos, a exemplo do pânico, ansiedade patológica e estresse pós-traumático.

Palavras-chave: núcleo incertus, reações defensivas, medo condicionado, respostas comportamentais, amígdala.

ABSTRACT

The research of neural mechanisms related to training of emotions has increased in recent years. Fear is a behavior originated in response to the dangers encountering by animals, originating in defensive responses displayed when exposed to threatening stimuli. Fear memory helps animals and humans recognize putative sources of danger and adopt the appropriate behavioral response. The primary neural circuits for fear acquisition and extinction involve connections between prefrontal cortex, ventral hippocampus and amygdala, and these áreas are modulated by brainstem networks. The nucleus (n.) incertus in the dorsal pontine tegmentum provides a strong GABAergic projection to these forebrain centers and is strongly activated by neurogenic stressors. In this study in male, adult rats, we injected miniruby anterograde tracer into n. incertus and delineated its projections to the amygdala; and examined the effect of electrolytic lesions of n. incertus on different stages of the fear conditioning-extinction process. N. incertus-derived nerve fibers were observed in anterior medial amygdala, endopiriform nucleus, intra-amygdala bed nucleus of stria terminalis, amygdalohippocampal transition area, and the ventromedial nucleus of the lateral amygdala, with a broad fiber band present between the basolateral amygdala and the olfactory nuclei of amygdala. In a conventional contextual fear conditioning paradigm, we compared freezing behavior in control (naïve) rats (n = 13), with that in rats after sham- or electrolytic lesions of n. incertus (n = 9/group). There were no differences between the three groups in the habituation, acquisition, or context conditioning phases; but n. incertus-lesioned rats displayed a markedly slower (delayed) extinction of conditioned freezing responses than sham/control rats; suggesting n. incertus-related circuits normally promote extinction through inhibitory projections to amygdala and prefrontal cortex. The results helps in understanding the neurobiological mechanisms involved and in development of the future biotechnological techniques to minimize the effects of disorders associated with fear in humans, such as panic, anxiety and posttraumatic stress disorder.

Key-words: nucleus incertus, defensive responses, fear conditioning, behavioral responses, amygdala.

LISTA DE ILUSTRAÇÕES

SUMÁRIO

1 INTRODUÇÃO

O núcleo incertus (NI) é um grupo de células distintas nas regiões caudoventral do núcleo periventricular pontino cinza, adjacentes à fronteira caudal do núcleo dorsal caudal tegmental. O termo "núcleo incertus" tem uma história complexa, sendo introduzido pela primeira vez em 1903 e recebendo, posteriormente, várias descrições em diferentes animais, tais como gatos, hamsters, porquinhos da Índia e ratos (CHATFIELD; LYMAN, 1954; WYSS, et al., 1979, GOTO, et al., 2001). No século passado, várias denominações também foram aplicadas à região, incluindo, "nucleus recessus pontis" e "nucleus 'O'" (OLUCHA-BORDONAU, 2003).

A utilização do termo "núcleo incertus" em referência a diferentes regiões encefálicas nas mais variadas espécies, bem como a utilização de diferentes denominações à região do NI dificultam as comparações entre trabalhos mais antigos e recentes. Como exemplo, Goto et al. (2001) cita que o NI conforme descrito pela autora e seus colaboradores foi anteriormente chamado de 'núcleo reccessus sulcos mediani" e de "parte ventromedial do núcleo dorsal tegmental" por outros autores. Em seu trabalho, Goto et al. (2001) diferenciam de forma clara duas divisões do núcleo: um grupo paramedial que foi chamado de núcleo incertus pars compacta (NIc) e uma divisão ventrolateral, com menor densidade neuronal, a pars dissipata (NId). Ambas as regiões compartilham características similares e por isso foram consideradas como partes do mesmo núcleo.

Para melhor caracterizar a região também foi necessário a realização da diferenciação dos limites do núcleo dorsal da rafe (DR) e NI, que se pode realizar a partir da diferente natureza neuroquímica, já que o DR possui natureza serotoninérgica e há presença de neurônios colecistocinina (CCK) positivos no NI, além de reatividade acetilcolinesterase positiva. Assim, os estudos anatômicos e das conexões da região do NI sistematicamente realizados pelos trabalhos de Goto et al. (2001) e Olucha-Bordonau et al. (2003) garantiram a classificação e a delimitação distinta do NI.

O mapeamento de transmissores presentes no NI começou com o trabalho de Ford et al. (1995) que mostraram a expressão do neurotransmissor GABA, no DR, que era na realidade o NI no cérebro do rato. Posteriormente, foi descrito um novo neuropeptídeo chamado relaxina-3, encontrado primeiramente no NI de rato e do camundongo (BATHGATE et al., 2002; BURAZIN et al., 2002) e co-expressado com a enzima GAD no rato (MA et al., 2007).

Os neurônios do NI expressam outros peptídeos, como a CCK e a neuromedina B (NMB) que, ao contrário da relaxina-3, são expressos em outras regiões encefálicas (KUBOTA et al., 1983, WADA et al., 1990; OLUCHA-BORDONAU et al., 2003). Neurônios da região limítrofe entre o NI e o núcleo da rafe também demonstraram uma imunoreatividade dupla para serotonina (5-HT) e relaxina-3 (TANAKA et al., 2005).

Todos os neurônios relaxina-3 no NI parecem co-expressar GABA, que são co-liberadas nos terminais, sendo que GABA atua sobre os receptores A e B produzindo inibição e a relaxina-3 atua sobre um receptor metabotrópico acoplado a proteína G, sendo, portanto, fatores na regulação gabaérgica do NI. Porém, neurônios relaxina-3 em outras regiões, como a área dorsal lateral e ventral da substância negra e o núcleo pontino da rafe, não tiveram essa particularidade caracterizada. Isso leva a crer que GABA e os peptídeos podem ser co-liberados sob várias condições fisiológicas e nos padrões diferentes em áreas diferentes do alvo, incluindo amígdala estendida e do hipocampo (MA et al., 2007).

Importante destacar, que no cérebro de ratos adultos estimou-se que o NI contém aproximadamente 2000 neurônios relaxina-3 positivos, número quatro vezes superior ao encontrado, por exemplo, na substância cinzenta periaquedutal anterior (TANAKA et al., 2005).

O primeiro estudo sistemático das conexões do NI que descreveu um sistema amplo de projeções envolvendo principalmente partes do chamado sistema límbico foi publicado por Goto et al., em 2001. Os autores concluíram à época que com base nas conexões encontradas, o NI exerceria influências significativas na modulação da atividade pré-frontal e cortical do hipocampo, na modulação de respostas motivacionais, estados de atenção e processos de aprendizagem (GOTO et al., 2001).

Dois anos depois, Olucha-Bordonau et al. (2003) destacaram o papel do NI e o seu envolvimento no controle do ritmo theta hipocampal e ritmos circadianos e observaram conexões do NI para a amígdala e núcleos supraquiasmáticos, que não foram descritos por Goto et al. (2001).

As projeções generalizadas dos neurônios do NI permitem a interação com diferentes circuitos envolvidos no controle de múltiplas funções fisiológicas, que variam de modulação de respostas ao estresse, influências sobre respostas excitatórias e a memória. A maioria da evidência experimental de estudos, atualmente derivam da ativação da atividade comportamental neural e estudos que utilizam peptídeos relaxina-3 relacionados. Muito menos evidências foram obtidas

tendo como base outras intervenções mais diretas, incluindo lesão ou inibição/ativação do NI (RYAN et al., 2011).

A pesquisa dos mecanismos neurais relacionados à formação das emoções tem crescido nos últimos anos. De acordo com Canteras (2003) isso decorre da definição dos sistemas neurais e eventos moleculares relacionados às repostas de medo condicionado obtidas a partir de condicionamento Pavloviano clássico.

Buscamos, assim, a partir da lesão do NI estudar a aquisição e extinção de memórias do medo que são processos neurais que permitem a animais e humanos o enfrentamento de desafios físicos e emocionais em um ambiente potencialmente perigoso. O foco do nosso trabalho está dentro de uma crescente e importante busca sobre os circuitos cerebrais que regulam a expressão do medo. Os resultados encontrados são o passo inicial para uma nova linha de investigação, com foco no NI, que auxiliará na compreensão dos mecanismos neurobiológicos envolvidos e no desenvolvimento futuro de técnicas terapêuticas visando minimizar os efeitos dos distúrbios associados ao medo em humanos, a exemplo do pânico, ansiedade patológica e estresse pós-traumático.

Esta tese está dividida em seis capítulos, sendo que neste apresenta-se a pesquisa e o histórico envolvido com a utilização do termo "núcleo incertus" resgatando as motivações para a realização deste trabalho.

No segundo capítulo, realizou-se a revisão da literatura acerca dos mecanismos defensivos do medo, os modelos de estudo do medo e as regiões encefálicas envolvidas no controle e modulação das respostas de medo, ou seja, a neurobiologia do medo condicionado.

No terceiro, são expostos os objetivos do nosso trabalho e no quarto capítulo apresenta-se a metodologia desenvolvida durante a pesquisa: animais utilizados nos experimentos, procedimento comportamental empregado, além de explicitar as análises histológicas e estatísticas.

No quinto capítulo são apresentados os resultados obtidos com as nossas experimentações e no sexto discute-se à luz de bibliografia recente e pertinente os resultados encontrados e sua importância dentro do contexto dos conceitos de medo condicionado.

Nas considerações finais apresentamos as principais conclusões do estudo e as implicações para futuras pesquisas.

Por fim, nos apêndices estão os artigos que foram produzidos durante nosso trabalho de pesquisa no período do doutorado.

2 REVISÃO DA LITERATURA

2.1 Medo condicionado

O medo é um comportamento originado em resposta aos perigos enfrentados pelos animais, tendo sua origem nas reações defensivas exibidas quando da exposição a estímulos ameaçadores provenientes do ambiente. A percepção desses estímulos pode ocorrer de maneira inata, independente de qualquer processo prévio, ou pode ser adquirida a partir de um processo de aprendizagem ao qual são submetidos os animais quando há uma ameaça a integridade física ou bem estar gerando um conjunto de respostas comportamentais e neurovegetativas que caracterizam a reação de defesa (LANDEIRA-FERNANDEZ, 1996; GRAEFF; BRANDÃO, 1999).

Em seu habitat natural, os animais exibem comportamentos que variam desde comportamentos agressivos a comportamentos de defesa. Blanchard e Blanchard (1988) exemplificam como o comportamento de defesa varia em relação a espécie, gênero e situação ao qual está submetido o animal no ambiente. Os autores definiram três níveis de perigo, potencial (incerto), distal e ameaça próxima, e que cada uma das formas de defesa deveria corresponder a um tipo de medo ou ansiedade, cada qual com substrato neural específico.

Em roedores, o comportamento de defesa é organizado a partir da avaliação da viabilidade de fuga e da distância entre a presa e o predador. A fuga é a resposta predominante, porém, se não houver uma distância segura para a presa empreendê-la, o congelamento, que é a ausência completa dos movimentos, será o mecanismo de defesa inicial, pois reduz a probabilidade de ser reconhecido pelo predador. Contudo, se o predador se aproxima, o congelamento é interrompido e o animal passa para um nível mais agressivo de defesa, onde utiliza saltos e mordidas na região olho-focinho do predador, para em seguida fugir (BLANCHARD; BLANCHARD, 1988).

McNaughton e Corr (2004) atualizaram os conceitos apresentados por Blanchard e Blanchard (1988) e sugeriram modificações nos níveis de defesa. Esses autores explicam a teoria segundo a qual o comportamento defensivo seria resultante da sobreposição de direção defensiva (comportamento de evitar o encontro) e da distância defensiva. Para eles, a distância defensiva operacionaliza uma definição cognitiva da intensidade da ameaça. É essa dimensão que controla o tipo de comportamento defensivo que será observado. Portanto, há diferentes níveis de defesa de acordo com as distâncias entre a presa e o predador, de modo

que em menores distâncias ocorrem ataques explosivos, em intermediárias ocorrem o congelamento e a fuga, e quando há distâncias muito grandes o comportamento defensivo desapareçe, reapareçendo um comportamento pré-ameaça.

O medo pode ser objetivamente estudado por meio de experimentos laboratoriais que analisam as respostas exibidas por animais expostos a diversas situações. Existem importantes razões pelas quais se deve estudar o comportamento do medo, pois modelos de medo são necessários para auxiliar-nos a entender como as emoções influenciam o comportamento e, além disso, experiências negativas são rapidamente aprendidas e recordadas por muito tempo pelos indivíduos, tornando o medo condicionado um excelente modelo para investigação dos processos e mecanismos subjacentes de aprendizagem e memória (FENDT; FANSELOW, 1999; LEDOUX, 2000).

O condicionamento aversivo clássico é um modelo experimental bastante utilizado e reconhecido para investigação dos mecanismos neurobiológicos do medo em diversas espécies e para o entendimento das raízes biológicas dos distúrbios associados ao medo em humanos, tais como pânico, ansiedade patológica e estresse pós-traumático. Neste modelo, durante a fase de aquisição, um estímulo sensorial neutro, chamado estímulo condicionado (EC), adquire a capacidade de obter respostas aversivas após o emparelhamento com um estímulo nocivo incondicionado (EI). Já na fase de expressão, o estímulo condicionado é apresentado sozinho e passa a provocar respostas condicionadas de medo. Esses estímulos tornam-se "avisos" de que situações ameaçadoras podem acontecer novamente (FENDT; FANSELOW, 1999; PEZZE; FELDON, 2004).

Sons, luzes, odores e estímulos táteis têm sido utilizados para o condicionamento e são chamados estímulos condicionados discretos, unimodais ou explícitos, com aplicação variando de alguns segundos a alguns minutos de duração. Na espécie humana, o medo incondicionado pode ser produzido, por exemplo, pela escuridão. Esses estímulos inicialmente neutros são associados a aversivos, particularmente aqueles que deflagram dor, causando a resposta aversiva (LANDEIRA-FERNANDEZ, 1996). O comportamento de congelamento também pode ser desencadeado por estimulação elétrica e/ou química de algumas estruturas encefálicas, como a substância cinzenta periaquedutal e os colículos inferiores (REIMER et al., 2009).

A avaliação do tempo de congelamento pode oferecer um método bastante conveniente e sensível para o estudo do medo condicionado, tendo em vista que é uma

resposta de elevado valor adaptativa, reflete medo e quaisquer alterações inesperadas no ambiente são suficientes para causar congelamento (HOFER, 1970).

O congelamento é um padrão comportamental bastante comum em ratos. De acordo com Blanchard e Blanchard (1988), quando a fuga ou ocultação é impossível, o congelamento é o único método eficaz de evitar o risco. Isto pode envolver imobilidade total ou parcial com movimentos de varredura da cabeça e vibrissas. À medida que o risco aparente diminui com o passar do tempo o animal volta a realizar a exploração do entorno para, finalmente, voltar ao comportamento normal (comer, beber, agressividade e atividade sexual). Os autores enfatizam que quando os estímulos de ameaça potencial continuam presentes, esse padrão de comportamento, exploração lenta e supressão de demais atividades, poderia continuar indefinidamente. De modo que, o congelamento, tido como a resposta mais dramática nesse padrão, é apenas a ponta do *iceberg* com referência aos comportamentos motivados pela avaliação padrão dos riscos.

Para Brandão et al. (2008) o congelamento consiste em um padrão comportamental complexo e coordenado, caracterizado pela ausência dos movimentos corporais, exceto movimentos respiratórios. Além disso, observamos um alto nível de alerta e considerável tonicidade muscular. Nessa condição ocorrem também alterações autonômicas como aceleração dos batimentos cardíacos, ritmo respiratório e pressão sanguínea periférica (HOFER, 1970).

Existe um interesse emergente na utilização do congelamento condicionado como medida de medo, pois ele constitui parte proeminente do comportamento defensivo de roedores, servindo como um indicador do nível de aprendizagem associativo entre o estímulo condicionado e o não condicionado. Além disso, inúmeras investigações têm sido conduzidas na tentativa de identificar os percursos que medeiam a expressão das respostas de medo condicionado (PARÉ et al., 2004).

2.2 Neurobiologia do Medo Condicionado

Cotidiamente fazemos avaliações acerca da segurança ou insegurança que um ambiente representa ao nosso bem estar. Sempre que percebemos um ambiente como "seguro", ocorre a ativação de mecanismos inibitórios atuando nas estruturas límbicas que controlam comportamentos de luta e/ou fuga, como as regiões lateral e dorsomedial da substância cinzenta periaquedutal. Tal mecanismo pode ser exemplificado pelas projeções

neurais do giro fusiforme e sulco temporal superior em direção ao núcleo central amigdaliano, inibindo-o. Assim, a amígdala não exerce seu papel normal, ou seja, a estimulação dessas vias na substância cinzenta periaquedutal. Por outro lado, sempre que se percebe o meio ambiente como “ameaçador”, a amígdala desencadeia estímulos excitatórios sobre a região lateral e dorsolateral da substância cinzenta periaquedutal, que então estimula as vias ventromediais, produzindo respostas de luta e/ou fuga (PORGES, 2003).

De modo que, a aquisição e a extinção das memórias provenientes do medo são processos neurais que permitem a animais e aos seres humanos enfrentar os desafios físicos e emocionais em um ambiente potencialmente perigoso. Nos mamíferos e, possivelmente, em outros vertebrados, o ponto central no cérebro de gerenciamento das informações relacionadas com o medo é a amígdala, que é um complexo formado por muitos núcleos localizados bilateralmente no lobo temporal anterior do encéfalo e na qual, foram identificadas aproximadamente 12 regiões distintas. Pesquisas demonstraram que os núcleos de maior relevância para o medo parecem ser o núcleo lateral, o núcleo basal, o núcleo basal acessório e o núcleo central, sendo os três primeiros muitas vezes agrupados para formar o complexo basolateral da amígdala (BLA) (LEDOUX, 2000).

Nader et al. (2001) demonstraram que o núcleo lateral da amígdala é o "ponto de partida" em que a informação sensorial, emocional sem sentido (estímulo condicionado, EC) adquire um valor emocional quando apresentado juntamente com um estímulo nocivo (estímulo incondicionado, EI).

Normalmente, o EC é um tom (som) e o EI é um choque nas patas que gera a resposta condicionada (RC), a qual pode ser interpretada como o nível de aquisição representado pela quantidade de tempo que o animal passa “paralisado” (congelamento) durante a apresentação dos estímulos pareados. Uma vez que os animais tenham adquirido uma RC, apenas o EC sem o EI provoca uma atenuação do desempenho da resposta condicionada. Esse fenômeno de inibição geralmente gradual é chamado extinção (VIANNA et al., 2004; CAMMAROTA et al., 2005).

A extinção é geralmente vista não como uma perda da resposta condicionada, mas como uma nova aprendizagem com base na nova associação do EC com a falta do EI. Assim, um animal que desenvolveu uma resposta condicionada ao ter somente a apresentação isolada do EC tenderá a associá-lo agora com a falta de perigo e medo e abster-se de execução do comportamento, por exemplo, de congelamento, o que gera uma nova resposta condicionada (RESCORLA, 2001).

Ao analisarmos o comportamento da extinção de maneira superficial, poderemos acreditar que o animal perdeu a memória ao final do processo de extinção e que, de alguma maneira, esta retornou novamente ao que havia antes da aquisição inicial. Inúmeros pesquisadores defendiam que o mecanismo da extinção consistia num enfraquecimento das representações formadas pela associação do EC e EI, até a quebra final dessa associação através da formação da extinção. Porém, a extinção não é um processo de esquecimento do medo adquirido e tais idéias se tornaram insustentáveis, uma vez que, muitas evidências mostram que dado um intervalo adequado entre uma sessão de extinção e os próximos, a resposta provavelmente extinta pode reaparecer (recuperação espontânea). Em realidade, grande parte dos pesquisadores sustentam que, a extinção consiste numa forma de aprendizado (RESCORLA, 2001; IZQUIERDO et al., 2004; MYERS; DAVIS, 2007).

As evidências têm demonstrado que a extinção é processada em várias áreas específicas do cérebro em diferentes conjuntos de eventos neuroquímicos, dependendo da tarefa. Sabe-se que as áreas e os mecanismos moleculares envolvidos na extinção variam de acordo com a tarefa. Nesse ponto, temos como certo que, o córtex pré-frontal ventromedial desempenha um papel fundamental na extinção de todas as tarefas estudadas até agora. Além disso, em todos os casos, a extinção requer uma expressão gênica e síntese de proteínas no início do processo, seja no córtex entorrinal, hipocampo, amígdala basolateral, ou córtex pré-frontal ventromedial, ou na totalidade ou em várias das áreas medidas, dependendo da tarefa (VIANNA et al., 2001, 2004). Isso sinaliza o fato de que a extinção implica um novo processo de aprendizagem, sobreposta ao da tarefa original e comportamentalmente maior, tendo em vista que o requisito de resposta de extinção é o oposto do anterior (CAMMAROTA et al., 2003).

Dentro desse contexto, aprioristicamente, a amígdala desempenha um papel-chave na aquisição do condicionamento e extinção da memória, enquanto que o armazenamento das memórias de extinção é realizado no córtex pré-frontal ventromedial (QUIRK; MUELLER, 2008). De modo que, a amígdala é a responsável pelas emoções relacionadas ao medo, bem como pelo reconhecimento de expressões faciais de medo e coordenação de respostas apropriadas à ameaça e ao perigo (HÖISTAD; BARBAS, 2008). Porém, a amígdala não parece estar relacionada somente ao reconhecimento de reações de medo, e sim, pode ser ativada tanto para respostas agradáveis como desagradáveis (HAMANN et al., 1999).

De acordo com Phan et al. (2002) a investigação da amígdala por meio de exames de imagem, como tomografia por emissão de pósitrons (PET) e ressonância magnética funcional

(fRMI), permitiu concluir que tal estrutura é ativada mesmo quando o indivíduo analisado não está submetido diretamente a uma situação que lhe provoque medo. Esse estudo confirmou, a partir de revisão de vários outros trabalhos, que a amígdala não é ativada apenas em processos que envolvem a sensação de medo, mas também durante situações mais positivas, como, por exemplo, durante o reconhecimento de expressões faciais de alegria, levando à conclusão de que a amígdala está envolvida na resposta a estímulos de importância emocional, independentemente de sua valência, ou seja, se o contexto é agradável ou desagradável, de modo que a amígdala responde a estímulos significativos em geral.

Inicialmente, acreditava-se que o hipotálamo exercia papel essencial entre as estruturas subcorticais relacionadas com o processamento das emoções. Porém, atualmente se reconhece que são as projeções da amígdala para o córtex que contribuem para o reconhecimento do vivenciamento do medo e outros aspectos cognitivos do processo emocional. Assim, projeções para o núcleo pontino caudal medeiam o sobressalto potencializado pelo medo; projeções para a substância cinzenta periaquedutal são importantes para as reações de congelamento e eferências para o hipotálamo lateral e bulbo medeiam respostas autonômicas (FENDT; FANSELOW, 1999; LEDOUX, 2000).

Como estrutura de ligação entre as áreas do córtex cerebral, a amígdala recebe informações de todos os sistemas sensoriais que, projetam-se para núcleos amigdalianos permitindo a integração da informação proveniente das diversas áreas do cérebro, por meio de conexões excitatórias e inibitórias a partir de vias corticais e subcorticais (GRAHAM et al., 2006; WILLIAMS et al., 2006). Os núcleos basolaterais são as principais portas de entrada da amígdala, recebendo informações sensoriais e auditivas; já a estria terminal estabelece conexão com o hipotálamo, permitindo o desencadeamento do medo. O núcleo central da amígdala é responsável pela interface com o sistema motor, conseqüentemente, lesões desse núcleo revelaram alterações na expressão das respostas ao medo condicionado (LEDOUX, 2003).

Em ratos, lesões na amígdala e na substância cinzenta periaquedutal levaram a uma diminuição do comportamento de medo eliciado pela apresentação de estímulos aversivos, demonstrando, uma vez mais, o envolvimento da amígdala com a regulação de um estado motivacional-emocional necessário para a produção ou manutenção das reações de defesa típicas de várias espécies (BLANCHARD; BLANCHARD, 1987; KIM et al., 1993).

A lesão da amígdala em humanos produz redução nas respostas emocionais e na capacidade de reconhecer o medo. Por outro lado, a estimulação da amígdala pode levar a um

estado de vigilância ou atenção aumentada, ansiedade e medo (WILLIAMS et al., 2006). Tal fato é confirmado por estudos de ressonância magnética funcional (fRMI) em humanos, nos quais, durante o condicionamento, se observou atividade da amígdala e atividade correlata no tálamo (LEDOUX, 2003).

Acredita-se que a amígdala recebe informações sobre estímulos visuais aversivos através de duas vias. Num primeiro momento, os estímulos são processados pelos núcleos intralaminares posteriores e parte medial do núcleo geniculado medial do tálamo, que transmite a informação diretamente para a amígdala. Essa transmissão rápida permite uma resposta imediata ao perigo potencial. Enquanto isso, o córtex visual, também recebe a informação do tálamo e, com maior complexidade e tempo, determina o grau de ameaça do estímulo. Dependendo do grau de aversividade, a informação é retransmitida à amígdala. Porém, se o córtex avaliar que o estímulo visual não gera risco para o organismo, uma mensagem para a amígdala irá suprimir a resposta do medo (PARÉ et al., 2004).

Além do córtex e do tálamo auditivos, áreas ventrais do hipotálamo projetam-se para os núcleos basolateral e basomedial da amígdala, havendo interferência na geração do condicionamento em casos de lesão dessas áreas (LEDOUX, 2003).

Antoniadis e McDonald (2000), através de múltiplas avaliações de medo, indicaram que a amígdala é uma estrutura que seletivamente medeia o condicionamento do ritmo cardíaco, enquanto que o hipocampo é importante na discriminação seletiva de um contexto associado ao choque, com alterações no controle da defecação e temperatura corporal, sugerindo que o hipocampo é importante ao possibilitar a discriminação entre contextos que compartilham um número de características similares. Além disso, o condicionamento de locomoção, congelamento e vocalizações ultrasônicas, exigem a participação de ambas as estruturas de memória, enquanto o condicionamento de micção não parece exigir qualquer participação do hipocampo ou amígdala. A visão proposta pelos autores atribui um papel igual no medo condicionado tanto a amígdala quanto ao hipocampo.

Tem sido sugerido que o papel do hipocampo no medo condicionado seria o de promover a transferência de uma configuração espacial do contexto para a amígdala, onde ocorreria então, a sua associação com os choques, determinando o processo de condicionamento (FENDT; FANSELOW, 1999). Lesões dessa estrutura, tanto eletrolítica quanto neuroquímica, levam a uma diminuição no condicionamento contextual de medo (FANSELOW, 2000).

Enfim, o quadro anatômico do processo de condicionamento e extinção é uma série de intrínsecas conexões da amígdala lateral, onde podemos dizer que "a aquisição emocional" começa, para a amígdala central, a qual sinaliza a resposta emocional adequada para ser executada (PITKÄNEN et al., 1997). Além disso, há ligações intrínsecas formadas por grupos de células GABAérgicas que ficam adjacentes ou entre os núcleos lateral e central. O processamento neural ao longo desta via é modulada por vários aferentes intrínsecos e extrínsecos, alguns deles derivados de dentro da amígdala.

O processamento dos sinais de condicionamento e de extinção pode ser alterada por sistemas modulatórios ascendentes do tronco cerebral. Por exemplo, a estimulação do locus coeruleus inibe neurônios da amígdala, a infusão intra-amígdala de norepinefrina melhora condicionamento de medo contextual, estimulação β-adrenérgica prejudica extinção, camundongos *knockout* para o transportador da serotonina apresentam um déficit seletivo na recordação de extinção das memórias de medo e projeções de neurônios, localizados entre o núcleo Barrington e locus coeruleus, contendo neuropeptídeo S facilita a extinção (LaLUMIERE et al., 2003; WELLMAN et al., 2007; CHEN; SARA, 2007; JUNGLING et al., 2008; DEBIEC et al., 2011; NARAYANAN et al., 2011). A distribuição da relaxina-3 dentro de regiões do tronco cerebral foi recentemente descrita em um dos nossos artigos (apêndice B).

Nossa hipótese é que o processo de condicionamento e extinção poderia ser afetado através de modulação a partir do NI do tegmento pontino. Apesar das projeções desta área para a amígdala terem sido inicialmente descritas como "escassas" estudos posteriores observaram diversas projeções para os núcleos basomedial, central, cortical, lateral, medial, basoleteral e área amidalahipocampal na amígdala. As principais áreas-alvo das aferências do NI incluem a amígdala, o septo medial e lateral, e o hipocampo ventral revelando um envolvimento putativo no controle de funções relacionadas a aspectos cognitivos e emocionais (GOTO et al., 2001; OLUCHA-BORDONAU et al., 2003).

Além disso, neurônios do NI expressam níveis elevados do receptor-1 do hormônio liberador de corticotropina (CRH-R1), consistente com a integração pelo NI de informação relacionados com estresse e sua transferência para centros cognitivos e emocionais telencefálicos. Pesquisas envolvendo camundongos *knockout* para relaxina-3 evidenciaram que esses animais exibem um fenótipo de hipoatividade circadiana especialmente durante a fase escura do ciclo biológico (BITTENCOURT; SAWCHENKO, 2000; VAN PETT et al., 2000; CANO et al., 2008; BANERJEE et al., 2010, SMITH et al., 2012).

Recentemente, também foi demonstrada uma importante participação do NI na ansiedade. Camundongos *knockout* para relaxina-3 exibiram um aumento de ansiedade no labirinto em cruz elevado em comparação com os animais controle (Watanabe et al., 2011). A partir de nosso trabalho sobre as projeções de septum (apêndice C) propomos uma explicação mecanicista para esse processo desde as projeções do septo medial para o NI e consequentemente a inibição da liberação da relaxina-3 para a amígdala ou hipocampo.

Além disso, vários estressores neurogênicos ativam o NI, como refletido pela aumento da expressão de c-Fos. Tanaka et al. (2005) submeteram ratos a uma imersão em água associado a uma imobilização que resultou numa exibição de forte indução da atividade c-fos nos neurônios relaxina-3 após 2-4h de submissão ao estressor. Contudo, a atividade de c-fos no NI pars dissipata foi menor em ratos re-expostos a um ambiente em que eles tinham experimentado exposição prévia a um gato, do que os animais não expostos (RIBEIRO-BARBOSA et al., 2005). Este resultado firma o entedimento que não é "todo e qualquer estressor psicológico" que ativará o NI, mas sim, somente ocorrerá a ativação quando o animal necessita de elevada "atividade comportamental sob uma situação estressante particular" (RYAN et al., 2011).

Além disso, o NI também possui projeções ascendentes para a rafe mediana, núcleo supramamilar, hipotálamo posterior, no septo medial, septo lateral e hipocampo, os componentes do sistema septohipocampal. Um papel proposto para o NI em modular o ritmo theta hipocampal foi apoiada por observações que estimulação elétrica do NI provocou um aumento da atividade theta do hipocampo em ratos anestesiados com uretano, e que a lesão do NI produziu ruptura da atividade theta do hipocampo induzida pela estimulação do reticularis pontis oralis (RPO), além da descrição da distribuição das projeções GABAérgicas e de relaxina-3 do NI para a região septal do rato (NUÑEZ et al., 2006; OLUCHA-BORDONAU, et al., 2012).

Importante destacar que existe uma relação estreita entre a sincronização de disparo neural na freqüência theta na amígdala e no hipocampo e o condicionamento de medo. Durante o medo relacionado à excitação emocional, os neurônios da amígdala lateral aumentam a atividade oscilatória na freqüência theta (PARÉ; COLLINS, 2000; PAPE et al., 2005). Além disso, tem sido mostrado que durante a consolidação e reconsolidação de medo condicionado, amígdala lateral e células da região CA1 do hipocampo aumentaram a sincronia entre a banda theta (SEIDENBECHER et al., 2003).

Lesting et al. (2011) afirmaram que há um “acoplamento theta”, coordenando uma rede sináptica que envolve a amígdala lateral, a região CA1 do hipocampo e a região infralímbica do córtex pré-frontal na resposta de condicionamento do medo e como todas essas áreas recebem projeções a partir de NI, temos a hipótese de que o NI desempenha um papel no controle de medo condicionado (apêndice A).

3 OBJETIVOS

3.1 Objetivo Geral:

- ✓ Determinar o envolvimento do NI na modulação da aquisição e extinção de memórias do medo;

3.2 Objetivos específicos:

- ✓ Determinar a atuação do NI, por meio de lesões eletrolíticas, sobre aquisição e extinção de memórias do medo utilizando o paradigma do medo condicionado;

- ✓ Identificar regiões alvo de projeções do NI na amígdala;

- ✓ Estabelecer novas bases sobre o conhecimento de circuitos cerebrais da expressão do medo com o envolvimento do NI.

4 MATERIAIS E MÉTODOS

4.1 Animais

Um total de 34 ratos adultos machos, da linhagem Sprague-Dawley, pesando entre 250-350gr foram utilizados neste estudo. Desse total, 3 ratos foram usados para os estudos neuroanatômicos e 31 ratos foram usados para os estudos comportamentais. Os animais foram alojados em gaiolas individuais com ciclo reverso 12:12 h claro/escuro durante 21 dias antes de iniciar os procedimentos comportamentais. Os ratos foram distribuídos aleatoriamente em grupos controle, cirurgia sem lesão ("sham"), e cirurgia com lesão eletrolítica e as cirurgias foram feitas 7 dias após a inversão do ciclo de luz.

Todos os procedimentos comportamentais de medo foram conduzidos durante a fase escura do ciclo biológico do animal. Todas as manipulações de animais foram aprovados pelo Comitê de Ética e Bem-Estar Animal da Universidade de Valência na Espanha e estavam de acordo com a normativa 86/609/CEE da Comunidade Européia relativa à proteção dos animais utilizados para fins experimentais e outros fins científicos.

4.2 Procedimentos cirúrgicos

4.2.1 Injeção do traçador neuroanatômico

Os animais foram anestesiados profundamente com ketamina 55 mg / kg (Imalgene, Merial Laboratórios SA, Barcelona, Espanha) e xilazina 20 mg / kg (Xilagesic, Laboratorios Calier, Barcelona, Espanha) e a anestesia foi mantida com isoflurano, conforme necessário. Sob controle estereotáxico, um pequeno orifício foi aberto no crânio e foi feita injeção de traçador anterógrado para o NI usando micropipetas de vidro de 40 μm (coordenadas AP -9,6 mm, ML 0 mm e DV 7,4 mm em relação ao bregma). Para o rastreamento anterógrado, usamos miniruby 15% (mR, Molecular Probes, Cat. D-3312, Paisley, Reino Unido) dissolvido em PB 0,1 M, pH 7,4. O traçador foi direcionado até a região do NI através de iontoforese pela passagem de uma corrente positiva de 1 mA, 2s em 2s, durante 15 min com um gerador de corrente modelo GC2N (Direlec, Madrid, Espanha). Após aplicação, a abertura cirúrgica foi suturada e os ratos foram injetados com buprex (0,05 mg / kg, ip, Lab Esteve, Barcelona, Espanha) para analgesia.

Em seguida, os ratos foram levados para sala de recuperação, e lá deixados por 7 dias antes do processamento adicional. Após 7 dias de sobrevivência, os ratos foram sacrificados com uma overdose de Nembutal (150 mg/kg Euthalender, ip, Normon, Barcelona, Espanha). Encéfalos foram perfundidos através de infusão transcardial de solução salina (250 ml) seguido por fixador paraformaldeído a 4% (em PB 0,1 M, pH 7,4). Após a infusão ocorreu a remoção dos encéfalos da caixa craniana e colocação no fixador durante a noite a 4 º C. No dia seguinte, os encéfalos foram transferidos para sacarose 30% em tampão PB 0,01 M pH 7,4.

4.2.2 Lesões eletrolíticas

Os ratos foram anestesiados profundamente com ketamina (Imalgene) e xilazina (Xilagesic) (55 mg / kg e 20 mg / kg, ip, respectivamente) e a anestesia foi mantida com isoflurano, quando necessário. Sob controle estereotáxico um eletrodo monopolar foi rebaixado para o interior do cérebro nas coordenadas AP -9,6 mm, ML 0 milímetros e DV -7,4 mm com relação ao bregma. Corrente positiva contínua de 1,5 mA foi aplicada durante 10s, por meio de um gerador de corrente (Cibertec, Madrid, Espanha). Cinco minutos após a lesão, o eletrodo foi removido e a ferida suturada. Os ratos foram injetados com buprex (0,05 mg / kg, ip, Lab Esteve) para analgesia pós cirurgia. Os ratos foram deixados em recuperação durante um período adicional de 15 dias antes da utilização nos procedimentos comportamentais.

4.3 Aparato e Mensuração do Congelamento

Os procedimentos comportamentais foram conduzidos num aparelho de medo condicionado contextual (Panlab, Barcelona, Espanha), composto por três gaiolas de 250 × 250 × 250 mm e um piso com uma grade com 22 hastes ligadas a um aparelho de choque e um alto-falante no teto. Em uma das laterais da parede havia uma luz suave. A gaiola onde ficaram os ratos estava dentro de um gabinete à prova de som de 600 (W) x 500 (D) x 500 (H) mm, que continha quatro lâmpadas de 9V. A bandeja que continha a grade foi suspensa sobre uma célula de carga que detectava os movimentos do animal na gaiola. Essa célula de carga transformava os movimentos dos animais em sinais elétricos que eram convertidos pelos software “Freezing” (Panlab, Espanha) em uma escala de 0-100. Após a verificação visual das

respostas, estabelecemos como congelamento sinais de movimento abaixo do nível 10 na escala por pelo menos 2 segundos.

4.4 Contextos Procedimentais utilizados

Dois tipos de contextos foram utilizados: no contexto A (aquisição), as paredes lateral e posterior da gaiola eram pretas, a parede da frente era de plexiglas, e a luz interior estava ligada (Figura 1). No contexto B (extinção), as paredes laterais e posterior possuíam tiras brancas e pretas na horizontal, vertical e diagonal e a grade do piso foi coberta com uma lâmina plexiglas branca, a luz interior era desligada e quatro tubos abertos contendo aroma de limão foram adicionados (Figura 2).

Figura 1: Aparato utilizado no contexto A (aquisição)

Figura 2: Aparato utilizado no contexto B (extinção)

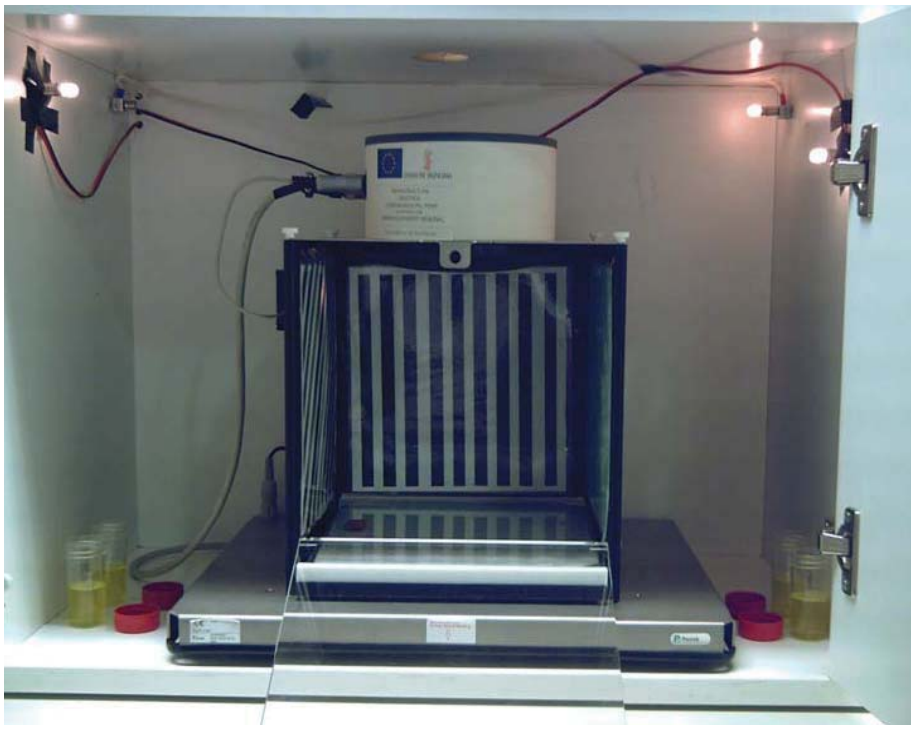

4.4.1 Procedimentos comportamentais

Todo o procedimento comportamental foi completado ao longo de 5 dias. Nos dias 1 e 2 cada rato visitou os contextos A e B por 15 minutos por sessão. No dia 3, os animais foram submetidos ao contexto da aquisição e receberam 3 pares de tom-choque no contexto A. O tom (2,8 kHz e 75 dB SPL) foi contínuo por 30s. O choque foi de 0,3 mA e 0,5s de duração e co-finalizado com o tom. Os tons e os choques foram apresentados aleatoriamente em seqüências de 180 ± 60s. No dia 4, cada animal foi novamente exposto a esses dois contextos, o contexto A, primeiramente, e duas horas mais tarde, o contexto B. No dia 5, no contexto B, os ratos receberam 5 tons de extinção (2,8 kHz e 75 db SPL) de 30s, apresentados com um atraso aleatório um do outro de 180 ± 60s e não receberam choques (Figura 3). Seguindo o procedimento, os ratos foram eutanasiados com uma overdose de Nembutal (150 mg / kg, i.p.). Encéfalos foram perfundidos através de infusão transcardíaca de solução salina (250 ml) seguido por fixador (paraformaldeído a 4% em 0,1 M PB, pH 7,4), removidos da caixa craniana, permanecendo no fixador “overnight” a 4ºC, transferidos no dia seguinte para o crioprotetor sacarose 30% em tampão PB 0,01 M, pH 7,4.

Figura 3: Paradigma utilizado nos experimentos

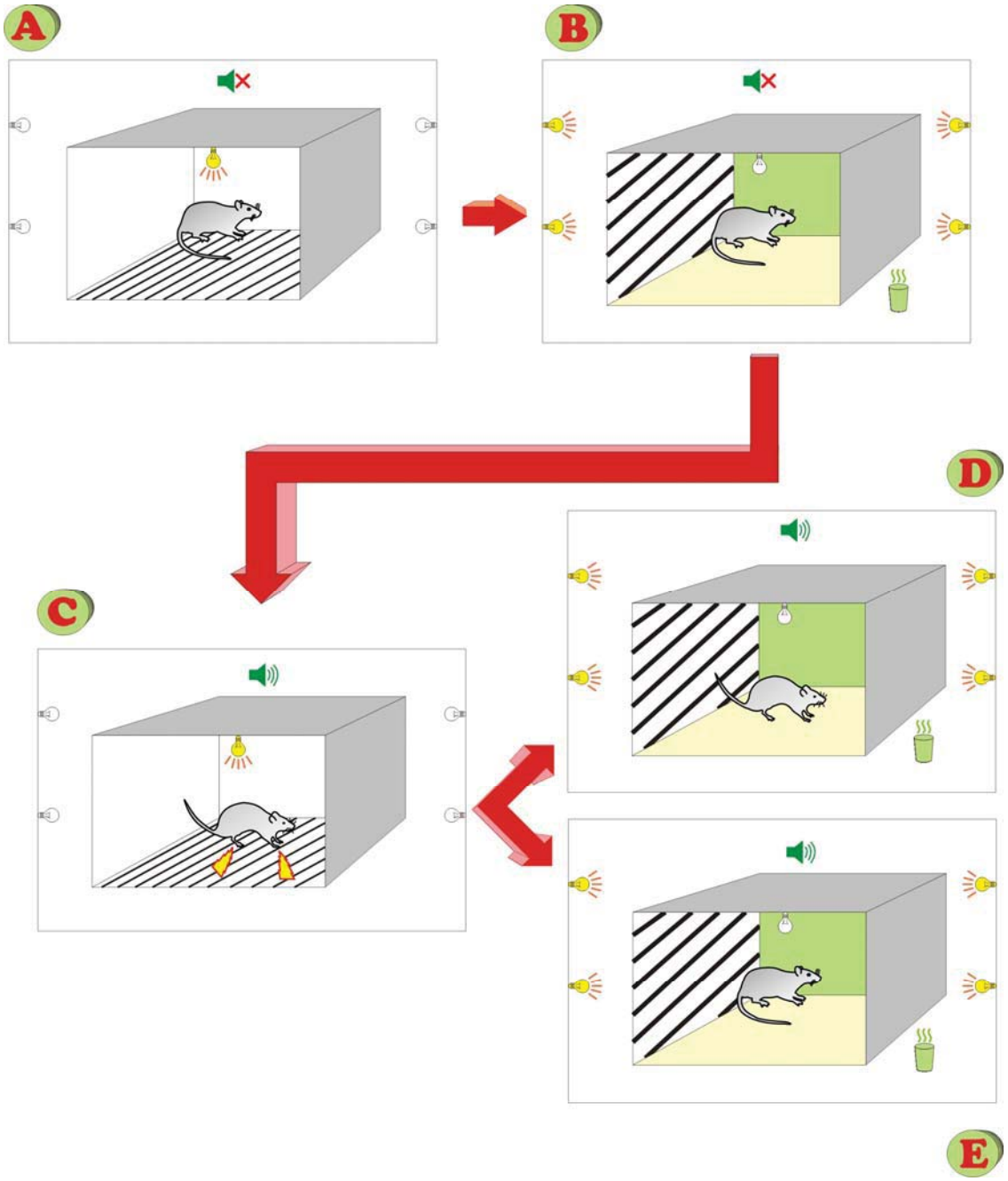

Fonte: imagem própria. Na parte superior observamos os contextos de habituação. Em "A" temos o contexto A, sem som e choque. Em "B" temos o contexto B, sem som e choque, mas com odores e superfícies revestidas. Na parte inferior, em "C" temos o contexto de condicionamento, com luz, som e choque (associado ao som) e o resultado observado em animais lesionados ("D") que não apresentam extinção, comportando-se com congelamento quando o som é novamente apresentado e animais sem lesão ("E") que comportam-se sem reação de congelamento por serem capazes de realizar o aprendizado de extinção.

4.5 Procedimentos histológicos

Encéfalos foram deixados em um tubo com crioprotetor durante 1-3 dias até depositarem-se no fundo do recipiente. Através de um criomicrótomo (Leica SM2010R, Leica Microsystems, Heidelberg, Alemanha) foram obtidos 6 séries de cortes coronais (40 μm) que foram conservados em PBS 0,01 M. Nos encéfalos de animais que tinham sido submetidos a cirurgia, utilizou-se imunohistoquímica para calretinina para determinar o grau de lesão neuronal no NI e áreas circunvizinhas. A distribuição de mR, após injeções do traçador para o NI, foi revelada utilizando o método ABC-DAB (avidina-biotinaperoxidase – diaminobenzidina) padrão.

4.5.1 Imunohistoquímica do traçador neuroanatômico

Os cortes foram lavados 2 × em TBS, transferidos para 1:100 ABC (Vectastain, Vector PK-6100, Vector Laboratories, Burlingame, CA, EUA) e incubados durante a noite a 4°C. Após lavagem (2 × TBS), o marcador foi revelado por imersão dos cortes em DAB 0,025%, sulfato de amônio e níquel 0,5%, H_2O_2 0,0024%, em Tris-HCl, pH 8,0. A reação foi interrompida após 15 min por acréscimo de TBS. Os cortes foram enxaguados (3 × PBS 0,01M, pH 7,4) e montadas em lâminas gelatinizadas, secas, desidratadas com etanol, fechadas com lamínulas e DPX.

4.5.2 Imunohistoquímica para calretinina

Os cortes foram lavados duas vezes em Tris 0,05 M tamponado com salina pH 8,0 (TBS) e transferido para solução de bloqueio (4% de "normal donkey serum" (NDS), 2% de albumina sérica bovina (BSA) e 0,2 % de Triton-X100 em TBS) durante 1 h à temperatura ambiente. Em seguida foram transferidos para meio de incubação contendo 1:2.500 "mouse anti-calretinin" (Swant, Bellinzona, Suíça), 2% NDS, 2% BSA e 0,2% Triton X100 em TBS durante 48 horas a 4ºC. A seguir foram enxaguados (2 × TBS) e transferidos para o anticorpo secundário biotinilado ("biotinylated donkey antimouse") (Jackson Laboratories, Cat. No. 715-065-150) durante 1 h. Os cortes foram então lavadas (2 × TBS) e imersos em 1:100 ABC (Vector) durante 1 h. Após a lavagem (2 × TBS), imunomarcação foi revelada por incubação

em DAB 0,025%, H_2O_2 0,0024% em tampão Tris HCl, pH 7,6. Após várias lavagens em PBS 0,01 M, os cortes foram montados em lâminas gelatinizadas, secas, desidratadas e limpas.

4.5.3 Análise histológica

Lesões e marcações anterógradas do traçador neuroanatômico foram fotografadas usando um microscópio Nikon Eclipse E600 com câmara digital DMX2000 (Nikon, Tokyo, Japão). Os mapas foram feitas com câmara clara acoplada a um microscópio Zeiss Axioskop (Zeiss, Munique, Alemanha) com objetiva 20x, digitalizado e reduzido ao tamanho final.

4.6 Análise estatística

Análise estatística utilizou two way ANOVA nos três grupos - lesão, cirurgia com lesão e cirurgia sem lesão (“sham”), usando o software GraphPad Prism. O teste de Bonferroni (post hoc) foi realizado para especificar as diferenças entre os pontos após a observação que o efeito da lesão foi significativo.

5 RESULTADOS

5.1 Projeções do NI para a amígdala

Em todos os três casos avaliados, a injeção do mR foi restrita ao NI, sem haver espalhamento para o núcleo dorsal tegmental ou o núcleo da rafe pontina (Figura 4). Fibras marcadas anterógradas entraram na amígdala a partir do prosencéfalo medial e da área subventricular. Dentro da amígdala, fibras anterogradamente marcadas foram observadas nos núcleos anterior da amígdala medial, enquanto que, em contraste, os núcleos da parte posterior da amígdala medial estavam livres de marcação. Fibras densamente concentradas estavam presentes na parte intra-amígdala do núcleo do leito da estria terminal (Figura 5). Algumas fibras também estavam dispersas em núcleos da base e da amígdala cortical e olfativa, e alguns destas fibras concentraram-se no núcleo endopiriforme, enquanto que os núcleos centrais estavam essencialmente livres de fibras marcadas. Finalmente, no complexo basolateral, fibras marcadas concentraram-se na divisão ventromedial da amígdala lateral (Figura 6).

Fig. 4: Injeção do mR no NI

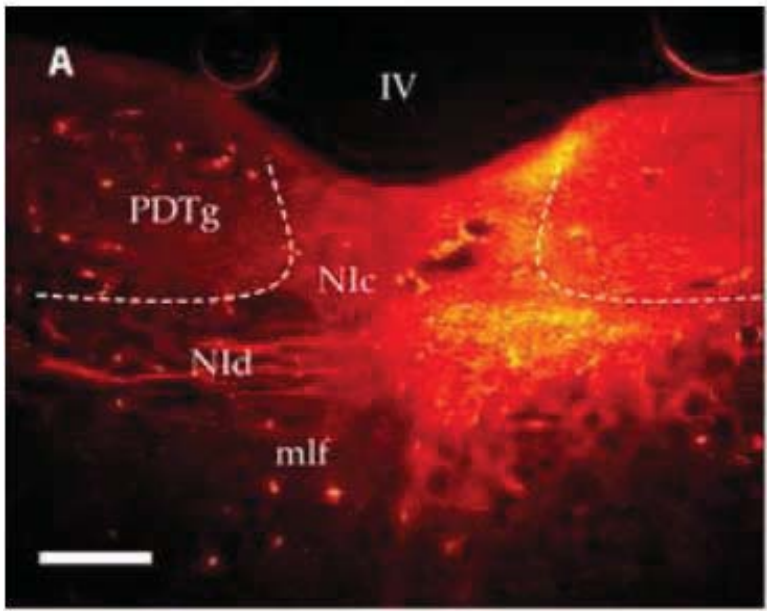

Fig. 5: Fibras marcadas na amígdala lateral ventromedial e no núcleo do leito da estria terminalis

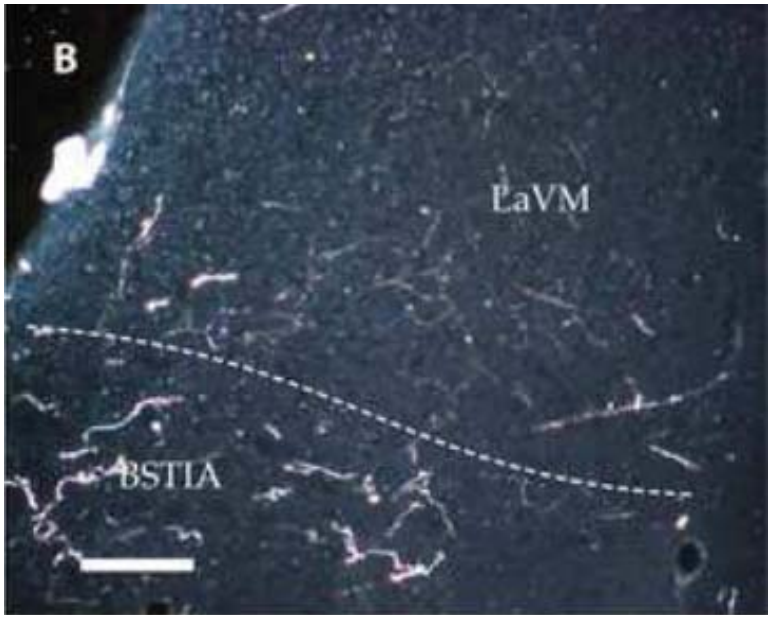

Fig. 6: Fibras marcadas nos núcleos amigdalianos

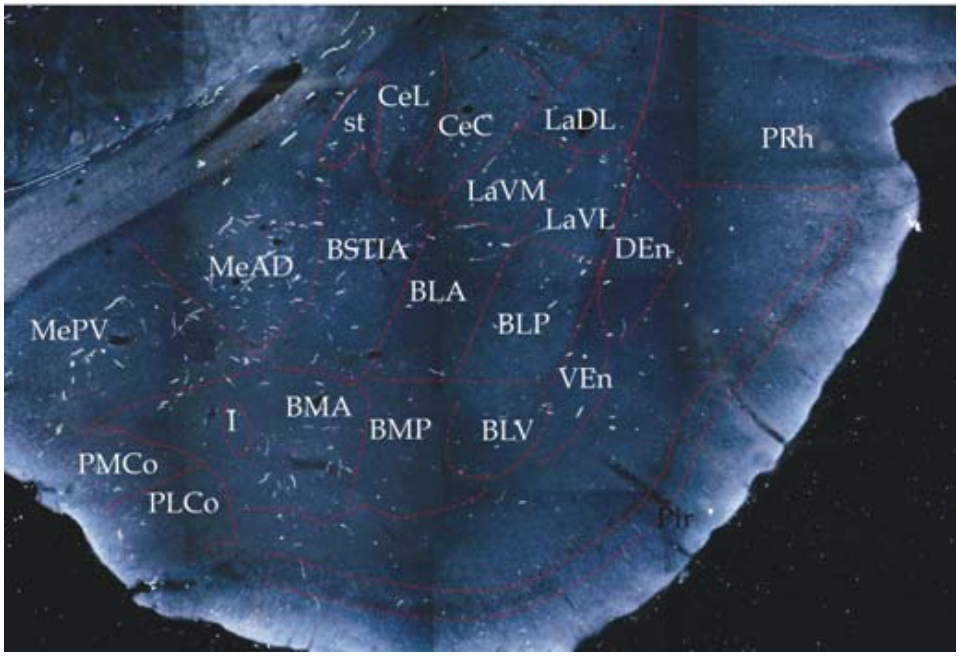

5.2 Estudos comportamentais

A extensão da lesão em cada rato estudado foi analisada por imunohistoquímica para calretinina. Em nenhum dos ratos lesionados analisados, a área danificada se espalhou para o

entorno de outros núcleos, e só algumas fibras/terminais lesionados foram observados no núcleo dorsal tegmental. Da mesma forma, não foram observadas alterações histológicas na rafe pontina, núcleo Barrington, ou locus coeruleus, apesar de alguns sinais de lesão terem sido observados no fascículo longitudinal medial que liga os núcleos envolvidos na coordenação oculomotora. Os ratos foram classificados, de acordo com a gravidade da lesão/danos ao NI como “lesionados” (perda substancial de neurônios calretinina-positivos), “operados sem lesão” (com o eletrodo colocado dorsalmente no cerebelo ou ventralmente na formação reticular) e "controle" (ratos que não foram submetidos a cirurgia) (Figura 7).

Fig. 7: Imunohistoquímica para calretinina

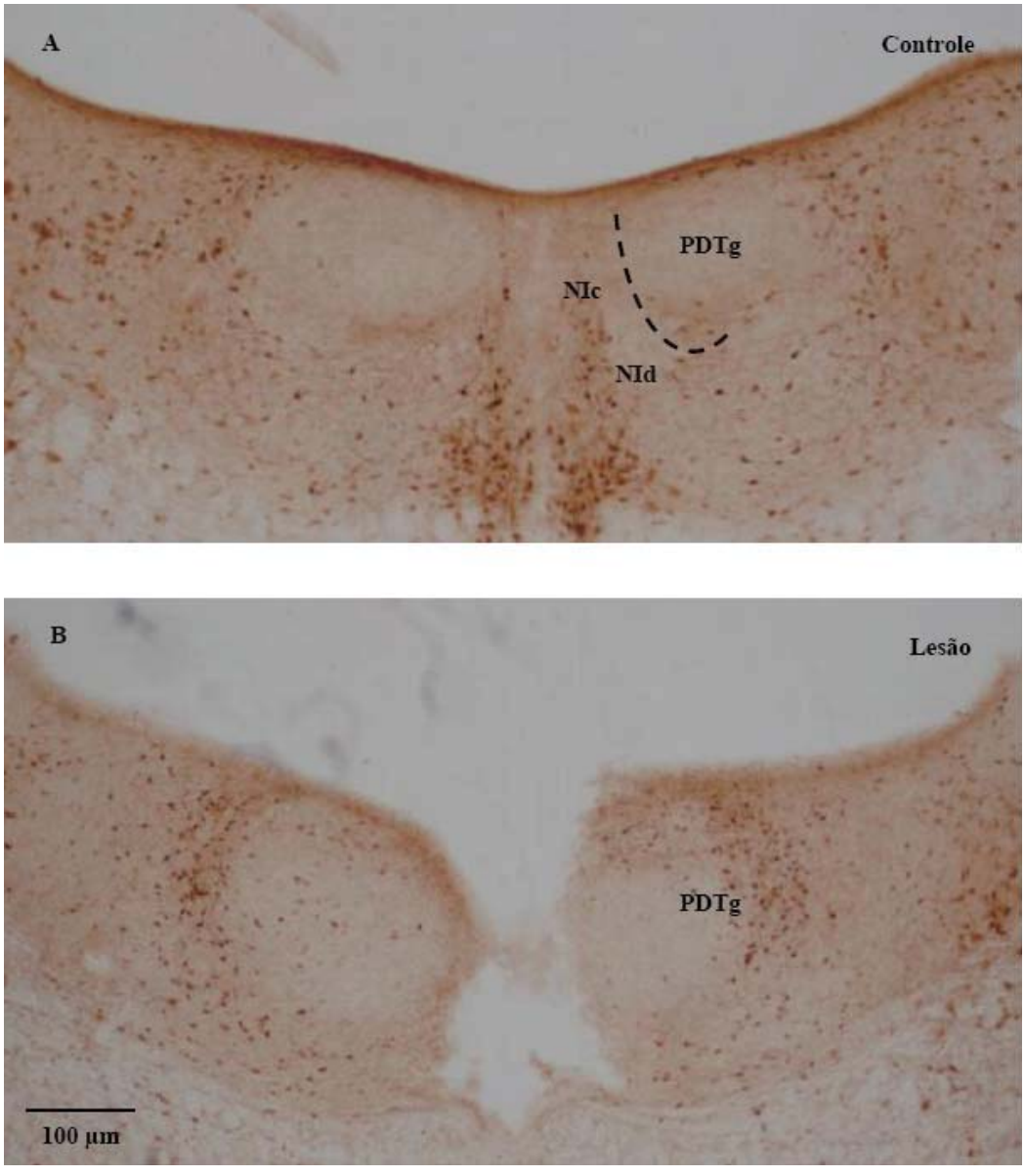

Evolução dos níveis de congelamento ocorreu durante o procedimento comportamental (Figura 8). Não houve alterações significativas no congelamento nos ensaios de habituação prévios à sessão de aquisição; não houve alterações significativas nos níveis de congelamento entre os grupos "lesionado", "operado sem lesão" e "controle" durante os ensaios de aquisição. Ratos inicialmente exibiram entre 10-20% congelamento durante o primeiro tom do emparelhamento, com uma mudança para 70-80% de congelamento durante o segundo tom do emparelhamento, e atingindo cerca de 90% durante o terceiro tom do emparelhamento. Na sessão seguinte foi avaliada a aquisição no condicionamento ao contexto. Com efeito, o nível de congelamento no contexto "A" mudou significativamente em comparação com a habituação passando para 50 - 70% durante a exposição ao mesmo contexto de habituação após a aquisição ($F(1,32) = 35,32$, $P < 0,0001$). No entanto, a lesão do NI não afetou o condicionamento ao contexto, e não houve significativas diferenças nos níveis de congelamento no contexto "B" antes e depois de aquisição em contexto A.

Fig. 8: Evolução dos níveis de congelamento

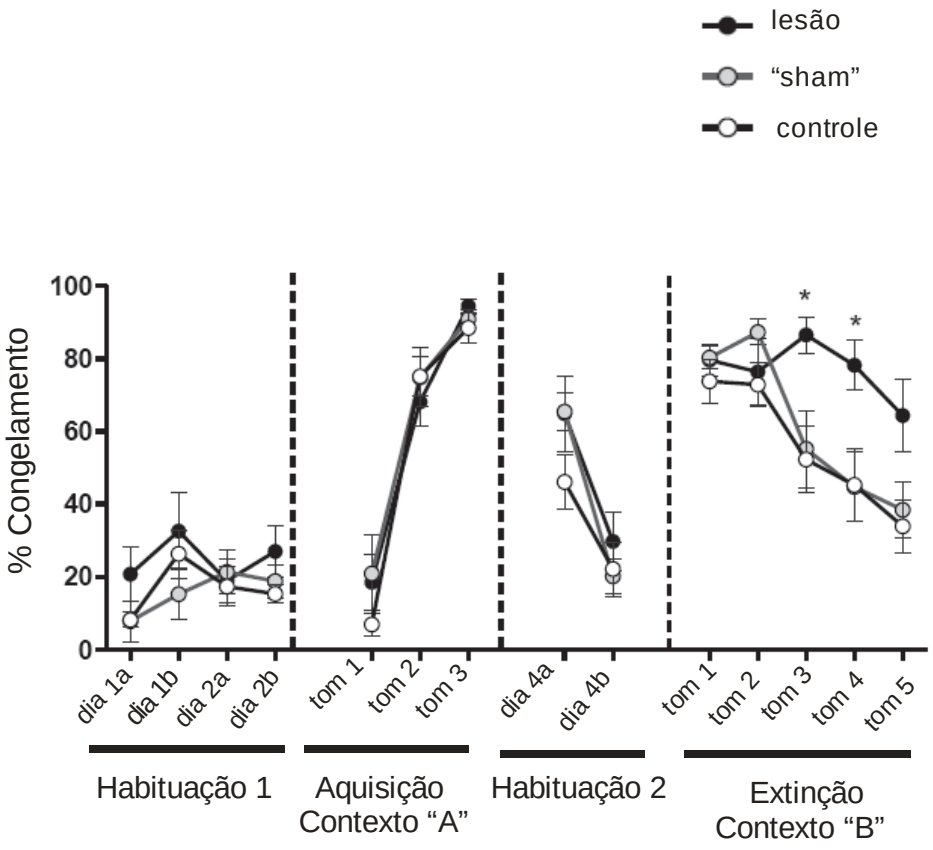

Durante os primeiros dois tons do processo de extinção não houve diferenças entre os grupos, indicando que o nível de retenção e de recuperação foi o mesmo. Entretanto, após o terceiro tom até o quinto tom, os níveis de congelamento de ratos operados sem lesão e controles foram similares, mas significativamente diferente dos ratos lesionados, que exibiram uma extinção mais lenta. ANOVA de duas vias revelou que a lesão tem um efeito significativo no tempo de congelamento ($F(2140) = 9{,}97$ $p < 0{,}0001$), e o teste de Bonferroni (post hoc) revelaram que as diferenças ocorreram após o segundo tom nos tons 3, 4 e 5 ($p < 0{,}05$) entre os animais lesionados e controle (Figura 9)

Fig. 9: Nível de "freezing" apresentado pelos animais no contexto de extinção

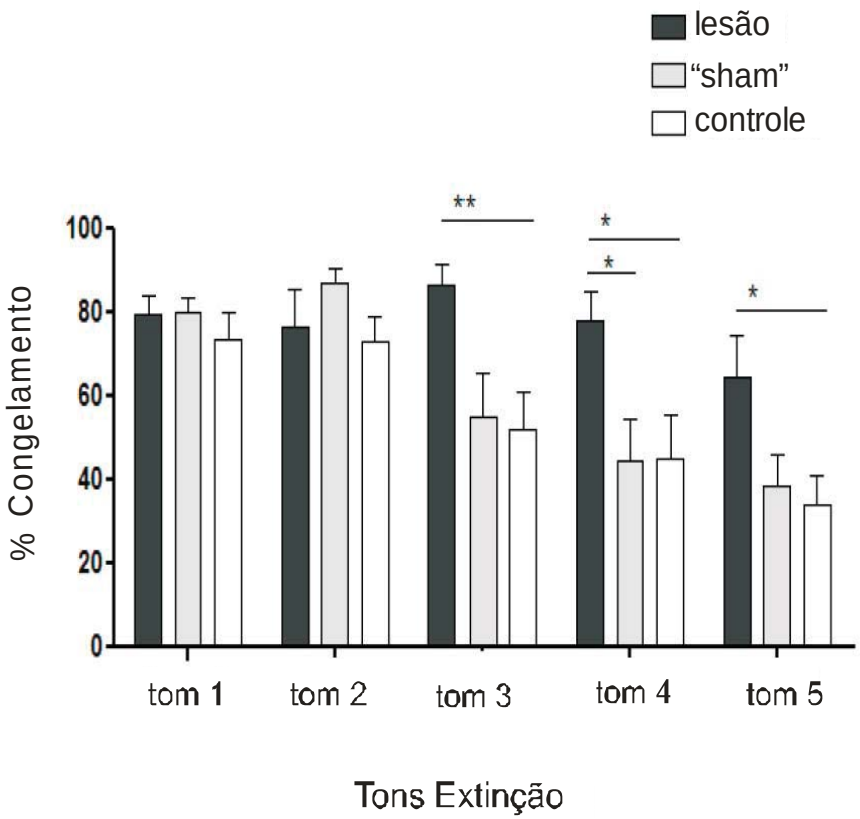

6 DISCUSSÃO

Neste estudo, utilizou-se técnicas de rastreio neurais para identificar a presença de projeções do NI dentro das estruturas da amígdala e adjacências. A presença desta inervação e outros aspectos da conectividade do NI apoiam a possibilidade de que essas projeções, em grande parte, inibitórias, possam modular os processos neurais associados com condicionamento de medo contextual. Com efeito, nós descobrimos que a lesão eletrolítica do NI, 14 dias antes de submeter ratos a um protocolo de condicionamento de medo contextual clássico, produziu um atraso específico de extinção do medo, mas não teve efeito sobre a aquisição do medo ou condicionamento ao contexto.

Os dados anatômicos encaixam com observações anteriores sobre marcação anterógrada de projeções de NI para a região da amígdala e, inclusive, ampliam essas observações (OLUCHA-BORDONAU et al., 2003). As fibras eferentes a partir do NI fazem plexos na parte intra-amigdalar do núcleo do leito da estria terminal, na área entre a amígdala olfativa e a amígdala basal e lateral, no subnúcleo ventromedial da amígdala lateral, e nos núcleos anterior e posteroventral da amígdala medial. Terminações densas também foram observadas no núcleo endopiriforme dorsal e ventral.

Já está estabelecido que a amígdala, especialmente o complexo basolateral (BLA), tem um papel crucial na aquisição e na expressão de respostas comportamentais relacionadas com o medo. Estudos mostraram que lesões na amígdala de ratos impedem a formação de memórias envolvendo medo condicionado pavloviano (SAH; LOPES DE ARMENTIA, 2003).

Adicionalmente, já foram identificados vários receptores e sistemas de sinalização intracelular na amígdala basolateral que regulam a formação da memória. De modo que, o modelo atual da extinção do medo condicionado admite a possibilidade de interação entre vários sistemas de sinalização intracelular. Resultados de estudos prévios indicam que a aquisição de extinção está associada com um aumento da fosforilação MAPK /ERK no BLA e que receptores para a bombesina/GRP no BLA estão envolvidos na consolidação da memória aversiva (ROESLER et al., 2004; HERRY et al., 2006). Outros autores indicam que a aprendizagem inibitória suposta pelo processo de extinção da memória do medo requer a ativação dos receptores NMDA dentro da amígdala basolateral e que ocorre uma plasticidade NMDA-dependente na amígdala lateral na aquisição da extinção do medo (SOTRES-BAYON et al, 2007; LAURENT et al., 2008).

Outros sistemas neuromoduladores, incluindo o sistema GABAérgico, também modulam a consolidação da memória pela regulação da liberação de norepinefrina (NE) dentro da amígdala. Evidências sugerem claramente que o GABA modula consolidação e extinção de memória de uma forma semelhante à da consolidação da memória original (BRIONI; MCGAUGH, 1988; BERLAU; MCGAUCH, 2006).

Estudos demonstraram que os neurônios no NI expressam ácido glutâmico descarboxilase (GAD) (FORD et al., 1995; OLUCHA-BORDONAU et al., 2003), consistente com a expressão do transmissor inibitório GABA por esses neurônios. Além disso, no rato, estes neurônios também expressam peptídeos, incluindo neurotensina, neuromedina B, CCK, peptídeo natriurético atrial e relaxina-3, importante neurotransmissor récem-descoberto, sugerindo que o GABA e esses peptídeos possam ser co-liberados sob várias condições fisiológicas e em diferentes padrões em áreas alvo diferentes, incluindo amígdala estendida e hipocampo. Dependendo da intensidade da atividade neuronal do NI e da distribuição dos diferentes receptores de GABA e peptídeos dentro das estruturas alvo, a transmissão GABA pode ter uma rápida e ação sináptica direta nas células alvo do NI, enquanto que os peptideos co-liberados podem ter uma via de ação mais lenta, mais dispersa em neurônios expressando concentrações elevadas de receptores em diferentes regiões da amígdala (BATHGATE et al., 2002; BURAZIN et al., 2002; MA et al., 2007).

Pesquisas atuais sugerem três principais estruturas cerebrais participantes de processos de extinção: hipocampo, amígdala e córtex pré-frontal. Já foi relatado que a consolidação da extinção do medo depende da proteína quinase ativada por mitógeno/proteína quinase regulada por sinal extracelular (MAPK/ERK) e síntese de proteínas no córtex pré-frontal medial (mPFC) e também já ficou demonstrando que a integridade do sistema interligado é importante para o processamento eficaz da extinção (PARE et al., 2004; HERRY et al., 2006; SIERRA-MERCADO et al., 2011).

No entanto, algum valor pode ser atribuída a uma estrutura particular nos aspectos específicos de extinção. Uma vez que lesões na córtex pré-frontal ventromedial não afetam a expressão da extinção, segue-se que aquisição de extinção deve ser processado a jusante das conexões pré-frontais para o núcleo central da amígdala, onde as reações de medo são elaboradas (QUIRK et al., 2000). Contudo, isto está na aparente contradição de experiências recentes em que a inativação pelo muscimol do córtex infralímbico resultou num atraso no processo de extinção, mas não teve nenhum efeito sobre a expressão de medo (SIERRA-MERCADO et al., 2011).

O córtex infralímbico induz rápida extinção através dos neurónios GABAérgicos intercalados inibitórios da amígdala, o que nos faz prever que a projeção inibitória GABAérgica a partir do NI atue sobre as funções da amígdala de uma maneira similar. Outro ponto que merece destaque são as projeções da área infralímbica do córtex pré-frontal aos núcleos intercalados da amígdala medial como parte de um circuito para a extinção do medo. Dados recentes comprovam a importância dessas projeções, uma vez que ficou comprovado, através de rastreamento anterógrado, a ligação da região infralímbica (IL) aos núcleos intercalados (ICN) por meio de projeções moderadas de IL ao ICN medial. No mesmo sentido, outro trabalho destacou a atuação do neuropeptídeo S aumentando a transmissão glutamatérgica para os neurônios GABAérgicos intercalados na amígdala (JUNGLING, et al., 2008; PINARD et al., 2012).

No que diz respeito ao efeito do lesão do NI sobre a extinção do medo, procurou-se eliminar qualquer efeito de uma lesão nas áreas circunvizinhas por apenas analisar os dados de ratos com lesões restritas ao NI e sem nenhum efeito aparente sobre as estruturas vizinhas. Nós não observamos diferenças entre os grupos controles (não-operados e não-lesionados) e lesionados no NI durante a aquisição do condicionamento do medo, ou na expressão de medo durante as etapas iniciais de extinção, indicando que a rede do NI não tem um papel importante nestes processos ou na recuperação da memória de medo. Os ratos lesionados também exibiram condicionamento normal ao contexto, bem como todos os grupos exibiram mais elevado nível de congelamento no contexto em que teve lugar condicionamento do que no contexto experimentado durante os ensaios de habituação antes da aquisição. Os padroões de congelamento exibidos pelos animais seguiram o modelo de aquisição proposto por Rescorla e Wagner (1972). Todos os ratos discriminaram bem entre os contextos, indicando que as lesões do NI não afetou a percepção e configuração do contexto.

No entanto, em resposta aos tons últimos apresentados durante a extinção, ratos com lesões do NI exibiram um maior nível de congelamento em comparação aos demais grupos, que extinguiram normalmente. Assim, concluímos que as lesões dos neurônios do NI e suas projeções prejudicam o processo de extinção, atrasando-o.

Sem nenhuma evidência explícita de uma projeção forte e direta a partir de NI para o núcleo central da amígdala, pode ser a projeção para a amígdala lateral e ventromedial que medeia este efeito. Caso contrário, os efeitos adicionais podem ser mediados por peptídeos que possuem densidades elevadas de receptores na amígdala central, através de efeitos oriundos de um volume mais lento de transmissão.

Observou-se, também, uma importante eferência do NI para a parte intra-amígdala do núcleo do leito da estria terminal, uma outra área que expressa níveis elevados de relaxina-3 e seu receptor (MA et al., 2007), mas para nosso conhecimento, uma contribuição específica desta área para o condicionamento do medo não foi descrita.

Uma consideração importante sobre a capacidade aparente do NI para modular a extinção do medo é a sua capacidade potencial para regular o disparo neuronal sincronizado entre populações de hipocampo, córtex pré-frontal e amígdala. A este respeito, trabalhos têm mostrado que a estimulação elétrica do NI induz o ritmo theta no hipocampo (NUÑEZ et al., 2006) e a estimulação do núcleo reticularis pontis oralis (RPO) resulta em sincronização entre o NI e o hipocampo (CERVERA-FERRI, et al., 2011).

Notavelmente, a sincronização neural na freqüência theta é uma característica associada com o condicionamento do medo e a atividade da amígdala lateral e área CA1 do hipocampo tornam-se sincronizadas em freqüência theta durante a consolidação e reconsolidação do medo condicionado (SEINDENBECHER et al., 2003). Além disso, a recuperação de memórias do medo aumenta acoplamento theta entre a amígdala lateral, córtex pré-frontal ventromedial e hipocampo e é reduzido durante a extinção (LESTING et al., 2011).

Em suma, descobriu-se que o NI parece ser modulador do amplo sistema neural associada com a extinção do medo e como neurônios do NI expressam altos níveis de CRH-R1 (BITTENCOURT; SAWCHENKO, 2000; VAN PETT et al., 2000), propomos que NI pode ser uma interface entre circuitos de sinalização e de estresse telencefálico envolvidos no processamento do medo. Se como aqui observado, o principal efeito de uma lesão discreta eletrolítica do NI é retardar o processo de extinção, um efeito também observado após inativação do córtex infralímbico, é possível que as ações normais de ambas vias ocorram em paralelo. Assim, o efeito da ativação infralímbica é transferida para os neurônios GABA intercalados e as projeções NI GABAérgicas podem sinalizar para os neurônios na amígdala lateral. Por sua vez, tanto neurônios GABA intercalados e da amígdala lateral projetam para neurônios do núcleo central, onde respostas comportamentais são evocadas.

Neurônios do NI expressam GABA e também sintetizam relaxina-3 e/ou CCK. Num estudo anterior demonstrou-se que a injeção de agonista de relaxina-3 receptor, R3/I5, no septo medial imita o efeito da estimulação do NI (isto é, aumenta ritmo theta hipocampal) (MA et al., 2009).

Neste estudo, foi demonstrado que NI parece participar nas redes de tronco cerebral que modulam a extinção do medo, mas o efeito específico de modulação/ativação dos transmissores diferentes dentro das populações de neurônios NI (GABA e os peptídeos, tais como a relaxina-3) sobre o processo de condicionamento do medo/extinção permanece a ser determinado.

7 CONCLUSÕES

1 – Através de técnicas de rastreio neurais ampliou-se a informação sobre as projeções do NI para a amígdala e adjacências apoiando assim, a possibilidade de que essa inervação possa modular processos neurais associados ao condicionamento do medo contextual, objeto desse estudo;

2 – A lesão eletrolítica do NI, 14 dias antes de submeter ratos a um protocolo de condicionamento de medo contextual clássico, produziu um atraso específico de extinção do medo, mas não teve efeito sobre a aquisição do medo ou condicionamento ao contexto;

3 – Esse efeito específico, de atraso na extinção do medo, pode ser oriundo da projeção do NI para a amígdala lateral e ventromedial, regiões alvos de projeções do núcleo incertus, que, então, mediariam o efeito final. Caso contrário, os efeitos adicionais podem ser mediados através de transmissores/peptídeos produzidos pelo NI que possuem densidades elevadas de receptores na amígdala central, através de efeitos oriundos de um volume mais lento de transmissão;

4 – Propõe-se que o NI pode ser uma interface entre circuitos de sinalização e de estresse telencefálico envolvidos no processamento do medo e os conhecimentos;

5 – Contudo, o efeito específico da modulação do NI sobre o processo de condicionamento do medo/extinção permanece a ser determinado.

8 REFERÊNCIAS

ANTONIADIS, E.A.; MCDONALD, R.J. Amygdala, hippocampus, and discrimination fear conditioning to context. **Behavioural Brain Research**, v. 109, n. 1, p. 141-142, 2000.

BANERJEE, A.; SHEN, P.J.; MA, S.; BATHGATE, R.A.; GUNDLACH, A.L. Swim stress excitation of nucleus incertus and rapid induction of relaxin-3 expression via CRF1 activation. **Neuropharmacology**, v.58, p.145-155, 2010.

BERLAU, D.J.; MCGAUGH, J.L. Enhancement of extinction memory consolidation: The role of the noradrenergic and GABAergic systems within the basolateral amygdala. **Neurobiology of Learning and Memory.** v. 86, p. 123-132, 2006.

BATHGATE, R.; SAMUEL, C.; BURAZIN, T.; LAYFIELD, S.; CLAASZ, A.; REYTOMAS, I.; DAWSON, N.; ZHAO, C.; BOND, C.; SUMMERS, R.; PARRY, L.J.; WADE, J.D.; TREGEAR, G.W. Human relaxin gene 3 (H3) and the equivalent mouse relaxin (M3) gene. **The Journal of Biological Chemestry**, v. 277, p. 1148–1157, 2002.

BLANCHARD, R. J.; BLANCHARD, D.C. An ethoexperimental approach to the study of fear. **The Psychological Record**, v. 37, n. 3, p. 305-316, 1987.

BLANCHARD, D.C.; BLANCHARD, R.J. Ethoexperimental Approaches to The Biology of Emotion. **Annu. Rev. Psychol,** v. 39, p. 43-68, 1988.

BITTENCOURT, J.C., SAWCHENKO, P.E. Do centrally administered neuropeptides access cognate receptors?: an analysis in the central corticotropin-releasing factor system. **The Journal of Neuroscience**, v. 20, p.1142-1156, 2000.

BRANDÃO, M.L.; ZANOVELI, J.M.; RUIZ MARTINEZ, R.C.; OLIVEIRA, L.C.; LANDEIRA-FERNANDEZ, J. Different patterns of freezing behavior organized in the periaqueductal gray of rats: association with different type of anxiety. **Behavioral and Brain Research**, v. 188, p.1-13, 2008.

BRIONI, J. D.; MCGAUGH, J. L. Post-training administration of GABAergic antagonists enhances retention of aversively motivated tasks. **Psychopharmacology**, v. 96, p. 505–510, 1988.

BURAZIN, T.; BATHGATE, R.; MACRIS, M.; LAYFIELD, S.; GUNDLACH, A.; TREGEAR, G.W. Restricted, but abundant, expression of the novel gene-3 (R3) relaxin in the dorsal tegmental region of brain. **Journal of Neurochemestry**, v. 82, p.1553–1557, 2002.

CAMMAROTA, M.; BEVILAQUA, L.R.M; KERR, D.S.; Medina, J.H; IZQUIERDO, I. Inhibition of mRNA and protein synthesis in the CA1 region of the dorsal hippocampus blocks reinstallment of an extinguished conditioned fear response. **The Journal of Neuroscience**, v. 23, n. 3, p. 737-741, 2003.

CAMMAROTA, M.; BEVILAQUA, L.R.; ROSSATO, J.I.; RAMIREZ, M.R.; MEDINA, J.H.; IZQUIERDO, I. Relationship between short and long-term memory and short- and long-term extinction. **Neurobiology of Learning and Memory**, v. 84, n. 1, p. 25-32, 2005.

CANO, G.; MOCHIZUKI, T.; SAPER, C.B. Neural circuitry of stress-induced insomnia in rats. **The Journal of Neuroscience**, v. 28, p. 10167-10184, 2008.

CANTERAS, N.S. Análise crítica dos sistemas neurais envolvidos nas respostas de medo inato. **Rev. Bras. Psiquiatr**. v. 25, sup. 2, 2003.

CERVERA-FERRI, A.; GUERRERO-MARTÍNEZ, J.; BATALLER-MOMPEÁN, M.; TABERNER-CORTES, A.; MARTÍNEZ-RICÓS,J.; RUIZ-TORNER, A.; TERUEL-MARTÍ, V. Theta synchronization between the hippocampus and the nucleus incertus in urethane-anesthetized rats. **Experimental Brain Research**. v. 211, n. 2, p. 177-192. 2011.

CHATFIELD, P.O.; LYMAN, C.P. An unusual structure in the floor of the fourth ventricle of the golden hamster (*Mesocricetus auratus*). **The Journal of Comparative Neurology**, v. 101, p. 225–235, 1954. Article first published online: 8 oct 2004.

CHEN, F.J.; SARA, S.J. Locus coeruleus activation by foot shock or electrical stimulation inhibits amygdala neurons. **Neuroscience**, v. 144, p. 472-481, 2007.

DEBIEC, J.; BUSH, D.E.; LEDOUX, J.E. Noradrenergic enhancement of reconsolidation in the amygdale impairs extinction of conditioned fear in rats--a possible mechanism for the persistence of traumatic memories in PTSD. **Depress Anxiety**, v. 28, p. 186-193, 2011.

FANSELOW, M.S. Contextual fear, gestalt memories, and the hippocampus. **Behavioural Brain Research,** v. 110, p. 73– 81, 2000.

FENDT, M.; FANSELOW, M.S. The neuroanatomical and neurochemical basis of conditioned fear. **Neuroscience and Biobehavioral Reviews,** v. 23, p. 743-760, 1999.

FORD, B.; HOLMES, C.J.; MAINVILLE, L.; JONES, B.E. GABAergic neurons in the rat pontomesencephalic tegmentum: codistribution with cholinergic and other tegmental neurons projecting to posterior lateral hypothalamus. **The Journal of Comparative Neurology,** v. 363, p. 177–196, 1995.

GOTO, M.; SWANSON, L.W.; CANTERAS, N.S. Connections of the nucleus incertus. **The Journal of Comparative Neurology**, v. 438, p. 86-122, 2001.

GRAEFF, F.G.; BRANDÃO, M.L. **Neurobiologia das Doenças Mentais.** 4. Edição. São Paulo: Editora Lemos, 1999, 188 p.

GRAHAM, R.; DEVINSKY, O.; LABAR, K.S. Quantifying deficits in the perception of fear and anger in morphed facial expressions after bilateral amygdala damage. **Neuropsychology,** v. 45, n. 1, p.42–54, 2006.

HAMANN, S. B.; ELY, T. D.; GRAFTON, S. T.; KILTS, C. D. Amygdala activity related to enhanced memory for pleasant and aversive stimuli. **Nature Neuroscience**, v.2, p. 289–293, 1999.

HERRY, C.; TRIFILIEFF, P.; MICHEAU, J.; LÜTHI, A.; MONS, N. Extinction of auditory fear conditioning requires MAPK/ERK activation in the basolateral amygdale. **European Journal of Neuroscience**, v. 24, n. 1, p. 261–269, 2006.

HOFER, M.A. Cardiac and respiratory function during sudden prolonged immobility in wild rodents. **Psychonomic Medicine,** v. 32, n. 6, p. 633-647, 1970.

HÖISTAD, M.; BARBAS, H. Sequence of information processing for emotions through pathways linking temporal and insular cortices with the amygdala. **Neuroimage**. v. 40 , n. 3, p. 1016-33, 2008.

IZQUIERDO, I.; CAMMAROTA, MARTÍN ; MEDINA, J.H.; BEVILAQUA, L.R.M Pharmacological findings on the biochemical bases of memory processes: A general view. **Journal of Neural Transplantation & Plasticity**, v. 11, p. 159-189, 2004.

JUNGLING, K.; SEIDENBECHER, T.; SOSULINA, L.; LESTING, J.; SANGHA, S.; CLARK, S.D.; OKAMURA, N.; DUANGDAO, D.M.; XU, Y.L.; REINSCHEID, R.K.; PAPE, H.C. Neuropeptide S-mediated control of fear expression and extinction: role of intercalated GABAergic neurons in the amygdala. **Neuron**, v. 59, p. 298-310, 2008.

KIM, J. J.; RISON, R. A.; FANSELOW, M. S. Effects of amygdala, hippocampus, and periaqueductal gray lesions on short- and long-term contextual fear. **Behavioral Neuroscience,** v. 107, n. 6, p. 1-6, 1993.

KUBOTA, Y.; INAGAKI, S.; SHIOSAKA, S.; CHO, H.J.; TATEISHI, K.; HASHIMURA, E.; HAMAOKA, T.; TOHYAMA, M. The distribution of cholecystokinin octapeptide-like structures in the lower brain stem of the rat: an immunohistochemical analysis. **Neuroscience** v. 9, p. 587–604, 1983.

LaLUMIERE, R.T.; BUEN, T.V.; MCGAUGH, J.L. Post-training intra-basolateral amygdala infusions of norepinephrine enhance consolidation of memory for contextual fear conditioning. **The Journal of Neuroscience,** v. 23, p. 6754-6758, 2003.

LANDEIRA-FERNANDEZ, J. Pavlovian context conditioning. **Brazilian Journal of Medical and Biological Research**, v. 29, p. 149-173, 1996.

LAURENT, V.; MARCHAND, A.R.; WESTBROOK, R.F. The basolateral amygdala is necessary for learning but not relearning extinction of context conditioned fear. **Learn. Mem.** v.15, p. 304-314, 2008.

LEDOUX, J.E. Emotion circuits in the brain. **Annu Rev Neurosci**, v. 23, p. 155-184, 2000.

LEDOUX, J.E. The Emotional Brain, Fear and the Amygdala. **Cellular and Molecular Neurobiology**, v. 23, n. 4/5, 2003.

LESTING, J.; NARAYANAN, R.T.; KLUGE, C.; SANGHA, S.; SEIDENBECHER, T.; PAPE, H.C. Patterns of Coupled Theta Activity in Amygdala-Hippocampal-Prefrontal Cortical Circuits during Fear Extinction. **PLoS One**, v. 6, n.6, e21714, 2011.

MA, S.; BONAVENTURE, P.; FERRARO, T.; SHEN, P.J.; BURAZIN, T.C.; BATHGATE, R.A.; LIU, C.; TREGEAR, G.W.; SUTTON, S.W.; GUNDLACH, A.L. Relaxin-3 in GABA projection neurons of nucleus incertus suggests widespread influence on forebrain circuits via G-protein-coupled receptor-135 in the rat. **Neuroscience**, v. 144, p. 165-190, 2007.

MA, S.; OLUCHA-BORDONAU, F.E.; HOSSAIN, M.A.; LIN, F.; KUEI, C.; LIU, C.; WADE, J.D.; SUTTON, S.W.; NUÑEZ, A.; GUNDLACH, A.L. Modulation of hippocampal theta oscillations and spatial memory by relaxin-3 neurons of the nucleus incertus. **Learn. Mem.** v. 16, p. 730-742, 2009.

MCNAUGHTON, N.; CORR, P.J. A two-dimensional neuropsychology of defense: fear/anxiety and defensive distance. **Neuroscience Biobehavioral Reviews**, v. 28, p. 285–305, 2004.

MYERS, K.M.; DAVIS, M. Mechanisms of fear extinction. **Molecular Psychiatry**, v. 12, p. 120–150, 2007.

NADER, K.; MAJIDISHAD, P.; AMORAPANTH, P.; LEDOUX, J.E. Damage to the lateral and central, but not other, amygdaloid nuclei prevents the acquisition of auditory fear conditioning. **Learning and Memory**, v. 8, n. 3, p. 156-163, 2001.

NARAYANAN V, HEIMING RS, JANSEN F, LESTING J, SACHSER N, PAPE HC, SEIDENBECHER T. Social Defeat: Impact on Fear Extinction and Amygdala-Prefrontal Cortical Theta Synchrony in 5-HTT Deficient Mice. **PLoS One**, v. 6, n. 6, e22600, 2011.

NUÑEZ A, CERVERA-FERRI A, OLUCHA-BORDONAU F, RUIZ-TORNER A, TERUEL V. Nucleus incertus contribution to hippocampal theta rhythm generation. **European Journal Neuroscience**, v. 23, p. 2731-2738, 2006.

OLUCHA-BORDONAU, F.E.; TERUEL, V.; BARCIA-GONZALEZ, J.; RUIZ-TORNER, A.; VALVERDE-NAVARRO, A.A.; MARTINEZ-SORIANO, F. Cytoarchitecture and efferent projections of the nucleus incertus of the rat. **The Journal of Comparative Neurology**, v. 464, p. 62-97, 2003.

OLUCHA-BORDONAU, F.E.; OTERO-GARCÍA, M.; SÁNCHEZ-PÉREZ, A.M.; NÚÑEZ, A.; MA, S. GUNDLACH, A.L.; Distribution and targets of the relaxin-3 innervation of the septal area in the rat. **The Journal of Comparative Neurology,** v. 520, n. 9, p. 1903–1939, 2012.

PAPE, H,C.; NARAYANAN, R.T.; SMID, J.; STORK, O.; SEIDENBECHER, T. Theta activity in neurons and networks of the amygdala related to long-term fear memory. **Hippocampus**, v. 15, p. 874-880, 2005.

PARÉ, D.; COLLINS, D.R. Neuronal correlates of fear in the lateral amygdala: multiple extracellular recordings in conscious cats. **The Journal of Neuroscience**, v. 20, p. 2701-2710, 2000.

PARÉ, D.; QUIRK, G.J.; LEDOUX, J.E. New vistas on amygdale networks in conditioned fear. **Journal of Neurophysiology,** v. 92, p. 1-9, 2004.

PHAN, K.L.; WAGER, T.; TAYLOR, S.F.; LIBERZON,I. Functional Neuroanatomy of Emotion: A Meta-Analysis of Emotion Activation Studies in PET and fMRI , **Neuroimage**, v. 16, n. 2, p. 331–348, 2002.

PINARD, C.R.; MASCAGNI, F.; MCDONALD, A. J. Medial prefrontal cortical innervation of the intercalated nuclear region of the amygdala. **Neuroscience**, v. 205, p. 112–124, 2012.

PEZZE, M.A.; FELDON, J. Mesolimbic dopaminergic pathways in fear conditioning. **Progress in Neurobiology,** v.74, p. 301-320, 2004.

PITKÄNEN, A.; SAVANDER, V.; LEDOUX, J.E. Organization of intra-amygdaloid circuitries in the rat: an emerging framework for understanding functions of the amygdala. **Trends Neuroscience**, v. 20, p. 517–523, 1997.

QUIRK, G.J.; RUSSO, G.K.; BARRON, J.L.; LEBRON, K. The Role of Ventromedial Prefrontal Cortex in the Recovery of Extinguished Fear. **The Journal of Neuroscience**, v. 20, n. 16, p. 6225–6231, 2000.

QUIRK, G.J.; MUELLER, D. Neural mechanisms of extinction learning and retrieval. **Neuropsychopharmacology**, v. 33, p. 56-72, 2008.

PORGES, S.W. Social engagement and attachement: a phylogenetic perspective. **Ann NY Acad Sci**, v.1008, p.31-47, 2003.

REIMER, A. E.; OLIVEIRA, A.R.de; BRANDAO, M.L. Involvement of GABAergic mechanisms of the dorsal periaqueductal gray and inferior colliculus on unconditioned fear. **Psychol. Neurosci. (Online)**, Rio de Janeiro, v. 2, n. 1, 2009. Disponível em: <http://www.scielo.br/scielo.php?script=sci_arttext&pid=S1983-32882009000100008&lng=en&nrm=iso>. Accesso em:19 Out 2011.

RESCORLA, R.A.; WAGNER, A.R. A theory of Pavlovian conditioning: Variations in the effectiveness of reinforcement and nonreinforcement, In: Black, A.H.; Prokasy, W.F. editor. Classical Conditioning II: Appleton-Century-Crofts, p. 64-99, 1972.

RESCORLA, R.A. Retraining of extinguished Pavlovian stimuli. **Journal of Experimental Psychology: Animal Behavior Processes** v. 27, n. 2, p. 115-124, 2001.

RIBEIRO-BARBOSA, E.R.; CANTERAS, N.S.; CEZARIO, A.F.; BLANCHARD, R.J.; BLANCHARD, D.C. An alternative experimental procedure for studying predator-related defensive responses. **Neuroscience and Biobehavioral Reviews,** v. 29, p. 1255–1263, 2005.

RYAN, P.J.; MA, S.; OLUCHA-BORDONAU, F.E.; GUNDLACH, A.L. Nucleus incertus-An emerging modulatory role in arousal, stress and memory. **Neuroscience and Biobehavioral Reviews**, v. 35, p. 1326-1341, 2011.

ROESLER, R.; LESSA, D.; VENTURELLA, R.; VIANNA, M.R.M.; LUFT, T.; HENRIQUES, J.A.P.;IZQUIERO, I.; SCHWARSTSMANN, G. Bombesin/gastrin-releasing peptide receptors in the basolateral amygdala regulate memory consolidation. **European Journal of Neuroscience**, v. 19, n.4, p. 1041-1045, 2004.

SAH, P.; LOPEZ DE ARMENTIA, M. Excitatory synaptic transmission in the lateral and central amygdala. **Ann NY Acad Sci**. v. 985, p. 67-77, 2003.

SEIDENBECHER, T.; LAXMI, T.R.; STORK, O.; PAPE, H.C. Amygdalar and hippocampal theta rhythm synchronization during fear memory retrieval. **Science**, v. 301, p. 846-850, 2003.

SIERRA-MERCADO, D.; PADILLA-COREANO, N.; QUIRK, G.J.; Dissociable roles of prelimbic and infralimbic cortices, ventral hippocampus, and basolateral amygdala in the expression and extinction of conditioned fear. **Neuropsychopharmacology,** v. 36, n. 2, p. 529-538, 2011.

SMITH, C.M.; HOSKEN, I.T.; SUTTON, S.W.; LAWRENCE, A.J; GUNDLACH, A.L Relaxin-3 null mutation mice display a circadian hypoactivity phenotype. **Genes Brain Behav**. v. 11, n. 1, p. 94-104, 2012.

SOTRES-BAYON, F.; BUSH, D.E.; LEDOUX, J.E. Acquisition of fear extinction requires activation of NR2B-containing NMDA receptors in the lateral amygdala. **Neuropsychopharmacology**. v. 32, n. 9, p. 1929-1940, 2007.

VIANNA, M.R.; SZAPIRO, G., MCGAUGH, J.L.; MEDINA, J.H.; IZQUIERDO, I. Retrieval of memory for fear motivated training initiates extinction requiring protein synthesis in the rat hippocampus. **Proc Natl Acad Sci**, v. 98, p.12251-12254, 2001.

VIANNA, M.R.; COITINHO, A.S.; IZQUIERDO, I. Role of the hippocampus and amygdala in the extinction of fear-motivated learning. **Current Neurovascular Research**, v. 1, n. 1, p. 55-60, 2004.

VAN PETT, K.; VIAU, V.; BITTENCOURT, J.C; CHAN, R.K.; LI, H.Y.; ARIAS, C.; PRINS, G.S.; PERRIN, M.; VALE, W.; SAWCHENKO, P.E. Distribution of mRNAs encoding CRF receptors in brain and pituitary of rat and mouse. **The Journal of Comparative Neurology**, v. 428, p.191-212, 2000.

TANAKA, M.; IIJIMA, N.; MIYAMOTO, Y.; FUKUSUMI, S.; ITOH, Y.; OZAWA, H.; IBATA, Y. Neurons expressing relaxin 3/INSL 7 in the nucleus incertus respond to stress. **European Journal Neuroscience**, v. 21,p. 1659-1670, 2005.

WADA, E.; WAY, J.; LEBACQ-VERHEYDEN, A.M.; BATTEY, J.F. Neuromedin B and gastrin-releasing peptide mRNAs are differentially distributed in the rat nervous system. **The Journal of Neuroscience**. v. 10, n. 9, p. 2917-2930, 1990.

WATANABE Y, TSUJIMURA A, TAKAO K, NISHI K, ITO Y, YASUHARA Y, NAKATOMI Y, YOKOYAMA C, FUKUI K, MIYAKAWA T, TANAKA M. Relaxin-3-deficient mice showed slight alteration in anxiety-related behavior. **Frontiers in Behavioral Neuroscience,** v. 5, 50, p. 1-11, 2011.

WELLMAN, C.L.; IZQUIERDO, A.; GARRETT, J.E.; MARTIN, K.P.; CARROLL, J.; MILLSTEIN, R.; LESCH, K.P.; MURPHY, D.L.; HOLMES, A. Impaired stress-coping and fear extinction and abnormal corticolimbic morphology in serotonin transporter knock-out mice. **The Journal of Neuroscience**, v. 27, p. 684-691, 2007.

WILLIAMS, L.M.; DAS, P.; LIDDELL, B.J.; KEMP, A.H.; RENNIE, C.J.; GORDON, E. Mode of functional connectivity in amygdala pathways dissociates level of awarwness for signals of fear. **The Journal of Neuroscience,** v.26, n. 36, p. 9264-9271, 2006.

WYSS, J.M.; SWANSON, L.W.; COWAN, W.M. A study of subcortical afferents to the hippocampal formation in the rat. **Neuroscience**, v. 4, n. 4, 1979, p. 463–476 Available online 17 March 2003.

APÊNDICE A

ELECTROLYTIC LESION OF THE NUCLEUS INCERTUS AND ITS ASCENDING PROJECTIONS RETARDS EXTINCTION OF CONDITIONED FEAR

PEREIRA, C.W.; SANTOS, F.N.; SÁNCHEZ-PÉREZ, A.M.; OTERO-GARCÍA, M.; MARCHIORO, M.; MA, S.K.; GUNDLACH, A.L.; OLUCHA-BORDONAU, F.E.

Observação: Os dados do artigo apresentado neste anexo da Tese são os mostrados nas figuras 4, 5,7, 8 e 9.

Elsevier Editorial System(tm) for Behavioural Brain Research
Manuscript Draft

Manuscript Number:

Title: Electrolytic lesion of the nucleus incertus and its ascending projections retards extinction of conditioned fear

Article Type: Research Reports

Keywords: Amygdala
Electrolytic lesion
Extinction
Fear memory
Neural tract-tracing
Nucleus incertus
Emotion

Corresponding Author: Mr Francisco E Olucha-Bordonau, PhD

Corresponding Author's Institution: Universitat de València

First Author: Celia W Pereira, PhD student

Order of Authors: Celia W Pereira, PhD student; Fabio N Santos, PhD student; Ana M Sánchez-Pérez, PhD; Marcos Otero-García, PhD student; Murilo Marchioro, PhD; Sherie K Ma, PhD; Andrew L Gundlach, PhD; Francisco E Olucha-Bordonau, PhD

Abstract: Fear memory helps animals and humans recognize putative sources of danger and adopt the appropriate behavioral response. The primary neural circuits for fear acquisition and extinction involve connections between prefrontal cortex, ventral hippocampus and amygdala, and these areas are modulated by brainstem networks. The nucleus (n.) incertus in the dorsal pontine tegmentum provides a strong GABAergic projection to these forebrain centers and is strongly activated by neurogenic stressors. In this study in male, adult rats, we injected miniruby anterograde tracer into n. incertus and delineated its projections to the amygdala; and examined the effect of electrolytic lesions of n. incertus on different stages of the fear conditioning-extinction process. N. incertus-derived nerve fibers were observed in anterior medial amygdala, endopiriform nucleus, intra-amygdala bed nucleus of stria terminalis, amygdalohippocampal transition area, and the ventromedial nucleus of the lateral amygdala, with a broad fiber band present between the basolateral amygdala and the olfactory nuclei of amygdala. In a conventional contextual fear conditioning paradigm, we compared freezing behavior in control (naïve) rats (n = 13), with that in rats after sham- or electrolytic lesions of n. incertus (n = 9/group). There were no differences between the three groups in the habituation, acquisition, or context conditioning phases; but n. incertus-lesioned rats displayed a markedly slower (delayed) extinction of conditioned freezing responses than sham/control rats; suggesting n. incertus-related circuits normally promote extinction through inhibitory projections to amygdala and prefrontal cortex.

Suggested Reviewers: Gregory J Quirk PhD
Professor, Department of Psychiatry , University of Puerto Rico School of Medicine
gregoryjquirk@gmail.com
He is an specialist in all processes controlling fear extinction

René García PhD
Professor, Laboratoire de Neurobiologie et Psychotraumatologie, Université de Nice-Sophia Antipolis, France
rene.garcia06@gmail.com
He is an specialist in modulation of fear extinction

Llorenç Diaz-Mataix PhD
PostDoc, Center for Neural Science, New York University
ldm5@nyu.edu
He is specialist in fear acquisition and emotional processes

Cover letter

VNIVERSITAT DE VALÈNCIA
Facultat de Medicina i Odontologia
Departament d'Anatomia i Embriologia Humana

FRANCISCO E. OLUCHA BORDONAU
Dep of Human Anatomy and Embryology
Fac. de Medicina y Odontología
University of Valencia

February 8, 2012

Professor Stephen Maren
Editor and Editor-in-Chief
Behavioral Brain Research

Dear Professor Maren,

Please find attached our manuscript entitled "Electrolytic lesion of the nucleus incertus and its ascending projections retards extinction of conditioned fear" by Pereira CW and others, which we submit for consideration by the *Behavioral Brain Research* as a Research Article.

We can confirm that this manuscript has been submitted solely to the Behavioral Brain Research and is not published, in press, or submitted elsewhere.

We can also confirm that all the research meets the ethical guidelines of the relevant agencies and Animal Welfare Committees.

We have endeavoured to adhere to the correct style and format requested for submissions.

We look forward to receiving editorial comments on our article in the near future.

Yours sincerely,

Francisco E. Olucha-Bordonau
Dep of Human Anatomy
Univ. Valencia, Spain

Research Highlights

- We studied the pontine n. incertus role in fear conditioning and extinction
- We have shown an important projection from the n. incertus to amygdala nuclei
- Lesions of the n. incertus do not affect to the acquisition or retrieval of fear to cue or context
- Lesions of the n. incertus delay the within trial extinction.
- Thus n. incertus facilitates extinction

Behavioural Brain Research, 8 February 2012

Electrolytic lesion of the nucleus incertus and its ascending projections retards extinction of conditioned fear

Pereira CW[a,b,†*], Santos FN[a,b,†*], Sánchez-Pérez AM[c], Otero-García M[d], Marchioro M[b], Ma S[e,f], Gundlach AL[e,g], Olucha-Bordonau FE[a**]

[a]Departamento de Anatomía y Embriología Humana, Facultad de Medicina, Universitat de Valencia, 46010 Valencia, Spain
[b]Universidade Federal de Sergipe, Laboratorio de Neurofisiologia, São Cristóvão, SE 49100-000, Sergipe, Brazil
[c]Departamento de Fisiología, Facultad de Medicina, Universitat de Valencia, 46010 Valencia, Spain
[d]Departamento de Biología Funcional y Antropología Física, Facultad de CC Biológicas, Universitat de Valencia, 46100 Valencia, Spain
[e] Florey Neuroscience Institutes, [f]Department of Medicine (Austin Health) and [g]Department of Anatomy and Cell Biology, The University of Melbourne, Victoria 3010, Australia

*These authors contributed equally to this research

†Current Address: Universidade Federal de Sergipe, Laboratorio de Neurofisiologia, Av Marechal Rondon, s/n, Jardim Rosa Elze, São Cristóvão, SE 49100-000, Sergipe, Brazil

**Corresponding author:
FE Olucha-Bordonau
Departamento de Anatomía y Embriología Humana
Universitat de Valencia
Av Blasco Ibáñez 15
46010 Valencia, Spain
Tel: +34 9 6398 3504 Fax: +34 9 6386 4159
E-mail: olucha@uv.es

Abstract

Fear memory helps animals and humans recognize putative sources of danger and adopt the appropriate behavioral response. The primary neural circuits for fear acquisition and extinction involve connections between prefrontal cortex, ventral hippocampus and amygdala, and these areas are modulated by brainstem networks. The *nucleus (n.) incertus* in the dorsal pontine tegmentum provides a strong GABAergic projection to these forebrain centers and is strongly activated by neurogenic stressors. In this study in male, adult rats, we injected miniruby anterograde tracer into n. incertus and delineated its projections to the amygdala; and examined the effect of electrolytic lesions of n. incertus on different stages of the fear conditioning-extinction process. N. incertus-derived nerve fibers were observed in anterior medial amygdala, endopiriform nucleus, intra-amygdala bed nucleus of stria terminalis, amygdalohippocampal transition area, and the ventromedial nucleus of the lateral amygdala, with a broad fiber band present between the basolateral amygdala and the olfactory nuclei of amygdala. In a conventional contextual fear conditioning paradigm, we compared freezing behavior in control (naïve) rats (n = 13), with that in rats after sham- or electrolytic lesions of n. incertus (n = 9/group). There were no differences between the three groups in the habituation, acquisition, or context conditioning phases; but n. incertus-lesioned rats displayed a markedly slower (delayed) extinction of conditioned freezing responses than sham/control rats; suggesting n. incertus-related circuits normally promote extinction through inhibitory projections to amygdala and prefrontal cortex.

Keywords: Amygdala, Electrolytic lesion, Extinction, Fear memory, Neural tract-tracing, Nucleus incertus

1. Introduction

Acquisition and extinction of fear memories are neural processes that allow animals and humans to face physical and emotional challenges in a potentially dangerous environment. In mammals and possibly other vertebrates, the central node for managing fear-related information in the brain is the amygdala [1]. Research over many years has established that the lateral nucleus of the amygdala is the 'starting point' where sensory, emotionally meaningless information (conditioned stimulus, CS) acquires emotional value when presented together with a meaningful stimulus (unconditioned stimulus, US) [2]. After acquisition, the presentation of the CS alone elicits the same response as those displayed after presentation of the US (conditioned response, CR).

Commonly, under experimental conditions the CS used is a tone, the US is a footshock and the CR, which can be interpreted as the level of acquisition, is the amount of time that the animal spends 'paralyzed' (freezing) during the presentation of the CS tone. If a CS is repeatedly presented without the US, the animal learns that the CS no longer predicts the occurrence of the US, a phenomenon known as extinction. While the amygdala plays a key role in acquisition of conditioning *and* extinction, extinction memories are thought to be stored in the ventromedial prefrontal cortex [3].

The anatomical framework of the conditioning-extinction process is a series of intrinsic connections running from the lateral amygdala, where the emotional acquisition commences, to the central amygdala, which signals the appropriate emotional response to be performed [4]. In addition, there are intrinsic connections formed by the intercalated GABAergic cell groups that lie adjacent to/between the lateral and central nuclei. Neural processing along this pathway is modulated by several intrinsic and extrinsic afferents, some of them derived from within the amygdala.

The processing of conditioning and extinction signals can be altered by modulatory systems ascending from the brainstem. For example, stimulation of the locus ceruleus inhibits amygdala neurons [5], intra-amygdala infusion of norepinephrine enhances contextual fear conditioning [6], β-adrenergic stimulation impairs extinction [7], basolateral noradrenergic activity mediates corticosterone enhancement of fear conditioning, [8], serotonin transporter knockout mice exhibit a selective deficit in extinction recall of fear memory [9, 10] and neuropeptide S containing projections from neurons located between Barrington's nucleus and locus ceruleus facilitates extinction [11].

We propose that the nucleus (n.) incertus in the pontine tegmentum is another area that could potentially affect the conditioning-extinction process. Although the projections from this area to the amygdala were initially described as 'sparse' [12], in subsequent studies we observed projections to several amygdala nuclei [13]. The main target areas of n. incertus afferents include the amygdala, medial and lateral septum, ventral hippocampus and

prefrontal and entorhinal cortex, revealing a putative involvement in the control of cognitive and emotion-related functions [12, 13]. Moreover, n. incertus neurons express high levels of the corticotrophin-releasing hormone receptor-1 (CRH-R1) [14, 15], consistent with the integration by n. incertus of stress-related information and its 'transfer' to telencephalic cognitive and emotional centers. In fact, several neurogenic stressors activate the n. incertus, as reflected by increased c-Fos expression [16-18] (see [19] for review).

Furthermore, ascending n. incertus projections target consecutively the median raphe, supramammillary nucleus, posterior hypothalamus, medial septum and hippocampus [12, 13], the components of the 'septohippocampal system' e.g. [20]. A proposed role for the n. incertus in modulating hippocampal theta rhythm was supported by observations that electrical stimulation of n. incertus increased hippocampal theta activity in urethane-anesthetized rats; and that lesion of the n. incertus produced disruption of hippocampal theta induced by stimulation in the *reticularis pontis oralis* (RPO) [21].

Importantly, there is a close relationship between synchronization of neural firing at theta frequency in the amygdala and hippocampus and fear conditioning. During fear-related emotional arousal, lateral amygdala neurons increase oscillatory activity at theta frequency [22, 23]. Moreover, it has been shown that during consolidation and reconsolidation of conditioned fear, lateral amygdala and CA1 cells increased synchrony between the theta band [24]. Furthermore, there is evidence of theta-related coordination between the hippocampus, amygdala and prefrontal cortex [25], and as all these areas receive projections from n. incertus, we hypothesized that the n. incertus plays a role in the control of fear conditioning.

Therefore, the goal of this study was to determine whether lesion of the n. incertus could markedly modulate fear expression and/or extinction behavior. We performed discrete electrolytic lesions of n. incertus in adult, male rats and tested the effect on performance in a paradigm of fear acquisition and extinction. In addition, we used neural tract-tracing to identify putative target regions in the amygdala that may mediate actions of increased or decreased n. incertus activity on fear processes.

(766 words)

2. Materials and Methods

2.1. Animals

A total of 34 adult, male Sprague-Dawley rats weighting 250-350 g were used in this study - 3 rats were used for the neuroanatomical tract-tracing study; and 31 rats were used for the lesion/behavioral study and were housed in individual cages with a reverse cycle 12:12 h light/dark (lights off at 8 am) for 21 days before commencing the behavioral procedures. Rats were randomly distributed in two groups; control and surgery, and lesion surgery was done 7 days after the reversal of the light cycle (Fig. 1). All behavioral procedures conducted during the dark phase. All animal manipulations were approved by the Committee of Ethics and Animal Welfare of the Universitat de Valencia, Spain and were in agreement with directive 86/609/EEC of the European Community on the protection of animals used for experimental and other scientific purposes.

2.2. Surgical procedures

2.2.1. Tracer injection

Rats were deeply anesthetized with ketamine 55 mg/kg (Imalgene, Merial Laboratorios SA, Barcelona Spain) and xylacide 20 mg/kg (Xilagesic, Laboratorios Calier, Barcelona, Spain) and anesthesia was maintained with isoflurane as required. Under stereotaxic control, a small hole was drilled in the skull and anterograde tracer injections were made into the n. incertus using 40 µm glass micropipettes (coordinates AP -9.6 mm, ML 0 mm and DV 7.4 mm with respect to bregma [26]. For anterograde tracing, we used 15% miniruby (mR, 10 kD biotinylated dextran amine rhodamine-labeled, Molecular Probes, Cat No. D-3312, Paisley, UK) dissolved in 0.1M PB, pH 7.4. Tracer was iontophoretically delivered into the n. incertus by passing a positive current of 1 µA 2 sec on 2 sec off over 15 min with a current generator (GC2N model, Direlec, Madrid, Spain). After injections, the surgical wound was sutured and rats were injected with buprex (0.05 mg/kg, i.p., Lab Esteve, Barcelona, Spain) for analgesia. Rats were then allowed to recovery, prior to further processing. After 7 days of survival time, rats were euthanized with an overdose of Nembutal (150 mg/kg, i.p. Euthalender, Normon, Barcelona, Spain). Brains were perfused by transcardial infusion of saline (250 ml) followed by fixative (4% paraformaldehyde in 0.1M phosphate buffer (PB), pH 7.4). Brains were then removed from the skull, postfixed in the same fixative overnight at 4ºC, and cryoprotected in 30% sucrose in 0.01 M PB, pH 7.4

2.2.2. Electrolytic lesions

Rats were deeply anesthetized with ketamine (Imalgene) and xylacide (Xilagesic) (55 mg/kg and 20 mg/kg, i.p., respectively) and anesthesia was maintained with isoflurane as required. Under stereotaxic control a monopolar electrode was lowered into the brain at coordinates

AP -9.6 mm, ML 0 mm and DV -7.4 mm with respect to bregma. Positive continuous current of 1.5 mA was injected for 10 sec by means of a current generator connected to a SIU (Cibertec, Madrid, Spain). Five min after the lesion, the electrode was removed and the wound sutured. Rats were injected with buprex (0.05 mg/kg, i.p., Lab Esteve) for post surgery analgesia. Rats were left to recover for an additional 15 days before use in the behavioral procedures.

2.3. Apparatus

The behavioral procedures were conducted in a contextual fear conditioning apparatus (Panlab, Barcelona Spain), consisting of three cages of 250 × 250 × 250 mm and a floor containing a 22-rod grid connected to a shocker and a speaker in the ceiling. On a lateral wall there was a soft light. The tray containing the grid was suspended over a load cell that detected movements of the rat in the cage. The rat enclosure was inside a sound proof cage of 600 (W) × 500 (D) × 500 (H) mm, which contained four 9V light bulbs. All procedures were controlled by the *Freezing* software (Panlab).

Two kinds of contexts were used. In context A (for acquisition), lateral and posterior walls were black and the front wall was Plexiglas, and the interior light was on. In context B (for extinction), the lateral and posterior walls were horizontal, vertical and diagonal black and white strips, the grid was covered with a white Plexiglas lamina, the interior light was off, the cage lights were on, and four open tubes containing lemon-flavored soap were added.

2.4. Behavioral procedures

The entire behavioral procedure was completed over 5 days (Fig. 1). On days 1 and 2 each rat visited contexts A and B for 15 min per session. On day 3 (acquisition), each rat received 3 tone-shock pairings in context A. The tone (2.8 kHz and 75 db SPL) was continuous for 30 sec. The shock was 0.3 mA and 0.5 sec duration and co-terminated with the tone. The tone and shock pairings were presented randomly at sequences of 180 ± 60 sec. On day 4, each rat was again exposed to the two contexts, first context A (acquisition) and two hours later, context B (extinction). On day 5, in context B, the rats received 5 extinction tones (2.8 kHz and 75 db SPL) of 30 sec, presented with a random delay from each other at times of 180 ± 60 sec. Following the procedure, rats were euthanized with an overdose of Nembutal (150 mg/kg, i.p.). Brains were perfused by transcardial infusion of saline (250 ml) followed by fixative (4% paraformaldehyde in 0.1M PB, pH 7.4). Brains were removed from the skull, postfixed in the fixative overnight at 4ºC, and cryoprotected in 30% sucrose in 0.01M PB buffer pH 7.4.

2.5. Behavioral measurements

The load cell at the bottom of the grid tray transformed horizontal movements into electrical signals that was amplified and converted into arbitrary signals. The interface magnified the signal 500× and the software amplified the signal a further 8 times. Under these conditions movements were displayed in a 0-100 scale. After visual checking of responses, we considered freezing as movement signals <10 lasting at least 2 sec. The *Freezing* software displayed freezing as a percentage of the total time of the step for each step of the protocol.

2.6. Histological procedures

Brains were left in cryoprotectant for 1-3 days until they had sunk to the bottom of the vessel. Coronal sections (40 µm) were obtained using a freezing slide microtome (Leica SM2010R, Leica Microsystems, Heidelberg, Germany). For each brain, 6 series of sections were obtained and collected in 0.01 M PBS. In brains from rats that had undergone surgery, calretinin immunohistochemistry was used to determine the degree of neuronal injury in the n. incertus and surrounding areas. The distribution of mR, following injections of the tracer into the n. incertus, was revealed using the standard ABC-DAB method.

2.6.1. Tracer histochemistry

Sections were rinsed in 2 × TBS and transferred to 1:100 ABC (Vectastain, Vector PK-6100, Vector Laboratories, Burlingame, CA, USA) and incubated overnight at 4°C. After rinsing (2 × TBS), the tracer was revealed by immersing the sections in 0.025% DAB, 0.5% ammonium nickel sulfate, 0.0024% H_2O_2 in Tris HCl, pH 8.0. The reaction was stopped after 15 min by adding TBS. Sections were rinsed (3 × 0.01 M PBS pH 7.4) and mounted on gelatin-subbed slides, air dried, dehydrated with graded ethanol, cleared and coverslipped with DPX.

2.6.2. Calretinin immunohistochemistry

Sections were rinsed twice in 0.05 M Tris-buffered saline pH 8.0 (TBS) and transferred to blocking solution (4% normal donkey serum (NDS), 2% bovine serum albumin (BSA) and 0.2 % Triton-X100 in TBS) for 1 h at room temperature. Sections were then transferred to incubation media containing 1:2,500 mouse anti-calretinin (Swant, Bellinzona, Switzerland) 6B3, 2% NDS, 2% BSA and 0.2% Triton X100 in TBS for 48 h at 4ºC. Sections were rinsed (2 × TBS) and transferred to the biotinylated secondary antibody (biotinylated donkey anti-mouse (Jackson Laboratories, Cat No. 715-065-150) for 1 h. Sections were then rinsed (2 × TBS) and immersed in 1:100 ABC (Vector) for 1 h. After rinsing (2 × TBS), immunolabeling was revealed by incubating the sections in 0.025% DAB, 0.0024% H_2O_2 in Tris HCl, pH 7.6. After several rinses in 0.01 M PBS, sections were mounted on chrome alum, gelatine-coated slides, air dried, dehydrated, cleared and coverslipped (Sigma-Aldrich).

2.7. Histological examination

Lesions and anterograde labeling were photographed using a Nikon Eclipse E600 microscope with a DMX2000 digital camera (Nikon, Tokyo, Japan). Mappings were made with a camera lucida tube attached to a Zeiss Axioskop microscope (Zeiss, Munich, Germany) with the 20× objective, scanned and reduced to the final size.

2.8. Statistical analysis

Two-way ANOVA statistical analysis was performed on the three groups - control, lesion and sham-operated, using GraphPad Prism software. Bonferroni's post-hoc test was performed to specify the differences between points after the lesion effect was found to be significant.

3. Results

3.1. Projections from the nucleus incertus to the amygdala

In all three cases assessed, the mR tracer injection was restricted to the n. incertus, with no spread to the dorsal tegmental nucleus or the pontine raphe nucleus (Fig. 2A). Anterogradely labeled fibers entered the amygdala complex from the medial forebrain bundle and the subventricular area (Fig. 2B,C). Within the amygdala, anterogradely labeled fibers were observed in the anterior nuclei of the medial amygdala, while, in contrast, the posterior nuclei of the medial amygdala were free of labeling. Fibers ran caudally and were densely concentrated in the intra-amygdala bed nucleus of the stria terminalis (IABST). Some fibers were also dispersed in the basal nuclei and the cortical and olfactory amygdala, and some of these fibers ran laterally and concentrated in the endopiriform nucleus, whereas the central nuclei were essentially free of labeled fibers. Finally, in the basolateral complex, labeled fibers concentrated in the ventromedial division of the lateral amygdala (Fig. 2C). Although not highly concentrated, some fibers were observed within the intercalated nuclei.

3.2. Behavioral studies

The extent of the lesion in each rat studied was analyzed by calretinin immunohistochemistry (Fig. 3A,B). In none of the lesioned rats analyzed, did the damaged area spread to the surrounding nuclei, and only a few 'injured' fibers/terminals were observed in the dorsal tegmental nucleus. Similarly, no histological alterations were observed in the pontine raphe, Barrington's nucleus or locus ceruleus, although some signs of injury were observed in the ventrally adjacent medial longitudinal fasciculus that connects nuclei involved in oculomotor coordination (Fig. 3B). According to the severity of the lesion/damage to the n. incertus, rats were classified as 'lesioned' (substantial loss of calretinin-positive neurons), 'sham' lesioned (with the electrode placed dorsally in the cerebellum or ventrally in the reticular formation) and 'control' (naïve rats that did not undergo surgery).

Evolution of the levels of freezing occurred during the behavioral procedure (Table 1; Fig. 4). There were no significant changes in freezing in the habituation trials prior to the acquisition session; and no significant changes in freezing levels between the lesioned, sham and control groups during the acquisition trials. Rats initially displayed 10-20% freezing, during the tone of the first pairing, with a shift to 70-80% freezing during the tone of the second pairing, and reaching close to 90% during the tone of the third pairing. This pattern followed the Rescorla and Wagner model of acquisition [27].

In the next session we assessed acquisition of conditioning to the context. Indeed, the level of freezing in context A shifted significantly from 20% for the last habituation trial to 50-70% during exposure to the same context after acquisition ($F_{(1,32)}$ = 35.32, P< 0.0001).

However, n. incertus lesion did not affect context conditioning; and there were no significant differences in freezing levels in context B before and after acquisition in context A (Fig. 4).

During the first two tones of the extinction process there was no differences between the different groups, indicating that the level of retention and retrieval was the same. However, by the third tone through to the fifth, freezing levels for sham and control rats were similar, but significantly different from lesioned rats, which displayed a slower extinction. Two-way ANOVA revealed that the lesion has a significant effect on freezing time ($F_{(2,140)}$ = 9.97 $p<0.0001$), and a post-hoc Bonferroni's test revealed that the differences occurred after the second tone at tones 3, 4 and 5 ($p<0.05$) between lesion and control (Fig. 4). Sham and control values were not significantly different, whereas sham and lesion were significantly different at tone 4 ($p<0.05$).

4. Discussion

In this study, we used conventional neural tract-tracing techniques to identify the presence of n. incertus projections within the amygdala and adjacent structures. The presence of this innervation and other aspects of the connectivity of the n. incertus support the possibility that this largely inhibitory projection might modulate neural processes associated with contextual fear conditioning. Indeed, we discovered that an electrolytic lesion of the n. incertus 14 days prior to subjecting rats to a classical contextual fear conditioning protocol produced a specific delay of fear extinction, but had no effect on the acquisition of fear or on contextual conditioning.

The anatomical findings fit with and extend our earlier observations on anterograde labeling of projections from n. incertus to the amygdala region [13]. Efferent fibers arising from the n. incertus make plexuses in the intra-amygdala bed nucleus of the stria terminalis, in the area between the olfactory amygdala and the basal and lateral amygdala, in the ventromedial subnucleus of the lateral amygdala, and in the anterior and posteroventral medial amygdala nucleus. Dense terminations were also observed in the dorsal and ventral endopiriform nuclei.

Neurons in the n. incertus express glutamic acid decarboxylase (GAD) [13, 28], consistent with the expression of the major inhibitory transmitter, GABA, by these large projections neurons. In the rat, these neurons also express a number of peptides, including neurotensin, neuromedin B, cholecystokinin, atrial natriuretic peptide and relaxin-3 (see e.g. [29], [30-32]; see [19] for review), suggesting GABA and peptides may be co-released under various physiological conditions and in different patterns in different target areas, including the extended amygdala and the hippocampus. Depending on the intensity of n. incertus neuron activity and the distribution of different GABA and peptide receptors within the target structures, GABA transmission may have a rapid and direct synaptic action on n. incertus target cells, while co-released peptides may have a slower, more dispersed action on neurons expressing high concentrations of receptors in different regions of the amygdala.

In related studies of the potential influence of the brainstem on fear memory, it has been shown that several pontine nuclei can have a modulatory effect on fear acquisition and/or extinction. For example, neuropeptide S projections arising from the pontine tegmentum enhance the actions of glutamatergic projections on the intercalated GABAergic neurons of the amygdala, thus potentiating extinction (e.g. [11]). With respect to the effect of the n. incertus lesion on fear extinction, we attempted to eliminate any effect of a lesion in surrounding areas by only analyzing data from rats with lesions restricted to the n. incertus and with no apparent effect on surrounding structures. We observed no differences between controls (non-lesioned and sham-lesioned) and n. incertus-lesioned groups during acquisition of fear conditioning, or in fear expression during the initial steps of extinction, indicating that

the n. incertus network does not have a major role in these processes or the retrieval of fear memory. The lesioned rats also displayed normal conditioning to context, as all groups displayed higher freezing in the context where conditioning took place than in the context experienced during habituation trials prior to acquisition. All rats discriminated well between the contexts, indicating n. incertus lesions did not affect the perception and configuration of a context. However, in response to the last tones presented during extinction, rats with lesions of the n. incertus displayed a higher level of freezing than sham and naïve rats, which extinguished normally. Thus, we conclude that lesions of n. incertus neurons and their projections impair the extinction process, delaying it.

Current reports suggest three main brain structures participate in extinction processes, i.e. hippocampus, amygdala and prefrontal cortex; and the integrity of this interconnected system is important for effective extinction processing [33, 34]. Nonetheless, some value can be attributed to a particular structure in specific aspects of extinction. Since lesions in the ventromedial prefrontal cortex do not affect 'within trial extinction' [35], it follows that acquisition of extinction must be processed downstream of the prefrontal connections to the central nucleus of the amygdala, where fear responses are elaborated. However, this is in apparent contradiction of recent experiments in which muscimol inactivation of the infralimbic cortex resulted in a delay in the extinction process, but had no effect on expression of fear [34]. However, in this latter experiment the prelimbic cortex was preserved. If the infralimbic cortex induces rapid extinction through the intercalated GABAergic inhibitory neurons of the amygdala [36], it is predicted that the inhibitory GABAergic projection from n. incertus to the amygdala functions in a similar way. With no overt evidence for a strong, direct projection from n. incertus to central amygdala, it may be the projection to the ventromedial lateral amygdala that mediates this effect. Otherwise, additional effects may be mediated by peptides that have high densities of receptors in the central amygdala, via slower volume transmission effects. We observed an important n. incertus input to the intra-amygdala bed nucleus of the stria terminalis, another area that expresses high levels of relaxin-3 and its receptor [29], but to our knowledge, a specific contribution of this area to fear conditioning has not been described. More generally, the amygdalohippocampal transition area and the medial amygdala receive a projection from the ventral subiculum of the hippocampus [37] and all of these areas are innervated by the n. incertus, increasing the potential modulatory role of the n. incertus over the amygdala.

An important consideration regarding the apparent ability of the n. incertus to modulate fear extinction is its potential ability to regulate the synchronized firing between the neuronal populations of hippocampus, prefrontal cortex and amygdala. In this regard, we have shown that electrical stimulation of n. incertus induces hippocampal theta rhythm [21] and stimulation of the RPO results in phase-locked synchronization between the n. incertus and

hippocampus [38]. Notably, neural synchronization at theta frequency is a feature associated with fear conditioning, and lateral amygdala and CA1 hippocampal activity becomes synchronized at theta frequency during consolidation and reconsolidation of conditioned fear [24]. In addition, retrieval of fear memories increases theta coupling between the lateral amygdala, ventromedial prefrontal cortex and hippocampus and is reduced during extinction [25].

In conclusion, we have discovered that the n. incertus appears to be modulator of the broader neural system associated with fear extinction and as n. incertus neurons express high levels of CRH-R1 [14, 15], we propose that n. incertus may be an interface between stress signalling and telencephalic circuits involved in fear processing. If as observed here, the main effect of a discrete electrolytic lesion of the n. incertus is to delay the extinction process, an effect also observed after infralimbic cortex inactivation, it is possible that the normal actions of both these pathways occur in parallel. Thus, the effect of infralimbic activation is transferred to the intercalated GABA neurons and the GABAergic NI projections may signal to the glutamate neurons in the lateral amygdala. In turn, both intercalated GABA and lateral amygdala glutamate neurons project to the central nucleus, where behavioral responses are evoked (Fig. 5).

N. incertus neurons express GABA and a majority also synthesize relaxin-3 and/or CCK. In an earlier study we demonstrated that injection of the relaxin-3 receptor agonist, R3/I5, into the medial septum mimics the effect of n. incertus stimulation (i.e. increasing hippocampal theta rhythm) [39]. In this study we have shown that n. incertus appears to participate in the brainstem networks that modulate fear extinction, but the specific effect of disruption/activation of the different transmitters within populations of n. incertus neurons (GABA and peptides, such as relaxin-3) on the fear conditioning/extinction process remains to be determined.

(1256 words)

Acknowledgements

This research was supported by grants from CAPES-Brasil Bex - 4494/09-1 (FNS) and 4496/09-4 (CWP) and Fapitec edital # 01/08 (FNS); the Ministry of Health, Spain - ISCIII-FIS PI061816 (FEO-B); the National Health and Medical Research Council of Australia - 520299 (SM); 277609 and 509246 (ALG); and the Victorian Government Operational Infrastructure Support Program (SM and ALG).

References

[1] LeDoux JE. Emotion circuits in the brain. Annu Rev Neurosci, 2000;23:155-184 doi: 10.1146/annurev.neuro.23.1.155.

[2] Nader K, Majidishad P, Amorapanth P, LeDoux JE. Damage to the lateral and central, but not other, amygdaloid nuclei prevents the acquisition of auditory fear conditioning. Learn Mem, 2001;8:156-163 doi: 10.1101/lm.38101.

[3] Quirk GJ, Mueller D. Neural mechanisms of extinction learning and retrieval. Neuropsychopharmacology, 2008;33:56-72 doi: 10.1038/sj.npp.1301555.

[4] Pitkanen A, Savander V, LeDoux JE. Organization of intra-amygdaloid circuitries in the rat: an emerging framework for understanding functions of the amygdala. Trends Neurosci, 1997;20:517-523.

[5] Chen FJ, Sara SJ. Locus coeruleus activation by foot shock or electrical stimulation inhibits amygdala neurons. Neuroscience, 2007;144:472-481 doi: 10.1016/j.neuroscience.2006.09.037.

[6] LaLumiere RT, Buen TV, McGaugh JL. Post-training intra-basolateral amygdala infusions of norepinephrine enhance consolidation of memory for contextual fear conditioning. J Neurosci, 2003;23:6754-6758.

[7] Debiec J, Bush DE, LeDoux JE. Noradrenergic enhancement of reconsolidation in the amygdala impairs extinction of conditioned fear in rats--a possible mechanism for the persistence of traumatic memories in PTSD. Depress Anxiety, 2011;28:186-193 doi: 10.1002/da.20803; 10.1002/da.20803.

[8] Roozendaal B, Hui GK, Hui IR, Berlau DJ, McGaugh JL, Weinberger NM. Basolateral amygdala noradrenergic activity mediates corticosterone-induced enhancement of auditory fear conditioning. Neurobiol Learn Mem, 2006;86:249-255 doi: 10.1016/j.nlm.2006.03.003.

[9] Wellman CL, Izquierdo A, Garrett JE, Martin KP, Carroll J, Millstein R, Lesch KP, Murphy DL, Holmes A. Impaired stress-coping and fear extinction and abnormal corticolimbic morphology in serotonin transporter knock-out mice. J Neurosci, 2007;27:684-691 doi: 10.1523/JNEUROSCI.4595-06.2007.

[10] Narayanan V, Heiming RS, Jansen F, Lesting J, Sachser N, Pape HC, Seidenbecher T. Social Defeat: Impact on Fear Extinction and Amygdala-Prefrontal Cortical Theta Synchrony in 5-HTT Deficient Mice. PLoS One, 2011;6:e22600 doi: 10.1371/journal.pone.0022600.

[11] Jungling K, Seidenbecher T, Sosulina L, Lesting J, Sangha S, Clark SD, Okamura N, Duangdao DM, Xu YL, Reinscheid RK, Pape HC. Neuropeptide S-mediated control of fear expression and extinction: role of intercalated GABAergic neurons in the amygdala. Neuron, 2008;59:298-310 doi: 10.1016/j.neuron.2008.07.002.

[12] Goto M, Swanson LW, Canteras NS. Connections of the nucleus incertus. J Comp Neurol, 2001;438:86-122.

[13] Olucha-Bordonau FE, Teruel V, Barcia-Gonzalez J, Ruiz-Torner A, Valverde-Navarro AA, Martinez-Soriano F. Cytoarchitecture and efferent projections of the nucleus incertus of the rat. J Comp Neurol, 2003;464:62-97 doi: 10.1002/cne.10774.

[14] Bittencourt JC, Sawchenko PE. Do centrally administered neuropeptides access cognate receptors?: an analysis in the central corticotropin-releasing factor system. J Neurosci, 2000;20:1142-1156.

[15] Van Pett K, Viau V, Bittencourt JC, Chan RK, Li HY, Arias C, Prins GS, Perrin M, Vale W, Sawchenko PE. Distribution of mRNAs encoding CRF receptors in brain and pituitary of rat and mouse. J Comp Neurol, 2000;428:191-212.

[16] Tanaka M, Iijima N, Miyamoto Y, Fukusumi S, Itoh Y, Ozawa H, Ibata Y. Neurons expressing relaxin 3/INSL 7 in the nucleus incertus respond to stress. Eur J Neurosci, 2005;21:1659-1670 doi: 10.1111/j.1460-9568.2005.03980.x.

[17] Cano G, Mochizuki T, Saper CB. Neural circuitry of stress-induced insomnia in rats. J Neurosci, 2008;28:10167-10184 doi: 10.1523/JNEUROSCI.1809-08.2008.

[18] Banerjee A, Shen PJ, Ma S, Bathgate RA, Gundlach AL. Swim stress excitation of nucleus incertus and rapid induction of relaxin-3 expression via CRF1 activation. Neuropharmacology, 2010;58:145-155 doi: 10.1016/j.neuropharm.2009.06.019.

[19] Ryan PJ, Ma S, Olucha-Bordonau FE, Gundlach AL. Nucleus incertus-An emerging modulatory role in arousal, stress and memory. Neurosci Biobehav Rev, 2011;35:1326-1341 doi: 10.1016/j.neubiorev.2011.02.004.

[20] Vertes RP, Kocsis B. Brainstem-diencephalo-septohippocampal systems controlling the theta rhythm of the hippocampus. Neuroscience, 1997;81:893-926.

[21] Nunez A, Cervera-Ferri A, Olucha-Bordonau F, Ruiz-Torner A, Teruel V. Nucleus incertus contribution to hippocampal theta rhythm generation. Eur J Neurosci, 2006;23:2731-2738 doi: 10.1111/j.1460-9568.2006.04797.x.

[22] Pare D, Collins DR. Neuronal correlates of fear in the lateral amygdala: multiple extracellular recordings in conscious cats. J Neurosci, 2000;20:2701-2710.

[23] Pape HC, Narayanan RT, Smid J, Stork O, Seidenbecher T. Theta activity in neurons and networks of the amygdala related to long-term fear memory. Hippocampus, 2005;15:874-880 doi: 10.1002/hipo.20120.

[24] Seidenbecher T, Laxmi TR, Stork O, Pape HC. Amygdalar and hippocampal theta rhythm synchronization during fear memory retrieval. Science, 2003;301:846-850 doi: 10.1126/science.1085818.

[25] Lesting J, Narayanan RT, Kluge C, Sangha S, Seidenbecher T, Pape HC. Patterns of Coupled Theta Activity in Amygdala-Hippocampal-Prefrontal Cortical Circuits during Fear Extinction. PLoS One, 2011;6:e21714 doi: 10.1371/journal.pone.0021714.

[26] Paxinos G, Watson C. The Rat Brain in Stereotaxic Coordinates. 3rd ed. New York: Academic Press, 1996.

[27] Rescorla RA, Wagner AR. A theory of Pavlovian conditioning: Variations in the effectiveness of reinforcement and nonreinforcement, In: "Black A.H." , "Prokasy W.F.", editor. Classical Conditioning II. : Appleton-Century-Crofts, 1972, 64-99.

[28] Ford B, Holmes CJ, Mainville L, Jones BE. GABAergic neurons in the rat pontomesencephalic tegmentum: codistribution with cholinergic and other tegmental neurons projecting to the posterior lateral hypothalamus. J Comp Neurol, 1995;363:177-196 doi: 10.1002/cne.903630203.

[29] Ma S, Bonaventure P, Ferraro T, Shen PJ, Burazin TC, Bathgate RA, Liu C, Tregear GW, Sutton SW, Gundlach AL. Relaxin-3 in GABA projection neurons of nucleus incertus suggests widespread influence on forebrain circuits via G-protein-coupled receptor-135 in the rat. Neuroscience, 2007;144:165-190 doi: 10.1016/j.neuroscience.2006.08.072.

[30] Sutin EL, Jacobowitz DM. Immunocytochemical localization of peptides and other neurochemicals in the rat laterodorsal tegmental nucleus and adjacent area. J Comp Neurol, 1988;270:243-270 doi: 10.1002/cne.902700206.

[31] Chronwall BM, Skirboll LR, O'Donohue TL. Demonstration of a pontine-hippocampal projection containing a ranatensin-like peptide. Neurosci Lett, 1985;53:109-114.

[32] Ryan MC, Gundlach AL. Anatomical localisation of preproatrial natriuretic peptide mRNA in the rat brain by in situ hybridisation histochemistry: novel identification in olfactory regions. J Comp Neurol, 1995;356:168-182 doi: 10.1002/cne.903560204.

[33] Pare D, Quirk GJ, Ledoux JE. New vistas on amygdala networks in conditioned fear. J Neurophysiol, 2004;92:1-9 doi: 10.1152/jn.00153.2004.

[34] Sierra-Mercado D, Padilla-Coreano N, Quirk GJ. Dissociable roles of prelimbic and infralimbic cortices, ventral hippocampus, and basolateral amygdala in the expression and extinction of conditioned fear. Neuropsychopharmacology, 2011;36:529-538 doi: 10.1038/npp.2010.184.

[35] Quirk GJ, Russo GK, Barron JL, Lebron K. The role of ventromedial prefrontal cortex in the recovery of extinguished fear. J Neurosci, 2000;20:6225-6231.

[36] Quirk GJ, Likhtik E, Pelletier JG, Pare D. Stimulation of medial prefrontal cortex decreases the responsiveness of central amygdala output neurons. J Neurosci, 2003;23:8800-8807.

[37] Kishi T, Tsumori T, Yokota S, Yasui Y. Topographical projection from the hippocampal formation to the amygdala: a combined anterograde and retrograde tracing study in the rat. J Comp Neurol, 2006;496:349-368 doi: 10.1002/cne.20919.

[38] Cervera-Ferri A, Guerrero-Martinez J, Bataller-Mompean M, Taberner-Cortes A, Martinez-Ricos J, Ruiz-Torner A, Teruel-Marti V. Theta synchronization between the hippocampus and the nucleus incertus in urethane-anesthetized rats. Exp Brain Res, 2011;211:177-192 doi: 10.1007/s00221-011-2666-3.

[39] Ma S, Olucha-Bordonau FE, Hossain MA, Lin F, Kuei C, Liu C, Wade JD, Sutton SW, Nunez A, Gundlach AL. Modulation of hippocampal theta oscillations and spatial memory by relaxin-3 neurons of the nucleus incertus. Learn Mem, 2009;16:730-742 doi: 10.1101/lm.1438109.

Tables

Table 1. Levels of freezing as % total time in each step of the conditioning-extinction procedure

Phase/Day	Context/Tone #	Lesion (n = 9) Mean ± SEM	Sham (n = 9) Mean ± SEM	Control (n = 13) Mean ± SEM
Habituation Day 1	Context B	21 ± 8	8 ± 6	8 ± 2
	Context B	33 ± 10	15 ± 7	26 ± 7
Habituation Day 2	Context A	19 ± 6	21 ± 6	17 ± 5
	Context B	27 ± 7	19 ± 5	15 ± 3
Acquisition Day 3	Tone 1	19 ± 8	21 ± 11	7 ± 3
Context A	Tone 2	68 ± 7	75 ± 8	75 ± 5
	Tone 3	94 ± 2	91 ± 3	89 ± 4
Day 4	Context A	65 ± 10	66 ± 5	46 ± 8
	Context B	30 ± 8	20 ± 5	22 ± 8
Extinction Day 5	Tone 1	80 ± 4	80 ± 3	74 ± 6
Context B	Tone 2	76 ± 9	87 ± 4	73 ± 6
	Tone 3	87 ± 5*	55 ± 11	52 ± 9
	Tone 4	78 ± 7*	45 ± 10	45 ± 10
	Tone 5	64 ± 10*	39 ± 8	34 ± 72

*P<0.05.

List of abbreviations

IV	4th ventricle
AStr	amygdalostriatal transition area
BLP	posterior basolateral amygdala
BLV	ventral basolateral amygdala
BMP	posterior basomedial amygdala
BSTIA	intraamygdalar part of the bed nucleus of the stria terminalis
DEn	dorsal endopiriformis
Ect	ectorhinal cortex
IC	intercalated nuclei of the amygdala
LaDL	dorsolateral division of the lateral nucleus of the amygdala
LaVL	ventrolateral division of the lateral nucleus of the amygdala
LaVM	ventromedial division of the lateral nucleus of the amygdala
Lent	lateral entorhinal cortex
MePD	posterodorsal division of the medial amygdala
mlf	medial longitudinal fascicle
mPFC	medial prefrontal cortex
NIc	nucleus incertus pars compacta
NId	nucleus incertus pars disipata
PDTg	posterodorsal tegmental nucleus
Pir	piriform cortex
PLCo	posterolateral division of the cortical amygdala
PMCo	posteromedial division of the cortical amygdala
PRh	perirhinal cortex
VEn	ventral endopiriform nucleus
vHip	ventral hippocampus

Figure captions

Fig. 1. Behavioral procedure for fear conditioning and extinction. Trials were performed during the active/dark phase. Surgery/lesions were done 15 days before the start of the behavioral procedures.

Fig. 2. Presence of n. incertus projections in the amygdala. The distribution of anterogradely-labeled fibers in the amygdala following miniruby injection into the n. incertus (NI) revealed the areas of amygdala receiving inputs from NI. **A**. Injection site in NI. Calibration bar, 100 μm. **B**. High power image of NI projecting fibers in the LaVM, observed by darkfield illumination. **C**. Collage of darkfield images of anterogradely labeled fibers in amygdala at a mid-caudal level. Dense NI projections are found in the BSTIA and ventromedial subnucleus of the lateral amygdala (LaVM). Scale bars, 100 μm for A-C.

Fig. 3. Electrolytic lesion of n. incertus (NI). (A) Calretinin immunoreactivity in the n. incertus of a sham surgery case. (B) Calretinin immunoreactivity in a rat with an electrolytic lesion. The lesion affected the n. incertus and medial longitudinal fasciculus, but not the adjacent posterodorsal tegmental nucleus. Scale bar, 100 μm.

Fig. 4. Lesion of the n. incertus impairs fear extinction. Graphs illustrate the level of freezing measured in each step of the behavioral protocol. All groups of rats displayed a similar level of fear expression in response to the acquisition protocol and handling. During the extinction protocol, controls and sham-operated rats behaved similarly, but rats with a lesion of the n. incertus displayed a significant delay in extinction. Rats were handled on the two days prior to the acquisition protocol in both contexts. * $P < 0.05$.

Fig. 5. Schematic of the putative connectivity and influence of the n. incertus (NI) on the amygdaloid nuclei involved in fear expression and extinction. The conditioned response is conveyed by the central nucleus which can be inhibited by intercalated neurons which receive projections from the infralimbic cortex, as it has been demonstrated previously, or by a direct inhibition of amygdala centers, which in turn project to the central amygdala (present study). Abbreviations: AHi, amygdalohippocampal area; BSTIA, bed nucleus of stria terminalis, intra-amygdala; Ce, central nucleus of amygdala; IL, infralimbic cortex; ITC, intercalated cells; LaVM, lateral amygdala, ventromedial subnucleus; +, excitatory input/effect; -, inhibitory input/effect.

Figure 1

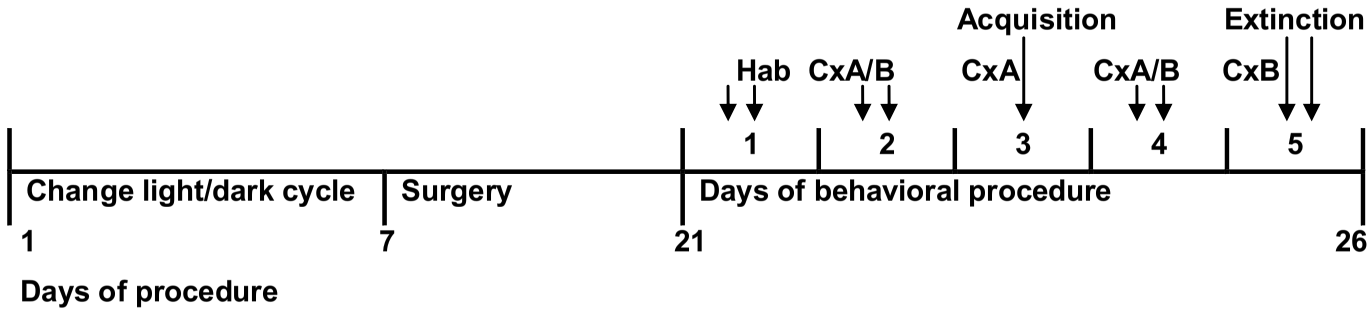
Acquisition
Extinction
Hab
CxA/B
CxA
CxA/B
CxB
1
2
3
4
5
Change light/dark cycle
Surgery
Days of behavioral procedure
1
7
21
26
Days of procedure

Figure 2
Click here to download high resolution image

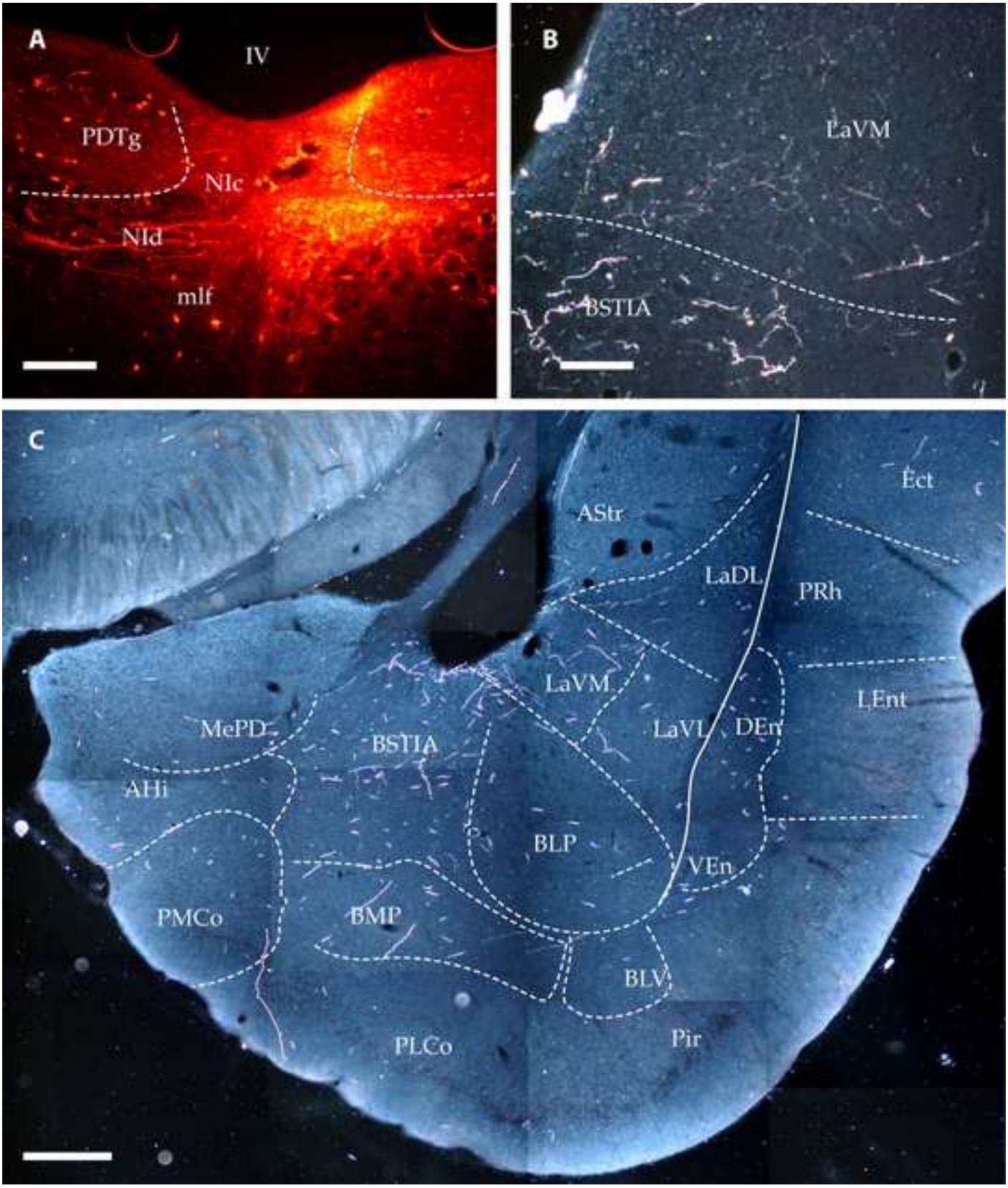

Figure 3
Click here to download high resolution image

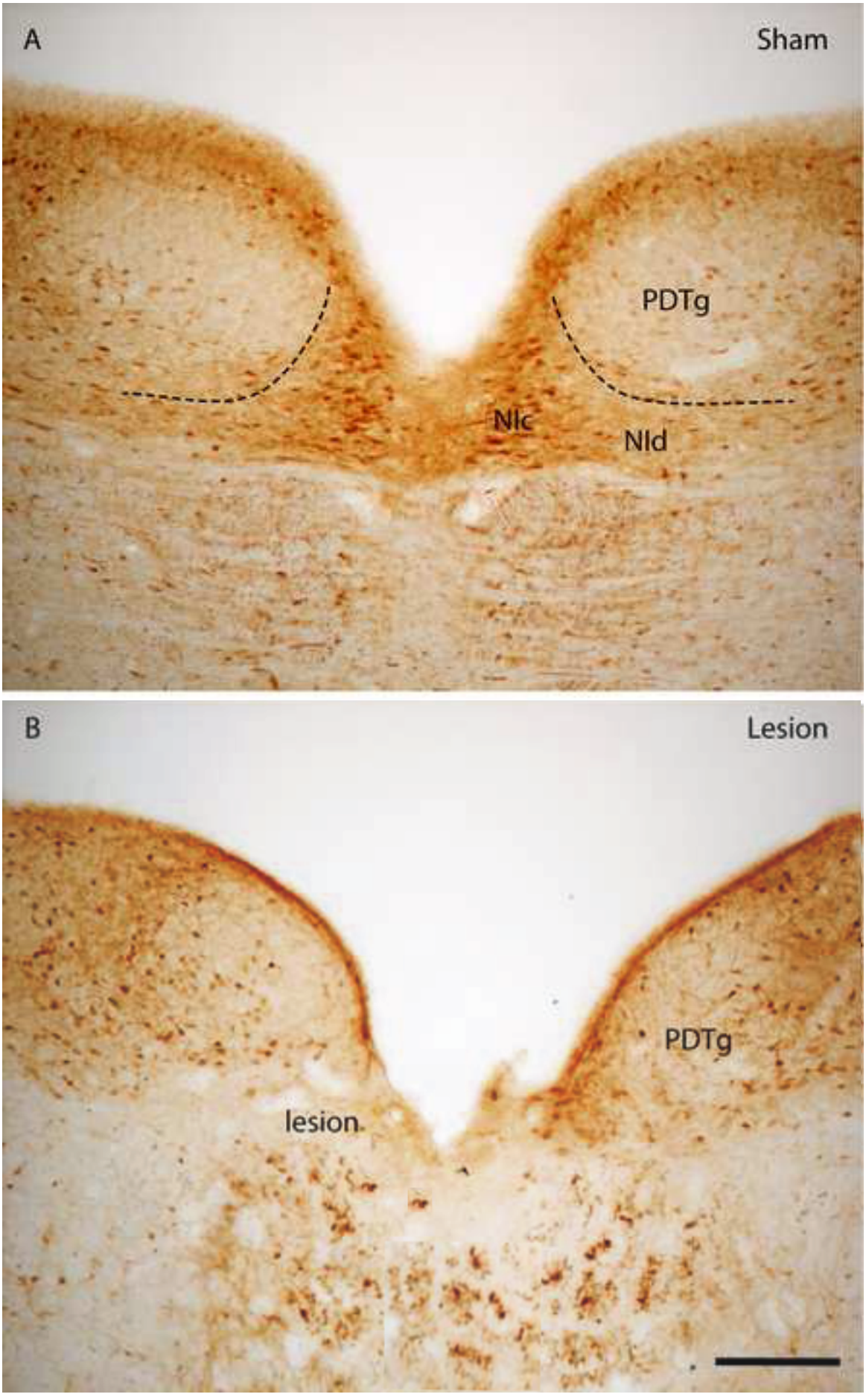

Figure 4

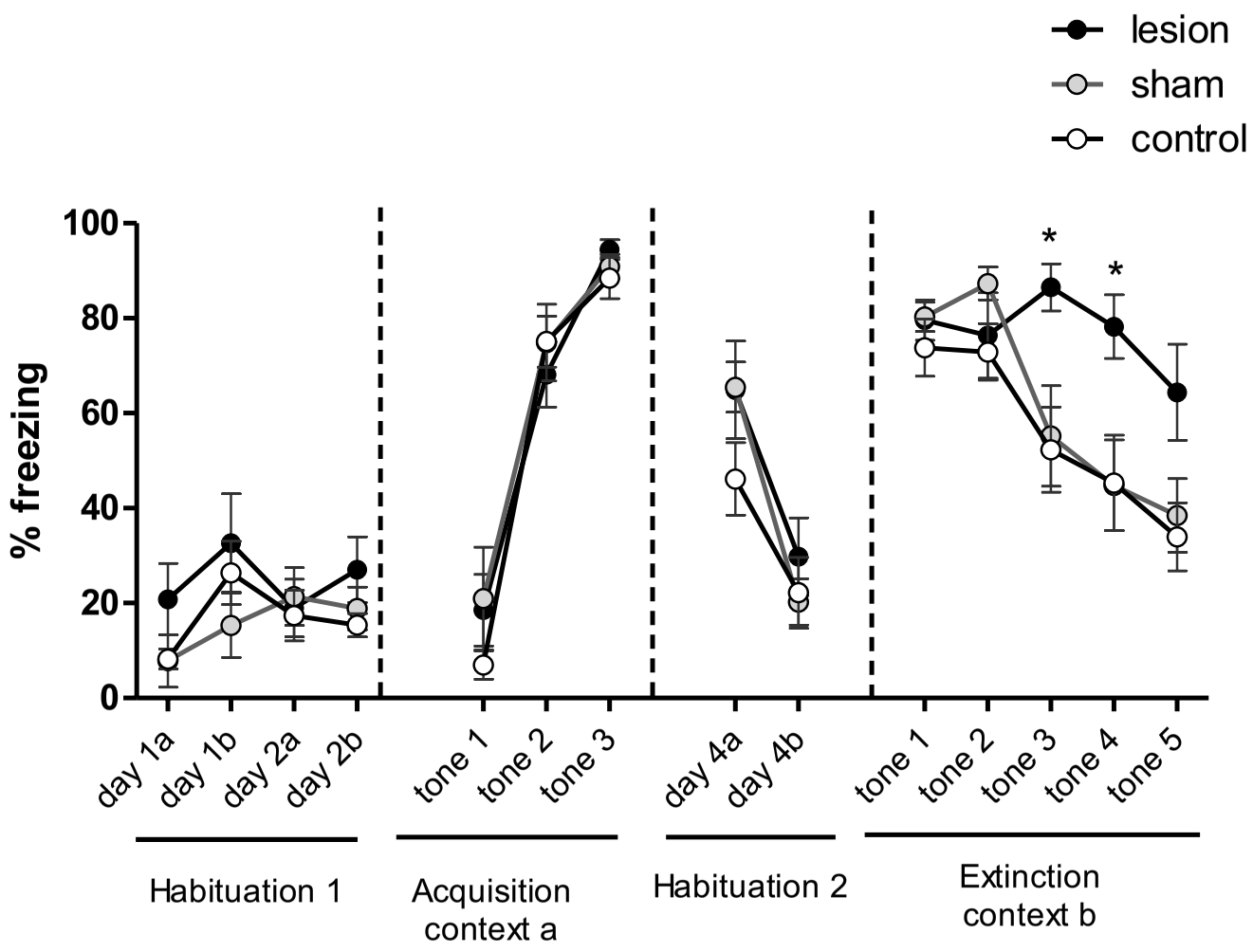
lesion
sham
control
% freezing
100
80
60
40
20
0
*
*
day 1a
day 1b
day 2a
day 2b
tone 1
tone 2
tone 3
day 4a
day 4b
tone 1
tone 2
tone 3
tone 4
tone 5
Habituation 1
Acquisition context a
Habituation 2
Extinction context b

Figure 5

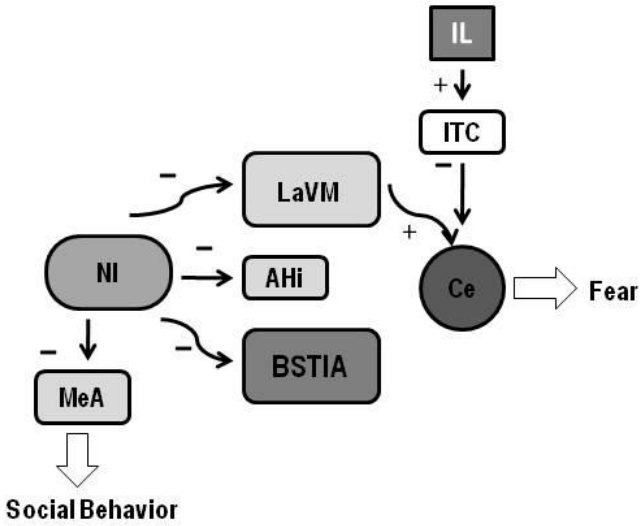

APÊNDICE B

DISTRIBUTION OF RELAXIN-3 INNERVATION OF TECTUM AND TEGMENTUM IN THE RAT SUGGESTS A ROLE FOR NUCLEUS INCERTUS IN CENTRAL DEFENSIVE NETWORKS

OTERO-GARCÍA, M.; PEREIRA, C.W.; SANTOS, F.N.; MARCHIORO, M.; MA, S.; GUNDLACH, A.L.; OLUCHA-BORDONAU, F.E.

Brain Structure and Function

Distribution of relaxin-3 innervation of tectum and tegmentum in the rat suggests a role for nucleus incertus in central defensive networks

--Manuscript Draft--

Manuscript Number:	
Full Title:	Distribution of relaxin-3 innervation of tectum and tegmentum in the rat suggests a role for nucleus incertus in central defensive networks
Article Type:	Original Article
Keywords:	Relaxin3-like immunorreactivity GABA attentional mechanisms defensive mechanisms stress monoamines nitric oxyde synthetase synaptophysin
Corresponding Author:	Francisco E Olucha-Bordonau, Ph.D Fac Medicina, Universidad de Valencia Valencia, Valencia SPAIN
Corresponding Author Secondary Information:	
Corresponding Author's Institution:	Fac Medicina, Universidad de Valencia
Corresponding Author's Secondary Institution:	
First Author:	Marcos Otero-García, PhD student
First Author Secondary Information:	
Order of Authors:	Marcos Otero-García, PhD student
	Celia W Pereira, PhD Student
	Fabio N Santos, PhD student
	Murilo Marchioro
	Sherie K-Y Ma, PhD
	Andrew L Gundlach, PhD
	Francisco E Olucha-Bordonau, Ph.D
Order of Authors Secondary Information:	
Abstract:	IIn mammals, tectal and tegmental divisions of the brainstem are involved in attentional mechanisms and responses to threatening stimuli such as predators. These centers are regulated by ascending connections, but the anatomical and neurochemical details of this drive are not fully known. The nucleus incertus (NI) in the pontine tegmentum is the source of ascending GABA projections to forebrain cognitive/emotional centers and NI neurons contain a number of neuropeptides, including relaxin-3 (RLN3). Tract-tracing studies have described NI projections within the tectum; and in this study we describe the distribution of relaxin-3 fibers within tectal and tegmental areas/nuclei of rat brain. RLN3-immunostained sections were also reacted with antisera against other neurochemical markers to assist in demarcation of the area. RLN3-containing fibers were concentrated in the medial, olivary and 'ventrolateral' pretectal nuclei; the medial intermediate grey layer of superior colliculus; and the pericentral area of inferior colliculus. Some labeled fibers were also detected in the cuneiform, parabigeminal and sagulum nuclei. RLN3 fibers were concentrated around the commissural bundles along the midline of the tectum, in the dorsal columns of the periaqueductal gray and in the dorsal raphe. In all areas, RLN3 and synaptophysin staining co-existed, indicating an

	association of the peptide with synapses. RLN3 projections target structures within the tectum and tegmentum that comprise the 'defensive system' involved in detection of and response to unexpected threatening stimuli. NI neurons, which are a major source of RLN3 fibers and express corticotrophin-releasing factor receptors, may contribute to these responses following activation by stress-related stimuli.
Suggested Reviewers:	Enrique Saldaña, MD PhD Associate Professor, Fac. Medicina, Universidad de Salamanca saldana@usal.es He is a specialist in audition and has recently decribed an important nucleus that runs all along the tectum
	Luis Martínez-Millán, PhD MD Professor, Universidad del País Vasco-EHU luis.martinezm@ehu.es He has worked and published important articles in intercollicular connections and an specialist in superior colliculus
	José Luis Lanciego, PhD MD Researcher, Universidad de Navarra jlanciego@unav.es He is an specialist in neuroanatomy specially in neuroanatomical methods and basal ganglia
	Newton S Canteras, PhD Professor, Universidade Sao Paolo newton@icb.usp.br He is an specilist on aggressive and defensive behaviors and the role of the periaqueductal gray in these processes
Opposed Reviewers:	

Brain Structure and Function - February 7, 2012

Distribution of relaxin-3 innervation of tectum and tegmentum in the rat suggests a role for *nucleus incertus* in central defensive networks

M Otero-García,[1] CW Pereira,[1,2] FN Santos,[1,2] M. Marchioro[2], S Ma,[3,4] AL Gundlach,[3,5] FE Olucha-Bordonau[1]*

[1] Departamento de Anatomía y Embriología Humana, Universidad de Valencia, 46010 Valencia, Spain
[2] Universidade Federal de Sergipe, Laboratorio de Neurofisiologia, Av. Marechal Rondon,s/n, Jardim Rosa Elze, São Cristóvão, SE. 49100-000, Sergipe, Brazil
[3]Florey Neuroscience Institutes, [4]Department of Medicine (Austin Health) and [5]Department of Anatomy and Cell Biology, The University of Melbourne, Victoria 3010, Australia

*Correspondence to:
FE Olucha-Bordonau
Departamento de Anatomía y Embriología Humana
Universidad de Valencia
Av Blasco Ibáñez 15
46010 Valencia, Spain
Telephone +34 9 6398 3504
FAX +34 9 6386 4159
E-mail: olucha@uv.es

Abstract

In mammals, tectal and tegmental divisions of the brainstem are involved in attentional mechanisms and responses to threatening stimuli such as predators. These centers are regulated by ascending connections, but the anatomical and neurochemical details of this drive are not fully known. The *nucleus incertus* (NI) in the pontine tegmentum is the source of ascending GABA projections to forebrain cognitive/emotional centers and NI neurons contain a number of neuropeptides, including relaxin-3 (RLN3). Tract-tracing studies have described NI projections within the tectum; and in this study we describe the distribution of relaxin-3 fibers within tectal and tegmental areas/nuclei of rat brain. RLN3-immunostained sections were also reacted with antisera against other neurochemical markers to assist in demarcation of the area. RLN3-containing fibers were concentrated in the medial, olivary and 'ventrolateral' pretectal nuclei; the medial intermediate grey layer of superior colliculus; and the pericentral area of inferior colliculus. Some labeled fibers were also detected in the cuneiform, parabigeminal and sagulum nuclei. RLN3 fibers were concentrated around the commissural bundles along the midline of the tectum, in the dorsal columns of the periaqueductal gray and in the dorsal raphe. In all areas, RLN3 and synaptophysin staining co-existed, indicating an association of the peptide with synapses. RLN3 projections target structures within the tectum and tegmentum that comprise the 'defensive system' involved in detection of and response to unexpected threatening stimuli. NI neurons, which are a major source of RLN3 fibers and express corticotrophin-releasing factor receptors, may contribute to these responses following activation by stress-related stimuli.

Key words: Relaxin3-like immunorreactivity, GABA, attentional mechanisms, defensive mechanisms Stress, monoamines, nitric oxyde synthetase, synaptophysin

Introduction

Adapting to threats from the environment and/or modifying behavior according to metabolic necessity requires coordination of multiple neural systems. In mammals, tectal and tegmental nuclei are involved in attentional mechanisms that direct sensory systems towards relevant target (Masino T, 1992); and to increase the effectiveness of this process, mechanisms of attention and performance must be optimized and coordinated during episodes of danger. In mammals, tectal and tegmental divisions of the brainstem are involved in coordinating attentional responses, including head- and eye-orienting movements, and responses to threatening stimuli such as predators. These centers, which include the pretectal area, superior and inferior colliculi, the mesencephalic periaqueductal grey, and the pontine central grey, are regulated by other ascending connections, but the anatomical and neurochemical details of this drive are not fully known.

The pretectal area is a collection of nuclei traditionally associated with the oculomotor system. Neuronal recordings and tracing of neural connections have shown that the olivary pretectal nucleus and the nucleus of the optic tract play critical roles in optokinetic nystagmus, short latency ocular following, smooth pursuit eye movements, and gain adaptation of the horizontal vestibulo-ocular reflex, as well as the pupillary light reflex (Klooster et al., 1995; Gamlin, 2006). The medial and posterior pretectal nuclei project to the intergeniculate leaflet (Mikkelsen and Vrang, 1994), which is activated by non-photic circadian stimulation (Mikkelsen et al., 1998).

The superior colliculus (SC) is a key component of circuits that mediate orienting responses to relevant sensory information (Grantyn, 1988; Munoz and Wurtz, 1992; Munoz et al., 1996; Krout et al., 2001). Direct topographic projections from the retina form a representation of the visual space over the superficial layers of SC (Stein et al., 1993). In addition to thalamic projections, the superficial layers project to deep layers of SC, where visual space overlaps with other sensory maps (Doubell et al., 2003). For audition, a topographic representation of the auditory space must be aligned with the coordinates of the visual space (King, 1999) in order to facilitate responses to stimuli derived from the same source (Stein and Meredith, 1990). The SC also contributes to defensive behaviors elicited by sensory inputs. Neurons located in medial aspects are maximally responsive to small objects slowly moving from the upper visual field (Drager and Hubel, 1975; Dean et al., 1989), which may warn of danger from airborne predators (Blanchard et al., 1986). In contrast, lateral aspects of SC are maximally responsive to objects in the lower visual field that is associated with potential food and elicits orienting, approach, hunting and consumption (Furigo et al., 2009; Furigo et al., 2010).

The inferior colliculus (IC) is a key node in the ascending auditory projection to the medial geniculate body. Two systems of auditory projections run in parallel - the tegmental pathway involves the central nucleus and projects to the main ventral nucleus of the medial geniculate body (Wenstrup et al., 1994; Winer et al., 1996); while the extra-tegmental pathway arises from the pericentral external cortex and dorsal nuclei (Ledoux et al., 1987). These areas project to nuclei around the ventral division of the medial geniculate body that are mainly involved in auditory emotional processing (LeDoux et al., 1984). An important efferent from the extra-tegmental pathway arising in the external cortex of IC reaches the inner layers of SC and the dorsolateral column of the PAG (Garcia Del Cano et al., 2006). The projection from the external cortex of IC to the deep layers of SC may contribute to the alignment of visual and auditory azimuthal maps (Thornton and Withington, 1996).

The mesencephalic periaqueductal grey (PAG) plays a central role in generating coping responses to different kinds of emotional stress and threats. Differential expression patterns of neuronal nitric oxide synthase (nNOS), acetylcholinesterase and $GABA_A$ receptors lead to a view that

PAG is organized in longitudinally arranged dorsomedial (DM), dorsolateral (DL), lateral (L) and ventrolateral (VL) columns (Onstott et al., 1993; Ruiz-Torner et al., 2001). Each column displays a different pattern of neural connections, and differential physiological effects of direct stimulation of the different regions (Bandler and Carrive, 1988; Bandler and Shipley, 1994; Bandler et al., 2000);(Subramanian et al., 2008) and c-*fos* expression patterns following different behavioral stimuli (Keay and Bandler, 1993; Keay et al., 1994); Carrive et al., (1997) have confirmed that the anatomically defined columns correlate with aspects of PAG function. For example, the DL column receives afferents from the prefrontal cortex and projects to the cuneiform nucleus, while the other PAG columns receive afferents from the amygdala and project to brainstem and spinal cord. Furthermore, the precommissural nucleus is considered a separate division, sharing some connections and physiological features with the PAG dorsolateral column (Canteras and Goto, 1999a); and it is activated when rats are exposed to a predator (Canteras and Goto, 1999a; Comoli et al., 2003; Sukikara et al., 2006; Mota-Ortiz et al., 2009; Motta et al., 2009).

The pontine central grey, lying caudal to PAG, is composed of several nuclei that are central to arousal mechanisms. The pontine and dorsal raphe nuclei contain serotonin neurons, which project widely over diencephalic and telencephalic centers to modulate several aspects of cognitive, emotional and mood behaviors (Jacobs and Azmitia, 1992; Vertes et al., 1994; Vertes et al., 2010). The locus coeruleus provides a widespread noradrenergic network of connections to the cerebral cortex (Jones and Yang, 1985) and is one of the main neural systems promoting wakefulness (Nelson et al., 2002; Nelson et al., 2003), with a close correlation between locus coeruleus activity and the level of arousal (Foote et al., 1980; Aston-Jones and Bloom, 1981). Neurons in the laterodorsal tegmentum and cholinergic neurons in the pontine tegmentum are thought to be involved in regulating rapid eye movement (REM) sleep since neurotoxic lesions of these neurons result in loss of REM sleep (Jones and Webster, 1988; Webster and Jones, 1988).

The *nucleus incertus* (NI) (or nucleus O) is located in the midline pontine tegmentum and sends prominent projections to various higher brain centers (Goto et al., 2001; Olucha-Bordonau et al., 2003). The first study of NI connectivity documented sparse projections to PAG and SC) . In a second study however, we observed a significant NI projection to SC that was confirmed by retrograde tracer injections from SC to NI (Olucha-Bordonau et al., 2003). We propose that NI may play a role in modulating attentional and behavioral responses through its widespread projections containing GABA and various neuropeptides. In this regard, the NI is characterized as a primary source of relaxin-3 (RLN3), the ancestral member of the relaxin peptide/hormone family (Burazin et al., 2002; Bathgate et al., 2003) , and its distribution appears conserved in mouse (Smith et al., 2010) rat (Tanaka et al., 2005; Ma et al., 2007) and macaque brain (Maet al., 2009). In the rat, NI sends ascending projections to cognitive, emotional and visceral processing brain areas, including dorsal and median raphé, interpeduncular and supramammillary nuclei, lateral hypothalamus, the perifornical area, medial and lateral septum, amygdala, hippocampus, and entorhinal and prefrontal cortex (Goto et al., 2001; Olucha-Bordonau et al., 2003). Importantly, brain areas containing anterograde fiber labeling following tracer injections into NI are largely identical to those containing RLN3 immunopositive fibers (see (Goto et al., 2001; Olucha-Bordonau et al., 2003; Tanaka et al., 2005; Ma et al., 2007)).

Anatomical studies conducted so far have lead to speculation about the likely functions of NI (Goto et al., 2001; Olucha-Bordonau et al., 2003) and the related relaxin-3 system (Liu et al., 2003; Sutton et al., 2004; Tanaka et al., 2005; Ma et al., 2007), and have provoked some functional testing of these possibilities. Central administration of RLN3 and selective RLN3 receptor agonist peptides

has been shown to increase feeding in satiated rats (McGowan et al., 2005; Hida et al., 2006; McGowan et al., 2006), but blockade of RLN3 receptor had no significant effect on feeding or body weight, (even in fasted rats; PJ Ryan, AL Gundlach, unpublished observation)), despite effective blockade of agonist-induced feeding (Kuei et al., 2007; Haugaard-Kedstrom et al., 2011). There is also considerable evidence that the NI and RLN3 signaling can modulate hippocampal theta rhythm (Ma et al., 2009b). Finally, neurogenic stressors, including forced swim stress (Tanaka et al., 2005; Banerjee et al., 2009) and stress-induced insomnia (Cano et al., 2008) activate NI neurons; and icv injection of CRF increases c-*fos* expression in NI and RLN3 neurons (Bittencourt and Sawchenko, 2000; Tanaka et al., 2005), suggesting a role of this nucleus in metabolic and behavioral adaptations to stress.

In studies aimed at better understanding the role of NI and RLN3 in the tegmentum, we used double-label immunohistochemistry to correlate the distribution of RLN3 positive fibers with differentiated neuronal subgroups in the tegmentum and pons using established neurochemical markers, including nNOS; the calcium binding proteins, calbindin-28kD (CB-28kD), calretinin(CR); the transmitter-associated enzyme, tyrosine hydroxylase (TH); and the transmitter, 5-hydroxytryptamine (5-HT). As the tegmentum is an area traversed by a high density of ascending fibers, we used double-labeling of RLN3 and synaptophysin (Jahn et al., 1985; Wiedenmann and Franke, 1985), to assess the localization of relaxin-3 at putative synaptic terminals.

(1450 words)

Materials and Methods

Animals

Male, Sprague-Dawley rats (300-400 g, n = 10) were used. All protocols were approved by the Animal Ethics Committee of the Universitat de València. All procedures were in line with directive 86/609/EEC of the European Community on the protection of animals used for experimental and other scientific purposes. Details of experimental procedures are provided in Table 1.

Brain fixation and sectioning

Rats were deeply anesthetized with an overdose of Nembutal (150 mg/kg, Euthalender, Spain) and transcardially perfused with 250 ml saline followed by 450 ml fixative (4% paraformaldehyde in 0.1 M phosphate buffer (PB), pH 7.4). After infusion of fixative over 30 min, the brain was removed from the skull and immersed in the same fixative for 4 h at 4°C. Brains were then cryoprotected by incubation in 30% sucrose in 0.01 M PBS pH7.4 for 48-72 h at 4°C. Coronal sections (40 µm) were cut using a freezing microtome (Leica SM2010R, Leica Microsystems, Heidelberg, Germany). For each brain, 6 series of sections were collected in 0.01 M PBS.

Double-label immunohistochemistry for relaxin-3 and nNOS, CB-28kD, CR, TH and 5HT

A double-label immunohistochemistry protocol was used to detect RLN3 immunoreactivity in nerve fibers and their distribution relative to various neuronal markers, including possible contacts with labeled target neurons. As the primary antibodies used were raised in different hosts (rabbit and mouse), protocols employed a combined single primary antibody incubation, followed by dual secondary antibody detection and visualization steps. For primary antibody incubations, sections were rinsed twice in Tris-buffered 0.05 M saline, pH 8.0 (TBS) and transferred to blocking solution (4% normal donkey serum (NDS), 2% bovine serum albumin (BSA) and 0.2 % Triton X100 in TBS) for 1 h at room temperature. Sections were then transferred to incubation media containing 1:2,500 rabbit anti-relaxin-3 (Ma et al., 2007; Ma et al., 2009b; Smith et al., 2009) and either 1:500 mouse anti-nNOS, AB144P (Chemicon, Temecula, CA, USA) 1:5,000 mouse anti-CB-28kD, Swant 300 (Swant, Bellinzona, Switzerland), 1:2,500 mouse anti-CR, Swant 6B3 (Swant), 1:10,000 mouse anti-TH, T1299 (Sigma, St Louis, MO, USA), or 1:50 mouse anti-5HT, H-209 (Abcam, Cambridge, MA, USA) diluted in 2% NDS, 2% BSA and 0.2% Triton X100 in TBS for 48 h at 4°C. RLN3 and different markers were then revealed in consecutive secondary antibody incubations.

For RLN3, sections were rinsed in 2 × TBS and incubated in 1:200 biotinylated donkey anti-rabbit IgG (711-065-152; Jackson Immunoresearch, West Grove PA, USA) for 0 h. Sections were then rinsed in 2 × TBS and transferred to 1:100 ABC (Vectastain PK-6100; Vector Laboratories, Burlingame, CA, USA). After rinsing (2 × TBS) the immunolabeling was revealed by immersing the sections in 0.025% DAB, 0.5% ammonium nickel sulfate, 0.0024% H_2O_2 in Tris HCl, pH 8.0 until a black colour reaction was observed. Sections were then rinsed for at least 2 h. Cell markers were then by incubation in 1:200 biotinylated donkey anti-mouse IgG (Jackson 715-065-150) for 0 h. Sections were then rinsed 2 × TBS and immersed in 1:100 ABC (Vector Laboratories) for 1 h. After rinsing (2 × TBS), the immunolabeling was revealed by incubating sections in 0.025% DAB, 0.0024% H_2O_2 in Tris HCl, pH 7.6 until a light-brown reaction was observed. Following several rinses in 0.01M PBS, sections were mounted onto gelatin-chrom alum-coated slides, air dried, dehydrated with graded ethanol, cleared with xylene, and coverslipped with DPX (Sigma).

Double-label immunofluorescence for relaxin-3 and nNOS, TH, 5HT, Syn

For detection of RLN3 and marker proteins/peptides/molecules, sections were rinsed 2 × 10 min and immersed in blocking media containing 4% NDS, 2% BSA and 0.1% Triton X-100 in TBS for 1 h at room temperature. Sections were then transferred to primary antibody solution containing 1:1,250 rabbit anti-RLN3 and either 1:1,000 mouse anti-Syn, S5768 (Sigma); 1:250 mouse anti-nNOS, N2280 (Sigma); 1:10,000 mouse anti-tyrosine hydroxylase, T1299 (Sigma); or 1:50 mouse anti-5HT, H-209 (Abcam) for 48h at 4°C. Sections were then rinsed 3 × in TBS and incubated in 1:200 FITC-labeled donkey anti-rabbit (711-095-152, Jackson Immunoresearch) and 1:200 Dylight-549 donkey anti-mouse (715-505-150, Jackson Immunoresearch) in TBS for 90 min. Sections were then briefly rinsed in 0.01 M PBS and rinsed 3 × 0.1 M PB with 2% porcine gelatine before mounting on clean slides. Slides were then air-dried, coverslipped with gelvatol and stored at -20°C.

Microscopic analysis

Permanent DAB immunohistochemistry was studied using a Nikon Eclipse E600 microscope with a DMX2000 digital camera (Nikon, Tokyo, Japan). Mappings were constructed using a camera lucida tube attached to a Zeiss Axioskop microscope (Carl Zeiss GmbH, Jena, Germany). Drawings at different coronal levels (see details below) were made with a 20× objective, then scanned and reduced to the final size. Confocal studies were conducted with a Leica TCS SPE (Leica Microsystems) using a 63× oil objective. Z-series of optical sections were obtained by sequential scanning and Z-stacks were processed with Image J software (NIH; http://rsb.info.nih.gov/ij). Wavelengths used to visualize FITC were excitation 499 nm and emission 520 nm; and for Dylight-549, excitation was 553 nm and emission 534 nm.

Results

In a series of comparative immunostaining experiments, we have documented the distribution of the relaxin-3 (RLN3) innervation within the tectum and tegmentum, relative to a number of neuronal populations labeled by characterized protein/enzyme markers, including the calcium-binding proteins calbindin-28kD (CB-28kD) and calretinin (CR); the transmitter synthetic enzymes neuronal nitric oxide synthase (nNOS) and tyrosine hydroxylase (TH); and the transmitter, serotonin (5-HT). A consistent pattern of RLN3 fibers and cells was observed in double immunostained sections, and in addition to their differential staining distribution, RLN3 fibers were morphologically different from those containing other markers - swelling in fibers with granular precipitates was commonly observed and RLN3 staining was rarely observed in smooth fibers. Lastly, because the brainstem area analyzed is traversed by a high density of ascending fibers that do not form synaptic contacts, RLN3 immunostaining was assessed for colocalization with synaptophysin (SYP) using confocal microscopy.

Comparative distribution of relaxin-3 and other markers in tectum and tegmentum

Relaxin-3 in pretectum

The distribution of RLN3 and marker protein immunoreactivity was assessed at four coronal levels within the pretectal area (Figs 1 and 2; Table 2). The pretectal area is composed of two groups of nuclei and is delineated medially by the posterior commissure, laterally by the latero-posterior thalamic nucleus and ventrally by the magnocellular nucleus of the posterior commissure. The medial group of nuclei is composed of the nucleus of the optic tract, olivary pretectal nucleus, posterior pretectal nucleus, medial pretectal nucleus and ventrolateral pretectal nucleus, while the lateral group of nuclei contains the dorsal and ventral anterior pretectal nuclei. The nucleus of the optic tract was void of nNOS- or CB-immunostaining. The olivary pretectal nucleus is composed of a central core that was void of nNOS and CB immunolabeling, although this was encapsulated by a shell that containing neurons immunopositive for both CB and nNOS. The medial pretectal nucleus also contained some CB-positive neurons that were located dorsally to the bundles of the posterior commissure, though they were void of nNOS-immunostaining. We have defined the ventrolateral pretectal nucleus as a wedge-shaped nucleus located medial to the anterior pretectal nucleus and containing disperse nNOS- and CB-labeled neurons. The posterior pretectal nucleus, lateral to the medial pretectal nucleus, was void of nNOS- and CB-immunostaining. The anterior pretectal nuclei were an irregular-shaped region that was void of CB- or nNOS-immunostaining.

A consistent pattern of RLN3-labeled fibers was observed in pretectal nuclei of all brains examined (n = 6). RLN3-positive fibers were present at all levels of the pretectal nucleus extending from level A the most rostral (bregma -4.5) to level D the most caudal (bregma -5.3). RLN3-labeled fibers were observed in the medial pretectal nucleus, olivary pretectal nucleus and ventrolateral pretectal nucleus. Immunostaining in the medial pretectal nucleus extended across the entire rostrocaudal extent of the posterior commissure. Immunolabeling in the olivary pretectal nucleus was evenly distributed in the core and shell. The ventrolateral pretectal nucleus also contained RLN3-positive neurons that extended from level B to D. Extensive colocalization of synaptophysin and RLN3-immunoreactivity was observed in nerve fibers in the medial pretectal area (MPT) (Fig. 3E-G) and other pretectal nuclei (Fig. 3), indicating the presence of putative synaptic contacts in these regions.

Relaxin-3 in the superior colliculus

RLN3 and marker protein immunoreactivity was assessed at five rostrocaudal levels in the superior colliculus (SC). The relative density of RLN3 labeling is summarized in Table 3. The presence of alternating grey and white matter layers and differential distributions of nNOS and CB immunoreactivity were used to define the layers of SC. The superficial grey layer below the zonal layer displayed a high density of small nNOS- and CB-positive neurons, whereas ventrally, the optic tract layer contained a lower density. The next intermediate grey layer displayed a high CB-positive neuron density and sparse nNOS-positive neurons. The intermediate white layer was void of CB-immunostaining, although it contained sparse nNOS-positive neurons. At caudal levels, the deep grey layer contained a moderate density of CB and nNOS neurons, while the deep white layer contained scarce CB and nNOS positive neurons. nNOS-labeled soma in the deep grey and deep white layers were continuous with the dorsolateral column of the periaqueductal gray (PAG).

A consistent pattern of RLN3-labeled fibers was observed throughout SC of all brains examined. This pattern differed along the rostrocaudal and mediolateral axis of each layer and was dependent upon layer stratification (Figs. 4 and 5). Level 1 corresponds to the posterior commissure at which some dispersed RLN3-labeled fibers were observed in the intermediate white layer.

A higher density of RLN3-labeled fibers was observed at the level of the SC commissure (level 2). RLN3-labeling was denser in the intermediate grey layer, which also displayed a higher density of CB-labeled neurons (Fig. 5B). Some scattered fiber staining was also observed in the optic and deep layers at this level. The most lateral area of the deep layers was void of both RLN3- and CB-labeling (Figs. 4 and 5B).

At level 3, nNOS positive cells of the dorsolateral PAG column were evident and extended to the deep layers of SC (Figs. 4 and 5C). In addition to their presence in the superficial gray layer (SuG), nNOS-labeled neurons were also concentrated in the intermediate (InG) and deep grey (DpG) layers (Fig. 4C). A high density of RLN3-labeled fibers was present in the InG, particularly in medial aspects. Some RLN3-labeled fibers were also observed in the medial aspects of the other deep layers and the optic layer (Op) (Figs. 4 and 5C).

At the level of the bed nucleus of the brachium of inferior colliculus (IC) (level 4), RLN3-labeled fibers were very dense in the medial area of InG compared to more rostral levels. Other deep layers also contained RLN3-labeling with a high to low gradient along the mediolateral axis (Figs. 4 and 5D). Presence of RLN3-labeled fibers coincided with areas containing nNOS-labeled cells (Fig 4,. Some RLN3-labeled fibers were also observed in lateral aspects of the Op (Figs. 4 and 5D).

At level 5, where the rostral external cortex of IC was present (Figs. 4 and 5E), dense RLN3-labeled plexuses were observed in the medial InG, coinciding with the distribution of CB-labeled soma (Fig. 5E). Some RLN3 fibers were detected in the medial aspects of the DpG and deep white (DpW) layers. The DpG layer displayed greater nNOS- and CB-labeling than adjacent white layers (Figs. 4 and 5E).

In addition to labeling in SC, dense RLN3 plexuses were observed in the area dorsal to the posterior and superior colliculus commissures that contained the tectal longitudinal column (Saldana et al., 2007). RLN3-labeled fibers were present in these columns at a similar density to that observed in medial aspects of SC (Figs. 3C,D, 4 and 5). Colocalization of synaptophysin and RLN3 in nerve fibers in the InG layer (Fig. 6E-G) and other deep layers indicated the presence of putative RLN3 synaptic contacts in these regions.

Relaxin-3 in inferior colliculus

Immunostaining was assessed at four rostrocaudal levels of IC. The relative density of RLN3-labeling is summarized in Table 4. The most rostral level 1 is predominantly occupied by the external cortex (EC). Neuronal NOS-labeled neurons were concentrated in layer 3 and were not observed in layers 1 and 2 (Fig. 7). The central nucleus of IC is composed of a dorsomedial area containing nNOS-positive neurons and an unlabeled lateral strip. Dorsal to the PAG, a medium density of nNOS-labeled neurons was observed in the dorsal nucleus of IC. Finally, no nNOS-labeling was detected in the intercollicular nucleus, which lies between the IC and PAG.

At levels 2 and 3, the external nucleus of IC (ECIC) occupies a superficial band of 3 layers and we observed dense nNOS-labeled neurons in layer 3 (Fig. 7). The central nucleus of IC was composed of a dorsomedial nNOS-positive area and a ventrolateral nNOS-negative area, with a gradual transition between them. The dorsal nucleus of IC contained some dispersed nNOS-positive cells intermingled with fiber bundles of the IC commissure. The intercollicular nucleus consisted of a band separating the central nucleus and PAG.

At level 4, the ECIC appeared displaced dorsally. The nNOS-negative area of the central nucleus largely occupied the ventrolateral aspects, with the nNOS-positive area restricted to the dorsomedial corner. The dorsal nucleus of IC and the intercollicular area were reduced to a thin strip. Dense RLN3-labeled plexuses were observed in the dorsal nucleus of IC (DCIC) and layer 1 of ECIC. The boundaries between layers of the external cortex were defined by NOS-positive cells in layer 3. Regions containing RLN3 fibers formed a band around the central and dorsal nuclei and were in continuity with the commissural and intercollicular areas medially, the sagulum and parabigeminal nuclei ventrolaterally, and the cuneiform nucleus ventrally (Figs. 7 and 8A-D). Colocalization of synaptophysin and RLN3 in nerve fibers in the DCIC (Fig. 8E-G) and ECIC, indicated the presence of putative RLN3-containing synapses.

Relaxin-3 in the periaqueductal grey

RLN3 and marker protein immunoreactivity was assessed at six levels of the periaqueductal grey (PAG), with reference to several anatomical landmarks. The relative density of RLN3 labeling is summarized in Table 5.

At level 1, the posterior commissure capped the aqueduct dorsally. Neurons around the aqueduct were classed as the precommissural nucleus (PrC) that extended rostrally (Canteras and Goto, 1999b). RLN3-labeled fibers were concentrated along the inner ring of the aqueduct and nNOS- and TH-positive cells were detected as two rows parallel to the aqueduct in the ventral half. The dorsal part contained a lower density of RLN3-labeled fibers where TH- or NOS-labeled neurons were absent. Nevertheless, some RLN3-labeled fibers were observed in the medio-dorsal tip, which we identified as the precommissural nucleus. Some RLN3-labeled fibers were observed ventrally between the bilateral Darkschewitsch nuclei together with a row of nNOS- and TH-positive neurons lying parallel to the ependyma. In the ventral tip of the aqueduct, RLN3-labeled fibers continued ventrally to the supramammillary nucleus and the posterior hypothalamic nucleus. In contrast, no RLN3 was observed in the parafascicular nucleus adjacent to the fasciculus retroflexus or in the subcommissural organ (Figs. 9 and 10A). nNOS-positive neurons and fibers extended ventrally between the medial forebrain bundle fascicles, in apparent continuity with the supramammillary nucleus (Fig. 9A).

At level 2, a region dorsal to the aqueduct, between the posterior and the superior colliculus commissures, was occupied by the intercommissural area (InC) and has not been formally described as part of PAG. Ventral to the InC, the lateral column flanked both sides of the aqueduct. At this level,

the InC nucleus contained dense plexuses of RLN3-labeled fibers that were largely confined to the posterior and the superior colliculus commissures. More ventrally, the lateral part of the PAG column lacked RLN3-immunostaining. In contrast, RLN3-labeling was denser in the juxta-aqueductal ring where some nNOS- and TH-positive cells of fusiform morphology were detected. Some RLN3-labeled fibers were observed in the Edinger-Westfal nucleus, among TH- and nNOS-positive neurons (Figs. 9 and 10B).

At level 3, the dorsomedial column (DM) replaced the intercommissural nucleus. Scattered RLN3-labeled fibers were detected in the outer division of the dorsomedial column, and a high density was observed in the inner division of the dorsomedial column. Sparse labeled fibers were observed in the lateral column, though denser labeling was observed in the inner half, where nNOS- and TH-positive cells and processes were observed. RLN3-labeled fibers coursed vertically through the Edinger-Westfal nucleus (Figs. 9 and 10C).

At level 4, the dorsolateral column (DL) appeared as a wedge-shaped nucleus containing nNOS-positive neurons that divided the PAG into the DM column located dorsally and the lateral column (L) ventrally. Ventral to the lateral column and dorsal to the accessory nucleus of the oculomotor nucleus (Su3), a row of nNOS-positive neurons were detected in the supraoculomotor cap (Su3C). RLN3-labeled fibers were observed among nNOS-labeled soma of the DL column, and densely near the aqueduct (Fig. 9D). Some labeling was also observed in the most medial division of the DM column. RLN3-labeling was absent in the L PAG column, although some labeling was detected in the inner half among TH-positive neurons. Some labeled fibers were also observed in the nNOS-positive Su3C and Edinger-Westfal nucleus (Figs. 9 and 10D).

At level 5, the DL column persisted and the mesencephalic trigeminal nucleus defines the lateral border of PAG. At this level, the PAG protruded laterally and is composed of the lateral (L) and the ventrolateral (VL) columns. The dorsal raphe nucleus lies ventral to the aqueduct, bordered by the medial longitudinal fascicle bundles. The trochlear oculomotor nucleus appears just dorsal to this fascicle. Dense plexuses of RLN3-labeled fibers were observed among nNOS-positive neurons of the dorsolateral column (Fig. 9E). Sparse fiber labeling was detected in the DM column, whereas RLN3-labeling in the lateral and ventrolateral columns was dense in the inner half. Densely RLN3-labeled fibers were detected in both the dorsal and ventral divisions of the dorsal raphe, which contained nNOS- and TH-positive neurons. In contrast, the trochlear oculomotor nucleus was void of any immunostaining (Figs. 9 and 10E).

Level 6 comprised of the expansion of the aqueduct into the fourth ventricle. Laterally and dorsally, the PAG was reduced to a strip of cells around the aqueduct, where nNOS-positive neurons were observed in the dorsal PAG, just above the ependyma. The L column extended to the dorsal border of the mesencephalic trigeminal nucleus. The VL column occupied the entire area ventrolaterally, bordered by the bundles of the medial longitudinal fascicle and medially, bordered by the dorsal raphe. RLN3-labeled fibers were densely observed in the DL and DM columns, and less labeling was observed in L and VL columns. RLN3-labeling was less evident in the dorsal, ventral and lateral divisions of the dorsal raphe, which contained nNOS- and TH-positive neurons (Figs. 9, 10F and 12A,B).

Dense RLN3 labeling in the DL coincided with nNOS-positive neurons. High magnification analyses of RLN3-labeled terminals revealed close synaptic contacts with nNOS-labeled soma and processes. In contrast, analyses of RLN3 and synaptophysin colocalization (Fig. 11I-K) indicate that the primary targets of RLN3-containing terminals are not nNOS neurons, but more likely another unknown population of neurons of the DL column.

Relaxin-3 in ventral tegmental nuclei

The cuneiform nucleus, microcellular tegmental nucleus and parabigeminal nucleus were observed ventral to the IC. At caudal levels, only the cuneiform nucleus and nucleus sangulum were detectable. RLN3-labeled fibers were observed in the nucleus sagulum and parabigeminal nucleus, and were absent in the microcellular tegmental nucleus and pedunculopontine tegmental nucleus (Fig. 7C-D). A band of RLN3-labeled fibers was observed between IC and PAG and continued into the cuneiform nucleus (Fig. 12C, D). Colocalization of synaptophysin and RLN3 was observed in nerve terminals in the cuneiform nucleus (Fig. 12E-G).

Relaxin-3 in pontine central grey

Immunostaining was assessed at five rostrocaudal levels of the pontine central grey (PCG) that extended from the dorsal raphe (DR) area to the prepositus hypoglossal nucleus. At level 1, the midline region is occupied by the DR, which contained nNOS- and 5HT-positive neurons. Laterally, we identified the dorsal tegmental nucleus (DTg) as a circular area that was void of any marker and flanked laterally by the PAG VL column. The median raphe (MnR) was located ventral to the DR. At this level of the pons, the central grey occupied the floor of the fourth ventricle (Figs. 13A, 14A and 15A). The rostral-most level is continuous with the caudal PAG. In the midline, the DR displayed a dense plexus of RLN3-labeled fibers, which was continuous with that in the median and paramedian raphe and in the caudal interpeduncular nucleus, which also contained 5-HT-positive neurons (Figs. 13A, 14A and 15A).

Levels 2 and 3 were characterized by the presence of the laterodorsal tegmental nucleus (LDTg), which contained a high density of nNOS-positive neurons and some TH-positive cells and processes. The pontine raphe nucleus (PnR) appeared as a midline group of 5HT- and nNOS-positive cells that lie between the medial longitudinal fasciculus (mlf) bundles. At these levels, sparse RLN3-labeled fibers were observed among nNOS-positive neurons of the LDTg (Fig. 13B,C), and the DTg was void of RLN3-immunostaining. In the midline, the DR contained a dense plexus of RLN3-labeled fibers intermingled among nNOS-positive neurons (Fig. 13B-D). This caudal area of the DR contained some nNOS-positive, but no TH-positive cells (Figs. 13BC, 14BC and 15B,C).

At level 4, the locus coeruleus (LC) was evident with dense TH-labeling and Barrington's nucleus (Bar) was identified between the LC and LDTg. At this level, RLN3-labeled neurons were observed intermingled with 5-HT-positive neurons of the midline PnR, this was considered the rostral-most extent of the NI. 5-HT-positive neurons were also encapsulated by dense RLN3-labeled fibers, which extended dorsolaterally and ventrolaterally around the unlabeled DTg. RLN3-immunostaining was dense in the LDTg and Bar, but was absent in LC (Figs. 13D, 14D and 15D).

At level 5, the NI pars compacta (NIc) was observed in the midline, which extended ventrolaterally as the pars dissipata (NId). The LDTg was not present at this level as reflected by the lack of nNOS-immunostaining. The NI contained the highest density of RLN3-labeled neurons, which were observed in both the midline NIc and lateral NId (Figs. 13, 14 and 15E). Higher magnification analyses of NI neurons revealed intense RLN3-immunoreactivity within the soma, and within neurites that co-localized with synaptophysin (Fig. 16 A, I-K). Interestingly, RLN3-positive fibers were observed to make close synaptic contact with 5-HT-labeled soma of DR (Fig. 16C-E) and colocalization of RLN3 and synaptophysin (Fig. 16F-H) was greatest in DR compared to other nuclei.

Discussion

In this study, we have constructed a detailed map of the distribution of RLN3 fibers throughout the dorsal mesencephalon and pons, which comprises the pretectum, colliculi, periaqueductal grey, ventral tegmental nuclei and pontine central grey. By employing double-label immunohistochemistry to stain coronal sections for RLN3 and specific markers of each of these major nuclei, this study accurately details the distribution of RLN3 elements in the tectum and tegmentum. Our observations reveal that RLN3 fibers preferentially target medial and olivary pretectal nuclei and an area identified as the ventrolateral pretectal nucleus. The innervated areas extend along the midline between cell groups located around the posterior SC and IC commissures. In the SC, RLN3 fibers target medial aspects of the InG and caudomedial aspects of deep layers. In the IC, labeled fibers encapsulate the central nucleus of layer 1 of the ECIC and DCIC, which extends rostrally to the brachium of the IC and ventrally to the cuneiform nucleus. In the PAG, RLN3 fibers principally target the dorsolateral column containing nNOS-positive neurons. At more caudal PAG levels, some fibers were observed in the medial half of the lateral and ventrolateral columns, which contained TH-positive neurons. RLN3 fibers were detected among nNOS- and TH-positive neurons of the LDTg and in DR and PnR, identified by the presence of 5HT-positive neurons.

One important aspect to be considered is the origin of the RLN3 immunoreactive fibers. Tracer methods reveal that the NI provides innervation to all labeled areas (Goto et al., 2001; Olucha-Bordonau et al., 2003). However, three other centers also display a few amount of RLN3 positive somata that are the lateral part of the substantia nigra, the rostral ventromedial part of the PAG and the raphe pontis nucleus (Tanaka et al., 2005; Ma et al., 2007). The possibility that part of the innervation to the areas described in this article arise from other RLN3 other than NI it is not excluded. Tracer injections in the peripeduncular area that surrounds, but may also include the substantia nigra pars lateralis, result in anterograde labeling in the superior and inferior colliculus, central grey and cuneiform nucleus (Arnault and Roger, 1987). It has been found connections from the ventral medial periaquerductal grey to the intergeniculate leaflet (Blasiak et al., 2009) , however, to our knowledge there is not a description of the efferent connections of this particularly small group of the PAG. Finally, the neurons in the pontine raphe nucleus could be considered as a rostral extension of the NI.

In general, unimodal sensory areas of SC and IC (i.e. superficial layers of SC and the central and dorsal nuclei of IC), are devoid of RLN3 fibers, while polymodal sensory areas such as the deep layers of SC and paracentral areas of IC are strongly innervated. Similarly, the anterior pretectal nuclei that are mainly involved in nociception are generally devoid of RLN3 fibers, in contrast to other pretectal nuclei involved in visuomotor control that receive a strong RLN3 innervation. Importantly from the point of likely functional activity, in all RLN3-positive areas, we observed colocalization of RLN3 with synaptophysin, indicating that RLN3 immunoreactivity is present in presynaptic structures, consistent with active sites of release. These observations are consistent with the presence of high concentrations of RLN3 receptors (RXFP3 mRNA and RLN3 agonist binding sites) in these areas (Sutton et al., 2004; Ma et al., 2007) . Some relevant technical issues and the specific and broader functional implications of this complex innervation pattern are discussed below.

Technical considerations

The specificity of the RLN3 antisera used has been validated in rat (Ma et al., 2007), mouse (Smith et al., 2010)and primate(Ma et al., 2009a), and the distribution of RLN3 observed in different species appears highly conserved. The distribution patterns observed for the different neurochemical

markers used (nNOS, CB, CR, TH and 5-HT) agree with previous findings (e.g. (Onstott et al., 1993), Paxinos and Watson, 1998). In addition to the NI, three other nuclei contain RLN3 expressing neurons - the PnR, the anterior-ventral part of PAG, and a region dorsal to the lateral substantia nigra in both rat (Tanaka et al., 2005; Ma et al., 2007) and mouse(Smith et al., 2010). While it is more likely, based on the dense labeling observed in the tectum and tegmentum following anterograde-tracing from the NI (Olucha-Bordonau et al., 2003), that the RLN3 innervation of these regions predominantly arises from the NI, these other nuclei may provide some tectal and tegmental RLN3-positive elements, and it will be of interest to assess this possibility in future studies.

Synaptophysin, a constituent of the synaptic vesicle membrane, is widely used as a marker of presynaptic terminals. Although there is some controversy about its exact role, synaptophysin is believed to be involved in transmitter secretion (Thomas and Betz, 1990), and synaptic vesicle recycling (Daly et al., 2000; Daly and Ziff, 2002; Pennuto et al., 2003). We observed widespread colocalization of RLN3 with granular synaptophysin immunoreactivity, suggesting the capability and occurrence of synaptic RLN3 transmission in the tectum and tegmentum under normal and/or pathological conditions (see(Tanaka et al., 2005; Ma et al., 2007)).

Functional considerations

Pretectum

In earlier studies, some anterograde labeling of efferents of the rat NI was observed in the posterior pretectum and medial pretectum (Olucha-Bordonau et al., 2003) and specific RLN3 immunostaining was observed in the rat medial pretectal nucleus(Ma et al., 2007). This study has provided further strong support for the existence of an NI/RLN3 projection to the pretectal area in the rat. We observed dense RLN3 fibers in the medial pretectal nucleus, and moderate labeling in the olivary pretectal nucleus, and in a triangular area just medial to the anterior pretectal nucleus and ventral to the olivary pretectal nucleus, which we named the ventrolateral pretectal nucleus. This area is clearly different from the surrounding nuclei based on its neurochemical content (Paxinos et al. 2008), and here we observed dense nNOS- and CR-positive cells with RLN3 fibers in the ventrolateral pretectal nucleus.

The olivary pretectal nucleus receives direct afferents from the retina that are thought to be responsible for the pupillary reflex (Klooster et al., 1995). Interestingly, efferent projections from the olivary pretectal nucleus innervate medial aspects of the intermediate grey layer of SC and the adjacent PAG (Klooster et al., 1995), which contain dense RLN3 fibers plexuses. The medial and posterior pretectal nuclei project to the intergeniculate leaflet and the suprachiasmatic nucleus and are involved in the regulation of behavior across the light/dark cycle. The intergeniculate leaflet receives a substantial RLN3 innervation (Tanaka et al., 2005; Ma et al., 2007) and projections exist from the NI to the ventral suprachiasmatic nucleus (Olucha-Bordonau et al., 2003), although the relative magnitude of the RLN3 innervation of the suprachiasmatic nucleus was not described (Tanaka et al., 2005; Ma et al., 2007). The medial pretectal nucleus contains a dense plexus of RLN3 fibers and the medial (and posterior) pretectal nuclei send projections to the thalamic nucleus reuniens (Krout et al., 2001) that in turn supplies a strong excitatory input to the CA1 field of hippocampus. A role for the medial pretectal nucleus in control of circadian activity has been suggested by results from studies in hamsters using non-photic circadian stimulation (Marchant and Morin, 1999). Furthermore, recent anatomical and physiological studies have revealed that the

intergeniculate leaflet in the rat receives its RLN3 innervation primarily from RLN3 neurons in the anterior PAG and IGL neuron activity is modulated by RXFP3 activation *in vitro* (Blasiak et al., 2009)

Superior colliculus

In previous studies, NI efferents were observed in superficial layers of rat SC following BDA injections into the NI (Olucha-Bordonau et al., 2003) and discrete RLN3 staining was reported in SC (Tanaka et al., 2005) (Ma et al., 2007). In the present study, a high density of RLN3 fibers was detected in the medial half of SC and a denser innervation of the intermediate grey layer than of adjacent layers. This pattern correlates well with that for the RLN3 receptor, RXFP3 in SC (Ma et al., 2007). *In situ* hybridization histochemistry for RXFP3 mRNA and radioligand binding autoradiography for RXFP3 protein revealed a very high density of receptors in the medial region of what appears to be the optic or intermediate grey layer(s). In fact, the pattern is consistent with the expression of receptor by neurons in such a 'cell-rich' layer and presence of receptor protein in axonal or dendritic elements of these cells in the most dorsal neuropil, immediately adjacent to the dorsal surface of the SC. Further studies of this anatomy and associated function are warranted.

Anatomical and electrophysiological studies of SC identify this region as a key 'warning' site in early orienting responses to relevant stimuli (Grantyn, 1988; Munoz and Wurtz, 1992; Munoz et al., 1996; Krout et al., 2001) independent of its modality (Stein and Meredith, 1990; Stein et al., 1993). The SC is suited to this function because it processes topographic, visual representations of the environment, whereby information from the retina is topographically represented in the superficial layers (Berman and Cynader, 1972). Visual information is then transferred to inner layers in such a way that the upper visual field is represented in the medial aspects of SC, while the lower visual field is represented in the lateral aspects (Meredith and Stein, 1990). In deep layers of SC, visual information converges with other auditory and/or somatosensory modalities (Wallace et al., 1998). This overlap and neural integration then enables an animal to localize the source of an auditory stimulus and direct its head and eyes towards it. In the case of auditory information, a tonotopic map must be adapted to the visual map and the convergence of these maps is organized by projections from the external cortex and the brachium of IC (Skaliora et al., 2004). In this study, we observed that these IC components receive an RLN3 innervation, suggesting that RLN3 transmission may help to shape these sensory maps.

In addition, we hypothesize that RLN3 projections to SC participate in defensive mechanisms. Different groups of SC cells are activated by particular types of stimuli. Medially located neurons are maximally responsive to small, dark and slowly moving objects from the upper visual field (Drager and Hubel, 1975; Dean et al., 1989). These signals may warn danger (e.g. for a rat, an airborne predator) and elicit freezing (Blanchard et al., 1986). In contrast, neurons in the lateral aspects of SC are maximally responsive to the lower visual field (e.g. associated with potential food in the rat) and may enable orienting, approach, hunting and consumption (Furigo et al., 2009; Furigo et al., 2010). As various stressors are able to activate NI neurons (Tanaka et al., 2005; Smith et al., 2009; Banerjee et al., 2010; Ryan et al., 2011), the NI/RLN3 projection to the medial deep layers of SC may provide a feedback regulatory modulation of the centers involved in performing an orienting response to threatening stimuli. An influence of RLN3 transmission on neurons in lateral areas involved more in approaching behavior, appears to be less important.

Inferior colliculus

Anterograde labeling in IC after BDA injections into the rat NI and RLN3 labeling in the region have not been reported (Olucha-Bordonau et al., 2003). However, here we observed a consistent tract of RLN3 fibers present in a thin band surrounding the external cortex and the dorsal nucleus of IC, while the central nucleus and the inner layers of both the external cortex and dorsal nucleus lacked labeling. These RLN3 fibers continued in a ventromedial band bordering the caudal levels of PAG and into the intercollicular nucleus. These areas are reported to belong to the extra-tegmental auditory pathway that projects to the inner layers of SC (Skaliora et al., 2004; Garcia Del Cano et al., 2006) and the paralaminar thalamic nuclei (Ledoux et al., 1987). The paralaminar thalamic nuclei, as a whole, project to the amygdala and the afferents from the IC are thought to transmit multisensory information. The projection mapped from the external cortex and dorsal nucleus of IC to SC (Garcia Del Cano et al., 2006) overlaps very closely the pattern of RLN3 fibers we observed in SC. In addition, the efferent fibers from the external cortex of IC to SC branched to the dorsolateral column of PAG (Garcia Del Cano et al., 2006), where a dense plexus of RLN3 fibers was observed. The projection from the external cortex and dorsal nucleus of IC to SC may be involved in the generation of an auditory map over SC (Skaliora et al., 2004).

Medial tectal groups

Throughout the rostrocaudal extent of the tectum, a plexus of RLN3-positive fibers was observed in the midline area of the posterior, SC and IC commissures, intermingled with fiber tracts and cell groups. Similar labeling has been observed around the commissure of IC (Tanaka et al., 2005) and the commissure of SC (Ma et al., 2007). In fact, the RLN3 projection to this area extends from the pretectal area to IC. RLN3 labeling was not restricted to the area of the defined tectal longitudinal column (Saldana et al., 2007; Aparicio et al., 2010), which receives projections from SC, IC and the brachium of IC, and is mainly involved in auditory processing (Aparicio and Saldana, 2009; Aparicio et al., 2010). The longitudinal organization of RLN3 projections over the midline tectum appears to parallel the longitudinal organization of PAG columns and appears superimposed on the nuclear organization of the pretectal area, the stratigraphical organization of SC and the concentric organization of IC. Notably, a similar pattern was observed in non-human primate brain (Ma et al., 2009a).

Periaqueductal gray

Anterograde-labeled NI efferents and RLN3 fibers have been described in PAG (Goto et al., 2001; Olucha-Bordonau et al., 2003) (Tanaka et al., 2005; Ma et al., 2007). In addition, RLN3-labeled soma are also observed in the ventral juxta-aqueductal ring (Tanaka et al., 2005; Ma et al., 2007; Brailoiu et al., 2009). Occasional soma were observed in the current study, but without colchicine pre-treatment to produce cellular accumulation of RLN3, somatic labeling was relatively poor. Nonetheless, on the basis of our double-label maps, the nNOS-positive DL column of PAG was the area most densely targeted by RLN3 fibers. Earlier *in situ* hybridization studies of RXFP3 expression revealed two strong hybridization signals, one in the dorsal aspects, which likely includes the dorsolateral and dorsomedial columns and another, corresponding to the ventrolateral column, with the lateral column unlabeled (Ma et al., 2007).

The best studied of PAG subdivisions, the dorsolateral column, was similarly targeted by RLN3 fibers, and has been documented to display strong c-*fos* activation following exposure to a predator (Canteras and Goto, 1999a). However, activation of the dorsolateral column induces inhibition of the ventrolateral column, resulting in inhibition of the freezing response (De Oca et al., 1998). This is

consistent with the view that PAG is organized so that dorsal and lateral columns drive active responses to threatening stimuli, while the ventrolateral column drives quiescent responses such as freezing (Bandler and Keay, 1996). According to this model, stress-induced activation of the NI could activate the GABA/RLN3 projection to the dorsolateral column reducing its inhibition of the ventrolateral column, and resulting in an increased freezing response. The dorsolateral column also has a putative role in the control of anxiety as different anxiogenic drugs induce c-*fos* in its rostral part (Singewald and Sharp, 2000). Infusion of a substance P receptor antagonist into the dorsolateral column, but not the deep layers of SC, reduced fear-potentiated startle (Zhao et al., 2009). The dorsolateral column, unlike other PAG columns, receives projections from areas 10m, 25 and 32 of prefrontal cortex (Sesack et al., 1989; An et al., 1998; Floyd et al., 2001; Gabbott et al., 2005); and projects to the cuneiform nucleus (Cameron et al., 1995); and both the prefrontal cortex and the cuneiform nucleus receive RLN3 fibers.

Notably, RLN3 fibers were observed in an area between the posterior and SC commissures that we termed the 'rostral PAG' which displayed different cytoarchitectonic features from the caudally located dorsomedial column (Ruiz-Torner et al., 2001). Cells of this rostral PAG are activated by predator encounter and c-*fos* activation diminishes at more caudal levels where the dorsomedial column is present (Canteras and Goto, 1999a). Furthermore, the density of neurons expressing estrogen receptor alpha is higher in the rostral tip of the PAG compared to the more caudally located dorsomedial column (VanderHorst et al., 1998), suggesting a different neurochemical profile for neurons in this area.

The lateral and ventrolateral PAG columns were essentially devoid of RLN3 innervation, although we did observe fibers in the inner area containing TH-positive cells and processes. This data supports the view that there are two regions within the lateral and ventrolateral columns (Ruiz-Torner et al., 2001) with different functional roles (e.g. predator-related behavior evokes c-*fos* activity specifically in the lateral half of the mid-rostrocaudal levels of the lateral PAG column(Comoli et al., 2003).

Lateral tegmental cell groups

RLN3 fibers were observed in several regions within the midbrain tegmentum, which comprises the cuneiform nucleus, the nucleus sagulum, the parabigeminal nucleus and the brachium of IC. The presence of RLN3 fibers in the latter area appears to be the continuation of fibres in the external cortex and dorsal nucleus of IC. Electrophysiological studies have shown that visual and auditory inputs from the superficial SC and the brachium of IC, respectively, are summed linearly in cells of deep layers of SC, thus providing a framework in which visual and auditory maps are aligned (Skaliora et al., 2004). The RLN3 projection to the brachium and deep layers of IC may contribute to the modulation of this process.

The parabigeminal nucleus is reciprocally connected with SC (Roldan et al., 1983; Usunoff et al., 2007) and projects to the amygdala (Usunoff et al., 2006). It is thought to participate in a 'multi-neuronal' pathway that conveys extra-geniculate visual information to the amygdala to mediate quick responses to threatening visual stimuli (Usunoff et al., 2007). The nucleus sagulum receives afferents from auditory cortical areas and projects to the dorsal nucleus of IC and the dorsal division of the medial geniculate body (Beneyto et al., 1998), with a role in processing auditory information. Thus together, the parabigeminal nucleus and the nucleus sagulum form a continuous visual and auditory lateral column involved in aspects of sensory processing that may be modulated by RLN3.

Anterogradely-labeled NI efferents were observed in the cuneiform nucleus (Olucha-Bordonau et al., 2003); and here we observed RLN3 fibers. The cuneiform nucleus, like the medial region of the intermediate grey layer of SC, receives projections from the so-called 'medial hypothalamic zone defensive system', comprising the anterior hypothalamic nucleus, dorsal ventromedial hypothalamic nucleus and dorsal premammillary nucleus (Canteras and Swanson, 1992). Notably, the cuneiform nucleus, like SC, responds to visual threatening stimuli such as suddenly expanding shadows in the upper visual field, and together with the dorsolateral PAG column is considered as part of the neural network involved in defense behaviors in response to predatory attacks (Canteras, 2002).

Pontine central grey

In the pontine central grey, RLN3 fibers avoid the DTg and LC (Tanaka et al., 2005; Ma et al., 2007),but strong labeling was observed in the DR and PnR, LDTg, and Barrington's nucleus. Like the NI, the DR and PnR display a widespread pattern of connections with 'prosencephalic' areas that are classified as 'limbic' structures. The raphe nuclei also project to midline and intralaminar thalamic nuclei (Vertes et al., 2010), but in contrast to the NI, few, if any, projections from the raphe nuclei reach the tectal area (Vertes and Kocsis, 1994). The raphe nuclei have been shown to modulate general arousal (Mendelson et al., 1987; Jacobs and Azmitia, 1992), and more recent evidence in the mouse suggests a role for RLN3 signaling in arousal regulation (Smith et al., 2010; Smith et al., 2011; Smith et al., 2012)

The LDTg is a cholinergic group considered to be involved in regulation of the sleep/wake cycle. Neurons of this area provide a major input to the thalamus (Wainer and Mesulam 1990) and activity of these neurons is linked to REM sleep (Steriade and McCarley 1990). In addition, hypocretin/orexin peptides linked to sleep-wakefulness, evoked prolonged firing of LDTg neurons and produced an increase in frequency and amplitude of EPSCs in these cells (Burlet et al., 2002). Thus, the RLN3 projection to the LDTg may provide modulation of systems involved in arousal during stress. For example, stress-induced insomnia produced a strong activation of NI neurons (Cano et al., 2008).

Conclusions

Our findings indicate that RLN3 projections originating predominantly from the NI avoid unimodal sensory areas and preferentially target tectal areas, including SC and IC, where different sensory modalities overlap. For example, the IC central nucleus and the SC superficial layer, corresponding to the primary auditory and visual areas, are not targeted by RLN3 fibers, whereas the multimodal peri-central area of IC and deep layers of SC contain a high density of RLN3-positive fibers. Another general principle evident from this data is that in most cases all components of an interconnected network receive equally weighted projections from the RLN3 (NI) system. For example, the external cortex of IC, the intermediate grey layer of SC, the DL column of PAG and the cuneiform nucleus are thought to be interconnected (Cano et al., 2008) and all are strongly innervated by RLN3 (NI) projections; consistent with a modulatory influence of RLN3 signaling over this system. Indeed, similar to the role of other widely projecting pontine nuclei, such as the LC or the raphe nuclei, the NI is not predicted to 'generate or drive' one or more major system(s) or function(s); but instead, is more appropriately predicted to play a modulatory role contributing to the fine-tuning of major functional systems.

In the current literature, there is strong evidence that an important trigger for increased NI (RLN3) neuron activity is stress and elevated brain levels of stress-related peptides (CRF), and the systems targeted and modulated by the NI during stressful conditions participate in the generation of

responses towards environmental threats. Several forms of neurogenic stressor have been shown to activate the NI (Tanaka et al., 2005; Cano et al., 2008; Banerjee et al., 2010) .This activation is likely via CRF_1 receptors that are highly expressed in the rat NI, relative to levels in other brainstem centers involved in arousal mechanisms such as the DR or LC (Bittencourt and Sawchenko, 2000; Van Pett et al., 2000). Additionally, the NI receives afferents from the prefrontal cortex that may drive goal-oriented behavior (Goto et al., 2001; Goto et al., 2001; Goto et al., 2001) in the context of both normal behavior and stress responses. In this regard, the network of interconnected tectal and tegmental regions subserve quick responses towards possible threatening stimuli. As mentioned, the external cortex of IC, the SC intermediate grey layer, the DL column of PAG and the cuneiform nucleus form an interconnected network activated by predator threats and targeted by the RLN3 and NI and may play a pivotal role in modulating behavior associated with such stressful episodes.

An important question beyond the scope of this study is the exact role of the RLN3 (NI) projections to the targeted tectal and tegmental areas. NI neurons are GABAergic and represent long ascending inhibitory projections that can likely be modulated by RLN3 transmission. Various findings, including recent effects of RLN3/RXFP3 signaling on theta rhythm in rats, allow us to postulate that RLN3 may potentiate the inhibitory action of GABA transmission in a cooperative fashion and these ideas as well as the precise underlying mechanisms are testable experimentally in future studies.

Acknowledgements

Grant sponsors: FNS received a grant from CAPES-Brasil Bex: 4494/09-1 and Fapitec edital # 01/08. CWP received a grant from CAPES-Brasil Bex: 4496/09-4. The Ministry of Health, Spain; Grant number: ISCIII-FIS PI061816 (to FEO-B); National Health and Medical Research Council of Australia; Grant number: 520299 (to SM); Grant number: 277609 and 509246 (to ALG); Johnson & Johnson Pharmaceutical Research & Development, LLC, San Diego, USA; Collaborative Research Grant (to ALG).

Tables

List of abbreviations

3PC	oculomotor nucleus, parvicellular part
3v	3rd ventricle
4	trochlear nucleus
4v	4th ventricle
5HT	5-Hydroxytryptamin
APTD	anterior pretectal nucleus, dorsal part
APTV	anterior pretectal nucleus, ventral part
Aq	aqueduct
Bar	barrington nucleus
BIC	brachium of the inferior colliculus
CB	calbindin 28 kD
cic	commissure of the inferior colliculus
CnF	nueclus cuneformis
CR	calretinin
csc	commissure of the superior colliculus
ctg	central tegmental tract
DCIC	dorsal nucleus of the inferior colliculus
Dk	nucleus of Darkschewitsch
Dlf	dorsal longitudinal fasciculus
DLPAG	dorsolateral column of the periaqueductal gray
DMPAG	dorsomedial column of the periaqueductal gray
DMTg	dorsomedial tegmental area
DpG	deep gray layer of the superior colliculus
DpMe	deep mesencephalic nucleus
DpWh	deep white layer of the superior colliculus
DRC	dorsal raphe nucleus, caudal part
DRD	dorsal raphe nucleus, dorsal part
DRV	dorsal raphe nucleus, ventral part
Dtg	dorsal tegmental bundle
DTgP	dorsal tegmental nucleus, pericentral part DTgP
ECIC	external cortex of the inferior colliculus
EW	Edinger-Westphal
fr	fasciculus retroflexus
icPAG	intercollicular area of the periaqueductal gray
iDM	dorsomedial column of the periaqueductal gray, intermediate part
IMLF	interstitial nucleus of the medial longitudinal fasciculus
InC	intercommissural nucleus of the periaqueductal gray
InCo	intercollicular nucleus
InG	intermediate gray layer of the superior colliculus
InWh	intermediate white layer of the superior colliculus
LC	locus coeruleus

LDTg laterodorsal tegmental nucleus
LDTgV laterodorsal tegmental nucleus, ventral part
LPAG lateral column of the periaqueductal gray
LPLC lateral posterior thalamic nucleus, laterocaudal part
LPMC lateral posterior thalamic nucleus, mediocaudal part
LPMR lateral posterior thalamic nucleus, mediorostral part
MCPC magnocellular nucleus of the posterior commissure
Me5 mesencephalic trigeminal nucleus
MG medial geniculate nucleus
MGD medial geniculate nucleus, dorsal part
MGM medial geniculate nucleus, medial part
MiTg microcellular tegmental nucleus
mlf medial longitudinal fasciculus
MnR median raphe nucleus
MPT medial pretectal nucleus
NIc nucleus incertus, pars compacta
NId nucleus incertus, pars disipata
NOS nitric oxide synthase
Op optic nerve layer of the superior colliculus
OPT olivary pretectal nucleus
OT optic tract
PAG priaqueductal gray
PBG parabigeminal nucleus
pc posterior commissure
PC paracentral thalamic nucleus
PCom nucleus of the posterior commissure
PDTg posterodorsal tegmental nucleus
PF parafascicular thalamic nucleus
PL paralemniscal nucleus
PLi posterior limitans thalamic nucleus
PmR `paramedian raphe
PnO pontine reticular nucleus, oral part
PnR pontine raphe nucleus
PPT posterior pretectal nucleus
PrC precommissural nucleus
RtTg reticulotegmental nucleus of the pons
Sag sagulum nucleus
SC superior colliculus
SCO subcommissural organ
SG suprageniculate thalamic nucleus
Sph sphenoid nucleus
Su3 supraoculomotor periaqueductal gray
Su3C supraoculomotor cap
SuG superficial gray layer of the superior colliculius
SuMM supramammillary nucleus, medial part

sumx supramammillary decussation
syn synaptophysin
RLN3 relaxin-3
TH tyrosine hydroxylase
VLPAG ventrolateral column of the periaqueductal gray
VTg ventral tegmental nucleus

Table 1. Details of the analysis and type of procedure conducted in these studies

Rat	Immunohistochemical Methods	Analysis
FH78, NIF2, PCM12 NIC6, MIC7, MIC8	Double immunohistochemistry - RLN3 and nNOS or CB-28kD or CR or TH or 5HT	Camera lucida
CNT2, CNT3, MIC9, MIC10	Double immunofluorescence - RLN3 and SP or nNOS or TH or 5HT	Confocal

Table 2. Semi-quantitative estimates of the distribution of RLN3 immunopositive fibers relative to neural markers in the pretectal area

Region/Marker	RLN3	nNOS	CB
MPT	+++	-	+
PPT	+	+	+++
VLP	++	++	+
OPT	++	+	+
OT	-	-	-
APTD	-	-	-
APTV	-	-	-
LPMR	++	-	+++
LPLC	++	-	+++
PLi	++	-	-

Semi-quantitative estimates were made by visual observation of microscopic fields using a 20× objective: (-) no labelling, (+) 1-4 labeled fibers or cells, (++) 5-8 labeled fibers or cells, (+++) 9-12 labeled fibers or cells, (++++) more than 12 labeled fibers or cells

Table 3. Semi-quantitative estimates of the distribution of RLN3 immunopositive fibers relative to neural markers in the superior colliculus

Region/Marker			RLN3	CB	nNOS
SuG	Anterior	Medial	+++	+++	-
		Lateral	+++	+++	-
	Posterior	Medial	++	+++	-
		Lateral	++	+++	-
Op	Anterior	Medial	-	-	-
		Lateral	-	+	+
	Posterior	Medial	+	-	-
		Lateral	-	-	++
InG	Anterior	Medial	+++	-	+
		Lateral	+	-	-
	Posterior	Medial	+++	+	++++
		Lateral	+	+	+
InWh	Anterior	Medial	-	-	-
		Lateral	-	+	+
	Posterior	Medial	-	+	++
		Lateral	-	-	-
DpG	Anterior	Medial	-	-	-
		Lateral	-	+	-
	Posterior	Medial	+	++	++
		Lateral	+	-	-
DpWh	Anterior	Medial	+	+	-
		Lateral	-	+	-
	Posterior	Medial	+	++	++
		Lateral	+	-	+

Semi-quantitative estimates were made by visual observation of microscopic fields using a 20× objective: (-) no labelling, (+) 1-4 labeled fibers or cells, (++) 5-8 labeled fibers or cells, (+++) 9-12 labeled fibers or cells, (++++) more than 12 labeled fibers or cells

Table 4. Semi-quantitative estimates of the distribution of RLN3 immunopositive fibers relative to neural markers in the inferior colliculus and lateral tegmental nuclei

Region/Marker	nNOS	RLN3
DCIC	+	+++
InCo	-	-
CIC medial	+++	-
CIC lateral	-	-
ECIC1	+	+++
ECIC2	+	-
ECIC3	+++	-

Region/Marker	nNOS	RLN3
Sagulum n.	-	+
Parabigeminal n.	-	++
Brachium of IC	++	+
Cuneiform n.	-	++
MiTg	-	-
Nuclei of lateral lemniscus	-	-

Semi-quantitative estimates were made by visual observation of microscopic fields using a 20× objective: (-) no labelling, (+) 1-4 labeled fibers or cells, (++) 5-8 labeled fibers or cells, (+++) 9-12 labeled fibers or cells, (++++) more than 12 labeled fibers or cells

Table 5. Semi-quantitative estimates of the distribution of RLN3 immunopositive fibers relative to neural markers in the periaqueductal gray

Region/Marker	RLN3	TH	nNOS
Dk	-	+++	++
DL-PAG	+++	-	++++
DM-PAG (inner iDM)	+++	-	+
DM-PAG (outer oDM)	+	-	-
EW	++	++	++
InC	++++	-	-
LPAG (medial)	+	++	+
LPAG (lateral)	-	-	-
MCPC	-	-	++++
PCom	-	-	-
PrC	++	-	-
SCO	-	-	-
Su3	-	-	-
Su3C	+	+	+++
SuMM	++++	+	++
TLC	++	-	-
VLPAG (medial)	+	+	+
VLPAG (lateral)	-	-	-

Semi-quantitative estimates were made by visual observation of microscopic fields using a 20× objective: (-) no labelling, (+) 1-4 labeled fibers or cells, (++) 5-8 labeled fibers or cells, (+++) 9-12 labeled fibers or cells, (++++) more than 12 labeled fibers or cells

Table 6. Semi-quantitative estimates of the distribution of RLN3 immunopositive fibers relative to neural markers in the pontine central gray

Region/Marker	nNOS	TH	5HT	RLN3
LDTg	++++	++	-	++
LDTgV	+	++	-	-
DRd	++	++	+	+++
DRv	++	-	++	+++
DTgP	+	-	-	-
DTgC	-	-	-	+
MnR	++	-	+	++
PMR	-	-	-	+
PnR	-	-	++	++
VTg	-	-	-	-
Bar	-	+++	-	+
LC	-	++++	-	+
DRC	-	-	++	+++
Sph	-	-	-	-
NIc	-	-	-	++++
NId	-	-	-	+++
PDTg	+	-	-	-

Semi-quantitative estimates were made by visual observation of microscopic fields using a 20× objective: (-) no labelling, (+) 1-4 labeled fibers or cells, (++) 5-8 labeled fibers or cells, (+++) 9-12 labeled fibers or cells, (++++) more than 12 labeled fibers or cells

References

An X, Bandler R, Ongur D, Price JL. (1998) Prefrontal cortical projections to longitudinal columns in the midbrain periaqueductal gray in macaque monkeys. J. Comp. Neurol. 401: 455-479..

Aparicio MA, Saldana E. (2009) Tectotectal neurons and projections: a proposal to establish a consistent nomenclature. Anat. Rec. (Hoboken) 292: 175-177.

Aparicio MA, Vinuela A, Saldana E. (2010) Projections from the inferior colliculus to the tectal longitudinal column in the rat. Neuroscience 166: 653-664.

Arnault P, Roger M. (1987) The connections of the peripeduncular area studied by retrograde and anterograde transport in the rat. J. Comp. Neurol. 258: 463-476.

Aston-Jones G, Bloom FE. (1981) Activity of norepinephrine-containing locus coeruleus neurons in behaving rats anticipates fluctuations in the sleep-waking cycle. J. Neurosci. 1: 876-886. .

Bandler R, Keay KA. (1996) Columnar organization in the midbrain periaqueductal gray and the integration of emotional expression. Prog. Brain Res. 107: 285-300.

Bandler R, Shipley MT. (1994) Columnar organization in the midbrain periaqueductal gray: modules for emotional expression? Trends Neurosci. 17: 379-389.

Bandler R, Carrive P. (1988) Integrated defence reaction elicited by excitatory amino acid microinjection in the midbrain periaqueductal grey region of the unrestrained cat. Brain Res. 439: 95-106.

Bandler R, Keay KA, Floyd N, Price J. (2000) Central circuits mediating patterned autonomic activity during active vs. passive emotional coping. Brain Res. Bull. 53: 95-104.

Banerjee A, Shen PJ, Ma S, Bathgate RA, Gundlach AL. (2010) Swim stress excitation of nucleus incertus and rapid induction of relaxin-3 expression via CRF1 activation. Neuropharmacology 58: 145-155.

Banerjee A, Shen PJ, Ma S, Bathgate RA, Gundlach AL. (2009) Swim stress excitation of nucleus incertus and rapid induction of relaxin-3 expression via CRF(1) activation. Neuropharmacology .

Bathgate RA, Samuel CS, Burazin TC, Gundlach AL, Tregear GW. (2003) Relaxin: new peptides, receptors and novel actions. Trends Endocrinol. Metab. 14: 207-213.

Beneyto M, Winer JA, Larue DT, Prieto JJ. (1998) Auditory connections and neurochemistry of the sagulum. J. Comp. Neurol. 401: 329-351.

Berman N, Cynader M. (1972). Comparison of receptive-field organization of the superior colliculus in Siamese and normal cats. J. Physiol. 224: 363-389 .

Bittencourt JC, Sawchenko PE. (2000) Do centrally administered neuropeptides access cognate receptors?: an analysis in the central corticotropin-releasing factor system. J. Neurosci. 20: 1142-1156.

Blanchard RJ, Flannelly KJ, Blanchard DC. (1986) Defensive behavior of laboratory and wild Rattus norvegicus. J. Comp. Psychol. 100: 101-107.

Blasiak A, Blasiak T, Czubak W, Gundlach A, Lewandowski M. (2009) Relaxin-3 innervation of the intergeniculate leaflet in the rat. .

Brailoiu E, Dun SL, Gao X, Brailoiu GC, Li JG, Luo JJ, Yang J, Chang JK, Liu-Chen LY, Dun NJ. (2009) C-peptide of preproinsulin-like peptide 7: localization in the rat brain and activity in vitro. Neuroscience 159: 492-500.

Burazin TC, Bathgate RA, Macris M, Layfield S, Gundlach AL, Tregear GW. (2002) Restricted, but abundant, expression of the novel rat gene-3 (R3) relaxin in the dorsal tegmental region of brain. J. Neurochem. 82: 1553-1557.

Burlet S, Tyler CJ, Leonard CS. (2002) Direct and indirect excitation of laterodorsal tegmental neurons by Hypocretin/Orexin peptides: implications for wakefulness and narcolepsy. J. Neurosci. 22: 2862-2872.

Cameron AA, Khan IA, Westlund KN, Willis WD. (1995) The efferent projections of the periaqueductal gray in the rat: a Phaseolus vulgaris-leucoagglutinin study. II. Descending projections. J. Comp. Neurol. 351: 585-601.

Cano G, Mochizuki T, Saper CB. (2008) Neural circuitry of stress-induced insomnia in rats. J. Neurosci. 28: 10167-10184.

Canteras NS. 2002. The medial hypothalamic defensive system: hodological organization and functional implications. Pharmacol. Biochem. Behav. 71: 481-491. *

Canteras NS, Goto M. (1999a). Fos-like immunoreactivity in the periaqueductal gray of rats exposed to a natural predator. Neuroreport 10: 413-418.

Canteras NS, Goto M. (1999b) Connections of the precommissural nucleus. J. Comp. Neurol. 408: 23-45.

Canteras NS, Swanson LW. (1992) The dorsal premammillary nucleus: an unusual component of the mammillary body. Proc. Natl. Acad. Sci. U. S. A. 89: 10089-10093.

Carrive P, Leung P, Harris J, Paxinos G. (1997) Conditioned fear to context is associated with increased Fos expression in the caudal ventrolateral region of the midbrain periaqueductal gray. Neuroscience 78: 165-177.

Comoli E, Ribeiro-Barbosa ER, Canteras NS. (2003) Predatory hunting and exposure to a live predator induce opposite patterns of Fos immunoreactivity in the PAG. Behav. Brain Res. 138: 17-28.

Daly C, Ziff EB. (2002) Ca2+-dependent formation of a dynamin-synaptophysin complex: potential role in synaptic vesicle endocytosis. J. Biol. Chem. 277: 9010-9015.

Daly C, Sugimori M, Moreira JE, Ziff EB, Llinas R. (2000) Synaptophysin regulates clathrin-independent endocytosis of synaptic vesicles. Proc. Natl. Acad. Sci. U. S. A. 97: 6120-6125.

De Oca BM, DeCola JP, Maren S, Fanselow MS. (1998) Distinct regions of the periaqueductal gray are involved in the acquisition and expression of defensive responses. J. Neurosci. 18: 3426-3432.

Dean P, Redgrave P, Westby GW. (1989) Event or emergency? Two response systems in the mammalian superior colliculus. Trends Neurosci. 12: 137-147.

Doubell TP, Skaliora I, Baron J, King AJ. (2003) Functional connectivity between the superficial and deeper layers of the superior colliculus: an anatomical substrate for sensorimotor integration. J. Neurosci. 23: 6596-6607.

Drager UC, Hubel DH. (1975) Responses to visual stimulation and relationship between visual, auditory, and somatosensory inputs in mouse superior colliculus. J. Neurophysiol. 38: 690-713.

Floyd NS, Price JL, Ferry AT, Keay KA, Bandler R. (2001) Orbitomedial prefrontal cortical projections to hypothalamus in the rat. J. Comp. Neurol. 432: 307-328.

Foote SL, Aston-Jones G, Bloom FE. (1980) Impulse activity of locus coeruleus neurons in awake rats and monkeys is a function of sensory stimulation and arousal. Proc. Natl. Acad. Sci. U. S. A. 77: 3033-3037.

Furigo IC, de Oliveira WF, de Oliveira AR, Comoli E, Baldo MV, Mota-Ortiz SR, Canteras NS. (2010) The role of the superior colliculus in predatory hunting. Neuroscience 165: 1-15.

Gabbott PL, Warner TA, Jays PR, Salway P, Busby SJ. (2005) Prefrontal cortex in the rat: projections to subcortical autonomic, motor, and limbic centers. J. Comp. Neurol. 492: 145-177.

Gamlin PD. (2006) The pretectum: connections and oculomotor-related roles. Prog. Brain Res. 151: 379-405.

Garcia Del Cano G, Gerrikagoitia I, Alonso-Cabria A, Martinez-Millan L. (2006) Organization and origin of the connection from the inferior to the superior colliculi in the rat. J. Comp. Neurol. 499: 716-731.

Goto M, Swanson LW, Canteras NS. (2001) Connections of the nucleus incertus. J. Comp. Neurol. 438: 86-122.

Grantyn R. (1988) Gaze control through superior colliculus: structure and function. Rev. Oculomot. Res. 2: 273-333.

Halliday G, Harding A, and Paxinos G. Serotonin and tachykinin systems. In: The Rat Nervous System, Ed Paxinos G. San Diego: Academic Press, 1995, p. 929-974.

Haugaard-Kedstrom LM, Shabanpoor F, Hossain MA, Clark RJ, Ryan PJ, Craik DJ, Gundlach AL, Wade JD, Bathgate RA, Rosengren KJ. (2011) Design, synthesis, and characterization of a single-chain peptide antagonist for the relaxin-3 receptor RXFP3. J. Am. Chem. Soc. 133: 4965-4974.

Hida T, Takahashi E, Shikata K, Hirohashi T, Sawai T, Seiki T, Tanaka H, Kawai T, Ito O, Arai T, Yokoi A, Hirakawa T, Ogura H, Nagasu T, Miyamoto N, Kuromitsu J. (2006) Chronic intracerebroventricular administration of relaxin-3 increases body weight in rats. J. Recept. Signal Transduct. Res. 26: 147-158.

Jacobs BL, Azmitia EC. (1992) Structure and function of the brain serotonin system. Physiol. Rev. 72: 165-229.

Jahn R, Schiebler W, Ouimet C, Greengard P. (1985) A 38,000-dalton membrane protein (p38) present in synaptic vesicles. Proc. Natl. Acad. Sci. U. S. A. 82: 4137-4141.

Jones BE, Webster HH. (1988) Neurotoxic lesions of the dorsolateral pontomesencephalic tegmentum-cholinergic cell area in the cat. I. Effects upon the cholinergic innervation of the brain. Brain Res. 451: 13-32.

Jones BE, Yang TZ. (1985) The efferent projections from the reticular formation and the locus coeruleus studied by anterograde and retrograde axonal transport in the rat. J. Comp. Neurol. 242: 56-92.

Keay KA, Bandler R. (1993) Deep and superficial noxious stimulation increases Fos-like immunoreactivity in different regions of the midbrain periaqueductal grey of the rat. Neurosci. Lett. 154: 23-26.

Keay KA, Clement CI, Owler B, Depaulis A, Bandler R. (1994) Convergence of deep somatic and visceral nociceptive information onto a discrete ventrolateral midbrain periaqueductal gray region. Neuroscience 61: 727-732.

King AJ. (1999) Sensory experience and the formation of a computational map of auditory space in the brain. Bioessays 21: 900-911.

Klooster J, Vrensen GF, Muller LJ, van der Want JJ. (1995) Efferent projections of the olivary pretectal nucleus in the albino rat subserving the pupillary light reflex and related reflexes. A light microscopic tracing study. Brain Res. 688: 34-46.

Krout KE, Loewy AD, Westby GW, Redgrave P. (2001) Superior colliculus projections to midline and intralaminar thalamic nuclei of the rat. J. Comp. Neurol. 431: 198-216.

Kuei C, Sutton S, Bonaventure P, Pudiak C, Shelton J, Zhu J, Nepomuceno D, Wu J, Chen J, Kamme F, Seierstad M, Hack MD, Bathgate RA, Hossain MA, Wade JD, Atack J, Lovenberg TW, Liu C. 2007. R3(BDelta23 27)R/I5 chimeric peptide, a selective antagonist for GPCR135 and GPCR142 over relaxin receptor LGR7: in vitro and in vivo characterization. J. Biol. Chem. 282: 25425-25435. .

LeDoux JE, Sakaguchi A, Reis DJ. (1984) Subcortical efferent projections of the medial geniculate nucleus mediate emotional responses conditioned to acoustic stimuli. J. Neurosci. 4: 683-698.

Ledoux JE, Ruggiero DA, Forest R, Stornetta R, Reis DJ. (1987) Topographic organization of convergent projections to the thalamus from the inferior colliculus and spinal cord in the rat. J. Comp. Neurol. 264: 123-146.

Liu C, Eriste E, Sutton S, Chen J, Roland B, Kuei C, Farmer N, Jornvall H, Sillard R, Lovenberg TW. (2003) Identification of relaxin-3/INSL7 as an endogenous ligand for the orphan G-protein-coupled receptor GPCR135. J. Biol. Chem. 278: 50754-50764.

Ma S, Sang Q, Lanciego JL, Gundlach AL. (2009a) Localization of relaxin-3 in brain of Macaca fascicularis: identification of a nucleus incertus in primate. J. Comp. Neurol. 517: 856-872.

Ma S, Olucha-Bordonau FE, Hossain MA, Lin F, Kuei C, Liu C, Wade JD, Sutton SW, Nunez A, Gundlach AL. (2009b) Modulation of hippocampal theta oscillations and spatial memory by relaxin-3 neurons of the nucleus incertus. Learn. Mem. 16: 730-742.

Ma S, Bonaventure P, Ferraro T, Shen PJ, Burazin TC, Bathgate RA, Liu C, Tregear GW, Sutton SW, Gundlach AL. (2007) Relaxin-3 in GABA projection neurons of nucleus incertus suggests widespread influence on forebrain circuits via G-protein-coupled receptor-135 in the rat. Neuroscience 144: 165-190.

Marchant EG, Morin LP. (1999) The hamster circadian rhythm system includes nuclei of the subcortical visual shell. J. Neurosci. 19: 10482-10493.

McGowan BM, Stanley SA, Smith KL, White NE, Connolly MM, Thompson EL, Gardiner JV, Murphy KG, Ghatei MA, Bloom SR. (2005) Central relaxin-3 administration causes hyperphagia in male Wistar rats. Endocrinology 146: 3295-3300.

McGowan BM, Stanley SA, Smith KL, Minnion JS, Donovan J, Thompson EL, Patterson M, Connolly MM, Abbott CR, Small CJ, Gardiner JV, Ghatei MA, Bloom SR. (2006) Effects of acute and chronic relaxin-3 on food intake and energy expenditure in rats. Regul. Pept. 136: 72-77.

Mendelson WB, Martin JV, Perlis M, Wagner R. (1987) Arousal induced by injection of triazolam into the dorsal raphe nucleus of rats. Neuropsychopharmacology 1: 85-88.

Meredith MA, Stein BE. (1990) The visuotopic component of the multisensory map in the deep laminae of the cat superior colliculus. J. Neurosci. 10: 3727-3742.

Mikkelsen JD, Vrang N. (1994). A direct pretectosuprachiasmatic projection in the rat. Neuroscience 62: 497-505.

Mikkelsen JD, Vrang N, Mrosovsky N. (1998) Expression of Fos in the circadian system following nonphotic stimulation. Brain Res. Bull. 47: 367-376.

Mota-Ortiz SR, Sukikara MH, Felicio LF, Canteras NS. (2009) Afferent connections to the rostrolateral part of the periaqueductal gray: a critical region influencing the motivation drive to hunt and forage. Neural Plast. 2009: 612698.

Motta SC, Goto M, Gouveia FV, Baldo MV, Canteras NS, Swanson LW. (2009) Dissecting the brain's fear system reveals the hypothalamus is critical for responding in subordinate conspecific intruders. Proc. Natl. Acad. Sci. U. S. A. 106: 4870-4875.

Munoz DP, Wurtz RH. (1992) Role of the rostral superior colliculus in active visual fixation and execution of express saccades. J. Neurophysiol. 67: 1000-1002. .

Munoz DP, Waitzman DM, Wurtz RH. (1996) Activity of neurons in monkey superior colliculus during interrupted saccades. J. Neurophysiol. 75: 2562-2580.

Nelson LE, Lu J, Guo T, Saper CB, Franks NP, Maze M. (2003) The alpha2-adrenoceptor agonist dexmedetomidine converges on an endogenous sleep-promoting pathway to exert its sedative effects. Anesthesiology 98: 428-436.

Nelson LE, Guo TZ, Lu J, Saper CB, Franks NP, Maze M. (2002). The sedative component of anesthesia is mediated by GABA(A) receptors in an endogenous sleep pathway. Nat. Neurosci. 5: 979-984. .

Olucha-Bordonau FE, Teruel V, Barcia-Gonzalez J, Ruiz-Torner A, Valverde-Navarro AA, Martinez-Soriano F. (2003) Cytoarchitecture and efferent projections of the nucleus incertus of the rat. J. Comp. Neurol. 464: 62-97.

Onstott D, Mayer B, Beitz AJ. (1993) Nitric oxide synthase immunoreactive neurons anatomically define a longitudinal dorsolateral column within the midbrain periaqueductal gray of the rat: analysis using laser confocal microscopy. Brain Res. 610: 317-324.

Paxinos G., Ashwell KWS, Kirkcaldie M (2008) Chemoarchitectonic Atlas of the Rat Brain. Academic Press 6th Ed, San Diego

Pennuto M, Bonanomi D, Benfenati F, Valtorta F. (2003). Synaptophysin I controls the targeting of VAMP2/synaptobrevin II to synaptic vesicles. Mol. Biol. Cell 14: 4909-4919.

Roldan M, Reinoso-Suarez F, Tortelly A. (1983) Parabigeminal projections to the superior colliculus in the cat. Brain Res. 280: 1-13.

Ruiz-Torner A, Olucha-Bordonau F, Valverde-Navarro AA, Martinez-Soriano F. (2001) The chemical architecture of the rat's periaqueductal gray based on acetylcholinesterase histochemistry: a quantitative and qualitative study. J. Chem. Neuroanat. 21: 295-312.

Ryan PJ, Ma S, Olucha-Bordonau FE, Gundlach AL. (2011) Nucleus incertus--an emerging modulatory role in arousal, stress and memory. Neurosci. Biobehav. Rev. 35: 1326-1341.

Saldana E, Vinuela A, Marshall AF, Fitzpatrick DC, Aparicio MA. (2007) The TLC: a novel auditory nucleus of the mammalian brain. J. Neurosci. 27: 13108-13116.

Sesack SR, Deutch AY, Roth RH, Bunney BS. (1989) Topographical organization of the efferent projections of the medial prefrontal cortex in the rat: an anterograde tract-tracing study with Phaseolus vulgaris leucoagglutinin. J. Comp. Neurol. 290: 213-242.

Singewald N, Sharp T. (2000) Neuroanatomical targets of anxiogenic drugs in the hindbrain as revealed by Fos immunocytochemistry. Neuroscience 98: 759-770.

Skaliora I, Doubell TP, Holmes NP, Nodal FR, King AJ. (2004) Functional topography of converging visual and auditory inputs to neurons in the rat superior colliculus. J. Neurophysiol. 92: 2933-2946.

Smith CM, Lawrence AJ, Sutton SW, Gundlach AL. (2009) Behavioral phenotyping of mixed background (129S5:B6) relaxin-3 knockout mice. Ann. N. Y. Acad. Sci. 1160: 236-241.

Smith CM, Hosken IT, Sutton SW, Lawrence AJ, Gundlach AL. (2012) Relaxin-3 null mutation mice display a circadian hypoactivity phenotype. Genes Brain Behav. 11: 94-104.

Smith CM, Ryan PJ, Hosken IT, Ma S, Gundlach AL. (2011) Relaxin-3 systems in the brain--the first 10 years. J. Chem. Neuroanat. 42: 262-275.

Smith CM, Shen PJ, Ma S, Sutton SW, Gundlach AL. (2009) Verification of a relaxin-3 knockout/LacZ reporter mouse as a model of relaxin-3 deficiency. Ann. N. Y. Acad. Sci. 1160: 259-260.

Smith CM, Shen PJ, Banerjee A, Bonaventure P, Ma S, Bathgate RA, Sutton SW, Gundlach AL. (2010) Distribution of relaxin-3 and RXFP3 within arousal, stress, affective, and cognitive circuits of mouse brain. J. Comp. Neurol. 518: 4016-4045.

Stein BE, Meredith MA. (1990) Multisensory integration. Neural and behavioral solutions for dealing with stimuli from different sensory modalities. Ann. N. Y. Acad. Sci. 608: 51-65; discussion 65-70.

Stein BE, Meredith MA, Wallace MT. (1993) The visually responsive neuron and beyond: multisensory integration in cat and monkey. Prog. Brain Res. 95: 79-90.

Steriade M, McCarley RW (1990) In: Brainstem Control of Wakefulness and Sleep. New York: Plenum.

Subramanian HH, Balnave RJ, Holstege G. (2008) The midbrain periaqueductal gray control of respiration. J. Neurosci. 28: 12274-12283.

Sukikara MH, Mota-Ortiz SR, Baldo MV, Felicio LF, Canteras NS. (2006) A role for the periaqueductal gray in switching adaptive behavioral responses. J. Neurosci. 26: 2583-2589.

Sutton SW, Bonaventure P, Kuei C, Roland B, Chen J, Nepomuceno D, Lovenberg TW, Liu C. (2004) Distribution of G-protein-coupled receptor (GPCR)135 binding sites and receptor mRNA in the rat brain suggests a role for relaxin-3 in neuroendocrine and sensory processing. Neuroendocrinology 80: 298-307.

Tanaka M, Iijima N, Miyamoto Y, Fukusumi S, Itoh Y, Ozawa H, Ibata Y. (2005) Neurons expressing relaxin 3/INSL 7 in the nucleus incertus respond to stress. Eur. J. Neurosci. 21: 1659-1670.

Thomas L, Betz H. (1990) Synaptophysin binds to physophilin, a putative synaptic plasma membrane protein. J. Cell Biol. 111: 2041-2052.

Thornton SK, Withington DJ. (1996) The role of the external nucleus of the inferior colliculus in the construction of the superior collicular auditory space map in the guinea-pig. Neurosci. Res. 25: 239-246.

Usunoff KG, Schmitt O, Itzev DE, Rolfs A, Wree A. (2007) Efferent connections of the parabigeminal nucleus to the amygdala and the superior colliculus in the rat: a double-labeling fluorescent retrograde tracing study. Brain Res. 1133: 87-91.

Usunoff KG, Itzev DE, Rolfs A, Schmitt O, Wree A. (2006) Brain stem afferent connections of the amygdala in the rat with special references to a projection from the parabigeminal nucleus: a fluorescent retrograde tracing study. Anat. Embryol. (Berl) 211: 475-496.

Van Pett K, Viau V, Bittencourt JC, Chan RK, Li HY, Arias C, Prins GS, Perrin M, Vale W, Sawchenko PE. (2000) Distribution of mRNAs encoding CRF receptors in brain and pituitary of rat and mouse. J. Comp. Neurol. 428: 191-212. .

VanderHorst VG, Schasfoort FC, Meijer E, van Leeuwen FW, Holstege G. (1998) Estrogen receptor-alpha-immunoreactive neurons in the periaqueductal gray of the adult ovariectomized female cat. Neurosci. Lett. 240: 13-16.

Vertes RP, Kocsis B. (1994). Projections of the dorsal raphe nucleus to the brainstem: PHA-L analysis in the rat. J. Comp. Neurol. 340: 11-26.

Vertes RP, Linley SB, Hoover WB. (2010) Pattern of distribution of serotonergic fibers to the thalamus of the rat. Brain Struct. Funct.

Vertes RP, Kinney GG, Kocsis B, Fortin WJ. (1994) Pharmacological suppression of the median raphe nucleus with serotonin1A agonists, 8-OH-DPAT and buspirone, produces hippocampal theta rhythm in the rat. Neuroscience 60: 441-451.

Wainer BH, Mesulam M-M (1990) Ascending cholinergic pathways in the rat brain. In: Brain Cholinergic Systems (Steriade M, Biesold D, Eds), pp 65-119. New York: Oxford University Press.

Wallace MT, Meredith MA, Stein BE. (1998) Multisensory integration in the superior colliculus of the alert cat. J. Neurophysiol. 80: 1006-1010.

Webster HH, Jones BE. (1988) Neurotoxic lesions of the dorsolateral pontomesencephalic tegmentum-cholinergic cell area in the cat. II. Effects upon sleep-waking states. Brain Res. 458: 285-302.

Wenstrup JJ, Larue DT, Winer JA. (1994) Projections of physiologically defined subdivisions of the inferior colliculus in the mustached bat: targets in the medial geniculate body and extrathalamic nuclei. J. Comp. Neurol. 346: 207-236.

Wiedenmann B, Franke WW. (1985) Identification and localization of synaptophysin, an integral membrane glycoprotein of Mr 38,000 characteristic of presynaptic vesicles. Cell 41: 1017-1028. .

Winer JA, Saint Marie RL, Larue DT, Oliver DL. (1996) GABAergic feedforward projections from the inferior colliculus to the medial geniculate body. Proc. Natl. Acad. Sci. U. S. A. 93: 8005-8010.

Zhao Z, Yang Y, Walker DL, Davis M. (2009) Effects of substance P in the amygdala, ventromedial hypothalamus, and periaqueductal gray on fear-potentiated startle. Neuropsychopharmacology 34: 331-340.

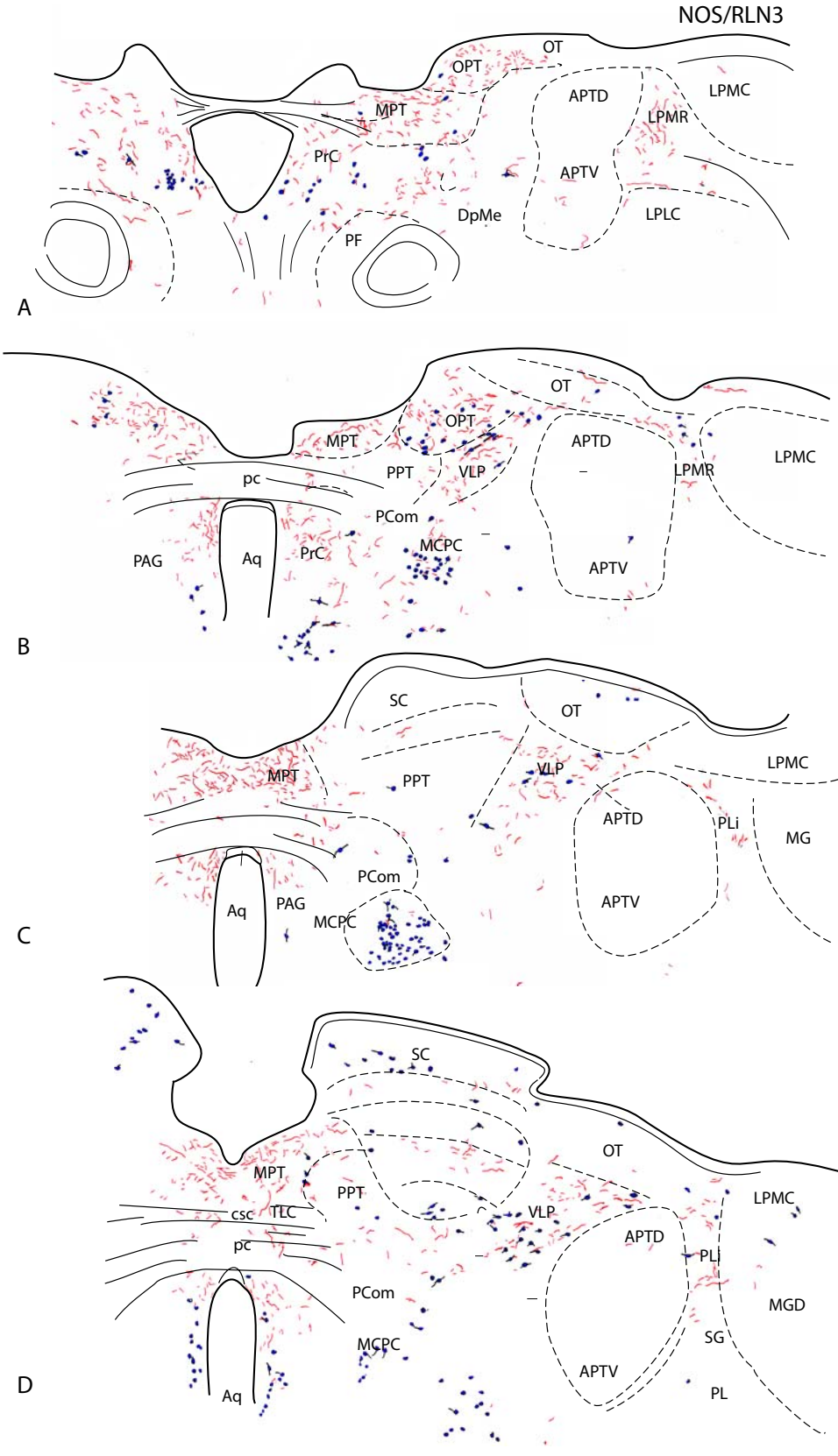

APTD anterior pretectal nucleus, dorsal part
APTV anterior pretectal nucleus, ventral part
Aq aqueduct
csc commissure of the superior colliculus
DpMe deep mesencephalic nucleus
LPLC lateral posterior thalamic nucleus, laterocaudal part
LPMC lateral posterior thalamic nucleus, mediocaudal part
LPMR lateral posterior thalamic nucleus, mediorostral part
MCPC magnocellular nucleus of the posterior commissure
MG medial geniculate nucleus
MGD medial geniculate nucleus, dorsal part
MPT medial pretectal nucleus
OPT olivary pretectal nucleus
OT optic tract
PAG priaqueductal gray
pc posterior commissure
PCom nucleus of the posterior commissure
PF parafascicular thalamic nucleus
PL paralemniscal nucleus
PLi posterior limitans thalamic nucleus
PPT posterior pretectal nucleus
PrC precommissural nucleus
SC superior colliculus
SG suprageniculate thalamic nucleus
TLC tectal longitudinal column
VLP ventroposterolateral nucleus

Figure 1. Distribution of RLN3-positive fibers within the pretectum mapped in sections immunostained for RLN3 and nNOS. Immunoreactivity was mapped using camera lucida and a 20× objective. RLN3 fibers and soma are indicated in red and nNOS positive soma and primary processes in blue. Boundaries of pretectal divisions were drawn in black and revectorized (for further details see Materials and Methods). The MCPC and PPT, containing nNOS-positive soma, are present at rostral levels, while an nNOS- and RLN3-immunopositive area identified as 'the ventrolateral pretectal nucleus' is present at caudal levels ventrolateral to SC. At level 4, SC stratification is clearly evident and nNOS positive soma in the MCPC are less abundant. Intense RLN3 labeling was observed in MPT and some labeled fibers were detected in the OPT and VLP. A RLN3 innervation reaches the LPMR and PLi, whereas the APT and OT are unlabeled. Scale bar: 500 µm. For abbreviations, see list.

Figure 2.

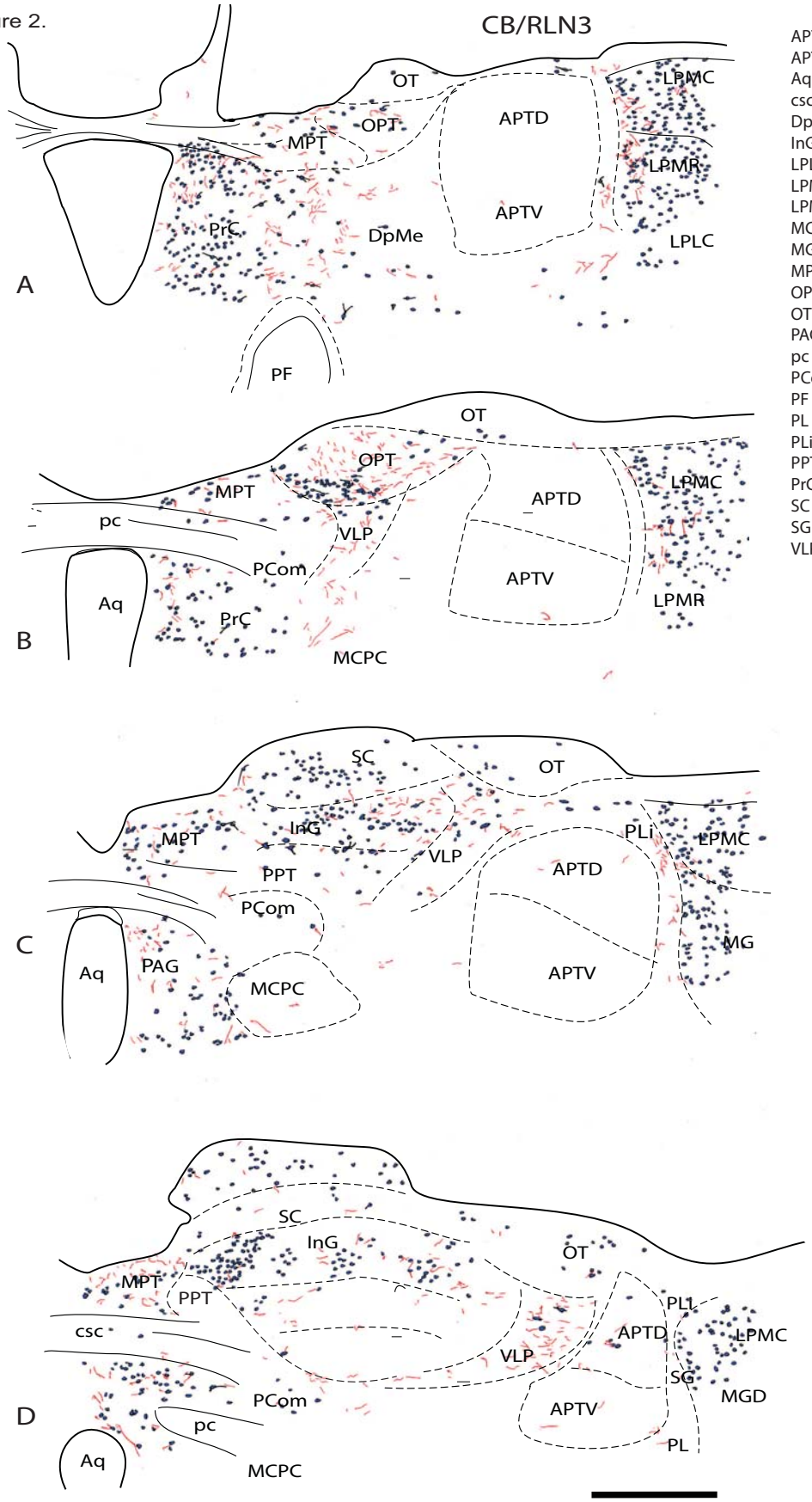

APTD anterior pretectal nucleus, dorsal part
APTV anterior pretectal nucleus, ventral part
Aq aqueduct
csc commissure of the superior colliculus
DpMe deep mesencephalic nucleus
InG intermediate gray layer of the superior colliculus
LPLC lateral posterior thalamic nucleus, laterocaudal part
LPMC lateral posterior thalamic nucleus, mediocaudal part
LPMR lateral posterior thalamic nucleus, mediorostral part
MCPC magnocellular nucleus of the posterior commissure
MG medial geniculate nucleus
MPT medial pretectal nucleus
OPT olivary pretectal nucleus
OT optic tract
PAG priaqueductal gray
pc posterior commissure
PCom nucleus of the posterior commissure
PF parafascicular thalamic nucleus
PL paralemniscal nucleus
PLi posterior limitans thalamic nucleus
PPT posterior pretectal nucleus
PrC precommissural nucleus
SC superior colliculus
SG supragenículate thalamic nucleus
VLP ventroposterolateral nucleus

Figure 2. Distribution of RLN3-positive fibers in sections of the pretectum immunostained for RLN3 and CB. For details of the mapping and boundaries of levels 1-4, see Fig. 1 legend. The adjacent PAG, LPM and MG contain dense CB labeling. The presence of CB positive soma in the PPT facilitates demarcation of the pretectal nuclei. Scale bar: 500 µm. For abbreviations, see list.

Figure 3.

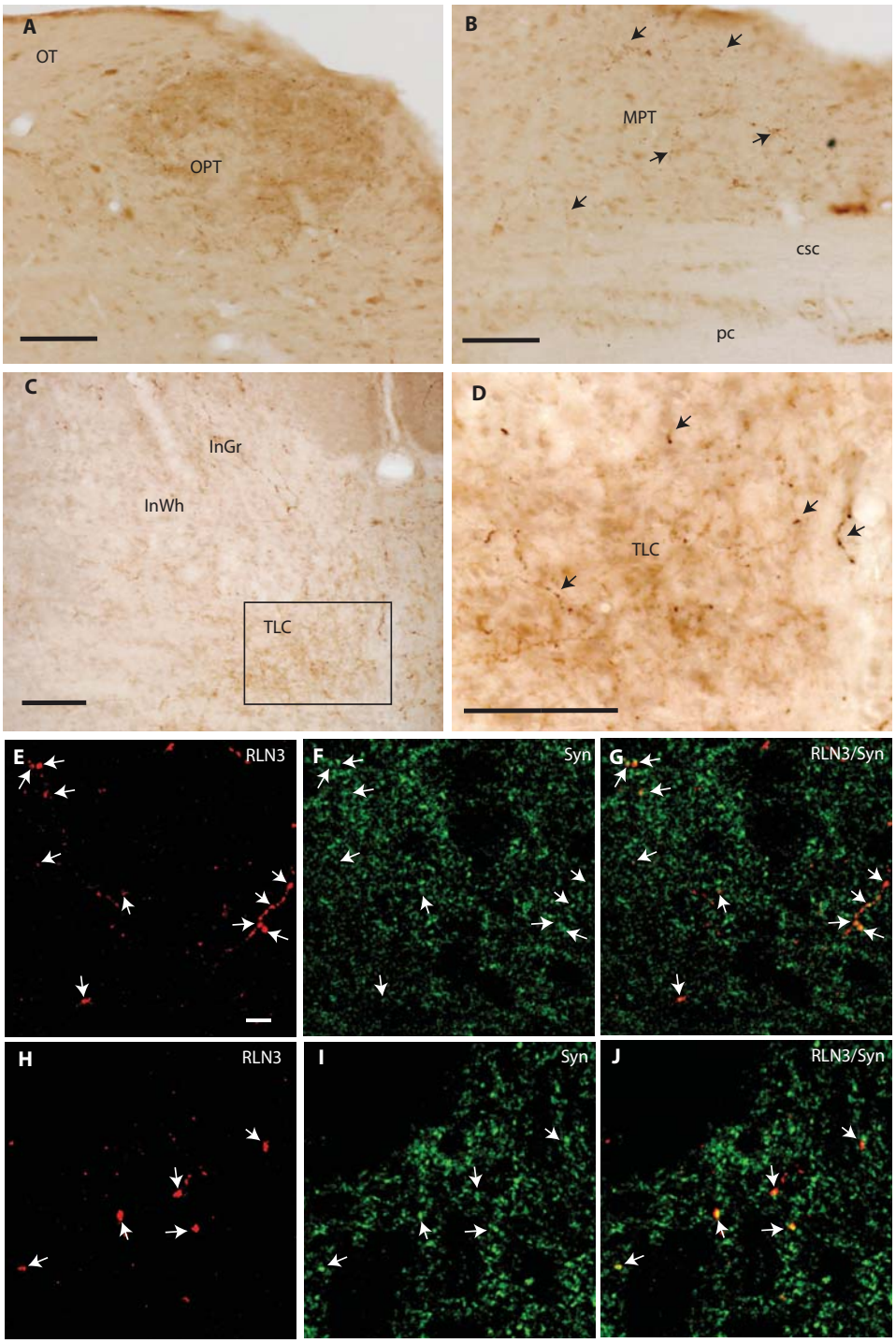

csc commissure of the superior colliculus
InGr intermediate gray layer of the superior colliculus
InWh intermediate white layer of the superior colliculus
MPT medial pretectal nucleus
OPT olivary pretectal nucleus
OT optic tract
pc posterior commissure
TLC tectal longitudinal column

Figure 3. Illustrative examples of RLN3 and marker immunostaining in different regions of the pretectal area. (A) The olivary pretectal nucleus contains a high density of RLN3 fibers in an nNOS labeled stained section. RLN3-labeling observed in the nNOS-negative core and in the shell containing some nNOS-labeled cells. (B) The medial pretectal nucleus, located dorsal to the posterior commissure, contains a high density of RLN3-labeled fibers. (C and D) RLN3-labeled fibers between the cellular groups around the bundles of the collicullar commissures. A section immunostained with RLN3 and TH, the tectal longitudinal column from the boxed area in C is magnified in D. Black arrows indicate RLN3-labeled fibers. Single confocal sections of 0.25 µm illustrating the coexistence of synaptophysin (green) and RLN3 (red) in nerve fibers within the medial pretectal area (MPT; E-G) and OPT (H-J). White arrows indicate putative synaptic contacts. Scale bar A-D: 100 µm; E-G: 10 µm. For abbreviations, see list.

Figure 4.

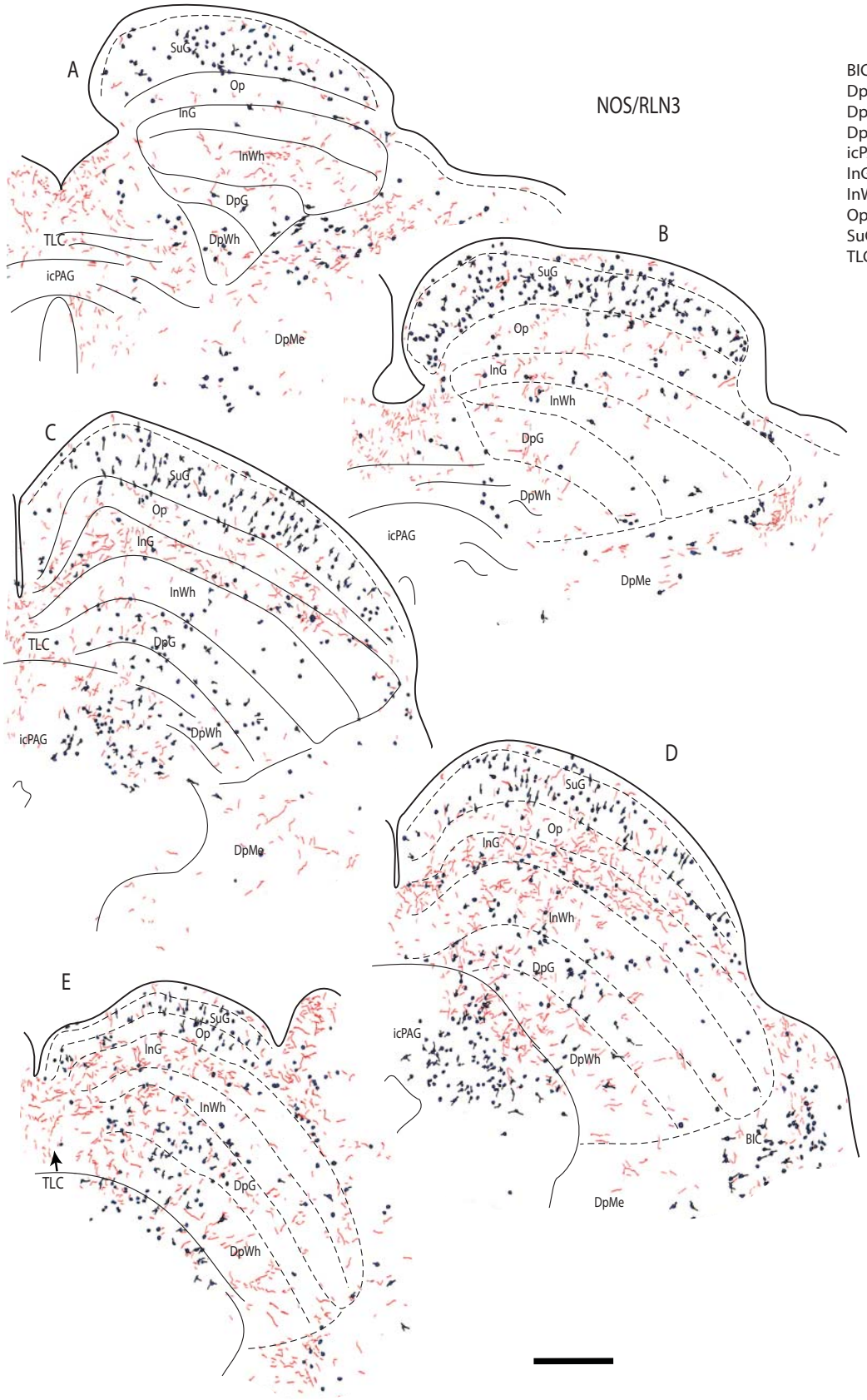

BIC brachium of the inferior colliculus
DpG deep gray layer of the superior colliculus
DpMe deep mesencephalic nucleus
DpWh deep white layer of the superior colliculus
icPAG intercollicular area of the periaqueductal gray
InG intermediate gray layer of the superior colliculus
InWh intermediate white layer of the superior colliculus
Op optic nerve layer of the superior colliculus
SuG superficial gray layer of the superior colliculius
TLC tectal longitudinal column

Figure 4. Distribution of RLN3-positive fibers within SC mapped in sections immunostained for RLN3 and nNOS. The superficial grey layer contains a dense population of nNOS-positive neurons at all levels. nNOS-labeled soma in DLPAG, BIC and deep layers of SC facilitate the demarcation of SC boundaries. RLN3 fiber plexuses are more dense at caudo-medial levels, especially in the InG layer. Scale bar: 500 µm. For abbreviations, see list.

Figure 5.

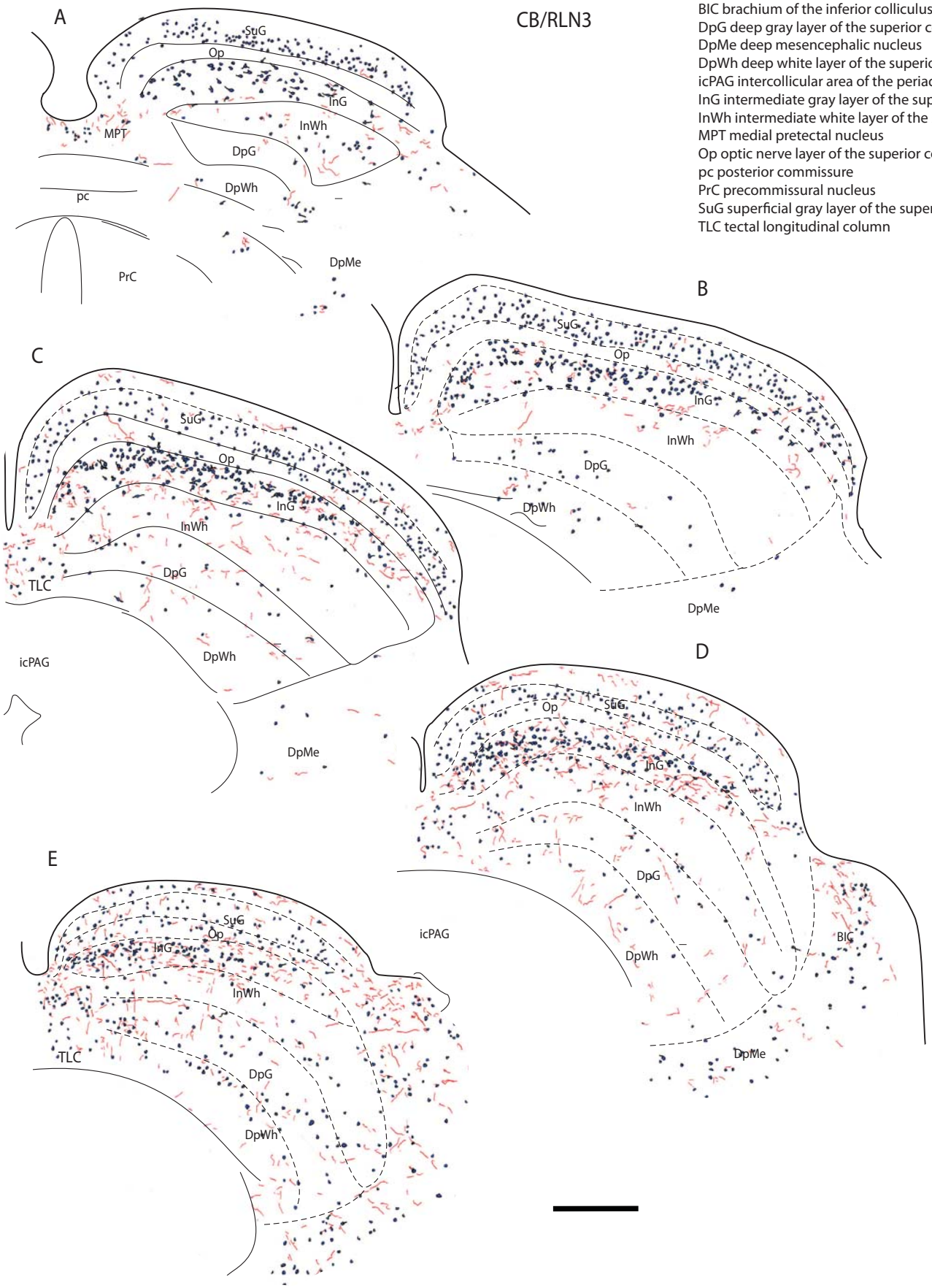

BIC brachium of the inferior colliculus
DpG deep gray layer of the superior colliculus
DpMe deep mesencephalic nucleus
DpWh deep white layer of the superior colliculus
icPAG intercollicular area of the periaqueductal gray
InG intermediate gray layer of the superior colliculus
InWh intermediate white layer of the superior colliculus
MPT medial pretectal nucleus
Op optic nerve layer of the superior colliculus
pc posterior commissure
PrC precommissural nucleus
SuG superficial gray layer of the superior colliculius
TLC tectal longitudinal column

Figure 5. Distribution of RLN3-positive fibers within SC mapped in sections immunostained for RLN3 and CB. Small and large CB-positive soma were observed in the SuG and InG layers, respectively. CBlabeling was virtually absent in the OP and InW layers. RLN3 fibers are concentrated in the medial aspects of the InG, where larger CB neurons were observed. Scale bar: 500 µm. For abbreviations, see list

Figure 6.

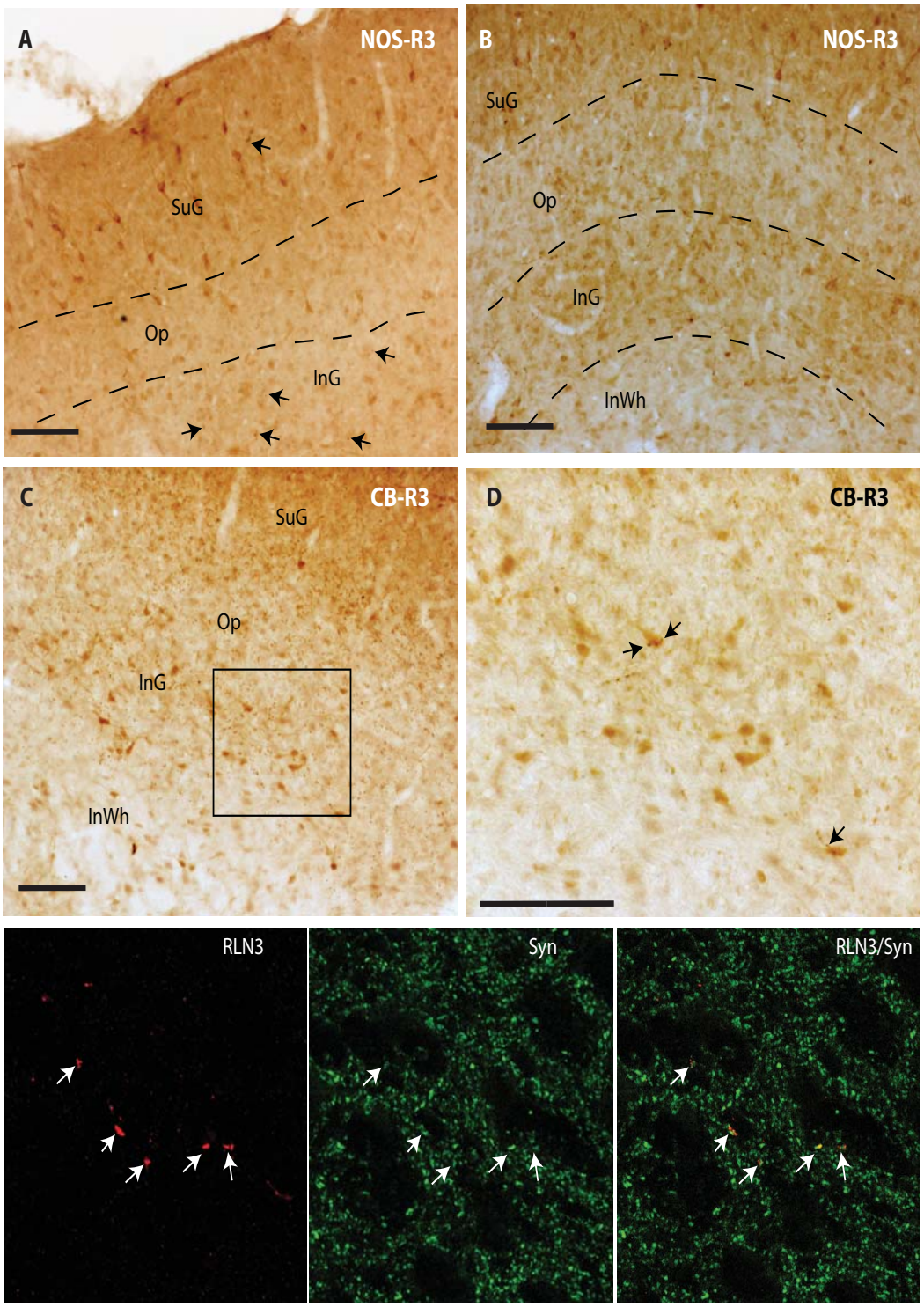

InG intermediate gray layer of the superior colliculus
InWh intermediate white layer of the superior colliculus
Op optic nerve layer of the superior colliculus
SuG superficial gray layer of the superior colliculius

Figure 6. Illustrative examples of RLN3 and marker immunostaining in different areas of SC. (A and B) SuG and particularly the InG contain the highest density of RLN3-labeled fibers (indicated by black arrows). (C and D) In deep layers of SC, a high concentration of RLN3-labeled fibers was present in the InG; and in some cases fibers were closely apposed to CR-labeled soma. (E-G) Single confocal sections of 0.25 µm illustrating the colocalization of synaptophysin (green) and RLN3 (red) in nerve fibers in the caudomedial InG layer. White arrows indicate putative synaptic contacts; stars indicate unlabeled neuronal soma. Scale bar A-D: 100 µm; E-G: 10 µm. For abbreviations, see list.

Figure 7.

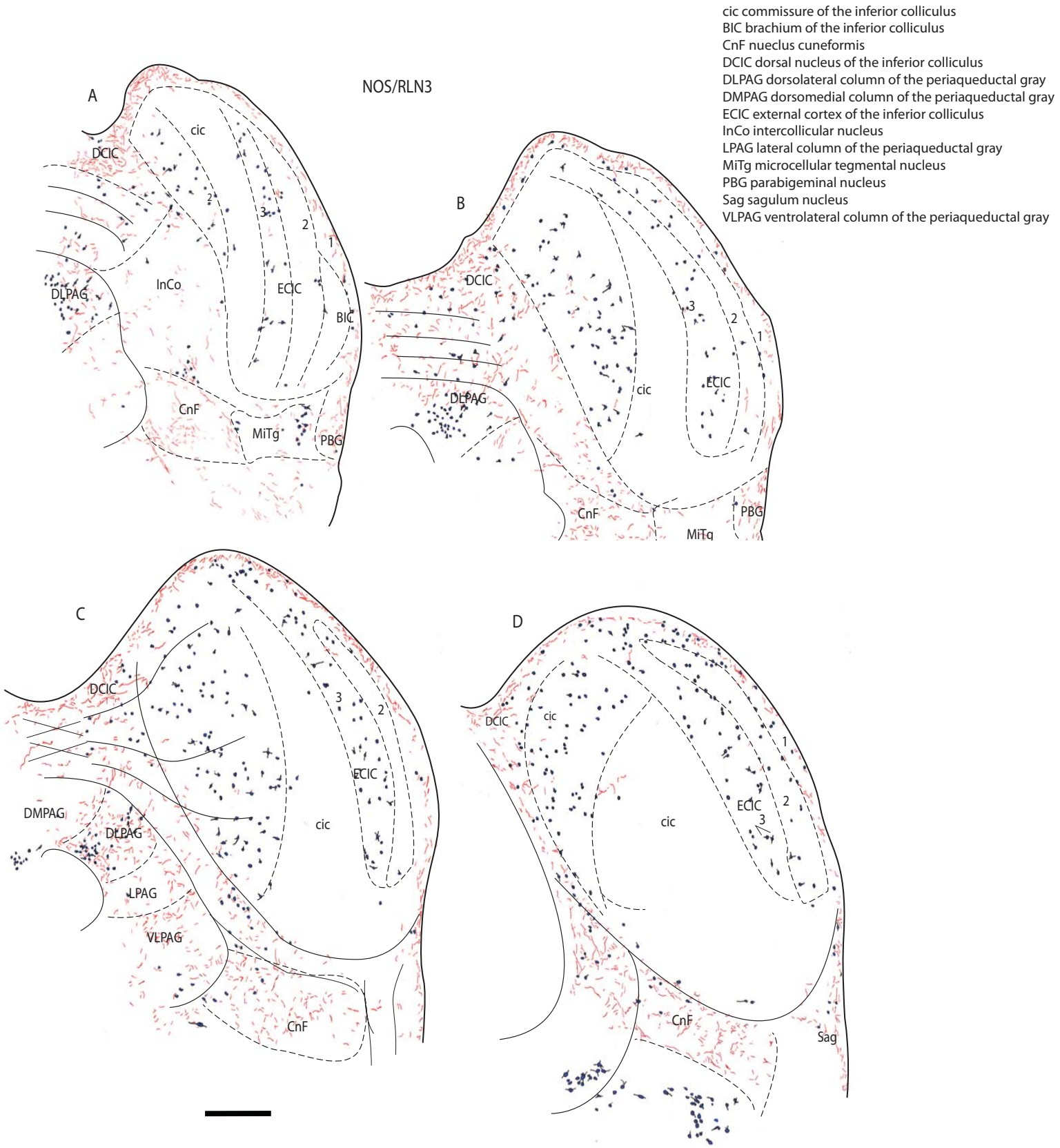

Figure 7. Distribution of RLN3-positive fibers within IC mapped in sections immunostained for RLN3 and nNOS. nNOS-positive populations are dense in the medial CIC and ECIC3 , but completely absent in the lateral half of the CIC. The RLN3 innervation avoids the central area of the IC and is particularly dense in layer 1 of DCIC and ECIC. Scale bar: 500 µm.

Figure 8.

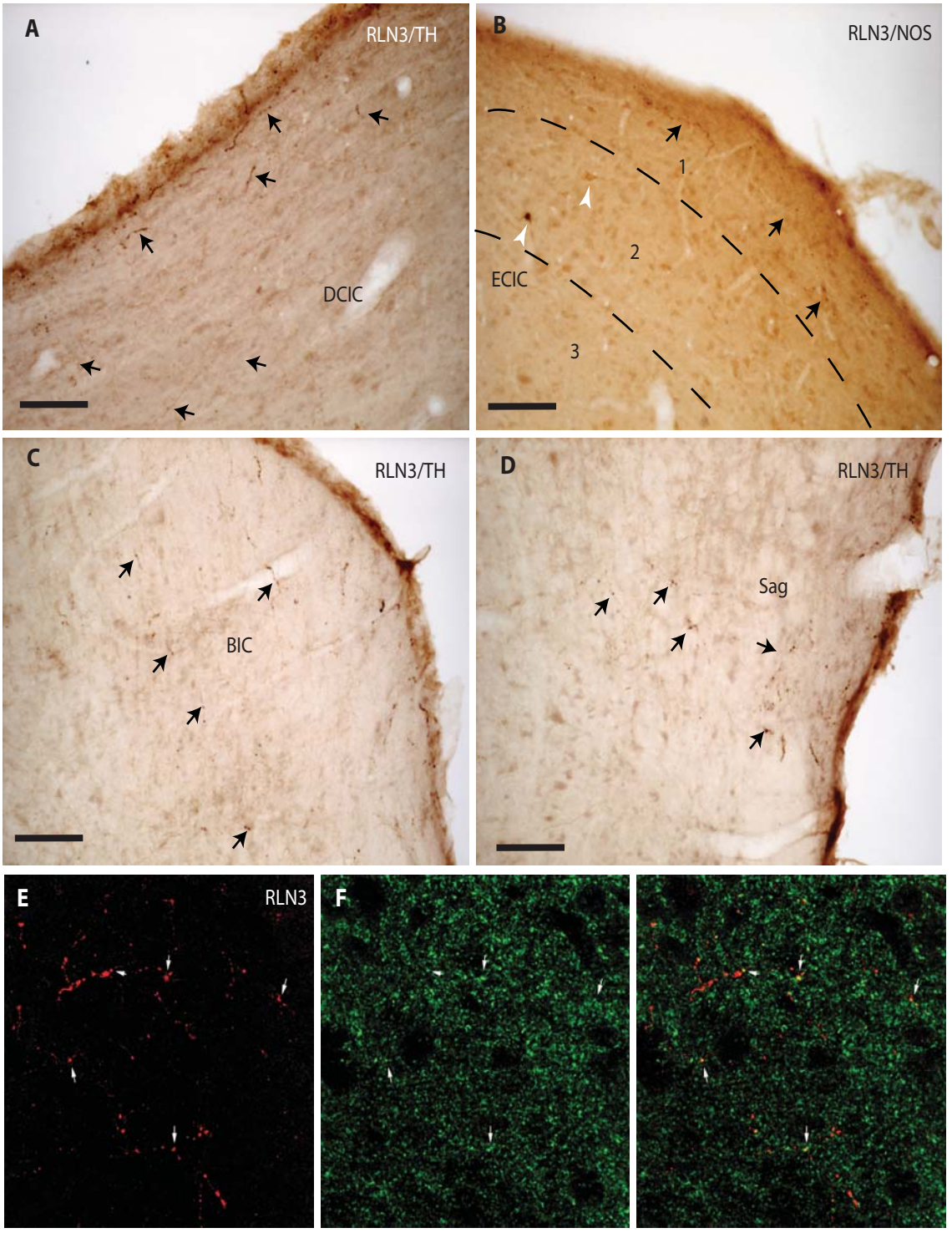

DCIC dorsal nucleus of the inferior colliculus
BIC brachium of the inferior colliculus
ECIC external cortex of the inferior colliculus
Sag sagulum nucleus

Figure 8. Illustrative examples of RLN3 and marker immunostaining in different areas of IC. (A) Dorsal cortex of IC in a section stained for RLN3 and TH. Black arrows indicate RLN3 fibers in the DCIC, BIC and Sag, respectively. (B) The external cortex contains RLN3 plexuses in layer 1 in a section immunostained for RLN3 and nNOS, arrowheads indicate nNOS cells in layer 2. (C) RLN3-labeled fibers in the brachium of IC. (D) RLN3 fibers (black arrows) and nNOS-positive cells in layer 2 (white arrowheads). (E-G) Single confocal sections of 0.25 µm, illustrating the colocalization of synaptophysin (green) and RLN3 (red) in nerve fibers in the DCIC. White arrows indicate putative synaptic contacts. Scale bar 10 µm. For abbreviations, see list.

Figure 9.

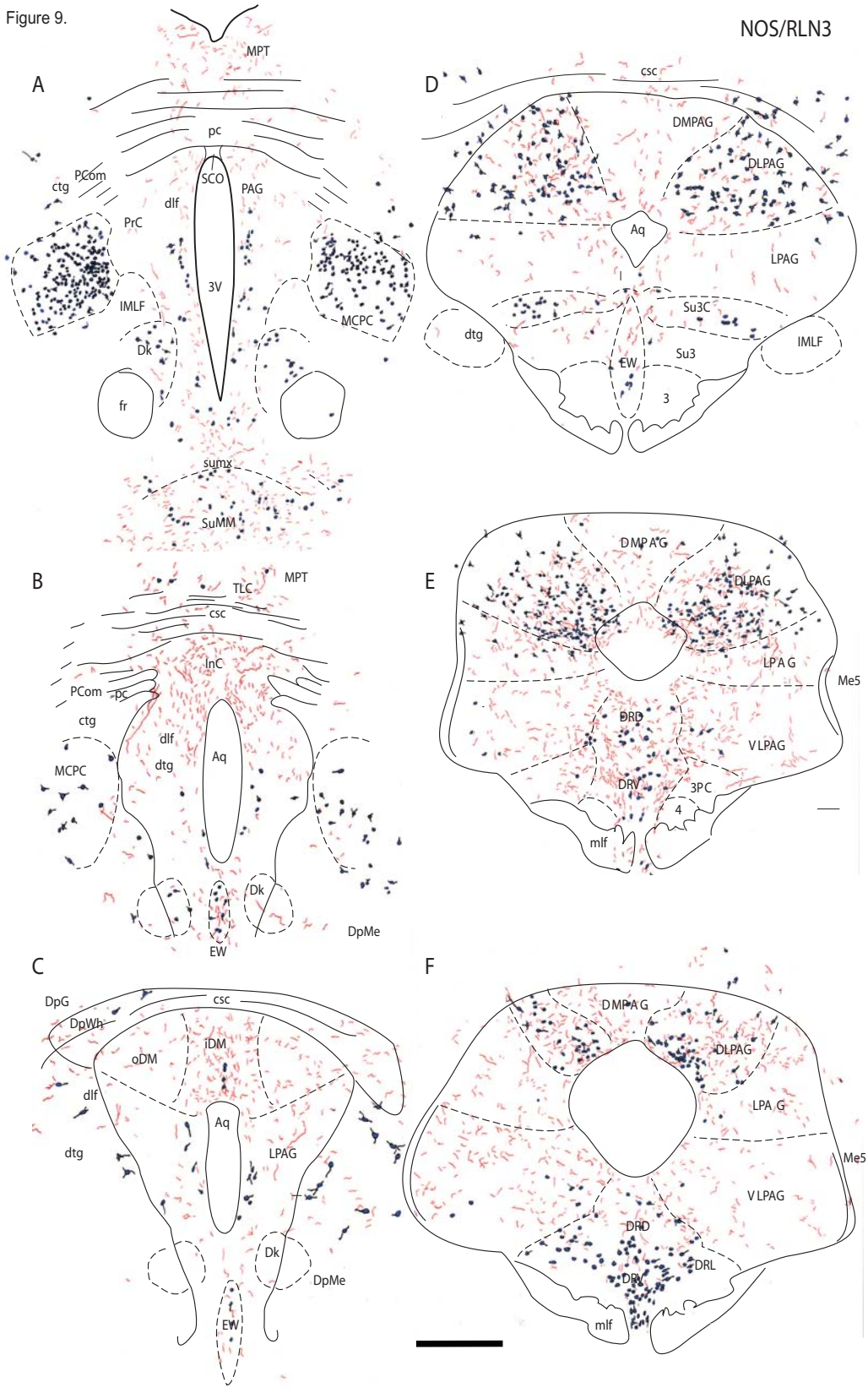

3PC oculomotor nucleus, parvicellular part
3v 3rd ventricle
4 trochlear nucleus
Aq aqueduct
csc commissure of the superior colliculus
ctg central tegmental tract
Dk nucleus of Darkschewitsch
dlf dorsal longitudinal fasciculus
DLPAG dorsolateral column of the periaqueductal gray
DMPAG dorsomedial column of the periaqueductal gray
DpG deep gray layer of the superior colliculus
DpMe deep mesencephalic nucleus
DRD dorsal raphe nucleus, dorsal part
DRL dorsal raphe nucleus, lateral part
DRV dorsal raphe nucleus, ventral part
dtg dorsal tegmental bundle
EW Edinger-Westphal
fr fasciculus retroflexus
iDM inner division of the dorsomedial column
IMLF interstitial nucleus of the medial longitudinal
IMLF interstitial nucleus of the medial longitudinal
InC intercommissural nucleus of the periaqueductal gray
LPAG lateral column of the periaqueductal gray
MCPC magnocellular nucleus of the posterior commissure
mlf medial longitudinal fasciculus
MPT medial pretectal nucleus
oDM outer division of the dorsomedial column
PAG priaqueductal gray
pc posterior commissure
PCom nucleus of the posterior commissure
PrC precommissural nucleus
SCO subcommissural organ
Su3 supraoculomotor periaqueductal gray
Su3C supraoculomotor cap
SuMM supramammillary nucleus, medial part
sumx supramammillary decussation
TLC tectal longitudinal column
VLPAG ventrolateral column of the periaqueductal gray

Figure 9. Distribution of RLN3-positive fibers within PAG mapped in sections immunostained for RLN3 and NOS. At rostral levels, nNOS-positive soma were observed in the MCPC, the periaqueductal ring and the EW nucleus. At levels 4 to 6, the nNOS-positive cells distribution allows the demarcation of the DL column and DR. At rostral levels the RLN3 innervation is concentrated in the InC and iDM. At caudal levels RLN3-positive fibers are observed in the DM column and the DR at level 4. RLN3-immunostaining is more intense in the medial half of the lateral column. Scale bar: 500 µm.

Figure 10.

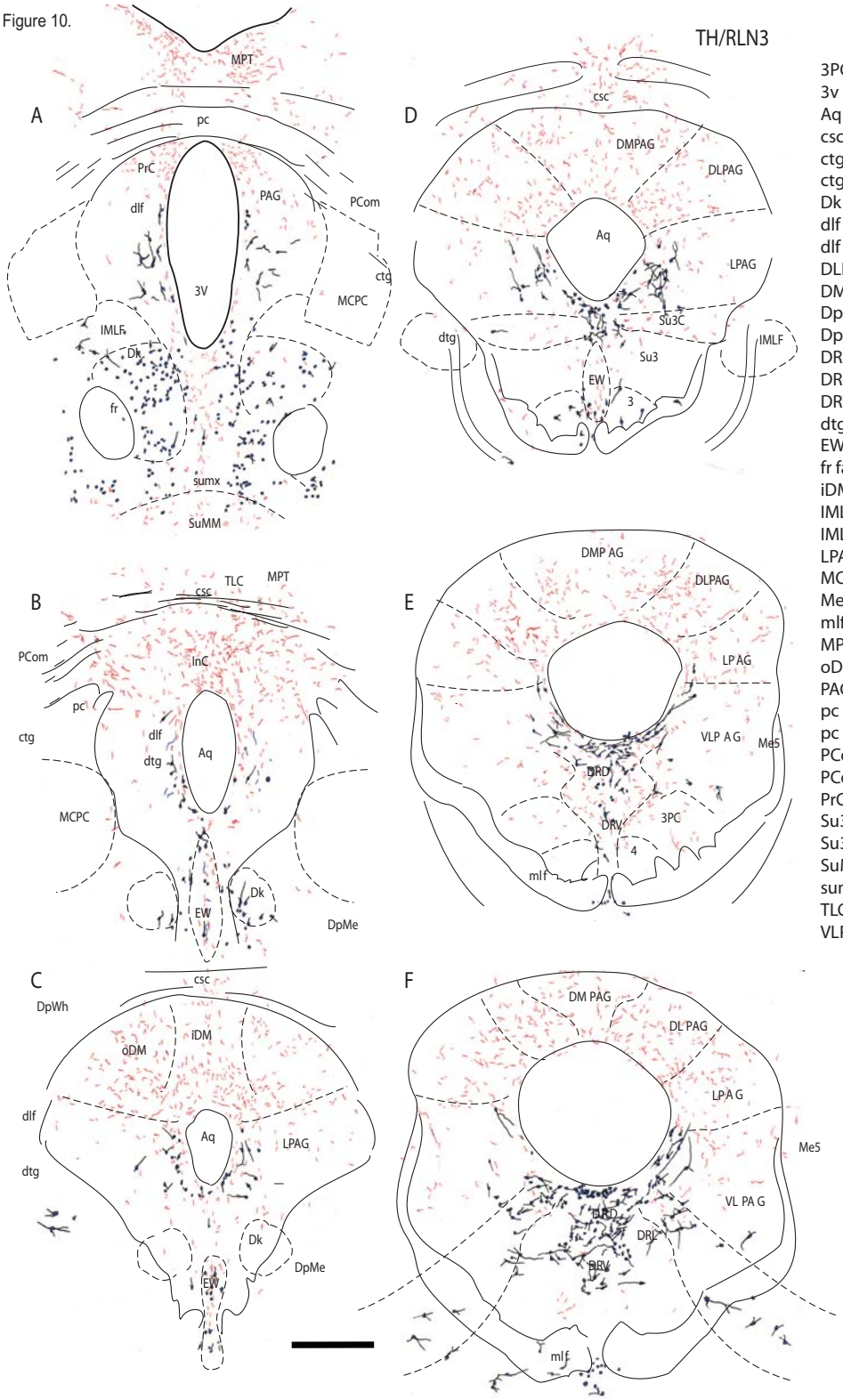

3PC oculomotor nucleus, parvicellular part
3v 3rd ventricle
Aq aqueduct
csc commissure of the superior colliculus
ctg central tegmental tract
ctg central tegmental tract
Dk nucleus of Darkschewitsch
dlf dorsal longitudinal fasciculus
dlf dorsolateral funiculus
DLPAG dorsolateral column of the periaqueductal gray
DMPAG dorsomedial column of the periaqueductal gray
DpMe deep mesencephalic nucleus
DpWh deep white layer of the superior colliculus
DRD dorsal raphe nucleus, dorsal part
DRL dorsal raphe nucleus, lateral part
DRV dorsal raphe nucleus, ventral part
dtg dorsal tegmental bundle
EW Edinger-Westphal
fr fasciculus retroflexus
iDM dorsomedial column of the periaqueductal gray, intermediate part
IMLF interstitial nucleus of the medial longitudinal
IMLF interstitial nucleus of the medial longitudinal fasciculus
LPAG lateral column of the periaqueductal gray
MCPC magnocellular nucleus of the posterior commissure
Me5 mesencephalic trigeminal nucleus
mlf medial longitudinal fasciculus
MPT medial pretectal nucleus
oDM outer division of the dorsomedial column
PAG priaqueductal gray
pc posterior commissure
pc posterior commissure
PCom nucleus of the posterior commissure
PCom nucleus of the posterior commissure
PrC precommissural nucleus
Su3 supraoculomotor periaqueductal gray
Su3C supraoculomotor cap
SuMM supramammillary nucleus, medial part
sumx supramammillary decussation
TLC tectal longitudinal column
VLPAG ventrolateral column of the periaqueductal gray

Figure 10. Distribution of RLN3-positive fibers within PAG mapped in sections immunostained for RLN3 and TH. At levels 5 and 6, TH-positive cells and processes in the DR facilitated the definition of its subdivisions. The ventral half of the juxta-aqueductal ring and EW also contain TH-positive labeling. At level 1, the PrC contains RLN3-positive fibers. Scale bar: 500 µm. For abbreviations, see list.

Figure 11.

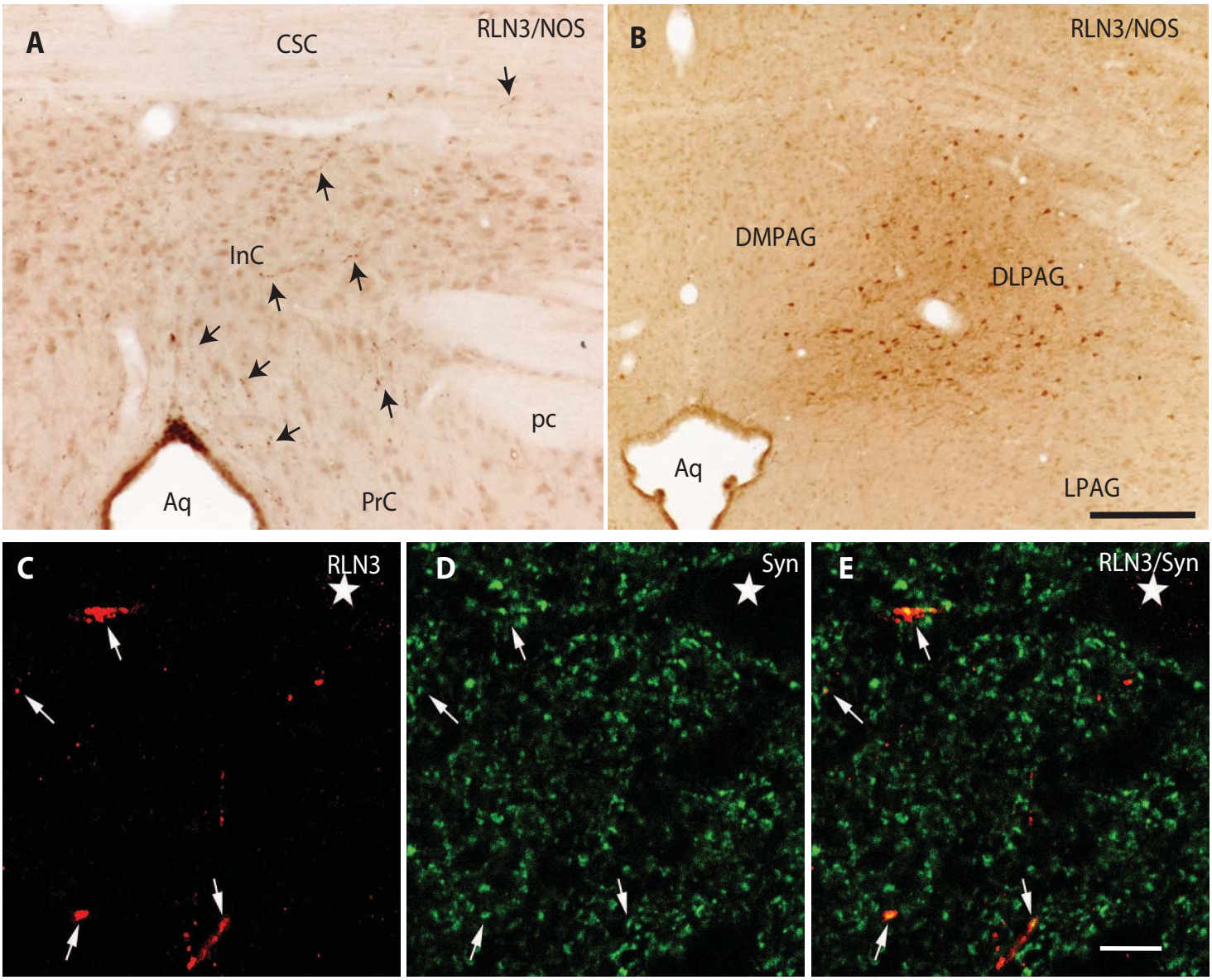

Figure 11. Illustrative examples of RLN3 and marker immunostaining in PAG. (A) Abundant RLN3-labeled fibers in the precommissural and intercollicular nuclei. (B) Intense nNOS-immunoreactivity in the DL column of PAG. (C-E) Single confocal sections of 0.25 µm illustrating the colocalization of synaptophysin (green) and RLN3 (red) in nerve fibers in the DL column. White arrows indicate putative synaptic contacts, stars point at putative neuronal somata.
LN3-positive fibers in the THpositive area of the ventrolateral PAG. Scale bar A,B: 200 µm, C-K: 10 µm. For abbreviations, see list.

Aq aqueduct
csc commissure of the superior colliculus
DLPAG dorsolateral column of the periaqueductal gray
DMPAG dorsomedial column of the periaqueductal gray
InC intercommissural nucleus of the periaqueductal gray
LPAG lateral column of the periaqueductal gray
pc posterior commissure
PrC precommissural nucleus

Figure 12.

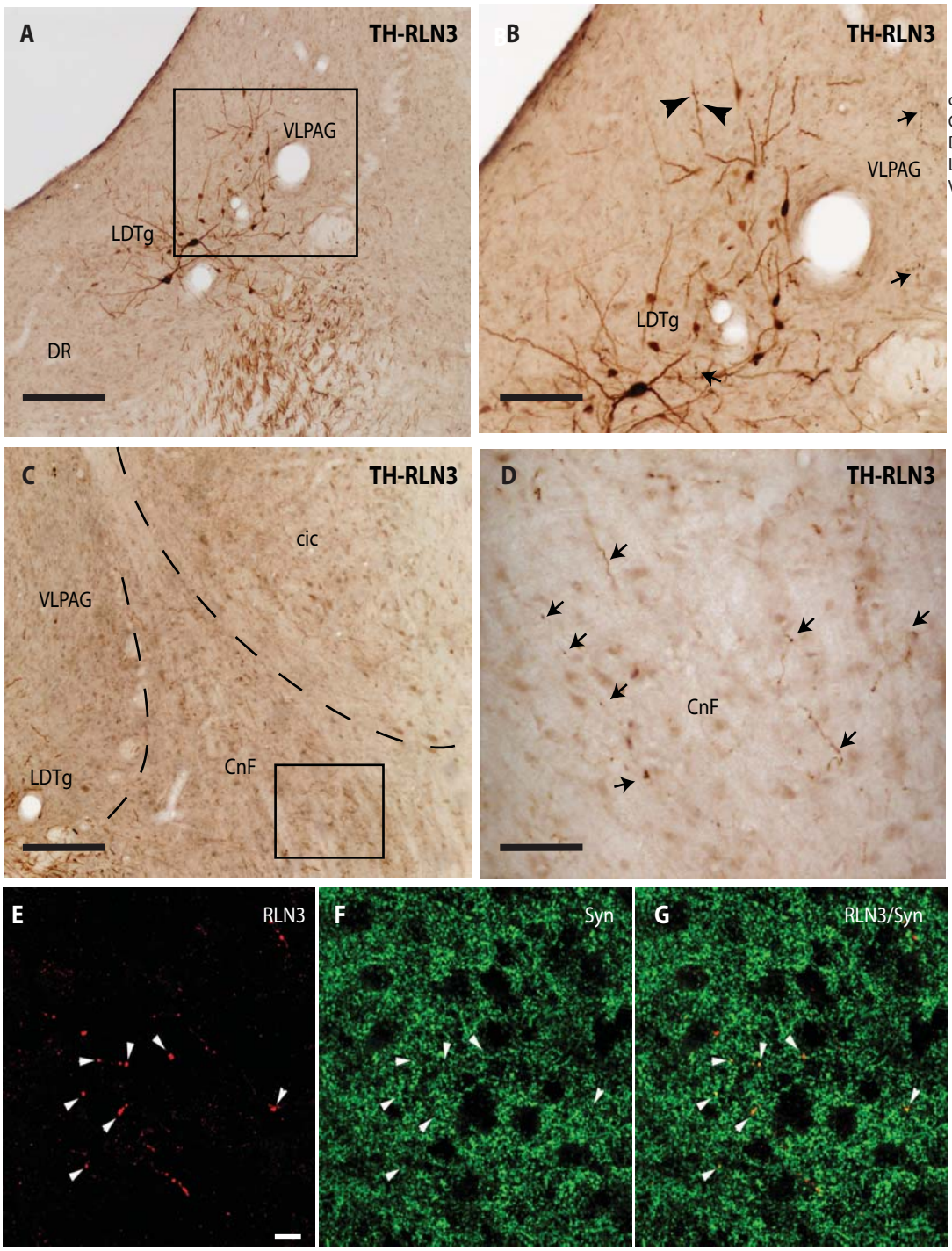

cic commissure of the inferior colliculus
CnF nueclus cuneformis
DR dorsal raphe nucleus
LDTg laterodorsal tegmental nucleus
VLPAG ventrolateral column of the periaqueductal gray

Figure 12. Illustrative examples of RLN3 and marker immunostaining in LDTg (A-B) and cuneiform nucleus (C,D). Confocal images illustrating the colocalization of synaptophysin (green) and RLN3 (red) in nerve fibers in the cuneiform nucleus (E-G). White arrows indicate putative synaptic contacts. Scale bars A 200 µm B-C: 100 µm, D: 50 µm, E-G: 10 µm.

Figure 13.

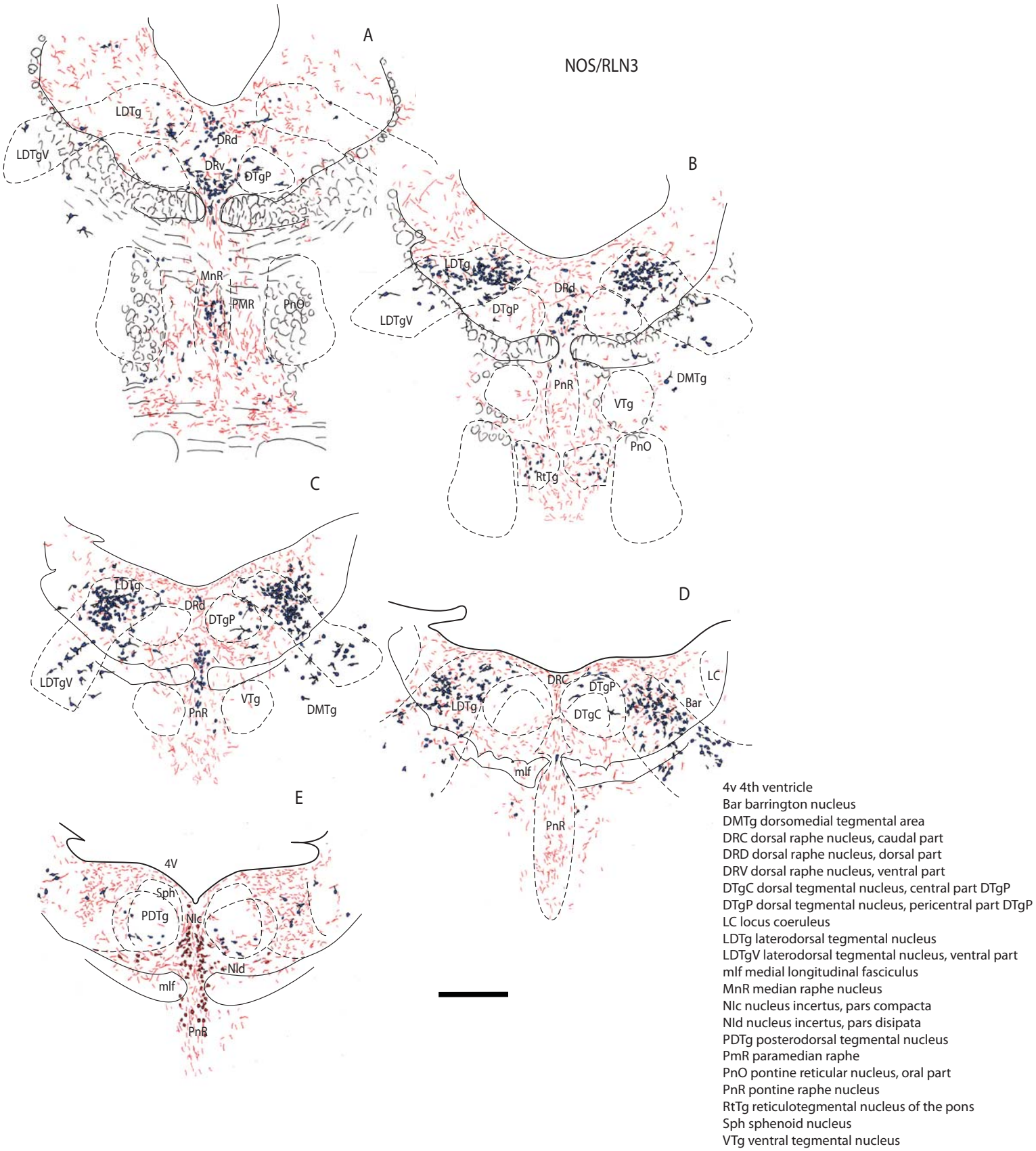

4v 4th ventricle
Bar barrington nucleus
DMTg dorsomedial tegmental area
DRC dorsal raphe nucleus, caudal part
DRD dorsal raphe nucleus, dorsal part
DRV dorsal raphe nucleus, ventral part
DTgC dorsal tegmental nucleus, central part DTgP
DTgP dorsal tegmental nucleus, pericentral part DTgP
LC locus coeruleus
LDTg laterodorsal tegmental nucleus
LDTgV laterodorsal tegmental nucleus, ventral part
mlf medial longitudinal fasciculus
MnR median raphe nucleus
NIc nucleus incertus, pars compacta
NId nucleus incertus, pars disipata
PDTg posterodorsal tegmental nucleus
PmR paramedian raphe
PnO pontine reticular nucleus, oral part
PnR pontine raphe nucleus
RtTg reticulotegmental nucleus of the pons
Sph sphenoid nucleus
VTg ventral tegmental nucleus

Figure 13. Distribution of RLN3-labeled fibers within the pontine central grey and DR mapped in sections immunostained for RLN3 and nNOS. nNOS staining distinguishes the LDTg nucleus at level 2 to 4 and divisions of DR from level 1 to 3. A high density of RLN3-labeled fibers is present in the Bar, LDTg and raphe divisions, whereas the DTgP is unlabeled. The rostral area of the NI containing RLN3 soma is observed at level 5. Scale bar: 500 µm. For abbreviations, see list.

Figure 14.

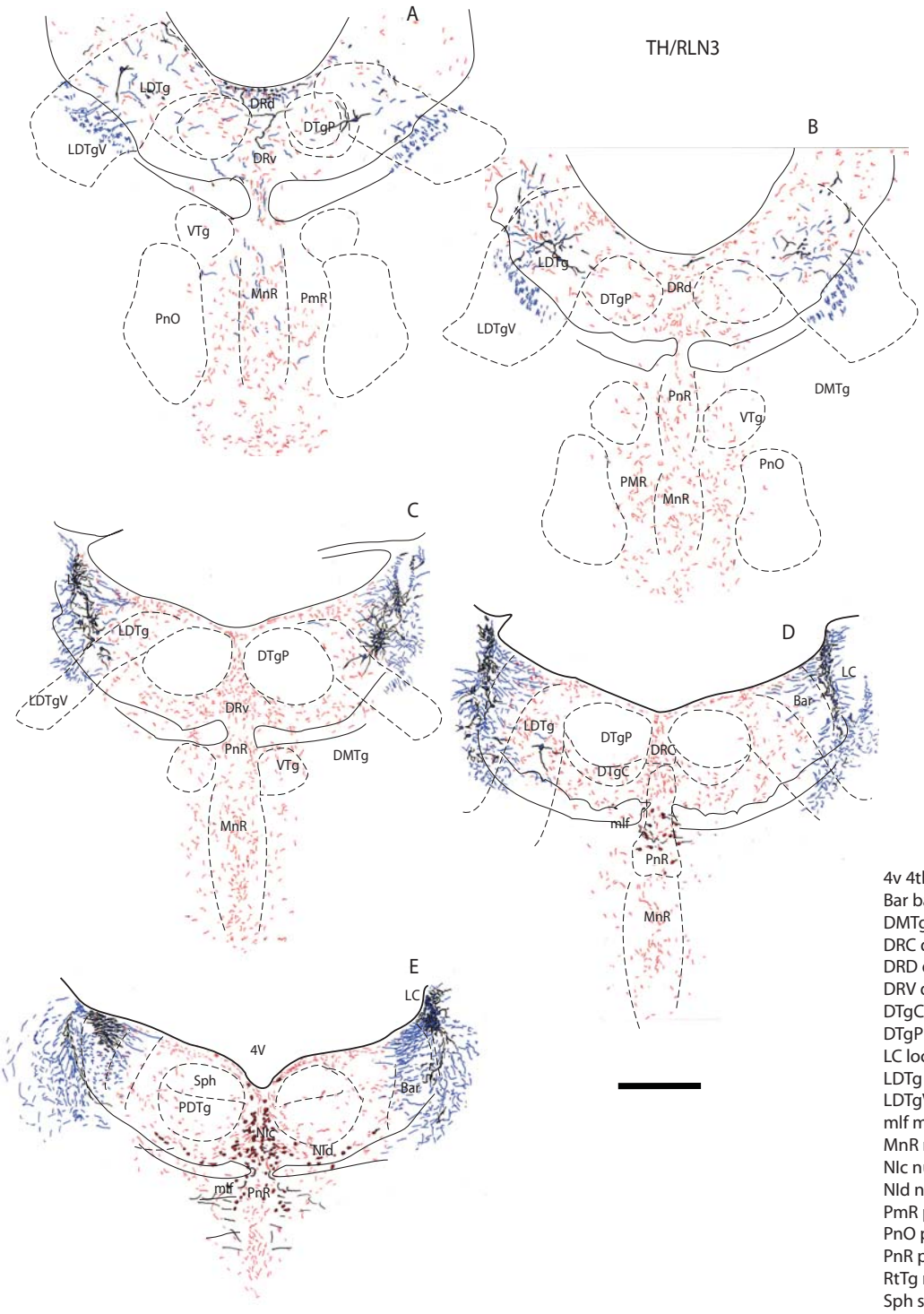

4v 4th ventricle
Bar barrington nucleus
DMTg dorsomedial tegmental area
DRC dorsal raphe nucleus, caudal part
DRD dorsal raphe nucleus, dorsal part
DRV dorsal raphe nucleus, ventral part
DTgC dorsal tegmental nucleus, central part DTgP
DTgP dorsal tegmental nucleus, pericentral part DTgP
LC locus coeruleus
LDTg laterodorsal tegmental nucleus
LDTgV laterodorsal tegmental nucleus, ventral part
mlf medial longitudinal fasciculus
MnR median raphe nucleus
NIc nucleus incertus, pars compacta
NId nucleus incertus, pars disipata
PmR paramedian raphe
PnO pontine reticular nucleus, oral part
PnR pontine raphe nucleus
RtTg reticulotegmental nucleus of the pons
Sph sphenoid nucleus
VTg ventral tegmental nucleus

Figure 14. Distribution of RLN3-labeled fibers within PCG and DR mapped in sections immunostained for RLN3 and TH. At level 1, DR contains TH-positive cells and processes. At rostral levels, THinmunoreactive tracts help define the LDTg nucleus. At levels 3, 4 and 5, intense TH-labeling appears in LC. RLN3-labeled fibers avoid the DTg and are dense in the midline and raphe nuclei. Scale bar: 500 µm. For abbreviations, see list.

Figure 15.

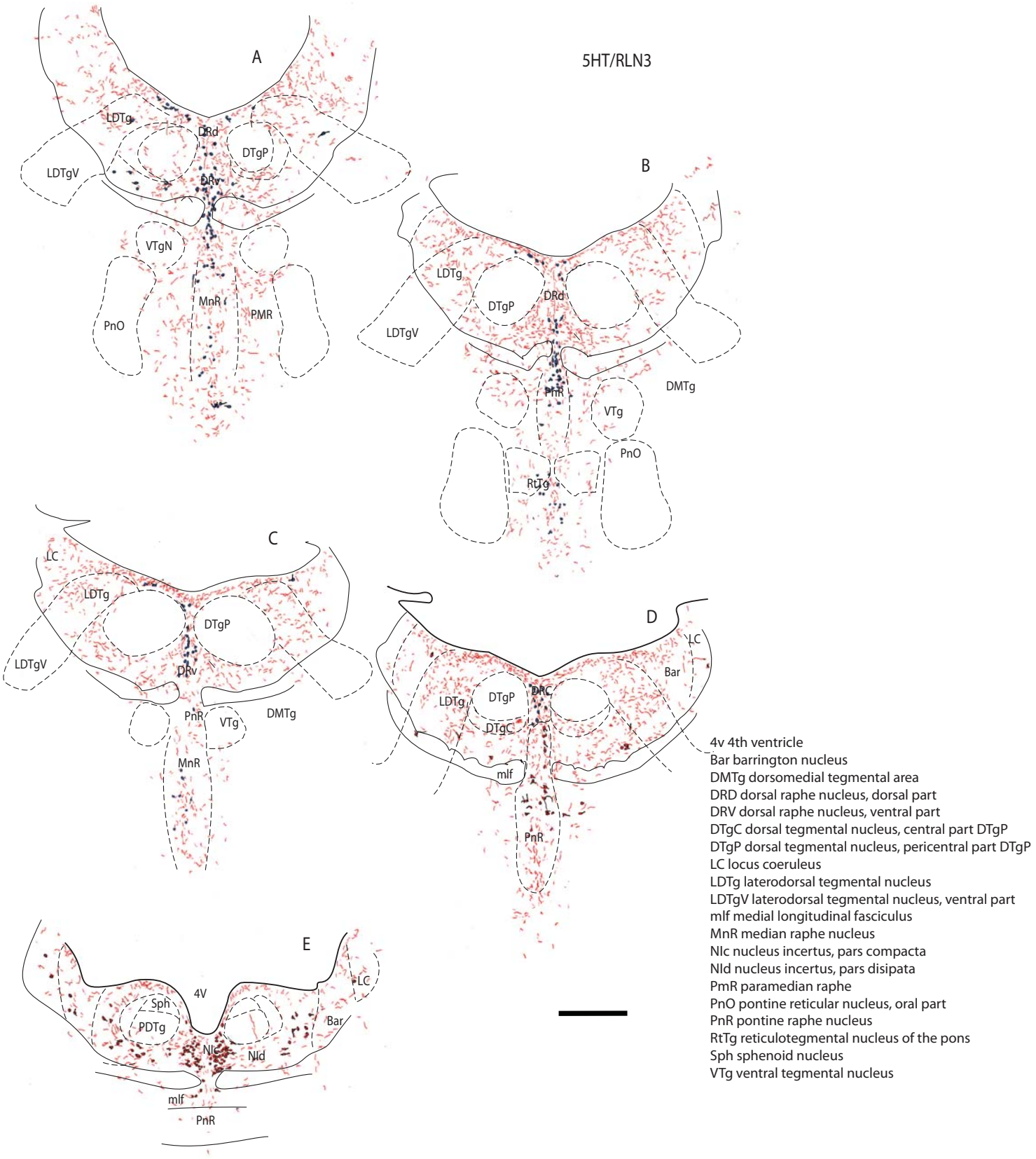

Figure 15. Distribution of RLN3-positive fibers in PCG and DR mapped in sections immunostained for RLN3 and 5HT. At levels 1 to 3, 5HT-labeled soma are present in DR and rostral PnR. MnR also contains some 5HT-labeled somata. At levels 4 and 5, RLN3-labeled soma appear in caudal PR and NI. The DTg contains no RLN3 fibers, although its surrounding area, midline region and raphe nuclei contain dense plexuses. Scale bar: 500 µm. For abbreviations, see list.

Figure 16.

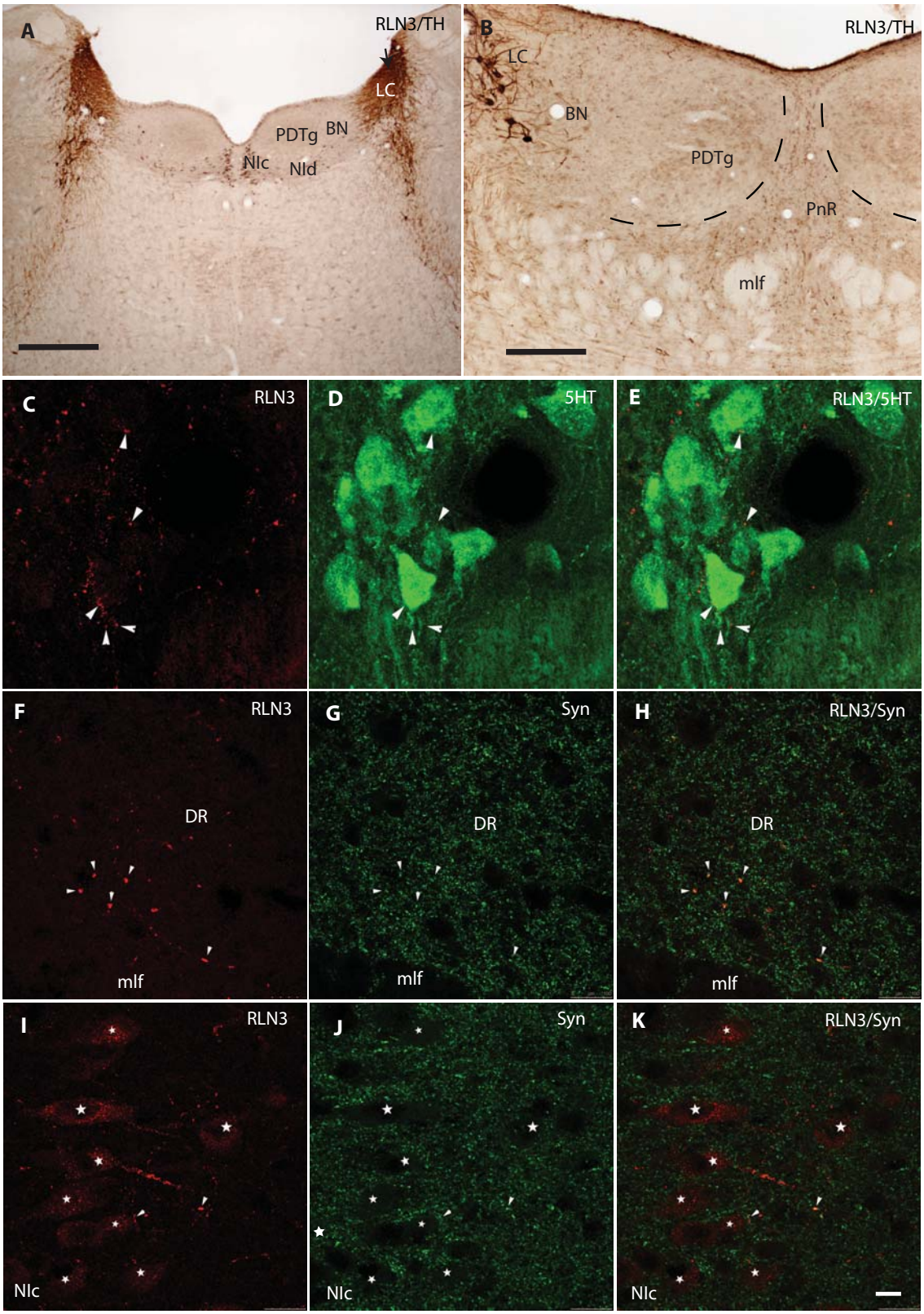

BN Barrington's nucleus
DR dorsal raphe nucleus
LC locus coeruleus
mlf medial longitudinal fasciculus
NIc nucleus incertus, pars compacta
NId nucleus incertus, pars disipata
PDTg posterodorsal tegmental nucleus
PnR pontine raphe nucleus

Figure 16. Illustrations of RLN3-labeling and marker immunostaining in pontine central grey. (A) Dense TH-immunoreactive cells and fibers (brown) in LC, and RLN3-labeled neurons in midline NIc (black), and lateral NId. (B) Abundant RLN3-immunoreactive fibers in the PnR between the PDTg and extending below the floor of the 3V. (C-E) Confocal images illustrating the presence of RLN3-labeled fibers (red) adjacent to 5HT-positive neurons (green) in caudal DR. White arrows indicate putative contacts. (F-H) Confocal images illustrating the colocalization of synaptophysin (green) and RLN3 (red) in the caudal DR. White arrows indicate putative synaptic contacts. (I-K) Confocal images illustrating the RLN3-containing neurons of the NI (asterisks) and possible synaptic contacts of RLN3-labeled fibers (white arrows). Scale bar A: 200 µm; B: 100 µm; C-K: 10 µm. For abbreviations, see list.

Figure 17.

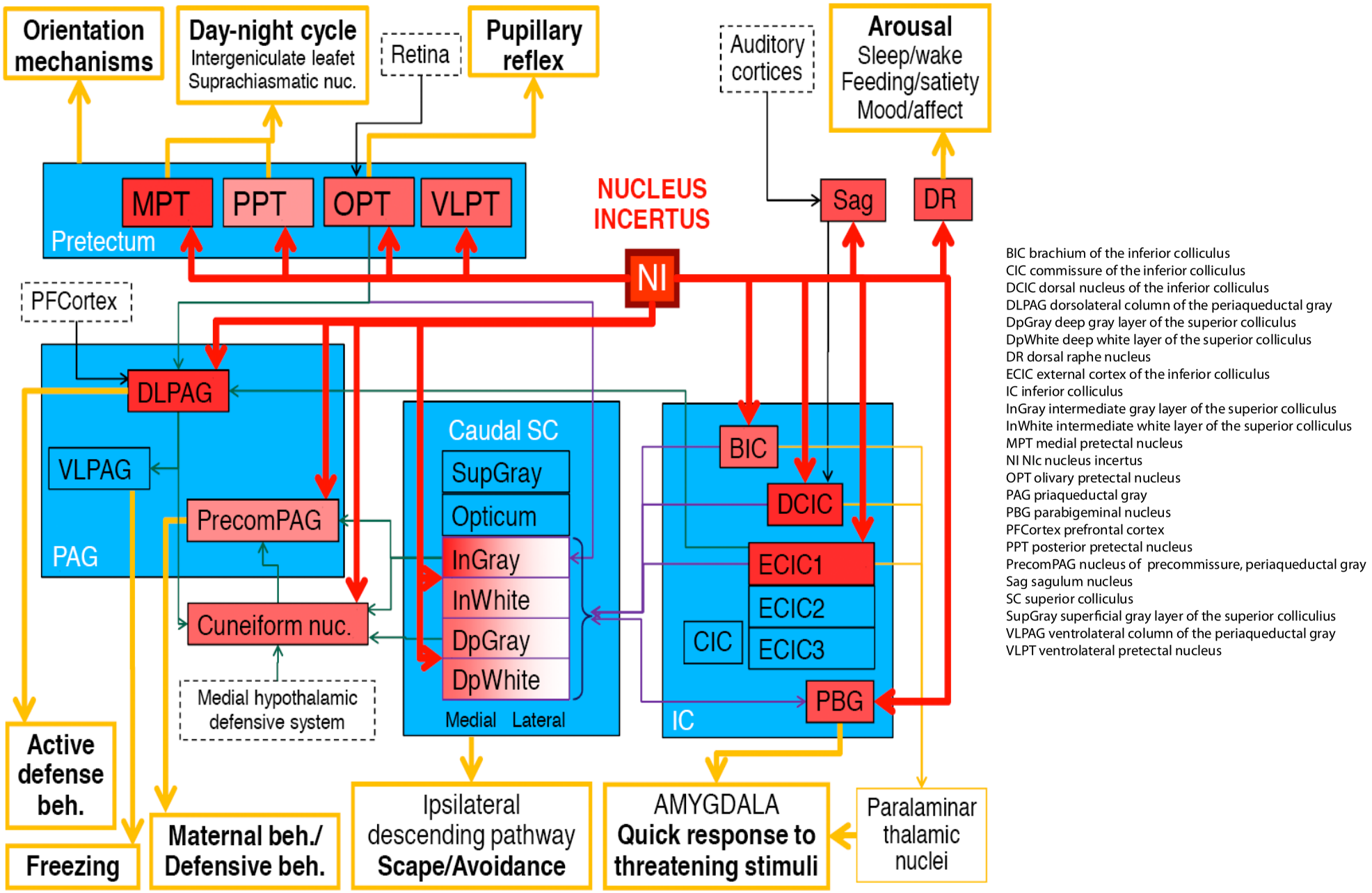

BIC brachium of the inferior colliculus
CIC commissure of the inferior colliculus
DCIC dorsal nucleus of the inferior colliculus
DLPAG dorsolateral column of the periaqueductal gray
DpGray deep gray layer of the superior colliculus
DpWhite deep white layer of the superior colliculus
DR dorsal raphe nucleus
ECIC external cortex of the inferior colliculus
IC inferior colliculus
InGray intermediate gray layer of the superior colliculus
InWhite intermediate white layer of the superior colliculus
MPT medial pretectal nucleus
NI NIc nucleus incertus
OPT olivary pretectal nucleus
PAG priaqueductal gray
PBG parabigeminal nucleus
PFCortex prefrontal cortex
PPT posterior pretectal nucleus
PrecomPAG nucleus of precommissure, periaqueductal gray
Sag sagulum nucleus
SC superior colliculus
SupGray superficial gray layer of the superior colliculius
VLPAG ventrolateral column of the periaqueductal gray
VLPT ventrolateral pretectal nucleus

Figure 17. A schematic illustration summarizing the RLN3-containing projections within the tectal and tegmental systems of rat brain. RLN3 projections are indicated by red arrows and many, if not all, of these may originate from the NI. Midbrain areas are grouped in blue squares. Main physiological and behavioral outputs of the targeted systems are indicated by yellow arrows.

APÊNDICE C

MEDIAL SEPTAL PROJECTIONS TO THE PONTINE TEGMENTUM TARGETS THE NUCLEUS INCERTUS

SÁNCHEZ-PÉREZ, A.M.; SANTOS, F.N.; PEREIRA, C.W.; MARCHIORO, M.; ELMLILI, N.; SANJUAN, J.; MA, S.; GUNDLACH, A.L.; OLUCHA-BORDONAU, F.E.

Journal of Comparative Neurology

Medial septal projections to the pontine tegmentum targets the nucleus incertus

Ana M Sánchez-Pérez[1], Fabio N. Santos[2], Celia W. Pereira[2], Murilo Marchioro[2], Nisrin ElMlili[3], Julio Sanjuan[4], Sherie Ma[5,6], Andrew L. Gundlach[5,6,7,] Francisco E. OluchaBordonau[8]*

[1]Department of Physiology. University of Valencia. [2] Department of Physiology, Universidade Federal de Sergipe, Aracaju, Brasil [3] Laboratoire de Neurobiologie et santé, Faculté des Sciences, Université Abdelmalek Essaadi, Tetouan- Morocco [4]Departamento de Medicina, Facultad de Medicina, Universidad de Valencia, 46010 Valencia, Spain. [5]Florey Neuroscience Institutes, [6]Department of Medicine (Austin Health) and [7]Department of Anatomy and Cell Biology, The University of Melbourne, Victoria 3010, Australia [8]Departamento de Anatomía y Embriología Humana, Facultad de Medicina, Universidad de Valencia, 46010 Valencia, Spain

*Correspondence to: Francisco E. Olucha-Bordonau Telephone +34-963983504 Facsimile +34-963864159 Email olucha@uv.es

Running title: Medial septal projections to the nucleus incertus

Key words: NI, nucleus incertus: septohippocampal system, hippocampal theta rhythm,

Grant sponsors: Fundation Alicia Koplowitz to AMSP; Capes Bex 4494/09-1 and Fapitec edital # 01/08 to FNS; Capes Bex 4496/09-4 to CWP (FNS); the Ministry of Health, Spain - ISCIII-FIS PI061816 (FEO-B); the National Health and Medical Research Council of Australia – 520299 (SM); 277609 and 509246 (ALG); and the Victorian Government Operational Infrastructure Support Program (SM and ALG)

ABSTRACT

Projections from the nucleus incertus of the pontine tegmentum to the medial septum are involved in modulating hippocampal theta rhythm. Hippocampal rhythmicity depends on the integrity of the system and adjustments may also be influenced by converging projections at the nucleus incertus. In this work we have studied these afferents that may provide a feed back modulation on the ascending projections from the nucleus incertus. Fluorogold injections into the nucleus incertus result in strong retrograde labeling in the medial septum area. Labeling was concentrated in the horizontal limb while scattered in the vertical limb of the medial septum. Double immunofluorescence of fluorogold and neuronal markers indicate that NI projecting and choline acetyl transferase positive cells occupy different compartments within the medial septum. In addition, FG labeling was seen in parvalbumin positive neurons. There was a high degree of co-localization between GAD65 positive neurons and FG labeling, indicating that the descending system is to some extent GABAergic. Anterograde tracer miniRuby injections in the medial septum reveal descending fibers running through the medial forebrain bundle which arrive to the median and paramedian raphe and continue caudally to reach the nucleus incertus. Interestingly, we found that anterogradely labeled terminal-like varicosities display co-localization with synaptophysin indicating that medial septal fibers make synapses on nucleus incertus neurons. Some anterogradely labeled fibers co-localize with GAD65 positive puncta and in some cases, these pucta contact with retrogradely labeled neurons from injections in either hippocampus or amygdala. These data provide evidence of a descending inhibitory pathway from the medial septum to the nucleus incertus that may work as a feedback loop, which may modulate ascending nucleus incertus projections to the hippocampus and amygdala.

INDEXING TERMS: nucleus incertus; relaxin-3; septohippocampal system; stress; theta rhythm, brain circuitries,

INTRODUCTION

Awakening processes adapt behavior to environmental conditions. One way to drive arousal mechanisms is a general and widespread activation of telencephalic centers that process information which flows in a particular moment. Research on general mechanisms of arousal activation started following the classical Morruzi and Magoon's experiments where an ascending system of connections arising from the reticular formation was found to activate telencephalic centers regulating awaking states.

The septal area has been traditionally viewed as a connecting interface between the so-called limbic telencephalon on one side and the hypothalamus and brainstem on the other. This concept arises from the complementary pattern of connections for the medial and the lateral septum. In a simplified view, while the medial septum receives ascending connections from the diencephalon and brainstem and relays them mainly over the hippocampus, cortex and amygdala (Vertes and Kocsis, 1997) the lateral septum receives projections from the hippocampus which, in turn, are relayed to the hypothalamus and brainstem (Leranth and Vertes, 1999). Consequent with this view, most of the physiological studies on medial septum have been centered in its role in driving hippocampal theta rhythm. Lesions in the medial septum result in impaired hippocampal theta rhythm (Andersen et al., 1979) (Vinogradova, 1995) (Petsche and Stumpf, 1962).

Moreover, recent EEG recordings in freely-moving rats demonstrated that the integrity of the entire medial and lateral septum-hippocampal network is critical for the generation of theta rhythm (Nerad and McNaughton, 2006). Different types of medial septal neurons display different roles in driving hippocampal activity. Slow-firing cholinergic neurons facilitate hippocampal activity (Sotty et al., 2003). On the other hand, fast-firing parvalbumin GABAergic neurons innervate GABAergic hippocampal interneurons driving disinhibition of pyramidal or granule cell. These two events, i.e. facilitation and desinhibition allow hippocampal synchrony at theta frequency (Freund and Antal, 1988)(Freund and Gulyas, 1997) (Toth, Freund, Miles, 1997) (Wu et al., 2000) (Sotty et al., 2003).

We have shown that stimulation of nucleus incertus in urethane-anesthetized rats increased theta and decreased delta activity of the hippocampus, whereas, electrolytic lesion of the nucleus incertus abolished hippocampal theta induced by stimulation of the *nucleus reticularis pontis oralis* (RPO) (Nunez et al., 2006) a key brainstem generator of hippocampal theta rhythm (Vertes, 1981; Vertes, 1982; Vertes et al., 1993)(Vertes and Kocsis, 1997)(Nunez, de Andres, Garcia-Austt, 1991).

In fact, the nucleus incertus is presumed to be the major relay station of RPO inputs to the medial septum (and hippocampus), as there are no direct projections from the RPO to hippocampus (Teruel-Marti, 2008). The hippocampal area where field potentials were recorded receives only sparse

inputs from the nucleus incertus. Thus, it was concluded that the influence of the nucleus incertus on hippocampal theta rhythm was most likely mediated by the medial septum and/or other lower brain structures. The nucleus incertus contains glutamic acid decarboxylase (GAD) positive neurons (Olucha-Bordonau et al., 2003) which are also characterized as the main source of relaxin3 (RLN3) (Ma et al., 2007). Fibres containing this peptide occur in the nucleus incertus' projection areas that are particularly conspicuous in the medial septum (Ma et al., 2009a; Olucha-Bordonau et al., 2011). Infusion of a RLN3 agonist into the medial septum results in increasing hippocampal theta rhythm and this effect was reverted by a previous infusion of an RLN3 antagonist (Ma et al., 2009b). Furthermore, injections of the antagonist in the medial septum revert the theta obtained by stimulation of RPO.

Although much has been said about the ascending connections over the septohippocampal system, there are few data on the afferent connections to the nucleus incertus, other than the pioneering work by (Goto, Swanson, Canteras, 2001) where the medial septal area was included within the list of telencephalic afferents to the nucleus incertus. As the septal area provides both ascending and descending connections, it is possible that a circuitry connecting septum and NI exists, forming a feed-back loop. The goal of the present work is to confirm and characterize septal projections to NI. In order to do that, we have made a comprehensive map of the nucleus incertus retrograde labeling and carry out characterization studies combining immunofluorescence maker with retrograde labeling. In addition, we have used anterograde labeling following injections in the septal area to prove the occurrence of septal arising fibers in the nucleus incertus. Furthermore, retrograde and anterograde tracing studies has been combined with GAD fluorescence to determine if neurons of the nucleus incertus projecting to hippocampus and amygdala receive GAD projections from the medial septum.

MATERIALS AND METHODS

Animals

Male Sprague-Dawley rats (300-400 g, n = 22) were used in this study. All protocols were approved by the Animal Ethics Committees of the Universitat de València (Spain), and Howard Florey Institute (Australia). All procedures were in line with directive 86/609/EEC of the European Community on the protection of animals used for experimental and other scientific purposes and the guidelines on animal welfare issued by the National Health and Medical Research Council of Australia. Details of the experimental protocols employed are provided below (see Table 1).

Tracer injections

Rats were anesthetized with ketamine (Imalgene 55 mg/kg i.p.) and xylacide (xilagesic 20 mg/kg i.p.) and trephine holes were drilled in the skull. Anterograde tracer injections into Medial Septum were made using 40 µm I.D. glass micropipettes (coordinates from bregma: AP 0.2 to -0.4 mm, ML 0.2-0.8 mm and DV -7 to -8 mm). For anterograde tracing, 15% miniruby (mR, 10 kD biotinylated dextran amine rhodamine-labeled, Cat No. D-3312, Molecular Probes, Paisley, UK) dissolved in 0.1M PB, pH 7.6 was iontophoretically delivered into the Medial Septum by passing a positive current of 1 µA, 2 sec on, 2 sec off over 20 min. The micropipette was left in place for an additional 10 min before withdrawal. Injections of 4% Fluorogold retrograde tracer dissolved in dH_2O (FG, 5-hydroxystabilamide (Cat No 80014, Biotium, Hayward, CA, USA), were made into the hippocampus (coordinates from bregma: AP -5.4 mm, ML 5 mm, DV 5 mm) the nucleus incertus (coordinates from bregma: AP -9.6 mm, ML 0 ± 0.2 mm and DV 7.4 mm) and amygdala (coordinates from bregma: AP
3.4 mm, ML 4 mm, DV -7.2 mm) Volumes of 0.04-0.08 µl of 4% FG in dH_2O were injected using a 40 µm I.D. glass micropipette attached to an IM-300 microinjector (Narishige, Tokyo, Japan) over 10 min. After injections, the surgical wound was sutured and rats were injected with Buprex (0.05 mg/kg, i.p., Lab Esteve, Barcelona, Spain) for analgesia. Rats were then allowed to recover for at least 7 days, prior to further processing.

Brain fixation and sectioning

For analysis of tracing studies, rats were deeply anesthetized with Nembutal (150 mg/kg i.p., Euthalender, Barcelona, Spain) and transcardially-perfused with saline (250 ml) followed by fixative (4% paraformaldehyde in 0.1M PB, pH 7.4) for 30 min (~500 ml). Brains were dissected and immersed in the same fixative for 4 h at 4ºC. They were then incubated in 30% sucrose in 0.01 M

PBS pH7.4 for 48 h at 4ºC. The brains were cut coronally at the level of the flocculi by using a rat's brain methacrylate matrix in order to obtain reliable sections displaying equal orientation. Coronal sections (40 μm) were collected using a freezing slide microtome (Leica SM2010R, Leica Microsystems, Heidelberg, Germany). For each brain, 6 series of sections were obtained and collected free-floating in 0.01M PBS plus 30% sucrose

Immunofluorescent detection of neuronal markers in the medial septum

For detection of medial septal marker proteins, sections were rinsed 2 × 10 min and immersed in a blocking media of TBS containing 4% NDS, 2% BSA and 0.1% Triton X-100 for 1 h at RT. Sections were then incubated in primary antibody solution containing 1:2,500 mouse anti-PV (Swant), 1:2,500 mouse anti-CB-28kD (Swant), 1:500 goat anti-ChAT (Chemicon), 1:1,000 mouse anti-GAD67 (Chemicon) or 1:5,00 mouse anti-synaptophysin (Sigma) in TBS containing 2% NDS, 2% BSA and 0.2% Triton X100 for 48 h at 4ºC. Sections were then rinsed (3 × TBS) and incubated in 1:200 488- donkey anti-ms) 1:200 Cy5labeled donkey anti-goat (Cat No. 705-175-003, Jackson) in TBS. Sections were then briefly rinsed in 0.01M PBS and mounted on chrome-alum gelatin-coated slides, air-dried, dehydrated in graded ethanol and coverslipped with DPX.

Antibody characterization

A number of characterized antisera were used in these studies (see Table 2). The goat polyclonal choline acetyltransferase (ChAT) antiserum (Cat No. AB144P, Chemicon, Temacula, CA, USA) stains a single band of 68-70 kD molecular weight on Western blot analysis of mouse brain lysate (manufacturer's technical data). Its antigen specificity has been determined by preadsorption with the appropriate purified protein (Rico and Cavada, 1998).

The CB-28kD antibody (Cat No. 300, Swant) is a mouse IgG1 produced by hybridization of mouse myeloma cells with spleen cells from mice immunized with CB-28kD purified from chicken gut (Celio et al., 1990). This antibody reacts specifically with CB-28kD on immunoblots of extracts of tissue originating from human, monkey, guinea pig, rabbit, rat, mouse and chicken, and does not cross-react with CR or other known calcium binding-proteins (manufacturer's technical data). The monoclonal parvalbumin (PV) antibody (Cat No. 235, Swant) was produced by hybridization of mouse myeloma cells with spleen cells from mice immunized with PV purified from carp muscles (Celio et al., 1988). It recognized a single 12 kD protein (pI 4.9) on a 2-dimensional immunoblot of rat cerebellar tissue; values identical to those expected for purified PV (Celio et al., 1988); and labeled a subpopulation of neurons in normal brain, but did not stain the brain of PV knockout mice

(manufacturer's technical data).

The antibody against glutamate decarboxylase-67 (GAD-67) (Cat No. MAB5406, Chemicon) reacts with the 67kD isoform of GAD from rat, mouse and human. It displayed no detectable cross reactivity with GAD65 on Western blots of rat brain lysate, compared to antibody AB1511 (Chemicon) that reacts with GAD65 and GAD67 (manufacturer's technical data). The tyrosine hydroxylase (TH) antibody (clone TH-2; Sigma) recognizes an epitope present in the N-terminal region (~aa 9-16) of both rodent and human TH and reacts with intact TH subunits. The synaptophysin antibody (clone SVP-38, Cat No. S5768, Sigma) is an IgG1 monoclonal antibody raised using rat retina synaptosomes as the immunogen and it labels synaptophysin in neurons (Booettger et al., 2003). The specificity of the FG antibody (Biotium) was verified by the presence and absence of labeling in rats injected or not injected with FG, respectively.

ImmunoFuorescence analyses

FG immunohistochemistry was studied using a Nikon Eclipse E600 microscope with a DMX2000 digital camera (Nikon, Tokyo, Japan) and maps were constructed using a camera lucida tube attached to a Zeiss Axioskop microscope (Zeiss, Munich, Germany) (Fig. 1). Drawings were made with 20× and 40 × magnifications, scanned and reduced to the final size.. Confocal immunofluoresence was analyzed with a laser confocal scan unit TCS-SP2 equipped with argon and helio-neon laser beams attached to a Leica DMIRB inverted microscope (Leica Microsystems). Wavelengths for FG excitation were 351 nm and 364 nm and for emission 382-487 nm; mR/Texas red wavelength for excitation was 433 nm and for emission 560-618 nm; 488 labeled antibodies wavelength of excitation was 488 nm and for emission was 510-570 nm; Cy5 wavelength of excitation was 633 nm and for emission 644719 nm. Serial 1-micron sections of captured images were obtained in the Z-plane and a ‘maximal projection’ was generated with Leica Confocal Software, Version 2.61.

RESULTS

We have observed retrograde labeling in the septal area after FG injection in the nucleus incertus (Figure 1A-D) and, conversely, anterograde labeling in the nucleus incertus after mR injection in the septal area (Figure 1 E-F) . Moreover, we have found that these afferents fibers arriving from septal area colocalized with neurons that in turn project to hippocampus and or amygdala, providing anatomical basis for an additional loop regulating hippocampal and amygdala function.

Septal terminology

We have adopted the same terminology used in our previous paper on relaxin3 projections to the septum (Olucha-Bordonau et al., 2011), based on the description by Jacab and Leranth of the medial and posterior septal areas (Jacab and Leranth, 1995), and the parcellation of the lateral septum described by Risold and Swanson (Risold and Swanson, 1997). Briefly, the medial septum was divided into the vertical (vMS) and the horizontal (hMS) medial septum. Within the lateral septum three main divisions were considered, rostral (LSr), caudal (LSc) and ventral (LSv). In addition, at caudal levels, corresponding to the area also known as posterior septum, we described the septofimbrial (SF) nucleus, an unpaired triangular shaped nucleus located centrally between the fornix bundles and the triangularis septalis (TS).

We have analyzed five rostrocaudal levels in coronal sections. Level 1 is the most anterior level and corresponds to the point in which the medial septum from both sides of the brain is separated by the ependymal (Figure 2A). Level 2 is the section where the medial septum consists of two clearly defined segments, the vertical and horizontal limbs (Figure 2B). At Level 3 the fiber tracts of the fornix became evident (Figure 2C). At level 4 the septofimbrial nucleus between the bundles of the fornix and the triangularis septalis is clearly distinguished (Figure 2D). And, finally, at level 5 the only representative of the septal complex is the hMS (Figure 2E).

Retrograde tracer injections in the nucleus incertus

Up to 5 cases showed optimal tracer injection located in the nucleus incertus (Figure 1A-B). In all of them some FG labeling spread to the surrounding dorsal tegmental nuclei and the reticular formation ventral to the medial longitudinal fascicle and no diffusion to the dorsal raphe nucleus were observed. The pattern of retrograde labeling in the septal area was similar in all 5 cases. As a representative injection, we show case CCH5 retrograde labeling in the septal area. Most FG positive neurons concentrated in the medial septum, although some disperse neurons could also be seen in the

lateral septal area (Figure 2)

At level 1, there was a row of retrogradely labeled neurons in the medial septum although some retrograde labeling also occurred in the lateral septum (Figure 2A). In the vMS, neurons appeared dispersed but in the hMS concentrated in the area just over the ependyma. Another group of cells appeared in a band just over the nucleus accumbens of the rostral lateral septum (LSr). Some other cells appeared scattered in the LSr but not in the LSc.

At level 2, only few dispersed retrogradely labeled neurons were seen in the lateral septum corresponding to the LSr, most retrograde labeling concentrated in the medial septum (Figure 2B). In the vMS disperse retrogradely labeled neurons were found mostly towards the centre. A rather concentrated cluster of labeled neurons appeared in the hMS in a deep area leaving a narrow superficial band unlabeled.

At level 3, virtually no FG labeling was found in the lateral septum contrasting with the intense labeling in the medial septum (Figure 2C). In medial septum retrogradely labeled neurons appeared dispersed in the vMS and concentrated in the hMS. Within the vMS labeled cells also occurred between the fiber bundles of the fornix. Labeled cells in the hMS became visible as a band at a certain distance of the septal surface.

At level 4, there was a group of labeled cells between the bundles of the fornix which belonged to the septofimbrial nucleus. No retrograde labeling occurred in the triangularis septalis or in the caudal lateral septum (LSc). We observed retrograde labeled neurons in the hMS and also some neurons appeared in the SIB (Figure 2D).

At level 5, there was no retrograde labeling in the posterior septal nuclei. In contrast, some labeling was observed in the hMS within the transition area between the preoptic hypothalamus and the basal forebrain. (Figure 2E).

Double labeling

In order to characterize the type of septal neuron projecting to the nucleus incertus, we performed double fluorescence to see putative co-occurrence between FG retrograde labeled neurons from injections in the nucleus incertus and specific neuronal markers within the medial septum.

No overlapping was seen between FG and ChAT immunofluorescence. In fact, ChAT occupied different compartments within the medial septum. In the vMS, ChAT positive neurons appeared dispersed in its lateral aspects, while retrograde FG labelled neurons located mainly in the medial aspects of the vMS. In contrast, ChAT positive neurons of the hMS form a rather concentrated cluster configuring a superficial band, while FG retrogradely labelled neurons grouped in another packed band in the deeper regions of the hMS. No double labelled neurons were observed in any subject studied.

Parvalbumin positive neurons appeared in a more dispersed way and in some cases it was possible to find FG and PV double labeling in both the vMS and the hMS.

In contrast to ChAT, we found a high degree of co-localization between GAD65 positive neurons and retrogradely labelled neurons. GAD positive neurons appeared dispersed, hMS and vMS. We found double labeled neurons in both vMS and hMS (Figure 3A-D).

Anterograde labeling in the nucleus incertus following mR injection in the medial septum

We performed mR injections in 12 cases (Figure 1). In 2 cases, large injections included vMS and hMS, In another 2 cases injections were located just outside the vMS and hMS; 4 subjects had very restricted injections of 150-250 um within the hMH and the 2 left had restricted injections in the vMS. In 6 of these subjects an additional FG injection were made in ventral hippocampus and in 4 cases an additional large FG injection was performed in the amygdala, In these cases, retrograde labelling in the hMS co-incided with the location of the miniruby injection (Figure 4).

Although with variable proportions, septal anterograde labeled fibers were always present in the NI. Labeling was more conspicuous when tracer was injected in the hMS (Fig 6A). Anterograde terminal-like labeling in the NI was present even in the smallest injection restricted to the hMS. In these cases, it was possible to follow labeled axons from the septal area, along the hypothalamus running through the medial forebrain bundle (mfb).and brainstem until the nucleus incertus (Figure 5). A dorsal tract was also seen, directed to the lateral habenula. Several labeled fibres were found primarily in the lateral preoptic area from where they dispersed over the perifornical area (Figure 5). More caudally, labeled fibers located in the lateral hypothalamic and perifornical areas. These fibers then entered into the dorsal and ventral premammillary nuclei (Figure 5). Then fibers locate in the lateral supramammillary nucleus (Figure 5), also some fibers were seen in the posterior hypothalamic nucleus (not shown). In the midbrain, a few labeled fibers were followed in the ventral tegmental area (Figure 5) and in the median and paramedian rafe (Figure 5). No labeled fibres were seen in the dorsal raphe in the restricted injections. Caudally, labelled fibres ran towards caudal regions, targeting the pontine raphe and continuing dorsally to get into the nucleus incertus. Although with ipsilateral dominance some fibres also entered into the contralateral nucleus incertus (Fig. 6).

Interestingly, in cases were the FG tracer was injected in the hippocampus and mR was injected in the medial septum we were able to find localization of anterograde fibers in the same areas containing retrograde labeling. This overlapping was fond in theta related areas like the supramammillary nucleus, median rafe as well as the nucleus incertus (Figure 7).

Characterization of anterograde labeling

As we found GAD positive retrogradely labelled neurons in the medial septum we studied if anterograde fibers also contained GAD punctae. We performed GAD65 immunofluorescence and studied the colocalization of miniruby fibers with GAD65 staining. Most, but not all mR labelled fibers also displayed GAD65 immunofluorescence. Also, many of the nucleus incertus cells displayed GAD65 immunofluorescence and part of them were retrogradely labeled from injections in the hippocampus or in the amygdala.

Finally, in a few cases, it was possible to find anterograde labeled fibers which also displayed GAD65 immunofluorescence on nucleus incertus cells that were retrogradely labeled from fluorogold injections in the amygdala or hippocampus. In order to know if anterogradely labeled fibers in the nucleus incertus from injections in the medial septum corresponded to synaptic terminals we have studied the co-localization of miniRuby fibers with synaptophysin immunofluorescence. Indeed co-localization occurred in the few terminal-like labeled fibers

DISCUSSION

In the current study, we have described descending projections arising from the medial septum and arriving to the nucleus incertus of the prepontine tegmentum. This projection arise from both the vMS and the hMS and has been confirmed with both anterograde and retrograde labelling. These connections provide anatomical basis for a feedback loop between the septal area and the nucleus incertus which may function controlling, as a whole, the hippocampus and amygdala activity. We have found that medial septal neurons projecting to the nucleus incertus also contain GAD. Moreover, we have shown that fibres that arise from the medial septum targets hippocampal and amygdala projecting neurons within the nucleus incertus. Double direction pathways from the hippocampus and/or amygdala to the nucleus incertus through the medial septum may provide an autoregulatory system that stabilizes hippocampal activity during active processes like exploration or theta synchronization.

Descending projections from the medial septum

Descending connections from the medial septum to the midbrain were described in the pioneering work by (Swanson and Cowan, 1979) where autoradiographic signal in the raphe nuclei and ventral tegmental area was observed after tritiated aminoacids injections in medial septum. However, they were not able to find H3-aspartate accumulation in the medial septum ruling out the possibility to be an aminoacid excitatory connection. In addition, retrograde tracer injections in the median and paramedian raphe revealed descending connections arising from the medial septum (Behzadi et al., 1990). Early works in cats also showed that while the vertical limb of the diagonal band projects primarily to the hippocampus, the main projection of the horizontal limb runs caudally to the ventral tegmental area (VTA) and interpeduncular nuclei (Krayniak, Weiner, Siegel, 1980).

Descending projections to the histaminergic neuronal groups of the posterior hypothalamus have been observed by injecting PHA-L in the medial septum and double immunolabeling with histamine decarboxilase (Wouterlood et al., 1988). Cornwall et al., (1990) observed retrograde labeling in the diagonal band after tracer injection in the laterodorsal tegmentum (LDTg) (Cornwall, Cooper, Phillipson, 1990). However these descending projections have not been confirmed until now by anterograde tracer injection into the medial septum. Our observations revealed that when anterograde tracer is placed into the medial septum (MS) labeled fibers do not appear in the LDTg but in the NI.

Descending projections from the medial septum has been displayed in the Allen's map with AAV injection in the septal area and two photon microscopic assembling of consecutive levels

(reference Allen's brain)

More recently, we have observed that activity of single nucleus incertus neurons can be recorded from both orthodromic (normal conduction from soma to axon terminals) and antidromic (opposite direction, stimulation of the target tissue can be registered in the origin) stimulation in the medial septum (Ma et al., submitted), confirming that the functional connexion between setpal area and NI is bidirectional.

The parcellation of the medial septum

We have previously demonstrated that the medial septum contains different groups of neurons that are not intermingled but occupy distinct areas within the vMS and hMS. We have already shown that the area located in the limit between the MS and the LS contains neurons projecting to the hypothalamus (Olucha-Bordonau et al., 2011). In the present paper we show that the neurons within the vMS projecting downwards to the NI occupy the outer layer of the vMS, closer to the LS. This situation reverses in the hMS, where descending neurons projecting to the NI reside in the inner band and ChAT positive neurons (presumably projecting to the hippocampus, amygdala and cortex) are located more superficially.

Wouterlood et al., 1988 showed that the medial septal projections to the histaminergic hypothalamic groups are also arranged in a band's pattern. Thus, anterograde tracer progressively injected towards the centre of the medial septum, resulted in a decreased number of labeled fibres and varicosities over the histaminergic hypothalamic neurons (Wouterlood et al., 1988). According to this analysis, a strip-fashion organization of the MS has also been documented recently by (Tsurusaki and Gallagher, 2006). These authors observed that the midline medial septal neurons are not cholinergic and display a different pattern of electrophysiological activity compared to more laterally located areas of the medial septum. Also afferent projections from a lateral strip of the medial septum innervates the hypothalamic attack area (Roeling et al., 1994). Taken altogether these findings suggest that the medial septum does not behave as a homogeneous nucleus but contains different neuronal groups with distinct function.

Theta rhythm as a consequence of a double direction pathway

During the 90s an important body of evidence was reported demonstrating the central role of ascending subcortico-hippocampal projections in driving the hippocampal theta rhythm (for review see (Vertes and Kocsis, 1997). According to this model, the nucleus reticularis pontis oralis (RPO) could activate theta through a series of ascending projections, involving the median raphe, the nucleus supramammillaris, and the medial septum. Each step of this pathway seems to regulate a particular

feature of the hippocampal theta rhythm. According to this model, the RPO is responsible for the induction of the rhythm (Nunez, de Andres, Garcia-Austt, 1991; Vertes et al., 1993). The median raphe can desynchronize theta (Kinney, Kocsis, Vertes, 1994; Vertes et al., 1994; Kinney, Kocsis, Vertes, 1995; Kocsis and Vertes, 1996; Viana Di Prisco et al., 2002). The supramammillary nucleus modulates the theta frequency (McNaughton et al., 1995; Kocsis and Vertes, 1997; Pan and McNaughton, 1997). Finally, the medial septum is considered the pacemaker (Nerad and McNaughton, 2006; Varga et al., 2008; Hangya et al., 2009). This model considers only the ascending path which collects projections from caudally placed nuclei to rostral regions.

Recently, new data have partially challenged this view. Experiments from Nerad and McNaughton showed that freely moving rats recorded at the hippocampus and septum simultaneously, displays a number of discrepancies in the synchrony between these nuclei. The authors, therefore, postulate that the pacemaker of hippocampal theta is "probably a set of functionally differentiated components rather than a single homogenous unit" (Nerad and McNaughton, 2006). In agreement with this hypothesis, our findings reveal a novel pathway involving septal descending projections to the NI that, in turn, project to hippocampus and amygdala. This circuitry implicates a higher degree of complexity since most (although not all) subcortical nuclei involved in theta generation and modulation, are also targeted by descending projections from the septal area (Goto et al., 2001). We postulate that this circuitry loop provides anatomical basis for the fine tuning of hippocampal rhythm pacemaking.

We have observed that an important cluster of medial septal neurons projecting to the nucleus incertus occurred in the hMS, an area that projects to amygdala. This relationship could be important in coupling theta rhythm between nucleus incertus, septum, hippocampus and amygdala. One of the best known roles of the amygdala is its contribution to emotional learning (LeDoux, 2000). Recently, it has been published that theta also occurs in the amygdala in different phases of the learning process (Pape et al., 2005). Theta coupling occurs in lateral amygdala, hippocampus and medial prefrontal cortex during retrieval of conditioned fear and declines during extinction trials. Moreover, during retrieval of the extinction memory there is a re-bound of theta in amygdala (Lesting et al., 2011). Interestingly, there is a high degree of theta coupling between the hippocampus and amygdala during memory consolidation (Seidenbecher et al., 2003) and reconsolidation (Narayanan et al., 2007). According to the model we are presenting, descending connections from the medial septum to the nucleus incertus could modulate the projections back to the hippocampus and amygdala in such a way that both structures may work simultaneously.

Implications for NI-Septum connections in behaviour.

There is not an only function assigned to the medial septum but in fact it participates in modulation of functions carried out buy other centers. Lesions in the medial septum induce an increase in open arm exploration and shock-probe burying test, indicating an anxiogenic role of medial septum (Lamprea, Garcia, Morato, 2010), (Menard and Treit, 1996) (Degroot, Kashluba, Treit, 2001)(Pesold and Treit, 1992; Menard and Treit, 1996; Menard and Treit, 1999).

This anxiogenic effect has been generally attributed to be mediated by the septohippocampal projection. According to the present results, the medial septal projection to the nucleus incertus could also contribute to the general effect of the medial septum over telencephalic centres managing anxiety. Interestingly, an important role of the nucleus incertus in anxiety has been described. Knock out mice for relaxin3, a peptide that is predominantly produced in this nucleus, display an increase of anxiety on the plus maze compared to control littermates (Watanabe et al., 2011). Thus, if lesions in medial septum lead to a less anxious behaviour whereas RLN3 knockout are more anxious, our results would provide an further mechanistic explanation, since medial septum would be inhibiting nucleus incertus activity and consequently RLN3 release, perhaps to amygdala or hippocampus.

McNaughton and Gray proposed that the septo-hippocampal pathway together with some related structures configure the behavioral inhibition system (McNaughton and Gray, 2000). Under that theory, the behavioral inhibition would compare the events that are actually happening with those expected. When there is a mismatch between them, the behavioral inhibition system would produce a significant output in order to halt the current motor program and most likely to reduce its activity in the future.

Under these circumstances, the septo-hypocampal pathway, as a behavioural inhibition system, would act in response to outside signals that can be aversive (punishment, physical pain, reward omission) or unexpected, novelty. Perceiving them as a potential threat, the actions of the septo-hypocampal pathway could lead to anxiety.

The medial septal projection to the nucleus incertus may provide a new source of inhibitory pathway over telencephalic centers. We report here that the medial septal projection is GABAergic and also targets GABAergic nucleus incertus neurons which project to the amygdala.

On the other hand, a great body of evidence have been reported in the last decades regarding the role of the medial septum and medial septum-hippocampus interactions in exploration, spatial navigation and object recognition (Poucet, 1989; Poucet and Buhot, 1994)(Okada and Okaichi, 2010). The occurrence of descending projections from the medial septum to the nucleus incertus and the subsequent ascending connections from the nucleus incertus to the hippocampus is configuring a loop which acts as a whole to generate a cognitive internal and external map. Specific disruption of relaxin

3 projections from nucleus incertus to the medial septum by infusing antagonist of relaxin3 receptor, results in impairment of spatial working memory in the spontaneous alternation test (Ma et al., 2009). Under the light of the present results, these data could be re-interpreted not only as a disruption of the septo-hippocampal but also the disruption of the septo-incertus pathway or more likely both.

CONCLUSIONS

Complex inhibitory systems converge into the nucleus incertus to perform behavioral responses towards particular situations. The majority of the stressors analysed to date induce c-fos activation in NI cells and over 50% of NI cells express CRH-R1. (Ma et al., 2012 submitted). Activation of NI results in increasing hippocampal theta activity, and this seems to be associated with an increase in exploratory behaviour. The fact that descending medial septum projection to the nucleus incertus is mainly GABAergic adds a component in the general inhibitory system. The septo-incertus hippocampal pathway also adds a level of complexity as NI efferent connections also target areas related to the regulation of the hippocampal theta rhythm (Figure 8). The fact that all components of the ascending projections to the hippocampus are connected in both directions and mostly through inhibitory systems may rise the possibility for an auto regulatory system that adjust firing as a result of overlapped projections. This may result in phase locking between the hippocampal field potentiual and the nucleus incertus neural firing.

It is important to point out the different role that descending projections from vMS and hMS may have on nucleus incertus activity. vMS mainly projects to the hippocampus while hMS projects mainly to the amygdala. Thus, a pathway could be outlined running from the hMS, which also controls the amygdala, to the nucleus incertus that, in turn, projects to the ventral hippocampus. This subregion is more closely related to emotional aspects of cognition as i.e. extinction of fear memories. This last process is context dependent and this dependency stands on ventral hippocampus connections to the prefrontal cortex and amygdala.

ACKNOWLEDGEMENTS

Grant sponsors: Fundation Alicia Koplowitz to AMSP; Capes Bex 4494/09-1 and Fapitec edital # 01/08 to FNS; Capes Bex 4496/09-4 to CWP; the Ministry of Health, Spain - ISCIII-FIS PI061816 (FEO-B); the National Health and Medical Research Council of Australia – 520299 (SM); 277609 and 509246 (ALG); and the Victorian Government Operational Infrastructure Support Program (SM and ALG)

LIST OF ABBREVIATIONS USED IN FIGURES

3V	third ventricle
ac	anterior commissure
Acb	accumbens nucleus shell
ADP	anterodorsal preoptic nucleus
ax	axon
APir	amygdalopiriform transition ares
BSTm	bed nucleus of the stria terminalis, medial
CA1	field CA1 of hippocampus
CB-28kD	calbindin 28 kD
ChAT	choline acetyltransferase
DG	dentate gyrus
f	fornix
FG	fluorogold
GAD	glutamic acid decarboxylase
hMS	medial septum, horizontal limb
I	intercalated nuclei
ICjM	insula of Calleja magna
is	injection site
Lent	lateral entorhinal area
LSc-d	lateral septum, caudal dorsal
LSc-v	lateral septum, caudal ventral
LSr-dl	lateral septum, rostral, dorsolateral division
LSr-m	lateral septum, rostral, medial division
LSr-vl	lateral septum, rostral, ventrolateral division
LSv	lateral septum, ventral
MnPO	median preoptic nucleus
MPA	medial preoptic area
mR	miniruby
NIc	Nucleus incertus pars compacta
NId	Nucleus incertus pars dissipata
oc	optic chiasma
PDTg	posterodorsal tegmental nucleus
Pe	periventricular hypothalamic nucleus

PV parvalbumin RLN3 relaxin-3 S subiculum SFi septofimbrial nucleus SHi septohippocampal nucleus SIB substantia innominata, basal part Syn synaptophysin TS triangular septal nucleus vMS medial septum, vertical limb

TABLES Table 1. Neural tracer treatments of rats and immunohistochemistry studies analysed

Table 1. Neural tracer treatments of rats and immunohistochemistry studies analysed

Case	Tracer injection	Immunohistochemical methods	Analysis
CCH5 CCH11 CCH12	FG nucleus Incertus	Tracer fluorescence and immuno-fluorescence for ChAT, PV, GAD 65	FG, and ChAT, PV,
CCH10	FG control		
RS2 RS5 RS6 RS7 RS10 RS15 RS16	mR Septum FG hypocampo	mR, FG and synaptophysin	Confocal co-location of mR, FG and synaptophysin
RS18 RS19	mR Septum FG amygdala	mR, FG and GAD65	Confocal co-location of mR, FG and GAD65

* These rats received a foot shock of 0.6 mA for 2 sec, 90 min prior to processing.

Table 2. List of Primary Antibodies Used in Immunoperoxidase and Immunofluorescence Staining

Antigen	Immunogen (MW)	Manufacturer, Host species, Ig isotype, Catalog number	Dilution used in IHC/IF[1]
Fluorogold	Fluorogold (5-hydroxystabilamide)	Chemicon, Temacula CA, USA, rabbit, polyclonal, AB-153	IHC 1:3,000
ChAT	choline acetyltransferase (70 kD)	Chemicon, Temacula CA, USA, goat, polyclonal, AB-144	IF: 1:500
CB-28kD	chicken calbindin D-28k (28 kD)	Swant, Bellinzona, Switzerland, mouse, monoclonal, McAB300	IF: 1:5,000
PV	parvalbumin (12 kD)	Swant, Bellinzona, Switzerland, mouse, monoclonal, McAB235	IF: 1:5,000
GAD-65	recombinant GAD-67 (67 kD)	Chemicon, Temacula CA, USA, mouse, monoclonal, MAB-5406	IF: 1:500
synaptophysin	rat retinal synaptosomes antigen (38 kD)	Sigma, St Louis, MO, USA, mouse, monoclonal, S5768	IF: 1:500

REFERENCES

Andersen P, Bland HB, Myhrer T, Schwartzkroin PA. 1979. Septo-hippocampal pathway necessary for dentate theta production. Brain Res. 165: 13-22.

Behzadi G, Kalen P, Parvopassu F, Wiklund L. 1990. Afferents to the median raphe nucleus of the rat: retrograde cholera toxin and wheat germ conjugated horseradish peroxidase tracing, and selective D-[3H]aspartate labelling of possible excitatory amino acid inputs. Neuroscience 37: 77-100.

Celio MR, Baier W, Scharer L, de Viragh PA, Gerday C. 1988. Monoclonal antibodies directed against the calcium binding protein parvalbumin. Cell Calcium 9: 81-86.

Celio MR, Baier W, Scharer L, Gregersen HJ, de Viragh PA, Norman AW. 1990. Monoclonal antibodies directed against the calcium binding protein Calbindin D-28k. Cell Calcium 11: 599-602.

Cornwall J, Cooper JD, Phillipson OT. 1990. Afferent and efferent connections of the laterodorsal tegmental nucleus in the rat. Brain Res. Bull. 25: 271-284.

Degroot A, Kashluba S, Treit D. 2001. Septal GABAergic and hippocampal cholinergic systems modulate anxiety in the plus-maze and shock-probe tests. Pharmacol. Biochem. Behav. 69: 391-399.

Freund TF, Gulyas AI. 1997. Inhibitory control of GABAergic interneurons in the hippocampus. Can. J. Physiol. Pharmacol. 75: 479-487.

Freund TF, Antal M. 1988. GABA-containing neurons in the septum control inhibitory interneurons in the hippocampus. Nature 336: 170-173.

Goto M, Swanson LW, Canteras NS. 2001. Connections of the nucleus incertus. J. Comp. Neurol. 438: 86-122.

Hangya B, Borhegyi Z, Szilagyi N, Freund TF, Varga V. 2009. GABAergic neurons of the medial septum lead the hippocampal network during theta activity. J. Neurosci. 29: 80948102.

Jacab RL, Leranth C. 1995. Septum. In The Rat Nervous System, Paxinos G (ed). Academic Press: 405-442.

Kinney GG, Kocsis B, Vertes RP. 1995. Injections of muscimol into the median raphe nucleus produce hippocampal theta rhythm in the urethane anesthetized rat. Psychopharmacology (Berl) 120: 244-248.

Kinney GG, Kocsis B, Vertes RP. 1994. Injections of excitatory amino acid antagonists into the median raphe nucleus produce hippocampal theta rhythm in the urethane-anesthetized rat. Brain Res. 654: 96-104.

Kocsis B, Vertes RP. 1997. Phase relations of rhythmic neuronal firing in the supramammillary nucleus and mammillary body to the hippocampal theta activity in urethane anesthetized rats. Hippocampus 7: 204-214.

Kocsis B, Vertes RP. 1996. Midbrain raphe cell firing and hippocampal theta rhythm in urethane-anaesthetized rats. Neuroreport 7: 2867-2872.

Krayniak PF, Weiner S, Siegel A. 1980. An analysis of the efferent connections of the septal area in the cat. Brain Res. 189: 15-29.

Lamprea MR, Garcia AM, Morato S. 2010. Effects of reversible inactivation of the medial septum on rat exploratory behavior in the elevated plus-maze using a test-retest paradigm. Behav. Brain Res. 210: 67-73.

LeDoux JE. 2000. Emotion circuits in the brain. Annu. Rev. Neurosci. 23: 155-184.

Leranth C, Vertes RP. 1999. Median raphe serotonergic innervation of medial septum/diagonal band of broca (MSDB) parvalbumin-containing neurons: possible involvement of the MSDB in the desynchronization of the hippocampal EEG. J. Comp. Neurol. 410: 586-598.

Lesting J, Narayanan RT, Kluge C, Sangha S, Seidenbecher T, Pape HC. 2011. Patterns of Coupled Theta Activity in Amygdala-Hippocampal-Prefrontal Cortical Circuits during Fear Extinction. PLoS One 6: e21714.

Ma S, Shen PJ, Sang Q, Lanciego JL, Gundlach AL. 2009a. Distribution of relaxin-3 mRNA and immunoreactivity and RXFP3-binding sites in the brain of the macaque, Macaca fascicularis. Ann. N. Y. Acad. Sci. 1160: 256-258.

Ma S, Olucha-Bordonau FE, Hossain MA, Lin F, Kuei C, Liu C, Wade JD, Sutton SW, Nunez A, Gundlach AL. 2009b. Modulation of hippocampal theta oscillations and spatial memory by relaxin-3 neurons of the nucleus incertus. Learn. Mem. 16: 730-742.

Ma S, Bonaventure P, Ferraro T, Shen PJ, Burazin TC, Bathgate RA, Liu C, Tregear GW, Sutton SW, Gundlach AL. 2007. Relaxin-3 in GABA projection neurons of nucleus incertus suggests widespread influence on forebrain circuits via G-protein-coupled receptor-135 in the rat. Neuroscience 144: 165-190.

McNaughton N, Gray JA. 2000. Anxiolytic action on the behavioural inhibition system implies multiple types of arousal contribute to anxiety. J. Affect. Disord. 61: 161-176.

McNaughton N, Logan B, Panickar KS, Kirk IJ, Pan WX, Brown NT, Heenan A. 1995. Contribution of synapses in the medial supramammillary nucleus to the frequency of hippocampal theta rhythm in freely moving rats. Hippocampus 5: 534-545.

Menard J, Treit D. 1999. Effects of centrally administered anxiolytic compounds in animal models of anxiety. Neurosci. Biobehav. Rev. 23: 591-613.

Menard J, Treit D. 1996. Lateral and medial septal lesions reduce anxiety in the plus-maze and probe-burying tests. Physiol. Behav. 60: 845-853.

Narayanan RT, Seidenbecher T, Sangha S, Stork O, Pape HC. 2007. Theta resynchronization during reconsolidation of remote contextual fear memory. Neuroreport 18: 1107-1111.

Nerad L, McNaughton N. 2006. The septal EEG suggests a distributed organization of the pacemaker of hippocampal theta in the rat. Eur. J. Neurosci. 24: 155-166.

Nuñez A, de Andres I, Garcia-Austt E. 1991. Relationships of nucleus reticularis pontis oralis neuronal discharge with sensory and carbachol evoked hippocampal theta rhythm. Exp. Brain Res. 87: 303-308.

Nuñez A, Cervera-Ferri A, Olucha-Bordonau F, Ruiz-Torner A, Teruel V. 2006. Nucleus incertus contribution to hippocampal theta rhythm generation. Eur. J. Neurosci. 23: 27312738.

Okada K, Okaichi H. 2010. Functional cooperation between the hippocampal subregions and the medial septum in unreinforced and reinforced spatial memory tasks. Behav. Brain Res.209: 295-304.

Olucha-Bordonau FE, Otero-Garcia M, Sanchez-Perez AM, Nunez A, Ma S, Gundlach AL. 2011. Distribution and targets of the relaxin-3 innervation of the septal area in the rat. J. Comp. Neurol.

Olucha-Bordonau FE, Teruel V, Barcia-Gonzalez J, Ruiz-Torner A, Valverde-Navarro AA, Martinez-Soriano F. 2003. Cytoarchitecture and efferent projections of the nucleus incertus of the rat. J. Comp. Neurol. 464: 62-97.

Pan WX, McNaughton N. 1997. The medial supramammillary nucleus, spatial learning and the frequency of hippocampal theta activity. Brain Res. 764: 101-108.

Pape HC, Narayanan RT, Smid J, Stork O, Seidenbecher T. 2005. Theta activity in neurons and networks of the amygdala related to long-term fear memory. Hippocampus 15: 874-880.

Pesold C, Treit D. 1992. Excitotoxic lesions of the septum produce anxiolytic effects in the elevated plus-maze and the shock-probe burying tests. Physiol. Behav. 52: 37-47.

Petsche H, Stumpf C. 1962. The origin of theta-rhytm in the rabbit hippocampus. Wien. Klin. Wochenschr. 74: 696-700.

Poucet B. 1989. Object exploration, habituation, and response to a spatial change in rats following septal or medial frontal cortical damage. Behav. Neurosci. 103: 1009-1016.

Poucet B, Buhot MC. 1994. Effects of medial septal or unilateral hippocampal inactivations on reference and working spatial memory in rats. Hippocampus 4: 315-321.

Rico B, Cavada C. 1998. Adrenergic innervation of the monkey thalamus: an immunohistochemical study. Neuroscience 84: 839-847.

Risold PY, Swanson LW. 1997. Chemoarchitecture of the rat lateral septal nucleus. Brain Res. Brain Res. Rev. 24: 91-113.

Roeling TA, Veening JG, Kruk MR, Peters JP, Vermelis ME, Nieuwenhuys R. 1994. Efferent connections of the hypothalamic "aggression area" in the rat. Neuroscience 59: 1001-1024.

Seidenbecher T, Laxmi TR, Stork O, Pape HC. 2003. Amygdalar and hippocampal theta rhythm synchronization during fear memory retrieval. Science 301: 846-850.

Sotty F, Danik M, Manseau F, Laplante F, Quirion R, Williams S. 2003. Distinct electrophysiological properties of glutamatergic, cholinergic and GABAergic rat septohippocampal neurons: novel implications for hippocampal rhythmicity. J. Physiol. 551: 927-943.

Swanson LW, Cowan WM. 1979. The connections of the septal region in the rat. J. Comp. Neurol. 186: 621-655.

Toth K, Freund TF, Miles R. 1997. Disinhibition of rat hippocampal pyramidal cells by GABAergic afferents from the septum. J. Physiol. 500 (Pt 2): 463-474.

Tsurusaki M, Gallagher JP. 2006. A distinct group of non-cholinergic neurons along the midline of the septum and within the rat medial septal nucleus. Neurosci. Lett. 410: 20-24.

Varga V, Hangya B, Kranitz K, Ludanyi A, Zemankovics R, Katona I, Shigemoto R, Freund TF, Borhegyi Z. 2008. The presence of pacemaker HCN channels identifies theta rhythmic GABAergic neurons in the medial septum. J. Physiol. 586: 3893-3915.

Vertes RP. 1982. Brain stem generation of the hippocampal EEG. Prog. Neurobiol. 19: 159 186.

Vertes RP. 1981. An analysis of ascending brain stem systems involved in hippocampal synchronization and desynchronization. J. Neurophysiol. 46: 1140-1159.

Vertes RP, Kocsis B. 1997. Brainstem-diencephalo-septohippocampal systems controlling the theta rhythm of the hippocampus. Neuroscience 81: 893-926.

Vertes RP, Kinney GG, Kocsis B, Fortin WJ. 1994. Pharmacological suppression of the median raphe nucleus with serotonin1A agonists, 8-OH-DPAT and buspirone, produces hippocampal theta rhythm in the rat. Neuroscience 60: 441-451.

Vertes RP, Colom LV, Fortin WJ, Bland BH. 1993. Brainstem sites for the carbachol elicitation of the hippocampal theta rhythm in the rat. Exp. Brain Res. 96: 419-429.

Viana Di Prisco G, Albo Z, Vertes RP, Kocsis B. 2002. Discharge properties of neurons of the median raphe nucleus during hippocampal theta rhythm in the rat. Exp. Brain Res. 145: 383-394.

Vinogradova OS. 1995. Expression, control, and probable functional significance of the neuronal theta-rhythm. Prog. Neurobiol. 45: 523-583.

Watanabe Y, Tsujimura A, Takao K, Nishi K, Ito Y, Yasuhara Y, Nakatomi Y, Yokoyama C, Fukui K, Miyakawa T, Tanaka M. 2011. Relaxin-3-deficient mice showed slight alteration in anxiety-related behavior. Front. Behav. Neurosci. 5: 50.

Wouterlood FG, Gaykema RP, Steinbusch HW, Watanabe T, Wada H. 1988. The connections between the septum-diagonal band complex and histaminergic neurons in the posterior hypothalamus of the rat. Anterograde tracing with Phaseolus vulgaris-leucoagglutinin combined with immunocytochemistry of histidine decarboxylase. Neuroscience 26: 827-845.

Wu M, Shanabrough M, Leranth C, Alreja M. 2000. Cholinergic excitation of septohippocampal GABA but not cholinergic neurons: implications for learning and memory. J. Neurosci. 20: 3900-3908.

LIST OF FIGURES

Figure 6. Anterograde labeling in the nucleus incertus after a very restricted injection in the hMS. C-terminal-like labeling occurred mainly in the ipsilateral medial septum although some labeling also occurred in the contralateral site all along its rostrocaudal extent.

Figure 7. Overlaping of areas containing anterograde labeling from injections in the vMS and retrograde labeling from injections in the ventral hippocampus.
A-C) supramammillary nucleus. D-F) median raphe. G-I) nucleus incertus.

Figure 8. A diagram model of the hippocampus-septum-incertus loop.
Over the traditional view of ascending projections from the NI to the hippocampus the descending projection from the septum to hypothalamus and nucleus incertus transform the ascending pathways into a double direction loop. Septum presents descending projections to Hypothalamic nucleus, Brain Stem and Nucleus Incertus. All these areas, in turn, innervate hippocampus in ascending projections. Because septum receives projections from all these nucleus, our data suggests a model for a feedback mechanism of septal function regulation.

Figure 1.

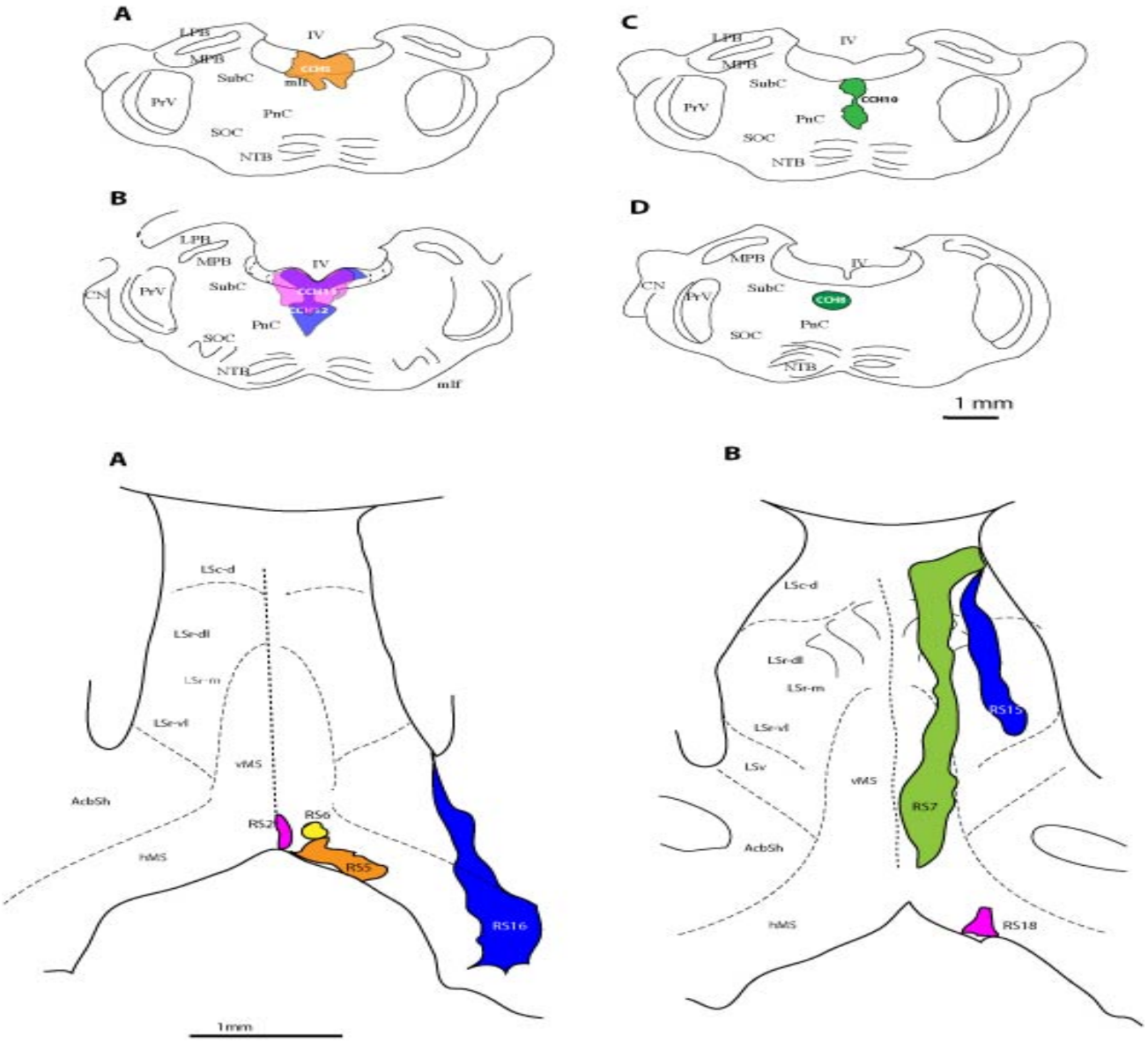
A
LPB
MPB
SubC
PrV
IV
CCH9
mlf
PnC
SOC
NTB
B
LPB
MPB
IV
CN
PrV
SubC
CCH11
CCH12
PnC
SOC
NTB
mlf
C
LPB
MPB
IV
SubC
PrV
CCH10
PnC
SOC
NTB
D
MPB
IV
CN
PrV
SubC
CCH8
PnC
SOC
NTB
1 mm
A
LSc-d
LSr-dl
LSr-m
LSr-vl
vMS
AcbSh
RS2
RS6
RS5
hMS
RS16
1mm
B
LSc-d
LSr-dl
LSr-m
RS15
LSr-vl
LSv
vMS
RS7
AcbSh
hMS
RS18

Figure 2.

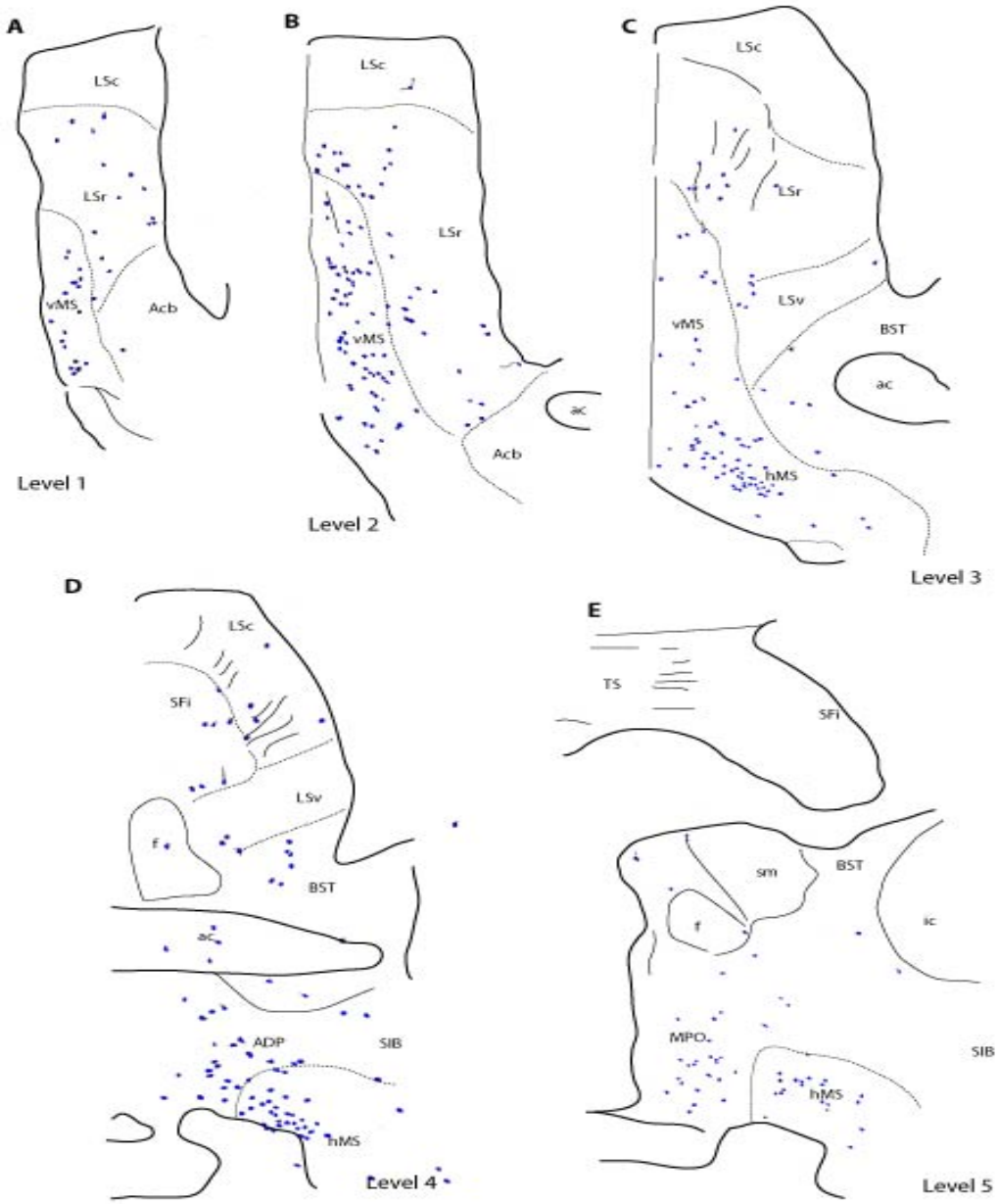
A
LSc
LSr
vMS
Acb
Level 1
B
LSc
LSr
vMS
ac
Acb
Level 2
C
LSc
LSr
LSv
vMS
BST
ac
hMS
Level 3
D
LSc
SFi
LSv
f
BST
ac
ADP
SIB
hMS
Level 4
E
TS
SFi
sm
BST
f
ic
MPO
SIB
hMS
Level 5

Figure 3.

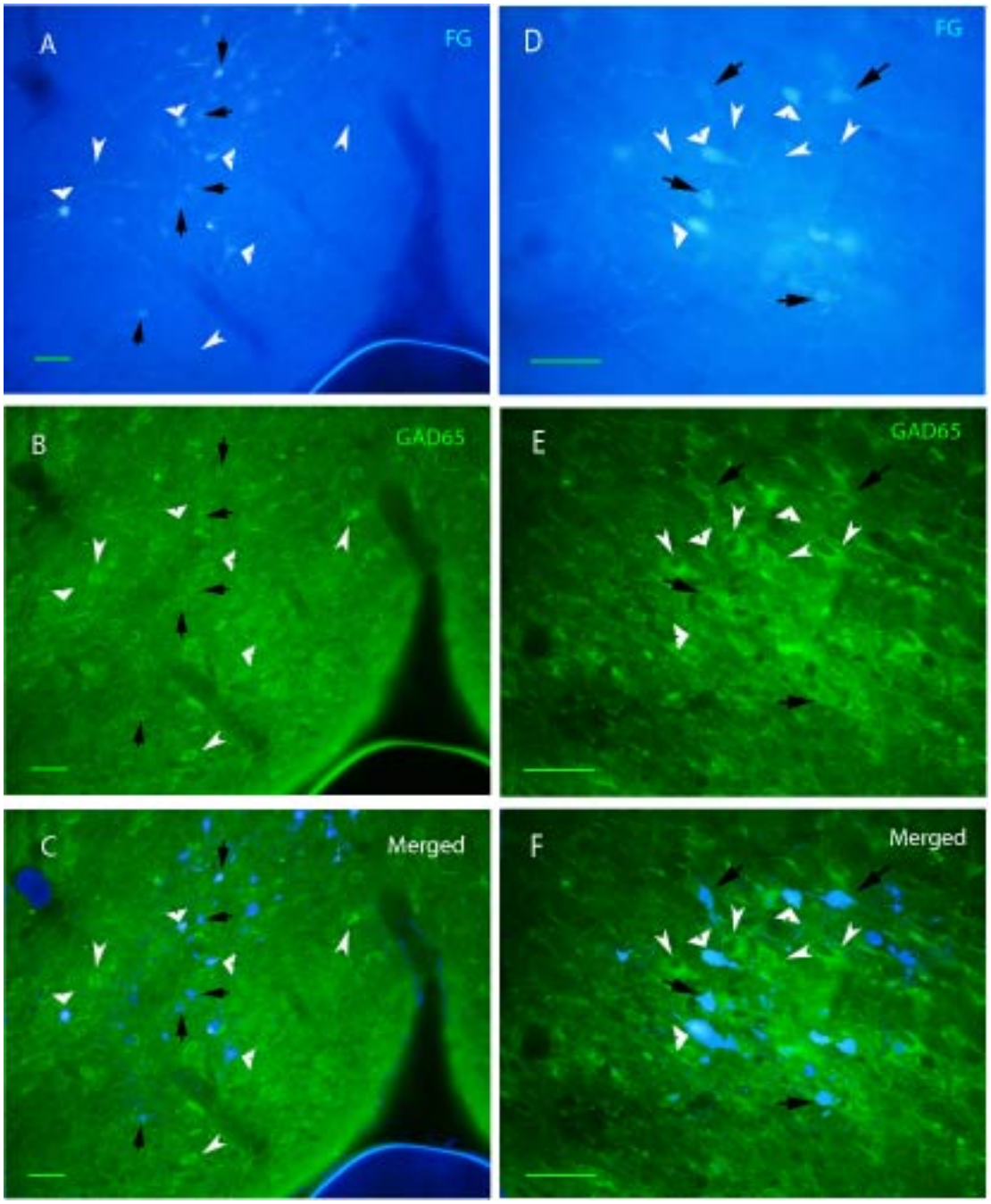

Figure 4.

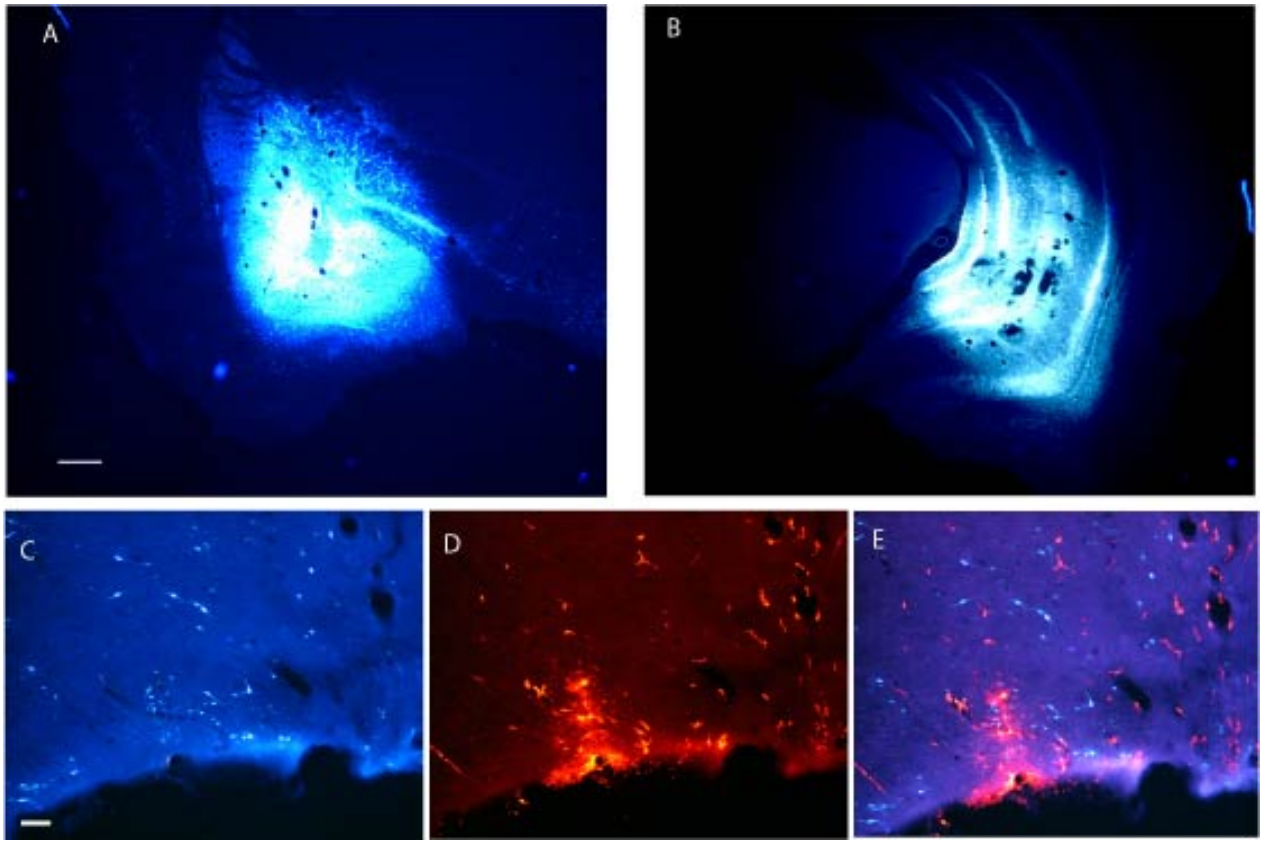

Figure 5.

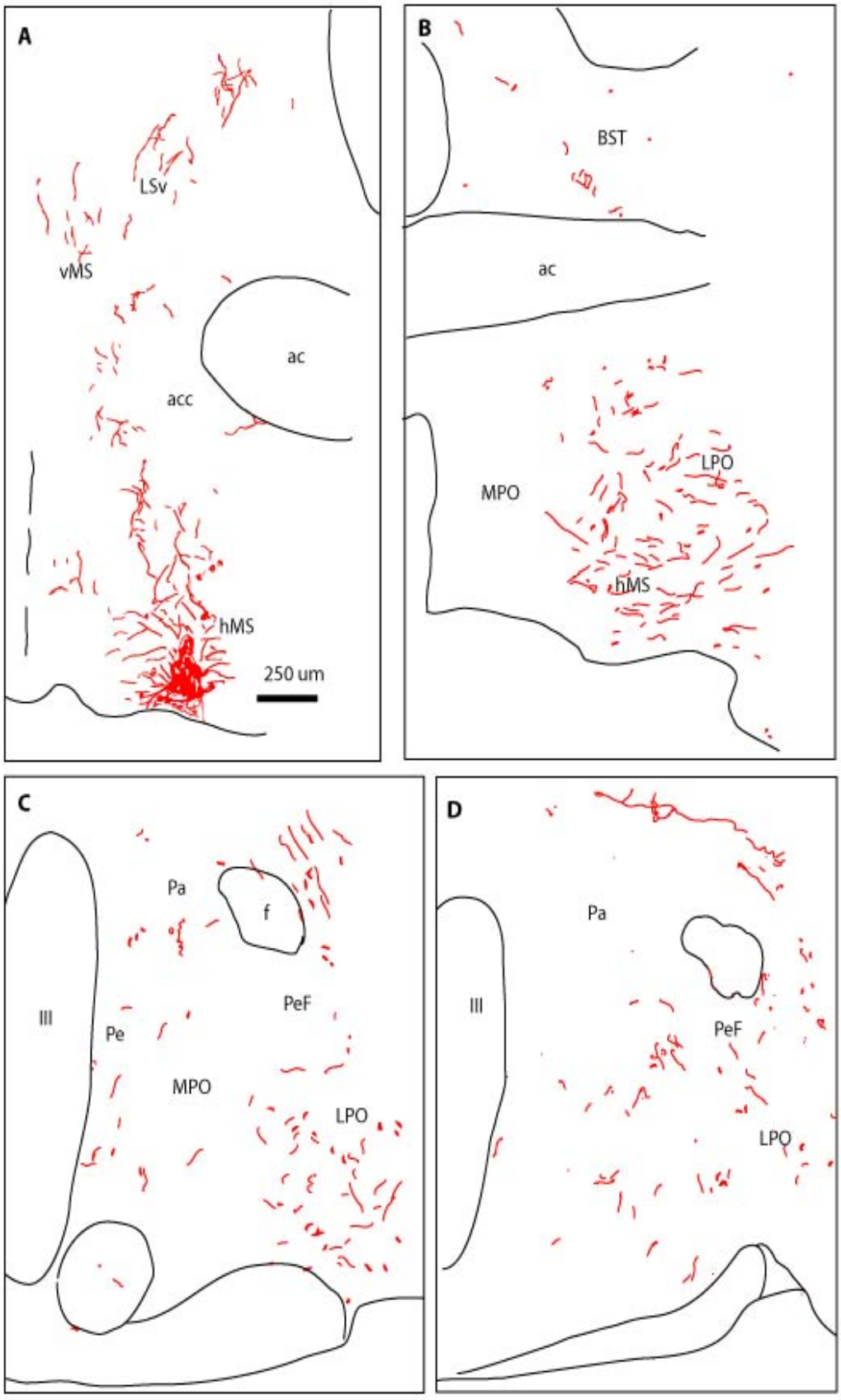
A
LSv
vMS
ac
acc
hMS
250 um
B
BST
ac
LPO
MPO
hMS
C
Pa
f
PeF
III
Pe
MPO
LPO
D
Pa
III
PeF
LPO

Figure 6.

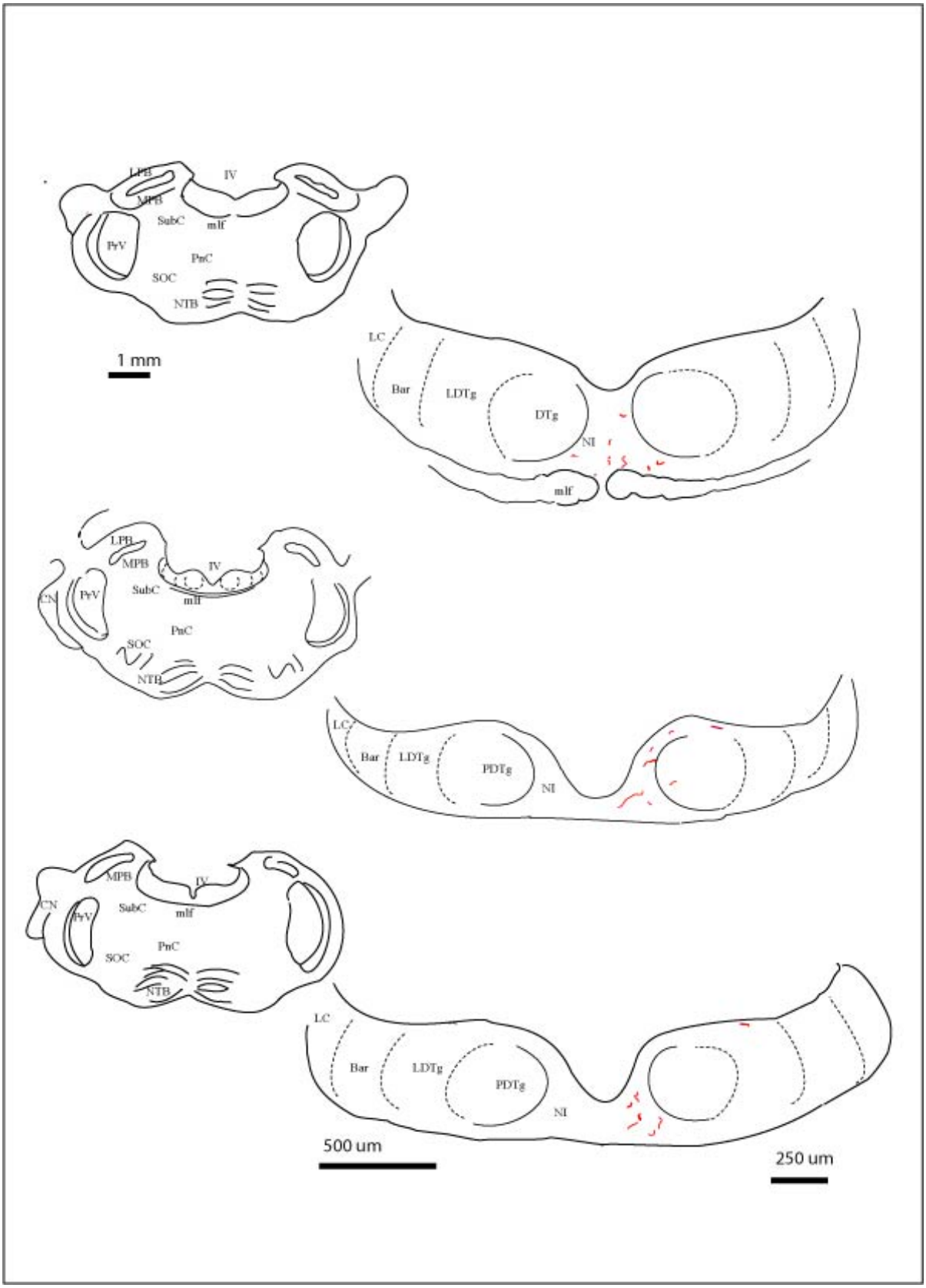
LPB
IV
MPB
SubC
mlf
PrV
PnC
SOC
NTB
1 mm
LC
Bar
LDTg
DTg
NI
mlf
LPB
MPB
IV
CN
PrV
SubC
mlf
PnC
SOC
NTB
LC
Bar
LDTg
PDTg
NI
MPB
IV
CN
SubC
mlf
PrV
PnC
SOC
NTB
LC
Bar
LDTg
PDTg
NI
500 um
250 um

Figure 7.

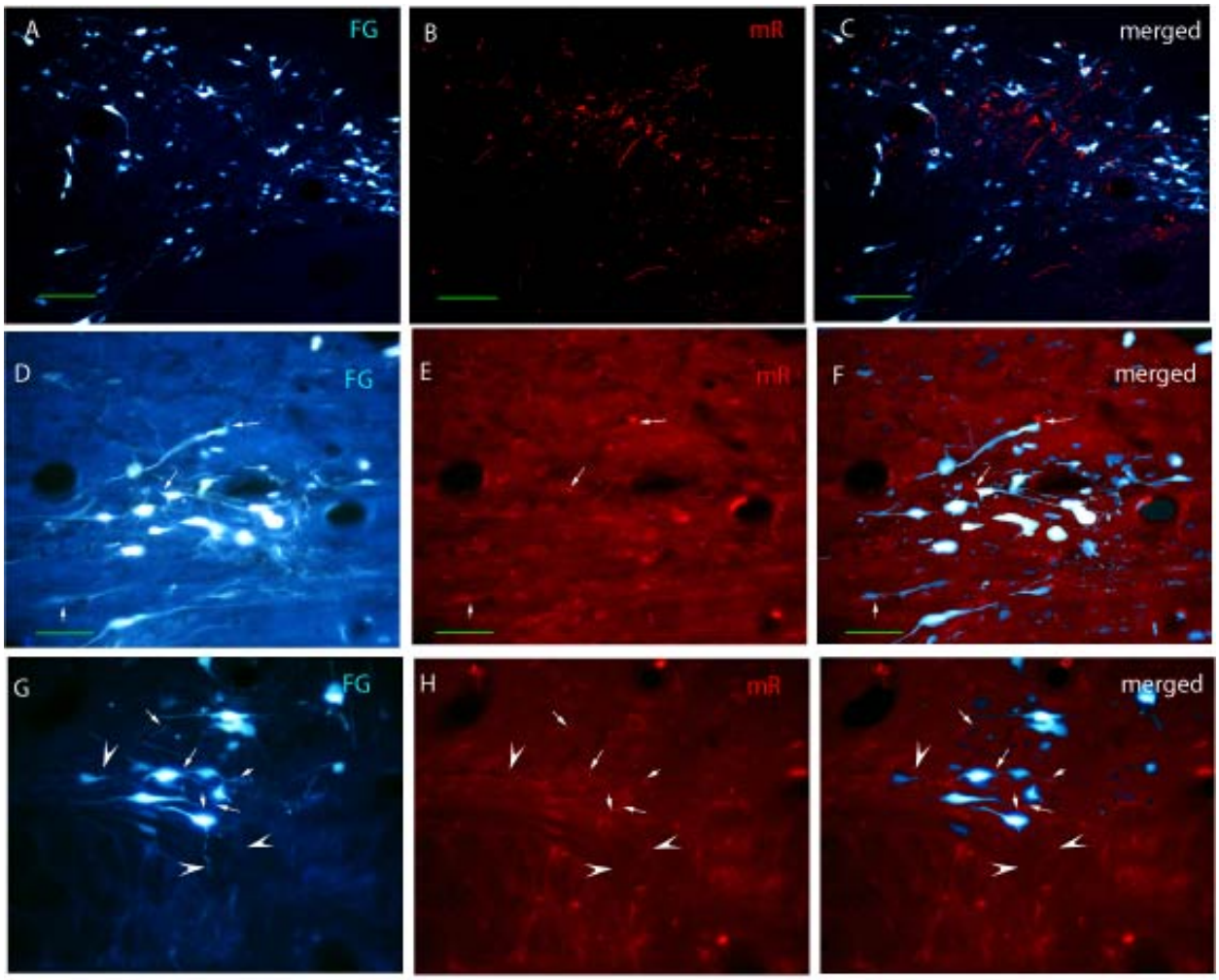

Figure 8.

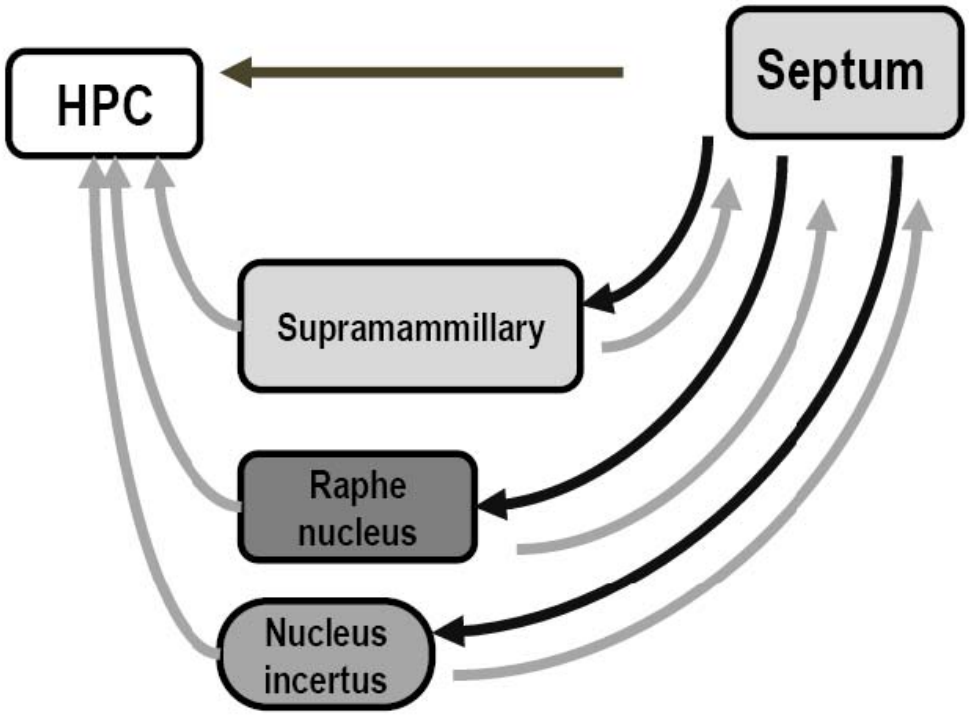
HPC
Septum
Supramammillary
Raphe nucleus
Nucleus incertus

APÊNDICE D

COMUNICAÇÕES PRODUZIDAS DURANTE O PERÍODO DE REALIZAÇÃO DO DOUTORADO (2008 – 2012)

Apêndice D

1. PEREIRA, Celia Waylan, SANTOS, Fabio Neves, MARCHIORO, Murilo, OLUCHA-BORDONAU, Francisco E. Atuação do Sistema Núcleo Incertus/Relaxina-3 Sobre o Condicionamiento Pavloviano In: **VII Reunião Regional da Fesbe**, 2012.

2. SANTOS, Fabio Neves, PEREIRA, Celia Waylan, MARCHIORO, Murilo, OLUCHA-BORDONAU, Francisco E. Papel do Núcleo Incertus na Modulação da Pressão Sanguínea In: **VII Reunião Regional da Fesbe**, 2012, Maceió. Anais., 2012.

3. OLUCHA-BORDONAU, Francisco E., SÁNCHEZ-PÉREZ, Ana M., SANTOS, Fabio Neves, PEREIRA, Celia Waylan, MA, Sherie, GUNDLACH, Andrew L. Behavioral effects of lesions of the nucleus incertus on fear conditioning and extinction and social exploration in rats In: **8th Fens – Forum of Neuroscience**, 2012, Barcelona. Fens Forum., 2012. v.Único.

4. SANTOS, Fabio Neves, OLUCHA-BORDONAU, Francisco E., OTERO-GARCIA, Marcos, PEREIRA, Celia Waylan. As projeções relaxina 3 sobre o tectum e tegmentum revelam um provável papel na modulação de respostas de atenção In: **XXXIV Congresso Anual da Sociedade Brasileira de Neurociências e Comportamento**, 2010, Caxambu. Anais., 2010. v.Único.

5. PEREIRA, Celia Waylan, OTERO-GARCIA, Marcos, OLUCHA-BORDONAU, Francisco E., SANTOS, Fabio Neves Distribuição de fibras relaxina 3 no diencéfalo de ratos In: **XXXIV Congresso Anual da Sociedade Brasileira de Neurociências e Comportamento**, 2010, Caxambu. Anais. , 2010. v.Único.

6. PEREIRA, Celia Waylan, SANTOS, Fabio Neves, OTERO-GARCIA, Marcos, NUÑEZ, Angel, MA, Sherie, GUNDLACH, Andrew L., OLUCHA-BORDONAU, Francisco E. Efectos de la Transmisión Núcleo Incertus/Relaxin3 Sobre la Modulación de la Presión Sanguínea In: **VII Congreso de la Sociedad Española de Psicofisiología y Neurociencia Cognitiva y Afectiva (SEPNECA)**, 2010, Valencia. VII Sociedad Española de Psicofisiología y Neurociencia Cognitiva y Afectiva. Barcelona: Viguera Editores, 2010. v.52. p.306 – 315. *Os anais do evento foram publicados na Revista de Neurologia*

7. OLUCHA-BORDONAU, Francisco E., OTERO-GARCIA, Marcos, PEREIRA, Celia Waylan, SANTOS, Fabio Neves, NUÑEZ, Angel, MA, Sherie, GUNDLACH, Andrew L. El núcleo incertus del tegmentum pontino: un sistema de proyecciones amplias para la modulación de procesos de atención y memória In: **VII Congreso de la Sociedad Española de Psicofisiología y Neurociencia Cognitiva y Afectiva** (SEPNECA), 2010, Valencia. VII Sociedad Española de Psicofisiología y Neurociencia Cognitiva y Afectiva. Barcelona: Viguera Editores, 2010. v.52. p.306 – 315. *Os anais do evento foram publicados na Revista de Neurología*

8. SANTOS, Fabio Neves, PEREIRA, Celia Waylan, OTERO-GARCIA, Marcos, NUÑEZ, Angel, MA, Sherie, GUNDLACH, Andrew L., OLUCHA-BORDONAU, Francisco E. Papel del Sistema Núcleo Incertus/Relaxin3 sobre el Condicionamiento Pavloviano In: **VII Congreso de la Sociedad Española de Psicofisiología y Neurociencia Cognitiva y Afectiva** (SEPNECA), 2010, Valencia. VII Congreso de la Sociedad Española de Psicofisiología y Neurociencia Cognitiva y Afectiva. Barcelona: Viguera Editores, 2010. v.52. p.306 – 315 *Os anais do evento foram publicados na Revista de Neurología*

9. OTERO-GARCIA, Marcos, PEREIRA, Celia Waylan, SANTOS, Fabio Neves, NUÑEZ, Angel, MA, Sherie, GUNDLACH, Andrew L., OLUCHA-BORDONAU, Francisco E. Relación de la Distribución de Fibras Relaxin3 en el Tectum y Tegmentum con Mecanismos Defensivos y Ofensivos In: **VII Congreso de la Sociedad Española de Psicofisiología y Neurociencia Cognitiva y Afectiva (SEPNECA)**, 2010, Valencia. Sociedad Española de Psicofisiología y Neurociencia Cognitiva y Afectiva. Barcelona: Viguera Editores, 2010. v.52. p.306 – 315. *Os anais do evento foram publicados na Revista de Neurología*

10. OLUCHA-BORDONAU, Francisco E., OTERO-GARCIA, Marcos, PEREIRA, Celia Waylan, SANTOS, Fabio Neves, BLASIAK, Anna, MA, Sherie, GUNDLACH, Andrew L. Tectal and tegmental targets of relaxin 3 fibers arising from the nucleus incertus in rat brain In: **40ª Annual Meeting Neuroscience** 2010, 2010, San Diego. Neuroscience Meeting Planner. San Diego: Society for Neuroscience, 2010. p.809.23.